University of Strathclyde – University of Glasgow

T cell Gene Therapy in Vascular Pathology

Peter Ross Gordon

Thesis submitted to the
University of Strathclyde for the
Degree of Doctor of Philosophy
September 2012

Containing studies performed in the Institute of Infection, Immunity and Inflammation, University of Glasgow, Glasgow G12 8TA and the Strathclyde Institute for Pharmacy and Biomedical Science, University of Strathclyde, Glasgow G4 0RE

Author's Declaration

'This thesis is the result of the author's original research. It has been composed by the author and has not been previously submitted for examination which has led to the award of a degree.'

Peter Ross Gordon

Signature:
Date:

Abstract

The immune system is a key contributor to atherosclerosis-related cardiovascular diseases (CVD) however, at present there are no targeted therapies specific for the inflamed vessel wall. Multiple leukocyte subsets have been shown to play a significant role in CVD and among them, CD4 T cells are receiving growing interest. Here we investigated whether T cells could be utilised as delivery vehicles in experimental atherosclerosis, for therapeutic molecules inserted via viral vector.

Using multiphoton microscopy, we developed a protocol for the imaging of immune cells within the atherosclerotic aorta, confirming homing of a relevant number of leukocytes to the inflamed vessel following adoptive transfer. Transferred cells in the aorta were found to behave in a similar manner to cells found in the peripheral lymph nodes. We then constructed GFP and IL-10 expressing adenoviral vectors and used them in the optimisation of CD4+ T cell transduction. The biological activity of the produced IL-10 was assessed and GFP transduced cells were transferred into recipient mice and their migration tracked using flow cytometry. Transduction of CD4+ T cells reached 80%. IL-10 produced by the transduced cells was shown to be biologically active and importantly, the transferred modified cells were shown to migrate and survive comparably to non-transduced cells in a non-inflamed context without causing liver toxicity. Unfortunately, transduction of B6 T cells through various means was found to be unsuccessful therefore we could not evaluate the effect of IL-10 secreting T cells in atherosclerotic mice.

In conclusion, the results of this thesis indicate that the use of genetically modified T cells could be a viable approach in the treatment of inflammatory disorders.

Table of Contents

List of tables

List of figures

Chapter 6

Acknowledgements

I would like firstly to thank my supervisor, Pasquale Maffia. He has been a great source of encouragement and support throughout my PhD, bringing his unique brand of Italian wisdom to this project and has also had to put up with me for the last 4 years, which is no mean feat. Although you were technically my boss I feel that we have become friends and I wish you all the best for the future Grande Puffo. Thanks also to Andrew Baker; you have been a pivotal source of knowledge and experience with all aspects of the project and I would not have been able to complete it without you. I would like to say a special thanks to Alan Parker who got dumped with me a few years back, but has helped me immensely with all aspects of virology and getting through my thesis. You offered endless support when I needed it and I wish you all the best in whatever you do; I couldn't have done this without you mate. A thank you also, to Hilary Carswell and Catherine Laurence for giving me moral support from Strathclyde and their advice on progressing through my PhD.

A huge thanks goes out to all the GBM posse. First up is Gary, you took me under your stylish and colour coordinated wing when I started my PhD which I'm really thankful for, helping me whenever I needed it with the world of the cardiovascular. You also taught me the meaning of "trendy" and gave me the material in order to do a jolly good impression of you. Sir Bob, you were my immunology encyclobobica and I'm really grateful for all the lab support and wisdom you gave me. From you I learned to love sit ups and I'll miss our discussions about various fighting styles, you'll have to find a new person to practice cross, jab, knee combos on now (Ross says he'd love that, try him). Agi, my Greek and significantly less handsome brother. Again I am thankful for all the help and support you have given me and the experiences of authentic Eastern cuisine. From you I have learned to enunciate and so many wonderful swear words I dare not type here. Thank

you to Gianluca who travelled all the way from Italy just to see and help me with my work, what a nice lad. From you I learned that red wine takes priority over sleep on occasions and that it is indeed possible to have stuble covering 90% of your head, marvellous. A big thank you to John (Jolly boy) for teaching me the ways of the microbiological and also for providing some of the biggest laughs in the lab and that goes for Ross too, if ever I need a slightly more flimsy stunt double I know who to call. Tovah, I miss our long chats whenever everyone went home from the lab and that silly way you pronounced things. If ever I was feeling overworked or stressed I'd just look at you and I would realise that it wasn't so bad, you were having a worse time of it. Tirthy boy, I have learned a lot about different cultures from you sir and also how the culture of Tirth has an inhuman love of chicken, good luck with the future and the new baby! Vivienne, Sharon and Owain I miss you guys too, Vivienne for unlocking gossiping skills I never knew I had, Sharon for awesome company and pub quiz organising and Owain for being the target of quite possibly the most accurate impression I can do of a "respected" academical figure. A massive thank you to Gayle, Felicity, Jamie and Jen for giving me the emotional support I needed to get me through this. You've had to put up with the grumpy, stressed, intoxicated and moaning versions of me and you're also amazing friends, our banterous times will go down in the scriptures of legend and hopefully many more will be added.

A big thank you to all the members of the BHF lab group, whether you were just helping me find plasmid kits in the maze like lab or giving me someone to talk to while I was changing media at an ungodly hour it was very much appreciated. Thank you to all the people in the BPU and CRF for all your support and helping my experiments come to fruition.

Finally, I would like to thank my family. Although none of you have taken the time to actually figure out what I do…I couldn't have done this without you. You have supported me all my life in whatever I wanted to do and I

hope I’ve done you proud. A special thanks to my sister for letting me stay over so often after long days and nights in the lab, I won’t stop giving you abuse though, it is my brotherly right.

Abbreviations

^{18}FDG	Fluoro-deoxyglucose
5-LO	5-Lipoxygenase
7-AAD	7-Aminoactinomycin D
AAV	Adeno-Associated Virus
ABCA1/G1	ATP-Binding Cassette Transporter A1/G1
ACE	Angiotensin Converting Enzyme
Ad(-5)	Adenovirus (serotype 5)
ADCC	Antibody-Dependent Cell Cytotoxicity
APC	Antigen Presenting Cell
ApoE/B	Apolipoprotein E/B
ATLO	Arterial Tertiary Lymphoid Organ
BCA	Bicinchononic Acid
C	Cysteine
CAD	Coronary Artery Disease
CAR	Chimeric Antigen Receptor
CAR	Coxsackie Adenovirus Receptor
CD	Cluster of Differentiation
CHD	Coronary Heart Disease
CMV	Cytomegalovirus
CPE	Cytopathic Effect
CSIF	Cytokine Synthesis Inhibitory Factor
CT	Computed Tomography
CVD	Cardiovascular Disease
DC	Dendritic Cell
DMEM	Dulbecco's Modified Eagle Medium
DMSO	Dimethyl Sulphoxide
DNA	Deoxyribonucleic Acid
EAE	Experimental Autoimmune Encephalomyelitis

ECM	Extracellular Matrix
EF1	Elongation Factor 1
ELISA	Enzyme Linked Immunosorbent Assay
EMA	Ethidium Monoazide Bromide
Enos	Endothelial Nitric Oxide Synthase
FACS	Fluorescence Activated Cell Sorting
FcR	Fc Receptor
FCS	Feotal Calf Serum
FX	Blood Coagulation Factor 10
GFP	Green Fluorescent Protein
GM-CSF	Granulocyte Macrophage Colony Stimulating Factor
gp	Glycoprotein
HDL	High Density Lipoprotein
HEK	Human Embryonic Kidney Cell Line
HeLa	Henrietta Lacks Cell Line
HEPES	4-(2-hydroxyethyl)-1-piperazineethanesulfonic acid
HEV	High Endothelial Venules
HO	Heme Oxygenase
HPETE	Hydroperoxyeicosatetraenoic Acid
HSPG	Heparin Sulphate Proteoglycans
HSV-TK	Herpes Simplex Virus-1 derived Thymidine Kinase
ICAM	Intracellular Adhesion Molecule
IFN	Interferon
IL	Interleukin
Iono	Ionomycin
IRES	Internal Ribosome Entry Site
L	Ligand
LDL	Low Density Lipoprotein
LFA	Lymphocyte Function-Associated Antigen

LN	Lymph Node
LPS	Lipopolysaccharide
LTA	Lymphotoxin Alpha
MACS	Magnetic-Activated Cell Sorting
MCP	Monocyte Chemotactic Protein
MCS	Multiple Cloning Site
M-CSF	Monocyte-Colony Stimulating Factor
MFI	Mean Fluorescence Intensity
MHC	Major Histocompatability Complex
MMP	Matrix Metalloproteinase
MOI	Multiplicity of Infection
MPLSM	Multi Photon Laser-Scanning Microscopy
MPO	Myeloperoxidase
MRI/MRA	Magnetic Resonance Imaging/Angiography
OCT	Optical Computed Tomography
ODN	Oligonucleotides
OVA	Ovalbumin
oxLDL	Oxidised Low Density Lipoprotein
PAMPS	Pathogen-Associated Molecular Patterns
PDGF	Platelet Derived Growth Factor
PE	Phycoerythrin
PFU	Plaque Forming Unit
PGK	Phosphoglycerate Kinase
pLN	Popliteal Lymph Node
PMA	Phorbol 12-Myristate 13-Acetate
R	Receptor
RA	Rheumatoid Arthritis
RANTES	Regulated and Normal T cell Expressed and Secreted
RBC	Red Blood Cell
RNA	Ribonucleic Acid
RPMI	Roswell Park Memorial Institute

scFV	Single Chain Variable Fragment
SCID	Severe Combined Immunodeficiency Disease
SEM	Standard Error Mean
SFFV	Spleen Focus Forming Virus
SPECT	Single Photon Emission Computed Tomography
SSC	Side Scatter
Tbet	T-box Expressed in T cells
TCR	T Cell Receptor
TGF	Transforming Growth Factor
Th	T Helper Cell
TIMP	Tissue Inhibitor of Matrix Metalloproteinases
TLO	Tertiary Lymphoid Organ
TLR	Toll-Like Receptor
TNF	Tumor Necrosis Factor
T-Reg	T Regulatory Cell
USP	Ultra Small Particles
UV	Ultraviolet
VALT	Vascular Associated Lymphoid Tissue
VCAM	Vascular Cell Adhesion Protein
VEGF	Vascular Endothelial Growth Factor
VLA	Very Late Antigen
VP	Viral Particle
VSV	Vessicular Stomatitis Virus
WT	Wild Type
WTD	Western Type Diet

Chapter 1: Introduction

1.1 Aims/General introduction

Atherosclerosis is defined as a progressive narrowing and thickening of the arterial wall due to the uptake of lipid molecules used to transport cholesterol from the liver to the tissues of the body [1] and is considered the main cause of cardiovascular disease (CVD).

Death rates in the UK from CVD are among the highest in the world, the majority of which comprising of coronary heart disease (CHD) and stroke, with heart disease killing 94,000 and stroke killing around 53,000 people in the UK alone each year (British Heart Foundation 1961-2011 and Stroke Association statistics 2009). In recent decades our understanding of the mechanisms involved in atherosclerosis has progressed significantly and the importance of inflammation at all stages of atherosclerotic plaque formation and development is now accepted [2]. As a result of this the immune system is now viewed as a possible novel target for prevention and treatment of CVD [3, 4] and in this thesis; T cells are suggested as a primary target to which therapeutic manipulation can be used. The significance of T-cell activity in atherosclerosis has been previously demonstrated in several ways. These studies have observed a reduction in the plaque formation in immune deficient mice [5], such as those with an absence of a specific subtype of T cell (Th1) [6] and aggravation of disease following reconstitution with T cells [5], All this supports the hypothesis that T cells have a key role in the pathology but also that they may localise to atherosclerotic vessels. As such they provide a potential vehicle to deliver therapeutics. The proposed method described in this thesis to utilize the T-cell as a therapeutic agent is via the use of gene therapy, a rapidly developing area of research particularly in the field of CVD. It is proposed that T-cells, moving to the inflamed vascular wall, would be ideal candidates for targeted delivery of therapeutic genes/agents. These therapeutic molecules will be inserted into the genome of the T cell by way of viral transduction and these molecules would be produced at areas

where the T cells reside, such as the atherosclerotic vessel. This thesis will discuss in greater detail atherosclerosis, the T-cells involvement in the disease and also the subject area of gene therapy, addressing the aims and results of the study.

1.2 Atherosclerosis

Atherosclerosis is defined as a progressive thickening and hardening of arterial walls due to the accumulation of fatty deposits such as cholesterol. It is a condition which develops gradually throughout the individual's life consisting of plaques forming in the walls of the large and medium sized arteries. These plaques are most prevalent at bifurcations in the arterial tree which is thought to be due to the turbulent blood flow at these sections of artery, creating hemodynamic strain upon the vessel wall. Plaque formation is driven by the uptake of cholesterol and fatty acid containing transport molecules into the vessel walls, this forming the core of the plaque itself along with cell debris, a large number of inflammatory cells and a covering "cap" of activated smooth muscle cells [7].

Although most developing atherosclerotic plaques do not cause any clinical symptoms the gradual thickening and in certain cases total occlusion of the artery, caused by the formation of a thrombus, can lead to acute ischemia in the dependent capillary beds and end organs such as brain or heart [8]. The area in which this occlusion occurs can affect which clinical symptoms develop, for example an occlusion of the coronary artery delivering blood to the heart can result in angina and myocardial infarction, an occlusion in the carotid artery leading to the brain can cause a transient ischemic attack or stroke whereas an occlusion in the lower limbs can result in gangrene. All of these are common clinical symptoms found in very high numbers throughout the world, particularly in Western societies.

1.3 Development of atherosclerosis

Atherosclerosis begins at a very young age and to a certain extent is a regular occurrence even in healthy individuals and is the result of the uptake of low density lipoprotein (LDL) from the blood into the sub-endothelial wall of the artery [9]. LDL is used by the body to transport cholesterol and fatty acids to various areas of the body, the cholesterol forming an integral component in the membrane stability of all cells and the fatty acids being stored in adipose tissue for use as an energy source. Following absorption into the vessel wall it can be re-introduced into the blood stream via a system based on high density lipoprotein (HDL) in which it is transported back to the liver and away from the tissue. It is when this absorption of LDL into the vessel wall reaches a critical point, in cases of hyperlipidemia, the very early stages of plaque formation begin. The process by which LDL enters the tunica intima is assisted by proteoglycans located in the extracellular matrix which bind to Apolipoprotein B molecules found on the LDL particles [10]. In the blood, LDL is protected from enzymatic degradation however, when it is taken into the intima it is subject to several types of oxygen radical and oxidising enzymes constitutively present in the tissue. The actions of these alter the lipid and protein composition of the LDL molecule resulting in it becoming oxidized, this new molecule being termed oxLDL [11]. In the vessel wall resides a tissue resident and also blood monocyte derived member of the innate immune system, the macrophage, who's role it is to sample areas of the surrounding tissue phagocytosing old cellular debris or molecules, including oxLDL, and also to ingest invading pathogens for destruction and later, presentation to the adaptive division of the immune system. The phagocytosis of the oxLDL particles found in the intima is triggered by a family of patter-recognition receptors termed scavenger receptors which recognize molecular patterns on the surface of the modified lipoprotein, these receptors also binding lipopolysaccharides, fragments of parasites and remnants left over from cellular apoptosis [12]. Under

hypercholesterolemic conditions the cholesterol contained within the LDL particles accumulate in the cytoplasm of the macrophage forming large droplets and transforms the macrophage into what is termed a foam cell, one of the most abundant forms of the immune cell found within the plaque. These foam cells give the vessel a discoloured off white to yellow appearance, this being termed a fatty streak which is often defined as the first visible signs of atherosclerosis [13]. Gradually as the foam cell is unable to digest and unload the cholesterol and fatty acids within its cytoplasm the cell will apoptose thus releasing these components back in to the intima creating lipid pools, these dead cells forming a necrotic core often found at the centre of plaques [14]. In a study to observe the effects of turning off this scavenger duty of the macrophage, therefore stopping ox-LDL uptake, it was found that if ox-LDL is left free within the intima it is capable of causing a more detrimental effect to the tissue than the production of foam cells [15] thus indicating the importance of the scavenging by the tissue resident macrophages.

The presence of oxLDL within the intimal layer promotes the influx of immune cells in 2 main ways. First is by the oxLDL particle itself as upon oxidation certain phospholipids are released which are able to activate the endothelial cells causing them to express the vascular adhesion molecules VCAM-1, ICAM and LFA [16]. The second is from the macrophage. After it has engulfed the oxLDL molecule it itself will release chemical signalling molecules such as cytokines and chemokines whose role is to attract further cells of the immune system to aid in dealing with the oxLDL, these molecules also activate the endothelial cells of the vessel and induce adhesion molecule expression [17]. It is on monocytes and lymphocytes circulating in the blood that the corresponding “counter receptor” for VCAM-1 is expressed, very late activation antigen 4 (VLA-4) [18] and thus binding between the two occurs which results in influx into the vessel wall. VCAM-1 expression can be further influenced by the additional hemodynamic strain present at these bifurcation points in the arterial tree

[19]. With regards to purely monocyte recruitment, upon arriving at the site of LDL accumulation these cells are acted upon by the cytokines and chemokines released by both macrophages and the surrounding smooth muscle cells, an example of which is macrophage colony stimulating factor (M-CSF), which promotes the differentiation of the monocytes into macrophages to help digest the oxLDL within the tissue. These monocytes upon receiving alternative chemical signals may also differentiate into dendritic cells (DCs), the role of which will be discussed later.

As mentioned previously, the area of plaque formation also contains many cells of the adaptive immune system [7] including a high number of T cells, a cell very important in the direction and coordination of the immune system and also memory responses to secondary exposures. As in accordance to the clonal expansion theory regarding T cell activation, the only method in which a T cell can become activated is by an antigen presenting cell (APC), presenting captured and digested pathogens/antigens specific to that particular T cell. This then activates the cell and induces the expression of adhesion molecules, such as VLA-4 allowing movement into the vessel wall via VCAM-1. It is important to note that the location in which this antigen presentation occurs is not known, e.g. if it occurs in a draining lymph node or if it occurs on site in the tissue as there has been no conclusive evidence of for either theory. To which antigen the adaptive response is reacting against has yet to be fully elucidated but there is evidence indicating oxLDL, endogenous heat shock protein 60 (HSP 60) [20] and also certain microbial components such as *Strep. Pneumonia* [21], suggesting molecular mimicry comes into play. As the T cell has now become activated and has migrated to the vessel wall, it then acts to fully activate the macrophage via cytokines such as IFN-γ, allowing a respiratory burst from the cell, the result of which is an increase in digestive peptides and enzymes and also generation of radicals e.g. superoxide and nitric oxide.

As the influx of immune cells and accumulation of lipid pools and foam cells increases within the plaque, secreted molecules promote migration of smooth muscle cells from the medial layer to move to under the endothelial layer in order to strengthen the cap of the forming plaque. The stability of the plaque lies in its ratio of smooth muscle cells to lipid core volume, the higher the smooth muscle cell population and lower the lipid level results in a stronger cap and a more stable plaque of which the reverse is true for unstable plaques. There is a constant balance between the events and signalling molecules of the immune reaction occurring in the plaque and also the signalling molecules released by activated smooth muscle cells located in and around the plaque. Collagen confers the majority of the strength of the plaque, its quantity dependant on both its production by smooth muscle cells and its digestion by the metalloproteinases involved in the inflammatory response. TGF-ß and PDGF are factors released by platelets activated at the area of atheroma which promote this collagen synthesis, which lend to a more stable plaque [22]. IFN-γ produced by the inflammatory response, specifically activated Th1 cells, strongly inhibits the production of interstitial collagen [23] thus resulting in poorer plaque stability. Degradation and erosion of the plaque fibrous cap is caused either by the immune reaction taking place within the plaque or due to physical factors such as hemodynamic strain on the vessel wall related to hypertension, allowing the material from the inflamed plaque core to be exposed to the blood. The core contains molecules which promote both platelet activation and clot formation, with platelets adhering to the ruptured plaque, aggregating and forming a small thrombus [24]. When coagulation factors bind and clot here, the thrombus grows rapidly and within minutes it can fill up the lumen of the vessel locally stopping the blood or it can embolize, the consequences of which are discussed later.

The way in which we study atherosclerosis is by using the apolipoprotein E $(ApoE)^{-/-}$ mouse. This mouse has been genetically altered so that the ApoE

molecule found on the molecules transporting cholesterol and lipid is deleted. This protein has an important role in the uptake of these transport molecules into the liver, especially LDL, and therefore as the molecules are not being absorbed by the liver the blood concentration of the cholesterol and fatty acids increases significantly encouraging high levels of LDL entry into the vascular tissue. The result is a mouse model which is capable of developing fatty streaks from the age of around 12 weeks. Although the pathology in humans and in mice has certain differences, the model allows us to observe atherosclerosis progression on a timescale more usable for our research needs.

1.4 Animal models of atherosclerosis

The study of CVD and in particular atherosclerosis is a complex, multi-faceted task requiring the examination of several disciplines and factors within the vessel wall and also systemically. Animal models of the disease offer the most complete tool for this task, allowing the measurement of several inter-connected variables. Mice are the most commonly used animal for the study of atherosclerosis however mice and humans differ in several areas that may influence atherogenesis. Lesions in humans occur primarily in the carotid, coronary and outermost blood vessels where as lesions in mice tend to form in the aortic root and aortic arch, however many of the critical features of atherogenesis are the same therefore allowing us detailed insight into the pathology, while allowing unique genetic modifications, therapy applications and the study of the disease over a reasonable time frame [25].

Larger animals are generally more expensive to purchase, maintain and feed than their smaller counterparts and the development of atherosclerosis tends to involve a longer time frame however, certain large animal models have certain advantages. Pigs will naturally develop atherosclerosis similar to humans which can be augmented using an atherogenic diet [26-28] and have vessel large enough to allow for noninvasive measurements of the vessels and allows for biopsies to be taken for analysis. Pigs also have a similar lipid profile to humans and develop lesions in generally the same arterial regions as humans [29] and at arterial bifurcation points [30]. Rabbits represent a species which are more sensitive to changes in dietary cholesterol levels [31] and share some of the same advantages as pigs, with the advantage of being cheaper. Rabbits have proven most useful in the study of lipid profiles such as familial hypercholesterolemia [32] and the study of different dietary fats on plaque [33]. The final large animal commonly used for atherosclerosis studies is the non-human primate. Non-human primates have all the experimental

advantages of having humanoid lipoproteins, including subclasses and also lipoprotein metabolism. Males tend to develop more atherosclerosis than females on a high fat diet which also mimics the human pathology [34-37]. As is true for all these large animal models, the size, upkeep, length of time required for pathological development and the lack of genetic modification have limited their usage for atherogenesis research.

Although there are several advantages to using larger animals, the mouse remains the favoured species due to its cheapness, ease of genetic manipulation and relative rapid atherogenesis. Genetic manipulation has played a major role in the dissection of the cellular and molecular mechanisms involved, in particular, with the role of the immune system in atherosclerosis. The ease and turnaround of breeding for mice allows for the modification of more than one gene in a single animal model, allowing fast cross breeding of transgenic strains, therefore offering a range of experimental opportunities. The 2 main models for atherosclerosis in use today are the $ApoE^{-/-}$ and low density lipoprotein receptor $(LDLr)^{-/-}$ models.

The $ApoE^{-/-}$ strain lacks the apolipoprotein E molecule, a class of apolipoprotein found in the fat and cholesterol transport molecules, chylomicrons and intermediate-density lipoproteins (IDLs) which binds to receptors on liver cells, resulting in the uptake of these molecules. The deletion of the ApoE molecule results in higher blood cholesterol and triglyceride levels which goes on to induced atherogenesis [38]. These lesions are comparable to human lesions and also develop spontaneously when fed on a normal “low-fat” diet, with lesion formation being significantly accelerated by the feeding of a high fat, high cholesterol Western type diet (WTD) [39]. Lesions formed while on the high fat diet do have a slightly different composition from those on no diet, mainly in the form of raised foam cell levels and lower lesion complexity [40]. In addition to altered lesion composition, the diet that the $ApoE^{-/-}$ strain are consuming can give differing experimental outcomes [39, 41]. Lesions will

form in the aortic root, brachiocephalic artery, main aortic tree, carotid and pulmonary arteries, with visible lesion development from around week 8 in high fat diet fed mice and 12 weeks on low fat diet fed mice. A disadvantage of using the $ApoE^{-/-}$ model is that the ApoE molecule has also been shown to have other functions affecting macrophage behaviour, immune function and adipocyte composition [42] which could all have an impact on the development of atherosclerosis independent of plasma cholesterol levels.

One of the advantages the $LDLr^{-/-}$ model has over the $ApoE^{-/-}$ is that the LDLr does not have these additional functions as described for ApoE. In a similar manner to $ApoE^{-/-}$, the deletion of LDLr results in increased circulating levels of LDL, a molecule highly indicated in atherosclerosis. Unlike $ApoE^{-/-}$ mice, significant lesion development relies on a high fat atherogenic diet [43, 44], which unfortunately means that as a variety of different diets with varying compositions are used, studies with this models are not often standardised and therefore hard to compare between studies. Lesions in these mice have a higher level of foam cell accumulation than standard diet fed $ApoE^{-/-}$ although the development of lesions in these mice has not been characterised to the same extent as with $ApoE^{-/-}$ mice. Neither the $ApoE^{-/-}$ or $LDLr^{-/-}$ models present lesion development in the coronary arteries however more complex models, such as an $ApoE^{-/-}$ scavenger receptor SR-B1 deficient mouse model develop obstructive coronary lesions resulting in myocardial infarction [45], a model more closely resembling human pathology.

1.5 Atherosclerosis as an inflammatory disease

Traditionally, atherosclerosis was thought to be a lipid related disease, based on strong clinical data and experimental data at the time between atheroma formation and hypercholesteremia [46]. Over the past two decades, however, it has come to be appreciated that there is a prominent role for inflammation in atherosclerosis and its associated complications. Although evidence supports the involvement of the immune response in a systemic nature towards hyperlipidemia [47, 48], a considerable amount of recent data suggests that a highly local immune response developing within the vessel wall itself may be of key importance [40, 49-51]. A range of both innate and adaptive elements are involved in the chronic response and their respective secreted molecules, some of which are discusses below.

1.6 Cellular components of the immune system involved in atherosclerosis

1.6.1 Monocytes

The precursor parent cell of both DCs and macrophages is the monocyte which circulates within the blood and differentiates into an effector cell (DC, macrophage) upon reaching tissue [52]. This homing of tissue is better understood in the context of atherogenesis due to the upregulated adhesion molecules and various signals from the damaged artery wall and immune cells, which act to promote further immune cell influx. In the context of a homeostatic method of homing, the mechanisms are less understood. Infiltration into inflamed tissue occurs in a P-selectin dependent manner, with L-selectin also aiding in monocyte endothelium rolling [53]. This rolling is followed by tight binding of VCAM-1, with chemokines/chemokine receptor interaction providing the directional signals for inter-tissue migration [53]. The monocyte will then differentiate

into a DC or macrophage depending on the conditions present within the tissue. Interference with monocyte recruitment to the vascular wall results in significant attenuation of the pathology [54-56], most likely due to the pivotal role that macrophages and DCs go on to play in the initiation and development of pathology.

1.6.2 Macrophages

Macrophages were identified to be one of the main components of atherosclerosis in some of the first studies on atherosclerosis in 1979 [57]. Their main function, in the context of atherosclerosis, is to scavenge the high levels of oxLDL found in the vessel wall, and re-circulate it back to the liver. These cells, found in the centre of forming plaques, express a range of receptors allowing for a duel role. They act as a scavenging cleaner of a variety of cellular debris and waste via scavenger receptors (SR) and also serving as a link between the innate and adaptive branches of the immune response via their expression of toll-like receptors (TLRs), which recognise pathogen associated molecular pathogens (PAMPS) [58]. Under normal conditions LDL transports cholesterol and fatty acids through the vessel wall to tissues around the body where it is used in a variety of ways, cell structure, energy storage etc. When the balance of influx and efflux of the LDL molecules is dysregulated, such as in cases of hypercholesterolemia, macrophages are required to absorb the excess levels of LDL within the vessel wall in an attempt to remove the oxLDL from the vascular tissue. The macrophage is capable of releasing the collected cholesterol again by way of ATP-binding cassette transporters (ABCA1/G1) to HDL molecules which then move the cholesterol back to the liver. Deficiency of these transporter molecules results in acceleration of atherosclerosis [59] and upregulation of enzymes aiding in this cholesterol efflux reduces plaque formation [60]. If the efflux of cholesterol and fatty acids is overwhelmed by the uptake by the macrophage, the macrophage becomes lipid laden,

and changes the morphology of the cell giving them the name foam cells. Both the M1 and M2 phenotypes of the macrophage are present within the plaque although they play opposite roles during inflammation. The M1 macrophages, induced by classical activation, release pro-inflammatory cytokines whereas M2 macrophages differentiate in the presence of IL-4, IL-13 or Vitamin D3 and release IL-10 thus implying they have a diverse role in the development of the pathology, not only pro-atherogenic [61].

Macrophages are present in both early and late stage atherosclerosis and are accepted to be fundamental to atherogenesis and plaque persistence; however the exact role of these cells in atherosclerosis is somewhat contentious. *In vitro* studies have shown that low ratios of macrophage to smooth muscle cells results in smooth muscle cell proliferation whereas higher ratios of macrophage to smooth muscle cells induce macrophage based smooth muscle death [62]. Macrophages are also able to promote the synthesis of new matrix components from smooth muscle cells but at the same time, release matrix metalloproteinases (discussed later) which degrade the extracellular matrix [63, 64]. The inhibition of their lipid scavenging role using SR KO mice with atherosclerosis has shown both a pro and anti-atherogenic role [15, 59]. Work carried out by Victoria Stoneman et al [65], used diphtheria toxin receptor transgenic mice to delete macrophages at different stages of atherosclerosis, finding that removal of macrophages at the early stages of atherosclerosis had a protective effect however deletion in mice with more developed atherosclerosis had minimal effect. Further work will be required to fully elucidate what role or roles macrophages play in atherosclerosis, with current data suggesting a slightly more convoluted role than first perceived.

1.6.3 Dendritic cells

Vascular dendritic cells (DCs) were discovered to be present in healthy arteries within the intimal layer in areas of plaque susceptibility [66], although their functional role in these prone arteries is largely unknown. Numbers of DCs found within atherosclerotic arteries is significantly higher than that of healthy vessels, the rise in number likely being the result of increased influx into the area with reduced efflux to secondary lymphoid structures. The classical role of this cell within the immune system is as a professional APC. The prime task of the DC is to uptake foreign molecules and present elements of these to cells of the adaptive immune system found in the draining lymph nodes of that particular tissue and therefore inducing the development of an adaptive immune response. Whether vascular DCs also present antigen in the context of atherosclerosis has not been yet been confirmed although if these DCs are isolated from aortic segments they are capable of presenting antigen as well as their bone marrow derived family members [40]. Vascular DCs have been found to be in close proximity to T cells, releasing chemokines which may play a role in the further recruitment of lymphocytes from the blood to the inflamed artery, this proximity implying possible antigen presentation. It is thought that DCs play a pro-atherogenic role due to their key role in the adaptive immune response. The clustering of T cells and DCs in the shoulders of vulnerable plaques have been shown to have upregulated co-stimulatory and activation markers [67] and this has been correlated with plaque destabilisation [68], as has been found in patients with angina [69]. In addition to promoting cell influx and activation, activated dentritic cells in the vessel have also been shown to inhibit the activity of the anti-atherogenic Treg cells [70]. There is also evidence for intimal resident DCs to become foam cells like their macrophage counterparts [67]. As the typical role of DCs differs from macrophages it could be that they retain their characteristics of antigen presenters and play a role in the initiation of atherosclerosis through presentation of ingested lipids. Human studies

have shown that higher densities of DCs were found in unstable plaques compared to stable [68, 71] which suggests that the presence of DCs in the vessel wall is associated with the progression of atherosclerosis and plaque instability. A study which extended the lifespan of DCs through over-expression of the anti-apoptotic gene hBcl-2, was actually associated with lower serum cholesterol levels and no acceleration of atherosclerosis [72], suggesting not only a pro-atherogenic role for this cell type. Converse to this, depletion of DCs using a diphtheria toxin ApoE$^{-/-}$ model resulted in enhanced hypercholesterolemia, indicating a close relationship between DCs and cholesterol levels [72], a finding further supported in similar depletion studies [73]. Taken together it is clear that DCs play an important role in atherosclerosis and represent a key link between lipid accumulation and immune activation, however what their role or roles are, are not yet clear.

1.6.4 Mast cells

Normally involved in allergy and mucosal immune responses, mast cells are also found at the site of plaque formation [74], especially in the location of rupture prone shoulder regions. If activated mast cells are capable of releasing a range of preformed or newly made mediators ranging from cytokines to enzymatic complexes such as proteases, it being these proteases that possibly lend to the destabilisation of the plaque. It has been shown that activation of these vascular mast cells correlates with intraplaque hemorrhage, macrophage and endothelial cell apoptosis and also further recruitment of immune cells into the arterial wall [75]. Cytokines released from mast cells have also been implicated in destabilisation, namely IFN-γ and IL-6, which have a role in promoting cysteine protainase cathepsin production and matrix metalloproteinases (MMP) [76], both of which lend to destruction of the vascular tissue, altering the before mentioned balance of tissue healing and the immune

system breakdown of extracellular matrix components. Atherosclerotic mice deficient in mast cells ($Kit^{W\text{-}Sh/W\text{-}Sh}$ /$LDLr^{-/-}$) show reduced local inflammation and plaque immune cell content but also increased levels of strengthening collagen and larger fibrous cap, therefore mast cells are presumed to have a detrimental role in atherosclerosis.

1.6.5 NKT, NK and Neutrophils

Natural Killer T cells (NKT cells) are innate-like T lymphocytes that recognize glycolipid antigens in the context of the MHC class I-related glycoprotein CD1d, found on DCs, as opposed to peptide based antigens. The reaction of these cells to the modified lipids within the plaque may have a large impact on the inflammatory response with NKT cells role being shown as being of a proinflammatory nature. $CD1d^{-/-}$/$ApoE^{-/-}$ have decreased lesion size of up to a quarter and if an agonist of the CD1d receptor is injected into an $ApoE^{-/-}$ mouse, it induced a 50% increase in atherosclerosis [77], suggesting a proatherogenic function.

Although for both these cell types more defined study into their roles is needed, natural killer (NK) cells and neutrophils are also present within the plaque area. Due to complications in developing a NK knock out mouse model, it is unclear what the role of these cells is. Absence of fully operating NK cells appears to reduce atherosclerosis although interference from the above mentioned NKT cells may have a role in this affect [78]. Neutrophil effects can be seen when blocking their efflux (CXCR4/CXCL12 dependent) thus inducing neutrophilia within the plaque, which is associated with increased apoptosis and a proinflammatory phenotype. This evidence suggests that neutrophils have a pro-inflammatory role in atherosclerosis with the likelihood being that they promote plaque instability.

1.6.6 B cells

B cells can be found in both the adventitia and within the plaque itself. In response to a pathogen, activated B cells form germinal centres with T cells (discussed later) which have also been activated to the same pathogen. Following events that develop within this germinal centre reaction, B cells generate antibodies to the specific pathogen which then move into systemic blood circulation, binding to the pathogen and aiding in its elimination. If B cells are depleted during atherosclerosis development, there is an increase in lesion size along with a decrease in the production of anti-oxLDL antibodies [79]. If B cells are transferred from aged $ApoE^{-/-}$ mice into young $ApoE^{-/-}$ mice induced a reduction in atherosclerosis [80], therefore suggesting that during the advancement of atherosclerosis, an atheroprotective immune response develops and it is B cells that are responsible for this, possibly through anti-oxLDL antibodies. There are conflicting and as of yet unanswered questions relating to how exactly B cells induce this anti-atherogenic response. Antibody producing cells can be subdivided into B1 and B2 cells, the latter being the subtype involved in a classical pathogen response, residing in the secondary lymphoid organs. The B1 subset of B cells produce “natural antibodies” which are of the IgM antibody subset and are found in the peritoneal and pleural cavities [81]. These B cells do not develop into memory cells at any point and continually produce broad specificity polyspecific IgM antibodies to self antigens, microbial peptides and viral infections. It is these B1 antibodies specific for oxLDL that recognise oxidised phospholipids from the ox-LDL molecule and can block binding and degradation of ox-LDL by macrophages *in vitro* [82]. Very little is known about B cells present in the secondary lymphoid organs in atherosclerotic mice and also the possible role of locally produced antibodies. The presence and apparent atheroprotective nature of antibodies drives the possibility of developing a vaccination towards the ox-LDL molecules, therefore producing a protective immune response for heart disease and stroke. Studies looking at vaccination have shown that a

protective response is indeed generated although the mechanisms of how exactly this works are still undefined [83]. Although the bulk of literature points towards a completely anti-atherogenic role for B cells and the resultant antibodies, some studies have shown that reducing the activation of B cells [84] or depleting their levels [85], reduces atherosclerosis. As with nearly all aspects of the immune systems involvement in atherosclerosis, the exact role of B cells is unclear.

1.6.7 T cells

T cells are the main cellular component of the inflamed atherosclerotic wall and play a pivotal role in the development and persistence of the pathology. This cell type is covered later in this thesis.

1.7 Cytokine involvement in atherosclerosis

1.7.1 TNFα

Tumor Necrosis Factor (TNF-α) is produced mainly by macrophages but also by a range of cells such as T cells, mast cells and endothelial cells. It is involved in systemic inflammation which effects a range of immune cells and has the capability to induce cell apoptosis, inhibit viral replication, tumor advancement and also to promote a pro-inflammatory immune response [86]. Absence of TNF-α from an $ApoE^{-/-}$ mouse can result in a decrease in lesion size also seemingly inducing the decease of adhesion molecule expression, VCAM-1, ICAM-1 and CCL2 [87]. More recently it has been shown that TNF-α affects the development of atherosclerosis at the fatty streak stage as opposed to sustaining more mature plaques [88].

1.7.2 Interleukin 12 (IL-12)

Interleukin 12 is classically released by DCs and macrophage in response to uptake and stimulation by antigen. It is involved in the development of naïve T cells into their respective effector/memory subset, and induces the production of interferon-γ (IFN-γ) and TNF-α mainly from T cells. IL-12 is found within atherosclerotic vessels of $ApoE^{-/-}$ mice and the addition of further IL-12 enhances lesion size [89]. Mice deficient for the p40 subunit of IL-12 ($IL12b^{-/-}/ApoE^{-/-}$) display a reduction in plaque size of up to 52% at 35 weeks but not at 45 weeks of age [90]. Together these two results support the view that IL-12 is proatherogenic.

1.7.3 IFN-γ

IFN-γ plays a critical role in both the innate and adaptive immune response. Following on from antigen presentation and IL-12 release via macrophage or DC, IFN-γ is produced by T cells, showing a range of biological activity. IFN-γ can permit full activation of macrophages, inducing upregulation of enzymatic activity allowing for use of reactive oxygen species to destroy phagocytosed pathogens. IFN-γ can also cause non-immune cells to upregulate class 1 MHC molecules which present internal cellular peptides, thus aiding in anti-viral responses [91]. Addition of IFN-γ to $ApoE^{-/-}$ mice accelerates atherosclerosis [92], conversely IFN-γ receptor deficient mice show a decrease in pathology[23]. IFN-γ also seems to play a role in late stages of atherosclerosis in that inhibition of its activities can reduce the size of plaque and stabilize its internal composition [93]. These results show that IFN-γ is a without doubt a proatherogenic cytokine.

1.7.4 Interleukin 4 (IL-4)

IL-4 is traditionally a cytokine which induces the development of Th2 cells as opposed to the IL-12 induced Th1. In context of a response to a pathogen, it is though that IL-12 and IL-4 compete in a manner as there is normally competition for numbers between Th1 and Th2, often when one subsides the other can expand. It would therefore be fair to assume that as atherosclerosis is a Th1 based pathology that IL-4 would possibly have an anti-atherogenic effect. This is not the case as neither deficiency or exogenous addition of IL-4 appears to have any effect on $ApoE^{-/-}$ mice fed on a high fat diet [94]. There is evidence from a long term study of $IL\text{-}4^{-/-}$ $ApoE^{-/-}$ mice on a high fat diet showing a reduction in plaque size at weeks 30-45 [90] which may indicate an anti-atherogenic role for IL-4 however more clarity is needed.

1.7.5 Interleukin 33 (IL-33)

IL-33 invokes its actions on atherosclerosis development through binding of the ST2 receptor, found on Th2 cells. Although this ST2 receptor is a member of the IL-1 (pro-inflammatory) receptor family, signalling through it induces a shift towards a Th2 response and away from the proatherogenic Th1. IL-33 administration can significantly reduce atherosclerosis by mechanisms involving this shift away from a Th1 dominated response to a Th2 response, identified as a in increase in IL-4, IL-5 and IL-13 production along with a decrease in IFN-γ. The resultant increase in Th2 levels may be responsible for production of anti-oxLDL antibodies thus further aiding in decreasing plaque development [95]

1.7.6 Interleukin 10 (IL-10)

IL-10 is a well known anti-inflammatory cytokine which is mainly expressed in monocytes and Type 2 T helper cells (Th2), mast cells, CD4+CD25+Foxp3+ regulatory T cells, and also in a certain subset of activated T cells and B cells. It is capable of inhibiting synthesis of pro-inflammatory cytokines like IFN-γ, IL-2, IL-3, TNF-α and granulocyte-macrophage colony-stimulating factor (GM-CSF) made by cells such as macrophages and the Type 1 T helper cells and also the ability to present antigen. Low levels of IL-10 correlate with more advanced plaques and increased atherosclerosis whereas a higher level of IL-10 is associated with decreased inflammation and therefore milder atherosclerosis [80, 96]. In IL-10 KO mice fed on an atherogenic diet it was found that lesion size was significantly increased as was IFN-γ, with decreased collagen, in comparison to a wild type mice. Intravenous delivery of IL-10 into these IL-10 KO mice induced a 60% reduction in lesion size. It was also observed that IL-10 addition at the early stages of atherosclerosis can significantly decrease fatty streaks [97]. In addition, if IL-10 production is induced in the vascular tissue through an intravenous viral vector (Adenovirus), % stenosis of the vessel decreased by 62%, serum cholesterol also decreased and monocyte deactivation was observed [98]. William Boisvert's group transplanted bone marrow from transgenic mice whose T cells secrete IL-10 (IL-10 gene linked to CD2 promoter) into LDLr null mice. It was found that these IL-10 secreting T cells induced a 47% decrease in lesion size, an 80% reduction in the necrotic core, a 50-80% decrease in cholesterol accumulation, the presence of the IgG_1 subset of antibodies which are associated with a Th2 response and a lower complexity to the plaques. In addition monocytes showed decreased activation and therefore lower levels of IFN-γ with the macrophages showing decreased apoptosis. The method of action for these significant alterations is suggested to be due to a phenotypic change in the response as it was seen that the response shifted from a Th1 to Th2 [96]. In a recent paper, *ex vivo* expanded Treg cells, a T

cell subset which naturally produce IL-10 *in vivo* to decrease inflammatory responses, were able to prevent the formation of transplant arteriosclerosis, reducing vascular inflammation and also smooth muscle neo-intimal formation [99]. This culmination of results demonstrates the anti-atherogenic properties of IL-10.

1.8 Chemokine involvement in atherosclerosis

1.8.1 MCP-1 and CCR2

Monocyte chemotactic protein-1 (MCP-1) also known as chemokine (C-C motif) ligand 2, is a chemokines which plays a role in the recruitment of monocytes, memory T cells and DCs to sites of injury and inflammation. Due to its high level of expression within atherosclerotic lesions and also due to the cell types it recruits, MCP-1/CCL2 is considered a key player in immune cells recruitment into the vessel wall [100-102]. In a number of models of atherosclerosis whereby the MCP-1 or its receptor CCR2 was deleted, the total number of macrophages decreased as did the formation of fatty lesions [103-105] as was also demonstrated in the use of gene therapies using a non-functional CCR2 for blocking MCP-1 [106, 107]. As might be expected, atherosclerotic lesions formation was accelerated in $ApoE^{-/-}$ mice following transplantation of bone marrow cells which overexpressed MCP-1 [108]. In humans, the raised levels of MCP-1 found in cases of coronary artery disease (CAD) or in patients with increased CAD risk factors, could possibly be used as a direct marker of inflammatory activity for use in early diagnosis [109].

1.8.2 RANTES, CCR1 and CCR5

RANTES (Regulated upon Activation, Normal T-cell Expressed and Secreted) aka CCL5, is chemotactic for T cells, eosinophils and basophils and plays an active role in recruiting leukocytes into area of inflammation, two receptors for which being CCR1 and CCR5. The expression of these two receptors on the surface of monocytes/macrophages and T cells combined with the raised ligand levels for these receptors (RANTES/CCL5, CCL3, CCL4) suggests a possibly considerable role for them in atherosclerosis [110-113]. It has been found that a modification/deletion to the CCR5 gene results in a reduced risk of myocardial infarct as well as severe CAD [114, 115]. Similarly blocking the receptors for RANTES with a peptide antagonist has been shown to halt lesion formation as well as leukocyte infiltration, providing a more stable plaque with higher smooth muscle cell and collagen levels [116]. Individual deletion and reconstitution via bone marrow transplant of CCR5 and CCR 1, showed that a lack off CCR5 resulted in a less inflammatory, more stable plaque [117] whereas a lack of CCR1 resulted in enhanced inflammation and lesion development [118], therefore demonstrating that CCR5 and CCR1 have opposing roles in atherosclerosis which is perhaps surprising considering that they share ligands.

1.8.3 CCR7

CCR7, also now known as CD197, is a member of the G protein-coupled receptor family and is expressed in various lymphoid tissues. It plays a large role in T cell migration in secondary lymphoid organs and more recently has been found to be involved in T cell and DC migration in non-lymphoid tissue also [119, 120]. The homeostatic chemokines CCL19 and CCL21 are the ligands for CCR7. In a clinical study increased chemokine expression was observed in the plasma of CAD patients as well as in the atherosclerotic lesion itself. It was also found that T cells found within these plaques had

enhanced CCR7 expression however in patients with angina; circulating T cells showed decreased CCR7 expression. The different developmental stages of lesions between CAD and angina patients may reflect redistribution of CCR7+ cells towards the inflammatory lesions during plaque progression [121]. In a model of atherosclerosis regression, a disappearance of foam cells from the vessel correlated with enhanced expression of CCR7 in these cells, which was supported by neutralising antibodies to CCL19 and CCL21 showing that CCR7 was required for plaque regression [122, 123].

1.8.4 IL-8 and CXCR2

Interleukin-8 (IL-8) also known as CXCL8 along with its receptor CXCR2, have an early role in the development of atherosclerosis. Oxidised LDL has been shown to induce the production of IL-8 in peripheral blood monocytes [124]. OxLDL also induces high levels of IL-8 by plaque isolated macrophages along with CXCR2 expression [125, 126]. If CXCR2 is removed (via bone marrow transplant from $CXCR2^{-/-}$ mice) in $LDLr^{-/-}$ mice, lesion size and cellular content (macrophages) inside the plaque are reduced [126]. IL-8/CXCR2s importance in lesion development, appears to come later in the pathology as opposed to early onset [127].

1.9 Enzymes involved in atherosclerosis

1.9.1 Matrix metalloproteinases and tissue inhibitor of metalloproteinases

Matrix metalloproteinases (MMPs) are a family of proteolytic enzymes which are members of the zinc dependent metzincin superfamily of enzymes. Generally, MMPs degrade various components of the extracellular matrix (ECM) with members of the MMP family including collagenases, gelatinases, stromelysins and membrane-type MMPs [128], and play an important role in vascular remodelling, cellular migration into tissue and the processing of ECM proteins and adhesion molecules [128, 129]. Inappropriate vascular remodelling plays a large role in atherosclerosis with direct implications on structural integrity and strength of the inflamed vessel. It has been found that the shoulder regions and regions of foam cell accumulation, local increased in MMP-1 stromelysin and MMP-9 can clearly be seen along with increased gelatinase activity, whilst in normal uninflamed arteries MMP and TIMP levels appear uniform [130]. In addition, overexpression of MMP, leads to further instability and hemorrhage in atherosclerotic lesions [131]. Immune cells also produce MMPs [132, 133] in order to facilitate their entry into tissue and can induce local tissue MMP expression through their pro-inflammatory cytokines. The high numbers of immune cells which accumulate at the site of plaque formation [40] may be a major source for these focal areas of MMP production. Under normal physiological conditions, MMP production is controlled at the transcriptional levels, modification of their pro-forms or zymogens and interaction with ECM components. In addition there are a family of counter MMP enzymes that play an important role in controlling high MMP levels. Tissue inhibitors of metalloproteinases (TIMPs) are specific endogenous inhibitors that bind MMPs with 4 TIMPs (1-4) having been identified in mammals. With the exception of TIMP-1 and membrane type 1 MMP, TIMPs inhibit all MMPs [134] and do so by wedging themselves into the active-site of the enzyme, replacing the substrate. It has been shown that overexpression of TIMP-2

can inhibit plaque growth and destabilisation, the effects of which are thought to be from modulation of macrophage behaviour [135], with similar effects being observed with TIMP-1 overexpression [136], suggesting TIMP based gene therapy as a future tool for treatment [137]. Careful testing of these MMP inhibitors is necessary to show that they have no adverse affect on angiogenesis [138], however results from MMP specific treatments are promising.

1.9.2 Lipoxygenase

The 5-lipoxygenase (5-LO) pathway is responsible for the production of the inflammatory mediators, leukotrienes, from membrane sourced arachidonic acid. These lipid mediators, designated LTA_4, B_4, C_4, D_4, E_4 and F_4, have a role in innate immunity such as chemotaxis [139] and increased phagocytosis [140] but have recently been shown to play a proatherogenic role [141], the expression of 5-LO and leukotriene A_4 hydrolase in atherosclerotic vessels correlating with plaque instability. 5-LO deficient $LDLr^{-/-}$ mice show a significant decrease in lesion size with macrophage 5-LO being chiefly responsible for atherogenesis [142].

12/15- lipoxygenase is a nonheme iron-containing dioxygenase which forms 12-hydroperoxyeicosatetraenoic acid (HPETE) and 15-HPETE from arachidonic acid which oxidise fatty acids in lipoproteins and phospholipids [11]. Based on the products, the enzyme is classed as 15-LO in humans and rabbits and 12-LO in pigs, rats and mice. In 12/15-LO deficient $ApoE^{-/-}$ mice, 12/15-LO has been found to have a proatherogenic effect, seemingly not only to have an effect on lipid peroxidation but also decreased oxLDL antibody levels suggesting a role in modifying the adaptive immune response [142]. Overexpression of this enzyme leads to an increase in fatty streak lesions [143], with its expression by bone marrow-derived cells being shown to be responsible for these proatherogenic properties [144].

Interestingly, rabbits overexpressing human 15-LO showed reduced lesion size which may be due to the range of 12/15-LO products, some pro and others anti-inflammatory [145].

1.9.3 Heme (Haem) Oxygenase-1

Heme (Haem) oxygenase (HO) is the catalytic enzyme which affects the rate limiting step in haem catabolism, haem being a prosthetic group that contains an iron atom at the centre of a porphyrin ring, mainly associated with haemoglobin. In the context of atherosclerosis, HO-1 induction reduced the chemotaxis of monocytes [146] and it's absence in HO-1 deficient $ApoE^{-/-}$ mice aggravated atherosclerosis with production by macrophages again being implicated in the process [147, 148].

1.10 Imaging of the atherosclerotic vessel

Traditionally, imaging of the cardiovascular system had focused solely on anatomy, regarding stenosis levels as the main characteristic of a plaques clinical fate. More recently, the recognition of atherosclerosis as an inflammatory condition has opened the way for other markers to be studied such as the qualitative structural aspects of the plaques as well as features of inflammation, offering an array of novel imaging targets.

1.10.1 Clinical imaging techniques

In the clinical setting, the common goals of all molecular imaging techniques are to increase the speed and quality of disease diagnosis and also to provide insights and guide possible novel therapies. To perform these roles, a range of methodologies have been and are, being developed across a number of imaging platforms.

1.10.1.1 Fluorescent imaging

Clinical optical imaging methods, such as fluorescence based, can offer a high level of sensitivity. Use of multiple fluorochromes targeting different molecules offers the ability for more complex imaging, enhancing clinical insight. The basic principle behind fluorescence systems is that a fluorophore, often bound to an antibody or targeting peptide, absorbs light energy (from a laser or diode) which transfers the electrons to an excited state, the return of this electron to the ground state releases energy in the form of light of a longer wavelength. Aside from imaging immune cell accumulation [51], probes can be constructed in which the fluorescent element is only released upon enzymatic cleavage, allowing the activity of clinically relevant enzymes to be mapped e.g. MMPs [149] and cathepsins [150, 151]. Unfortunately an inherent difficulty with fluorescence imaging

is tissue penetrance, which can vary based on the fluorochrome used and also the tissue being studied. As a result these systems remain for use in the experimental field; however there is hope that with the development of fibre optic catheter mounted devices [152] fluorescence will, in the future, become a viable diagnostic tool if used in conjunction with other imaging methods e.g. Optical Computed Tomography (OCT).

1.10.1.2 Optical computed tomography

OCT, sometimes referred to as "optical ultrasound" uses reflected light, often in the infrared range, to construct real time 3 dimensional (3D) images with a sensitivity of around 10μm, filtering out scattered light which can cause "glare". Using this catheter based system produces images of high enough detail to observe the major components of the vessel such as intimal layer, tunica media, adventitia and even the elastic lamina. The ability of this system to characterise plaque components shows promise for allowing the observation of morphological changes in plaques thought to be at risk [153].

1.10.1.3 Single positron emission tomography

A high degree of sensitivity can also be reached using radionuclides, whereby the gamma radiation emitted from the radionuclide is used to form multiple 2D images/slices. Single positron emission tomography (SPECT) has previously been used to track monocytes in mouse models of atherosclerosis [154]. SPECT imaging using Fluoro-deoxyglucose (^{18}FDG) has shown the most promise in vascular tissue. FDG is taken up by cells undergoing glycolysis but is not itself broken down and instead accumulates within the cell. Accumulation in the aorta and carotid arteries has been

shown to correlate with levels of macrophage accumulation [155]. Do to the high turn over energy of the myocardium and resultant wide spread accumulation; ^{18}FDG cannot be used for imaging of the coronary artery, a clearly important target for the assessment of pathology. The lack of anatomical detail in SPECT images can be aided with its use in conjunction with either computed tomography (CT) or magnetic resonance imaging (MRI).

1.10.1.4 Magnetic resonance imaging/angiography

In MRI/MRA (magnetic resonance angiography) a powerful magnetic field is applied which acts on certain nuclei, creating a rotating magnetic field that is detectable by the scanning equipment, allowing both 2D and 3D images to be created of the sample. Unlike SPECT or fluorescent imaging techniques, MRI/MRA requires the use of contrast agents such as gadolinium [156], which provide the vessels with contrast to the surrounding tissue, or more recently ultrasmall superparamagnetic iron oxide particles (USPIO). The paramagnetic properties of the contrast agents mean that their magnetic properties are only activated when an external magnetic field is applied. These USPIO particles, approximately the same size as LDL particles, enter atherosclerotic plaques due to the inflammation induced increase in endothelial permeability, and accumulate in the atheroma [157]. A further enhancement to MRI probes, whereby gadolinium is concealed within a complex until cleavage with an endogenous enzyme takes place, have allowed for MRI imaging of myeloperoxidase (MPO), an enzyme released from activated neutrophils and macrophages and is also elevated in blood in angina and myocardial infarction [158]. However, although MRI is capable of providing excellent anatomical detail and is widely used, it but does not provide the resolution required for molecular imaging. This is true also for ultrasound techniques with the added advantage of portable and cheap apparatus.

1.10.1.5 Ultrasound

In ultrasound, soundwaves of a frequency of >20kilohertz, are fired into tissues and the reflection signature analysed. As with the tailored probes, the practicality and resolution of ultrasound has been enhanced via the use of gas-filled microbubbles such as liposomes [159]. These microbubbles produce powerful sound wave reflection and have mainly allowed ultrasound imaging of adhesion molecules associated with atherosclerotic plaques, ICAM-1 [159], VCAM-1 [160], and integrins [161].

1.10.2 Experimental imaging techniques

In the experimental field, many of the above mentioned tools are often used in a similar fashion, however, the *in vivo* or *ex vivo* setting holds certain advantages, consequently clinically unsuccessful techniques such as fluorescence based imaging can be utilised to reveal an array of information at the molecular level, such as confocal and 2 photon microscopy.

1.10.2.1 Confocal microscopy

Confocal microscopy is an imaging technique originally patented in 1957 its purpose being to overcome certain limitations of fluorescent microscopy faced at that time. In conventional fluorescent microscopy, the labelled sample is excited evenly by light from the light source (laser/diode/mercury lamp). All parts of the specimen in the path are excited at the same time which is then picked up by the microscope's photodetector, which will include a large amount of unfocused background fluorescence, resulting in decreased image quality. A confocal microscope

eliminates this background fluorescence with the use of a pinhole, the term "confocal" deriving from the pinhole being conjugate to the focal point of the lens. Only the emitted light from the sample which passes through the pinhole is measured by a detector, with all other emitted light not in focus at the pinhole site being excluded. The result of this blocking means that there is never a complete image of the sample at any given instant and so repeated scanning of the sample, altering the focal point, allows the creation of 3D images made up from the many 2D slices taken. The main advantage of confocal microscopy is in its ability to produce these 3D images of samples at high resolution, allowing increased spatial awareness when studying samples. With respect to its use in atherosclerosis, the high resolution and 3D imagery has allowed for the study of various plaque attributes such as volume [162], lipid content, collagen, smooth muscle content and cellularity [163], therefore allowing comparisons between wild type and atherosclerotic mice ($ApoE^{-/-}$) [164] in a range of different pathological contexts [165]. Although allowing high definition imaging, the nature of the excitation light can have adverse affects such as photobleaching, defined generally as the photochemical destruction of a fluorophore, which occurs due to constant excitation by a high intensity light source e.g. laser. The degradation of the fluorphore over time will decrease the fluorescent intensity given off by a fluorophore and so decrease imaging depth and can also have an affect on time lapse imaging. As the laser light is stimulating the entire sample simultaneously in a confocal system, the fluorophores throughout the sample will become photobleached over prolonged imaging, resulting in decrease image quality. In addition to the bleaching, the high intensity laser light can also cause damage to the cells themselves. One final factor that confocal microscopy does not address is the interactions of moving elements in a tissue sample, e.g. cells, as it just takes one snapshot in time of whatever is being imaged. No extra information regarding where cells may be moving to, how they move or if they interact with other factors can be ascertained, unless using a multiphoton (2 photon) system as described below.

1.10.2.2 Multiphoton microscopy

Two-photon excitation microscopy (2 photon), is similar to confocal microscopy in many ways but differs in that it offers higher tissue penetration and also the ability to take 3D image stacks through time, giving a 3D movie of the sample being scanned. In the early 90's Webb and colleagues developed multi photon laser-scanning microscopy (MPLSM) [166]. The concept of MPLSM is based on the idea that two photons of comparably lower energy than the energy needed for one photon excitation (e.g. in Confocal Microscopy) can also excite a fluorophore if both photons excite the flourophore in the same quantum event. The excitation photons will carry approximately half the energy required to induce excitation and so the system relies on these photons exciting the fluorophore at exactly the same time. To increase the probability of this near-simultaneous absorption, a higher flux of excitation photons is required which is usually supplied by a femtosecond laser. As the probability of two-photon absorption depends on the square of the intensity of the excitation light, the excitation only occurs in a very small volume (~femtolitre) at the focal position of the microscope, therefore out of focus excitation light and scattering are absent. Due to this system of excitation, MPLSM allows for deeper tissue penetration, good resolution optical sectioning and a large reduction in any photo-toxicity/bleaching of the fluorescently labelled sample as only a small target area of the sample is being excited. These advantages in combination with the systems ability to take optical sections over time, permits the capturing of high resolution three dimensional movies from which the study of individual cells dynamics can be made within the vessel wall[167-169]. This study of cellular dynamics will be described later.

The use of molecular imaging of the vasculature now has an established and expanding role in elucidating the biology of pathological syndromes at the

molecular level, in particularly, to visualise inflammation in atherosclerosis [51, 170].

1.11 Current treatments for vascular pathology

Inflammation, from the Latin “inflammo” meaning “to ignite”, is part of a complex biological system attempting to protect the host from tissue damage or infection and to initiate tissue repair. The classic characteristics of redness, swelling, heat, pain and loss of function can be attributed to an increase of blood flow and fluid into the site of injury as well as the release of inflammatory molecules from damaged tissues, all of which aiding in the recruitment of immune cells to the site of damage. In the case of atherosclerosis, the site of “damage” is the vascular wall, with cells of the immune system homing to the atheroma and adventitial regions of the vessel.

1.11.1 Clinical therapies

1.11.1.1 Anti-coagulant therapies

Current and emerging therapies used for the treatment of atherosclerosis are broad ranging. Clinically approved methods used at present include antiplatelet drugs such as aspirin, clopidogrel, prasugrel and ticagrelor [171, 172]. Aspirin acts to inhibit the production of thromboxane (A2) via inhibiting the production of precursors by the enzyme cyclooxygenase, present in the platelets [173]. Thromboxane itself promotes the aggregation of platelets by upregulating levels of glycoprotein IIb/IIIa, a receptor for fibrinogen, which then binds the platelets together. Aspirin is often given over long periods of time at a low dose and has proven effective in treating patients with atherosclerosis-related pathology [174].

Clopidogrel, Prasugrel and Ticagrelor all act in a similar fashion by inhibiting the P2Y12 subtype of ADP receptors found on platelets [175], which plays an important role in the release of pro-coagulative granules [176], activation of the GPIIb/IIIa receptor and also in thrombus formation [177-180]. These medications are often given along with low dose aspirin and have proven themselves as an effective therapy.

1.11.1.2 Anti-hypertension therapies

Anti-hypertensive drugs are also widely used and act to decrease the pressure exerted by the blood on the plaque, therefore reducing chance of rupture and atheroma formation. ß-blockers (ß-adrenergic antagonists), such as bisoprolol, carvedilol and metoprolol are often used in adjunct with ACE (angiotensin converting enzyme) inhibitors and induce decreased blood pressure mainly through their actions on the heart where they decrease cardiac contractile force [181]. ß-blockers can also act through their affect on the renin/angiotensin system in the kidneys which controls blood volume levels, inhibition of the kidney ß1 resulting in a decrease in renin secretion [182]. Briefly, in response to low blood volume kidneys release rennin, this then carries out the conversion of angiotensinogen in the liver into angiotensin I. This is then converted by ACE into angiotensin II which is a potent vasoconstrictor and also stimulates the release of aldosterone from the adrenal cortex which acts on the kidneys to increase blood volume. As mentioned previously, ACE inhibitors also act as anti-hypertensives by inhibiting this conversion of angiotensin I to II and have proven to be an effective anti-hypertensive [183].

1.11.1.3 Statins

Statins (e.g. atorvastatin, simvastatin, etc.), also known as HMG-CoA reductase inhibitors, are in widespread use due to their ability to lower circulating cholesterol levels in patients and relatively low risk of side effects [184]. HMG-CoA reductase is the rate limiting enzyme in the metabolic pathway (mevalonate pathway) which produces cholesterol, acting as a competitive antagonist for HMG-CoA. Somewhat surprising anti-inflammatory affects of statins have also been studied which, in addition to lowered cholesterol, will aid in treatment of atherosclerosis. In a completely lipid level independent manner [185, 186], statins are able to restore endothelial function [187, 188] e.g. retain their anti-adhesive properties and regulate vascular tone, in models of hypercholesteremia and atherosclerosis [189]. Additional effects on the endothelium include decreased expression of adhesion molecules [190-192], increased eNOS levels [193] and decrease production of pro-coagulant factors [194]. Statins are also being used more and more in the field of transplantation owing to their ability to decrease the incidence of tissue rejection [195, 196], seemingly due to suppressive effects on local natural killer cells [197]. Indeed this general immunosuppressive property has also found support in cases of patients being treated with statins which also have cases of osteoperosis, multiple sclerosis and rheumatoid arthritis [198]. Statins have also been found to inhibit the recruitment of immune cells to the inflamed vessel wall, inhibiting monocyte derived chemokines [199-202] and directly bind lymphocyte function-associated antigen 1 [203], resulting in a general decrease in immune cell content in the vessel wall [190, 192, 204]. An inhibitory effect on endothelial MHC II levels may also play a role in the previously mentioned immunosuppression [198] and can also inhibit T cell proliferation and activation which in turn leads to a decrease in pro-inflammatory cytokines and even and increase in anti-inflammatory cytokines [205, 206].

1.11.2 Experimental therapies

1.11.2.1 High density lipoprotein mimicry

Novel therapies currently in the research phase offer an alternative approach to tackling atherosclerosis. Synthesised high density lipoprotein (HDL) mimetics have shown some promise in treating atherosclerosis. Naturally occurring HDL is generally known as "good cholesterol" as it takes up cholesterol from foam cells for further processing in the liver, thereby decreasing lesion size. HDL mimetics have shown promise in promoting cholesterol efflux by binding to oxidised LDL (oxLDL), exerting anti-inflammatory properties and may prove particularly effective if used in conjunction with statins [207-209].

1.11.2.2 Gene therapy

Current gene therapy approaches have also shown some promise, these mainly concerning themselves with inducing angiogenesis in ischemic tissues [210] or focusing on affecting initiation and development of vascular inflammation [211]. Non-viral approaches have a significant advantage over current viral vectors due to their relative safety *in vivo*, however this is accompanied by comparatively inefficient transduction levels. This, sometimes transient, low level gene expression can in some cases be advantageous as in the cases of angiogenic growth factors [212-215], such as vascular endothelial growth factor (VEGF) which is extremely potent, low level transduction and transient expression aid in avoiding any deleterious affects caused by high expression levels [216, 217]. This low level transduction is not ideal for all transgenes to be effective and so the potent transduction levels that viral vectors confer is an obvious advantage. By far the most characterised of current vectors, adenovirus serotype 5 has proven itself a potent tool in *in vivo* based gene

transduction into vascular cells [218-220], indeed success was had utilising an IL-10 expressing adenovirus in reducing atherosclerotic pathology in rabbit models of disease [98], this study using Ad IL-10 in an alternative approach. Although these vectors allow effective transduction of vascular cells, this is relatively small in comparison to the level of hepatocyte associated with *in vivo* use [221]. Re-targeting of these vectors for more efficient vascular wall transduction involves altering the tropism of the virus [222], altering the serotype of the vector [223, 224] or modifying peptides located on the fibre domain of the vector [225]. In addition to these targeting issues is the ability of the recipients immune system to clear the viral vector and thus limit the ability to induce long-term gene expression in the target tissues [226].

1.11.2.3 Vaccination

From an immunological perspective, a large amount of research has been carried out in developing a vaccination strategy for atherosclerosis. This method has proven extremely effective in other disease pathologies and would allow a highly specific immune response to the target antigen. Unfortunately an inherent issue faced in this approach is that the specific antigen or antigens to which the immune response is directed are unknown, with current data indicating a range of possible targets. Relative success has come from vaccinating against the highly immunogenic molecule, oxidised LDL [227]. A range of differing immunisation protocol have been studied [228-231] however most gave similar results, these being an increase in oxLDL specific IgG antibodies, decrease in circulating cholesterol and most importantly attenuation of lesion size and development. Further experiments focusing on vaccination with ApoB100, the primary apolipoprotein of LDL, again showed inhibition of lesion formation [232] . Despite the amount of experimental data, the underlying mechanism of this protection remains elusive. Heat shock proteins (HSPs)

have also been identified as possible pathological antigens. HSPs are involved in a range of cellular processes and are regulated in endothelial cells and macrophages upon sheer stress, ox-LDL exposure and hypoxia, all traits of atherosclerosis [233-235]. Subcutaneous vaccination using HSPs (HSP60/65) resulted in larger fatty streak formation in $LDLr^{-/-}$ mice [236], whereas experiments aimed at inducing tolerance, via oral/mucosal routes, have proven to attenuate lesion formation through induction of Treg and IL-10 production [237, 238]. DNA vaccines, whereby the target of interest is cloned into an expression plasmid which itself is incorporated into, for example *Salmonella typhimurium*, have displayed some success in immunising mice against pro-atherogenic cytokines such as IL-15 [239] and vascular growth factors [240]. This method of immunisation involves the oral delivery of the *Salmonella typhimurium*, which themselves produced the target protein.

1.12 T cells in atherosclerosis

1.12.1 The role of T cells in atherosclerosis

The presence of T cells in human atherosclerotic plaques was first documented in 1985 [241]. At this stage, macrophages and foam cells were already known to reside in the plaque but the prospect of the involvement of the adaptive immune system had not been considered. Later studies would go on to show that the number of T cells residing in the inflamed vessel wall would outnumber macrophages and play a prominent role in the pathogenesis [40].

Briefly, a T cell response is generated when the naïve T cell encounters an antigen presenting cell which is presenting the peptide for which the T cell receptor (TCR) is specific for. This initial activation takes place within a secondary lymph node to which these antigen laden APCs migrate. These

activated T cells then migrate from the secondary lymphoid tissues to the inflamed tissues, therefore naïve cells are rarely found in high numbers in nonlymphoid tissue. The majority of T cells found within the plaque are effector cells [242] with the proportion of activated cells increasing with the severity of pathology [243, 244]. Both $CD4^+$ and $CD8^+$ T cells are present in lesions but $CD4^+$ cells dominate in numbers [245] and of these the cells are generally of a TCRα/ß configuration with lower numbers expressing TCRγ/δ [242, 246].

The key trait of the adaptive immune response is that its members e.g. T and B cells can only become activated by the presentation of the antigenic peptide they are specific for. The presence of T cells at the inflamed vessel wall therefore indicates that the T cells are responding to eradicate a particular pathogen however the peptides responsible for initiating the disease have not yet been identified, with the probability being that no singular antigen drives this disease. The presence of Chlamydia, herpes simplex, and cytomegalovirus have all been detected within atherosclerotic plaques [247] in addition to high antibody titres to these pathogens with the addition of Helicobacter pylori, which indicates the role of the adaptive immune system [248]. Similarities between the microbial heat shock protein (HSP) 65 and human HSP60 can result in the immune response being directed towards the human protein (molecular mimicry), which is found within human atherosclerotic lesions [246]. An immunisation against HSP65/60 aggravates fatty streak formation [249] which indicates that the adaptive immune response to these proteins promotes atherogenesis, this correlating with higher HSP65/60 antibody titres in patients with atherosclerosis [250, 251].

The oxidation of LDL which occurs in the vascular wall and the resultant immune response to these modified self proteins is also thought to play a significant role in the pathogenesis [252]. Lipid peroxidation of fatty acids in the phospholipids and cholesterol esters of lipoproteins results in the

production of reactive aldehydes which may bind to apolipoprotein B and other proteins resulting in immunogenic neopeptides. The oxidation of LDL results in oxidised phospholipids to which, increased antibody titres in atherosclerotic mice have been found [253] and have been documented in some human patients [254].

B2-glycoprotein I is another possible candidate for the immune system. It is a protein found on platelets, endothelial cells and atherosclerotic plaques [255] which binds phospholipids and in patients with a range of inflammatory disease including atherosclerosis, raised ß2GPI antibody titres have been found [256]. Immunisation with ß2GPI accelerates lesion development which may be linked to its downstream effects of increasing oxLDL uptake by macrophages [257].

The significance of the role that T cells play can be demonstrated in animal models with either the addition or removal of these cells. In an immunodeficient scid/scid ApoE$^{-/-}$ mouse model, the addition of CD4+ T cells reversed the decrease in fatty streak formation and increased the pathology past that observed in immunocompetent ApoE$^{-/-}$ mice [5], the same effect being observed when the T cells being transferred were specific for oxLDL [258]. T cells from a ß2GPI-immunised donor increased fatty streak development [259] as was also the case following the transfer of cells from HSP-immunised mice [260]. Taken together, it is clear that although atherosclerosis was first, and to some extent still is, perceived as a monocyte macrophage inflammatory disease, T cells have a crucial role in the development and perpetuation of the pathology.

1.12.2 T Cell subsets in atherosclerosis

1.12.2.1 Th1

The two main subsets of $CD4^+$ T cells found in atherosclerosis are Th1 and Th2 cells, both integral parts of the adaptive immune system. The majority of T cells in atherosclerosis are of the Th1 phenotype, producing high levels of IFN-γ. Atherosclerosis is commonly defined as a Th1 driven pathology. The concomitant cytokine IFN-γ produced by these cells is known to activate monocytes/macrophages and DCs, inducing further production of pro-inflammatory components, leading to the continuation of the pathogenic Th1 response. It is thought that IFN-γ potentiates most stages that lead to inflammation and atherosclerosis, with atherogenic properties including increasing immune cell recruitment to the plaque, increased APC/phagocyte activation, decreasing smooth muscle cell proliferation and increasing their MMP production [261-263]. Deficiency in the IFN-γ receptor or IFN-γ significantly reduces lesion development and enhanced the stability of the plaque via increased collagen production [23, 92]. IL-12, the cytokine produced by DCs and monocytes/macrophages plays a decisive role in Th1 differentiation at the time of $CD4^+$ activation. $ApoE^{-/-}$ mice deficient for the IL-12p40 subunit showed considerable reduction in plaque development [90] and the addition of recombinant IL-12 enhances disease development through its pro-INF-γ activity [89]. The transcription factor T-bet is integral to Th1 differentiation and consequently T-bet knockout atherosclerotic mice display reduced lesion development, this effect being possibly due to the dominance of a Th2 phenotype [6].

1.12.2.2 Th2

The second most abundant CD4+ T cells phenotype is the Th2 subset. The major cytokines secreted by Th2 cells, IL-4, IL-5, IL-10 and IL-13, among

other things, provide help for antibody production by B cells. The production of IL-4 and IL-5 downregulate IFN-γ, therefore a Th2 biased response would be proposed to antagonise the pro-atherogenic Th1 effects and so therefore represent an anti-atherogenic response. The proposition that Th2 is anti-atherogenic remains controversial however as the effects of a Th2 response differ depending on the stage or the site of the lesion as well as the model used. A Th2 biased response in low level hypercholesterolemia models has been shown to protect against fatty streaks [264]. In $LDLr^{-/-}$ models the evidence is not so straight forward with contradicting evidence showing that deficiency of IL-4 has no significant effect on lesion development [94] with work carried out by the same research group showing that it does [265]. Severe long term hypercholesterolemia is associated with a switch to a Th2 phenotype and IL-4 production however at these late stages the Th2 bias does not decrease lesion progression [266] suggesting that a Th1 phenotype plays a key role in the early stages of atherosclerosis, but at later stages there is a natural switch whereby a Th2 phenotype takes over in driving pathology. Other Th2 derived cytokines, IL-5 and IL-33 have anti-atherogenic properties. Following immunisation with oxLDL, $ApoE^{-/-}$ mice had reduced lesion size which was related to high levels of IgM anti-oxLDL antibodies derived from IL-5 stimulated B1 cells [6]. IL-33 has also shown athero-protective effects which have been discussed in an earlier chapter.

1.12.2.3 Treg

Many mechanisms have evolved to maintain immunological tolerance and to limit an overactive response to antigens whose main products include IL-10 and TGF-ß, both well studied anti-inflammatory cytokines. Regulatory T cells (Treg) are a subpopulation of T cells which come in many forms, the best characterised of which being $CD4^+CD25^+$ T regs and represent 5-10% of the circulating peripheral $CD4^+$ cells [267]. The presence of Treg cells in

both human and mouse atherosclerotic lesions has been firmly established [268, 269] as has the impact of their anti-inflammatory properties on lesion development. Ait-Oufella et al [270] showed that depletion of the Treg population, either through genetic knockout or anti-CD25 neutralising antibodies, resulted in enhanced lesion development in both $LDLr^{-/-}$ and $ApoE^{-/-}$ mice respectively. It was found that Treg depletion had no influence on lesion size when the host T cells were engineered to be insensitive to TGF-ß, suggesting that TGF-ß is required for the atheroprotective effects of Tregs [271]. Further to this, the adoptive transfer of $CD4^{+}CD25^{+}$ Tregs into $ApoE^{-/-}$ recipients, reduced atherosclerosis [270, 272]. The use of these cells as an antigen-specific immunotherapy for atherosclerosis has met some success. Atherosclerosis in $ApoE^{-/-}$ mice can be attenuated by the transfer of Tregs specific for HSP60 generated *in vitro* [273], with the induction of Tregs via oral tolerance against HSP60 also proving to be effective in $LDLr^{-/-}$ mice [238]. Although it would appear that Tregs play a critical role in atherosclerosis the mystery of whether their suppression is antigen specific, cytokine or contact and where this regulation occurs is still unresolved.

1.12.2.4 Th17

A relatively novel lineage of CD4 T cell, Th17 cells, has been characterised [274], named so due to its ability to produce IL-17 and also IL-23 which act as potent proinflammatory mediators and synergise with TNF-α and IL-1 [275]. IL-17 has been linked to several autoummune and inflammatory diseases [275] but there is not a great deal of information on its role in atherosclerosis, however, a recent study showed that Th17 numbers were increased in $ApoE^{-/-}$ mice compared to wild-type as was the levels of IL-17 in the plaque laden arterial wall. Addition of neutralising IL-17 antibodies resulted in inhibition of lesion development whereas the addition of recombinant IL-17 increased pathology [276]; taken together this demonstrates that Th17 cells may have a critical role in atherosclerosis.

1.12.2.5 CD8

$CD8^+$ T cells have been shown to be present in atherosclerotic plaques however their role in the pathology remains unclear. A possible protective role for MHC I/$CD8^+$ has been indicated in MHC I deficient $ApoE^{-/-}$ mice in which larger atherosclerotic lesions were observed in comparison to the wild-type [277]. More recently $CD8^+$ T cell activation was found to occur in the early stages of hypercholesterolemia-induced atherosclerosis [278], which may indicate that hypercholesterolemia results in the formation of autoantigens to which these $CD8^+$ cells react to however direct experimental data on the role of $CD8^+$ cells is lacking.

1.13 The aortic tertiary lymph node (ATLO)

The majority of studies of atherosclerosis have focused on the lesions located in the tunica intima, comprising of the lipid laden foam cells, macrophages, T cells and smooth muscle cells etc. As discussed previously, the adaptive immune response plays a significant role in the development and perpetuation of pathology and there is increased recruitment of these cells into the arterial wall at all stages of atherosclerosis [40, 51].

A unique occurrence found at the very late stages of disease progression is the development of fully structured adventitial aortic tertiary lymphoid organs (ATLOs). Although the accumulation of leukocytes in the adventitia was first described in the 70's by Gerrity et al [57], it would be 1997 before they would be considered part of the vascular associated lymphoid tissue (VALTs) [279]. Tertiary lymphoid organs (TLOs), also called tertiary lymphoid tissues, are ectopic accumulations of lymphoid cells which occur in chronic inflammation, this being termed lymphoid neogenesis, in

typically non-lymphoid locations. TLOs have been described in autoimmunity [280-282], microbial infection [283, 284] and chronic allograft rejection [285, 286].

The precise signals which result in the formation of these on site lymphoid structures is still unknown however a combination of cytokines [287, 288], chemokines [289], adhesion molecules [290] and survival factors are all indicated as features in lymphoid structuring and the chronic expression of these, from cases of non-resolving inflammation would set the correct environment for the formation of these TLOs.

These structures contained B cell zones, germinal centres, plasma cells and T cells zones and high endothelial venules (HEVs) [49, 50] all structures that are found within secondary lymphoid organs. The presence of germinal centres and proliferating cells in particular [291], illustrates that the ATLO could be an area for a locally generated immune response. Although it could be assumed that arterial wall inflammation spreads from the intima to the adventitia, the role that the adventitial immunity plays is still unknown, as is how these two elements are connected as passage of cells through the tunica media is typically very low [292]. The elegant immunohistochemistry carried out by Grabner at al [50] showed that there is a reticular fibre network extending from the tunica media in to the ATLO itself, interconnecting with the ATLOs HEVs. These conduits were not big enough to allow cellular transport but can instead carry small molecules, ~10kD, acting in a similar way to lymph node conduits in size and transport function, and perhaps form the link between intimal and adventitial connectivity. The question of whether the ATLO has a beneficial or harmful role in atherosclerosis has still to be defined, as is its role in the previously mentioned autoimmune disease and microbial infections. In some cases of autoimmune disease, the formation of a TLO is accompanied by tissue destruction, whereas in microbial infections TLOs seem to develop to sequester pathogens away from the rest of the body. Even though the

internal structure of the ATLO has been revealed, whether this evidence of a locally generated immune response is perpetuating or aiding in resolving the pathology has still to be studied.

1.14 CD4 T cell transduction

1.14.1 The use of T cells as therapeutic delivery vehicles

As described previously, atherosclerosis and the development and progression of arterial plaques is due in part to an inflammatory response situated in the sub-endothelial layers of large and medium sized arteries. Not only is the innate wing of the immune system (e.g. macrophages) present at this site but also cells of the adaptive immune response (e.g. T cells) are also found reacting and directing the immune response to an as yet undefined antigen, present within the vessel [14]. Further studies looking into the composition and role of immune cells at this site of inflammation have shown the presence of a large range of immune and inflammatory cells but it was the work of Elena Galkina's group who first gave a quantitative account of the immune cell presence in the arterial wall [40]. They showed that the cell type most prevalent in the arterial wall was the T cell, outnumbering the macrophage which was typically thought to be the stereotypical cell of the plaque.

The impact and role of these T cells at the plaque has been demonstrated in a number of ways by many studies. In a study by [258] it was shown that if an animal which developed atherosclerosis was immunodeficient the severity of the pathology was reduced thus demonstrating the role the immune response plays in the disease. Furthermore if only T cells were re-introduced into an immunodeficient, atherosclerotic mouse then it was found the pathology increased showing that T cells on their own are capable of having a large effect on disease progression. It also was found

that the dominant subtype of T cell present was the Th1 subset, traditionally known as a promoter of cell mediated immunity. It was shown that when this Th1 subset was switched to a Th2 subset (humoral immunity), that the Th2 cells had anti-atherogenic properties, this result supported by studies in which pathology decreased following the knockout of Tbet in T cells, a factor essential for Th1 development which also results in Th2 development in its place [6]. The results from these studies underline the importance of the role that T cells themselves have in atherosclerosis, their removal decreasing pathology, their re-introduction increasing pathology and more specifically identifying one subset of T cell, the knock out of which decreasing the pathology. In conjunction with their significant role in atherosclerosis, T cells have been found to be present at all stages of the disease. Importantly, T cells along with other immune cells have been found to be present in the sub-endothelial layer and the adventitia in the arterial wall before any plaque formation has developed in the mouse [51]. As shown, T cells have a significant role in atherosclerosis, are present throughout disease progression and can also home normal and inflamed vascular tissue. This presents the CD4+ T cell as an encouraging target for manipulation, offering the possibility to affect atherosclerosis not only during progression but also at the time of onset, this T cell manipulation being the initial aim of this study.

The driving concept behind this project is that the T cell is utilized as a homing vehicle, delivering a customizable gene product. In addition to their presence and obvious significance, work by our lab and others [51] has shown that intravenous adoptive transfer of labelled lymphocytes are capable of homing to the vascular wall, this most likely occurring due to expression of adhesion molecules, chemokines and their co-receptors on the T cell. Thus this indicates that *in vitro* manipulated T cells can make their way to the vessel unaided post transfer.

1.14.2 Adenovirus

The adenovirus consists of a non-enveloped; double stranded DNA enclosed in a protein coat termed the nucleocaspid. There are 52 different serotypes of the adenovirus with serotype 5 being the best characterized of the family. With regard to binding the adenovirus utilizes the knob, shaft and penton base domains each with its own role. The initial binding occurs by the knob domain attaching to the coxsackie adenovirus receptor (CAR). A second interaction between the penton base and the integrins αvβ3/αvβ5, thought to be held in proximity to CAR via a lipid raft [293], induces endocytosis of the viral particle allowing it to enter the cell. It has also been found that the coagulation factor 10 (FX), which binds to the hypervariable regions (HVR) on the hexon molecules, is capable of targeting certain adenovirus serotype 5 (Ad5) through heparin sulphate proteoglycans (HSPGs). Other serotypes of adenovirus e.g. Ad35 are not influenced as heavily by FX presence [294]. Once inside the cell, the viral particles capsid degrades under the increasingly hostile conditions within the endosome and so the viral DNA is released and transported to the nucleus via intracellular transport mechanisms where it associates with a histone molecule forming a complex. It is in this state that replication of the viral DNA can occur, the virus taking advantage of the various enzymes and molecules involved in normal genetic replication to start the reproduction cycle. It is important to note that although this replication does occur in the nucleus, adenoviral DNA is not integrated into the host genome as is the case with retroviruses, discussed later. This therefore means that the expression induced by the adenovirus is relatively transient as without integration into the host genome each division of the cell can result in lower numbers of virus within the cell, cell division rates etc. having an effect on this transience. Adenoviral vectors are currently the most often used for gene transfer in cardiovascular tissue due in part to their ability to infect both replicating and non-replicating cells. Although the general expression of adenoviruses is brief, the short term gene products could be sufficient and appropriate

for treatments under which long-term exposure would lead to toxicity, such as in the case of angiogenic factors.

A factor that may be involved in the short lived gene expression found with adenovirus may be due to the hosts inflammation response against viral encoded proteins, hence repeated administrations are unfeasible as neutralization of the virus would be swift and futile [295]. The next generations of adenoviral vectors are under an ongoing developmental process to overcome these problems, which should lead to a more advanced delivery system.

With regard to this project previous work by Casey Weaver's group [296], has shown that adenoviral transduction of T cells is a successful and viable method in which to transfer a therapeutic gene of our choice. As mentioned previously the standard adenovirus gains entry into a cell via binding to the CAR receptor thus meaning that if an adenoviral vector is to be used, the target cell must express a form of the CAR receptor. Casey's group also [296] developed a transgenic mouse, whose T cells carried the human form of the CAR receptor, termed hCAR, achieved by subcloning the hCAR fragment into a CD2 minigene. It is with this hCAR mouse that we intend to use for adenoviral T cell transduction *in vitro*, prior to transfer into the $ApoE^{-/-}$ mouse.

1.14.3 Lentivirus

The lentivirus replication is different from the adenovirus in that the genetic information held in it is in the form of single strand RNA. The virus is enclosed by an outer envelope containing the binding domains for viral entry. Within this envelope is what is termed membrane associated proteins (p17) which itself encompasses the capsid protein shell. Inside the capsid shell lays the RNA molecules along with the preformed enzymes

Reverse Transcriptase and Integrase which are vital to virus production [297]. Using the example of HIV as a lentivirus, it too uses a primary and secondary signalling mechanism, similar to adenovirus, to gain entry into a cell. The knob domain of the lentivirus, termed gp120, binds the CD4 molecule on the surface of a T helper cell. The secondary signal comes from the shaft component termed gp41 which then binds to the chemokine receptor CCR5 and it is this dual signalling pathway that leads to entry into the cell [298]. Once inside the cell as with adenovirus the acidic conditions within the endosome cause degradation of the protein components surrounding the viral genome and thus the RNA is released. It is at this point that the preformed enzymes that were held with the RNA within the capsid are allowed to initiate. Firstly the RNA strands are acted on by Reverse Transcriptase which consequently modifies the RNA into viral DNA. This DNA is then integrated by the enzyme Integrase into the host's resident DNA inducing long term expression of the gene/virus [299].

These vectors are appropriate for *ex vivo* gene transfer where removal of target cells or organs is involved in the process of gene therapy, mainly due to safety issues. A lack of highly specific targeting envelopes would result in intravenous administration being at a high risk of non-specific integration of a relatively permanent gene in inappropriate tissues. As Retroviruses are only able to transduce actively replicating cells, this limits their efficacy for gene transfer into fully differentiated cells such as cardiac myocytes. Additionally, the safety of using retroviral vectors is a concern because introducing replication-competent retrovirus into a cell with a random insertion pattern can generate insertional mutagenesis, leading to disruption of normal cellular gene expression [300].

Relating to its use in this project, the lentivirus has been pseudo typed with outer membrane components of the vesicular stomatitis virus's glycoprotein G (VSV-G). This replaces the gp120 and gp41 mentioned previously which in effect re-targets the virus away from specific binding to

CD4 and CCR5. It is believed that the pseudo typed vector infects target cells by endocytosis followed by acid induced fusion with phospholipid components of the endosome [301], thus giving it a broad host cell range as it is capable of transfecting many forms of cellular membrane. There has been little previous work carried out using lentivirus on murine T cells in comparison to that done on human T cells although from the literature it suggests long term gene expression using the lentivirus is a viable option [302, 303]. Unpublished work by groups from Bristol and Oxford has very recently been able to achieve high transduction levels in murine T cells.

1.14.4 Adeno-associated virus

An alternative viral vector which has shown to be successful is Adeno-Associated Virus (AAV). As with lentiviral vectors, AAV vectors are able to transduce non-dividing cells and is not currently known to cause any disease, consequently causes a very mild immune response towards it if used *in vivo*. AAV vectors have shown to transduce the smooth muscle cells of the vessel wall [304] with relative success following local delivery [305, 306] however the bulk of success has been achieved in myocardial tissue using AAV serotype 2 obtaining long term gene expression [307, 308], although serotype 6 has also shown itself to be efficient in heart tissue [309]. Variations in the size of the vectors and availability of receptors, is thought to contribute to the favoured tropism for smooth muscle cells over endothelial cells for which adenovirus has natural tropism [304, 310]. As with adenoviral and lentiviral vectors, in order to generate a more efficient and selective system using AAV, modification to targeting proteins/serotype switching is required but has met with some success [311]. In terms of transduction of T cells, there has been no literature using AAV vectors.

1.14.5 Non-viral vectors

Generally, nonviral vectors are relatively inefficient for efficient high level gene transfer however avoid major safety issues related to viral vector such as immune response and tissue toxicity. Examples of non-viral vectors include naked plasmid DNA, gene gun (using bioballistic bombardment of DNA-coated gold particles to penetrate target organs or single cell layer), plasmid-liposome complexes (lipoplex), polymer-DNA complexes (polyplex), and liposome-polymer-DNA complexes (lipopolyplex). Alternative lipid based systems include Lipid Integrin DNA complexes (LID) which consist of a liposome and DNA component which is additionally complexed with an integrin as a targeting peptide. As the target integrins are expressed on vascular cells they can be taken advantage to increase cell specific transfection [312]. Unlike viral vector DNA, internalization of naked DNA or DNA-conjugates can occur either in a random manner or upon binding to a specific receptor depending on the type of vector used. A successful strategy in targeted nonviral vector gene transfer includes transcription factor decoy using antisense oligodeoxynucleotides (ODNs). When the gene is known that is affecting or causing the pathology, DNA or RNA can be introduced into the cell which binds to the mRNA of that gene thus, as mRNA needs to be in single strand format to be made by the ribosome, the now double stranded gene will be effectively turned off. These ODNs have been used in gene therapy and studies of gene expression in CVD, including restenosis after angioplasty, hypertension, transplant vasculopathy, myocardial reperfusion injury, and graft failure [313]. Electroporation, whereby an electrical current is applied to the target cell thereby creating small pore in the membrane through which genetic material can travel, is the only non-viral approach which has achieved some success in the transduction of T cells [314]. It is this system that the Nucleofection system from Amaxa [315] is also based on which we have used in this project. As with AAV strategies, these non-viral methods, with the exception of

electroporation, have had little or no success in the transduction of CD4 T cells.

Although a number of advantages are held by other vector strategies, due to the published success of transduction of CD4+ T cells [296] combined with the expertise and established protocols present in Prof. Baker's lab, adenoviral vectors were used in this thesis for T cell transduction experiments.

1.15 Interleukin 10, an anti-atherogenic molecule

Interleukin 10 (IL-10), originally entitled cytokine synthesis inhibitory factor (CSIF) [316], is a well documented and studied anti-inflammatory cytokine, chiefly produced by monocytes and lymphocytes, primarily regulatory T cells and is pleiotropic, inducing anti-inflammatory effects on a range of cells types. On cells of a myeloid origin e.g. dendritic cells (DCs), monocytes and macrophages, IL-10 can modulated the expression of cytokines, soluble mediators and cell surface molecules with important consequences for their ability to initiate and maintain an inflammatory response. IL-10 inhibits the production of the pro-inflammatory cytokines IL-1, IL-6, IL-12, IL-18, TNF-α and a range of growth factors such as GM-CSF, granulocyte colony stimulating factor (G-CSF) and macrophage colony stimulating factor (M-CSF) by activated monocytes and macrophages [317-320]. In addition to inhibiting cytokine production, IL-10 also inhibits MHC class II antigen expression on these cells and co-stimulatory molecules CD54, CD80 and CD86 [321-324], all of which play a key role in the initiation of an adaptive T cells response. As a result of the effects on antigen presentation to T cells, a knock on effect is observed and the resultant cytokines produced by the activated T cells are also decreased/inhibited [317, 321]. Acting directly on the T cells, IL-10 is capable of inhibiting IL-2, TNF-α and IL-5 production [325-327] as well

altering the cells chemotaxis [328]. The activation of T cells in the presence of IL-10 can induce a state of nonresponsiveness or anergy [329], which cannot be undone by a second round of activation using IL-2 or TCR stimulation [329]. This induction of tolerance or anergy can be replicated via continuous antigenic challenge [330] or by specific immunotherapies [331] and is often related to the induction of a regulatory subset of T cells that produce high levels of IL-10 [332, 333]. In addition, IL-10 also inhibits pro-inflammatory cytokines from neutrophils [334] but appears to have a limited effect on B cells *in vivo* [335].

In terms of atherosclerosis, the ability for IL-10 to decrease these key aspects of the immune response bodes well for its use in halting the chronic inflammation occurring beneath the growing plaque, with studies whereby the immune response particularly in T cells [5, 6, 258] is altered, showing decreased pathology. It has been shown in several papers that IL-10 can be a valid therapeutic molecule in models of atherosclerosis. In IL-10 deficient mice fed an atherogenic diet there was a 3 fold increase in lipid accumulation along with decreased collagen content and increased IFN-γ levels. Transfer of IL-10 into these mice resulted in a 60% reduction in lesion size [97]. Similar results were also found by Caligiuri et al. [80] in IL-10 KO mice, reporting increased levels of MMPs, systemic markers of coagulation and Th1 response. In looking at more advanced stages of plaque formation, bone marrow of 14 week old $LDLr^{-/-}$ mice was replaced with the marrow from $IL\text{-}10^{-/-}$ mice. Here it was found that the IL-10 deficiency resulted in a 35% increase in lesion size, with an increase in lymphocyte and macrophage accumulation along with a decrease in collagen content also being observed [336]. The use of systemic IL-10 encoding adenoviral vectors has also shown promise. In a model of atherosclerosis using a perivascular silastic collar, systemic injection of Ad IL-10 decreased the lumen stenosis by 62%, induced monocyte deactivation and lowered cholesterol levels [98]. In a similar approach to this project, the use of cells overexpressing IL-10 has also been shown to have anti-

atherogenic effects. The use of retrovirally transduced bone marrow cells under the CD68 promoter (a glycoprotein expressed by monocytes/macrophages) and their subsequent presence in the plaque resulted in reduced cholesterol ester accumulation, reduced apoptosis, pro-inflammatory cytokines and enzyme along with increased uptake and efflux of cholesterol [337]. Further in line with our approach, the use of T cells over expressing IL-10 from a bone marrow transplant into $LDLr^{-/-}$ recipients, decreased lesion size, lesion complexity, the necrotic core, cholesterol accumulation and showed a switch to a Th2 phenotype among other anti-atherogenic properties [96].

Taking both the general anti-inflammatory properties of IL-10 and also the range of data showing anti-atherogenic effects into account, IL-10 presents itself as an ideal candidate for our therapeutic molecule to be inserted into the adoptively transferred T cells.

1.16 Aims of the project

The aim of this project was to investigate the feasibility of using T cell gene therapy in experimental atherosclerosis. Firstly, two photon microscopy was used to confirm immune cell homing of the atherosclerotic vessels and study vascular immune cell dynamics in real time (Chapter 3). Secondly, we refined the introduction of custom genetic information into the T cell using a range of techniques. Following this optimisation, genes of interest (GOI) were inserted into the T cell for it to be produced by the internal machinery of the cell, in this case IL-10 or GFP (Chapter 4 and 5). Thirdly, these transduced T cells were then transferred into recipient mice mice in order to test their anatomical distribution and viability (Chapter 6). The final aim of the project was to transfer IL-10 secreting T cells into $ApoE^{-/-}$ recipient mice and evaluate their anti-inflammatory/atherogenic effect. Due to technical limitations this part of the project was completed.

Chapter 2: Methods

2.1 Mice

Aged male or female ApoE$^{-/-}$ mice and male C57BL/6 (80-90 weeks old; kindly gifted by Prof. Andreas Habenicht, University of Jena, Germany) were used as recipients. C57BL/6 mice (12-16 weeks old; Harlan, Shardlow, UK) were used as donors.

BALBc and C57BL/6 mice aged between 6-12 weeks were purchased from Harlan, UK and were used as recipient mice for adoptive transfers and as wild type non-hCAR expressing cells.

hCAR DO11.10 mice expressing the human coxsackie adenovirus receptor (CAR) and the MHC class II DO11.10 TCR specific for chicken OVA peptide 323-339 were used for all the CD4+ T cell transduction experiments.

hCAR OT-I mice (kindly gifted by Prof. Kristin Hogquist, University of Minnesota, US) expressing the human coxsackie adenovirus receptor (CAR) and also the MHC class I restricted OT-I TCR specific for ovalbumin peptide, 257-264.

All mice used were maintained on a 12/12 h light/dark cycle with free access to food and water at the Biological Procedures Unit, University of Strathclyde and at the Central Research Facility, University of Glasgow. All the procedures performed in accordance with local ethical and UK Home Office regulations.

2.2 Cell lines

The Human Embryonic Kidney cell (HEK 293) cell line was used for propagation of replication deficient adenoviral constructs. HEK 293 cells are human embryonic cells transformed by sheared adenovirus type 5 DNA first described in 1977 [338]. HEK293 cells produce the adenoviral E1 gene, allowing the production of infectious particles when cells are infected with E1 deleted adenovirus vectors. The HeLa cell line was used in various transduction experiments as they are easily transduced and propagated, originally derived from cervical cancer cells from Henrietta Lacks in 1951 [339]. 293T cells were used for the production of lentiviral vectors. 293T cells are also human embryonic kidney cells but express the simian vacuolating virus 40 large T antigen on their surface, allowing for episomal expression of the transfected plasmids.

2.3 CMTPX labelling and transfer of lymphocytes

A single cell suspension was prepared as described below (see 2.24) from peripheral and mesenteric lymph nodes of C57BL/6 mice. Cell Tracker Red CMTPX (Molecular Probes, Invitrogen) was prepared as a 10 mM stock solution by dissolving the CMTPX powder in dimethyl sulphoxide (DMSO) at RT, 50 µg CMTPX powder in 7.3 µl DMSO. Cells were resuspended with CMTPX at a concentration of 0.5 µl CMTPX stock/$1x10^7$ cells/ml of pre-warmed CO_2-independent RPMI media. Cells were incubated at 37^oC for 45 mins in a 50 ml falcon tube (Corning, UK) with a loosely fitted lid and gently agitated every 15 minutes. Cells were then centrifuged at 350 x g for 5 minutes, the supernatant aspirated and the pellet resuspended in pre-warmed complete RPMI and incubated for a further 30 minutes at 37^oC. Cells were then washed twice in pre-warmed PBS and resuspended for adoptive transfer. $4x10^6$ cells injected intravenously into aged $ApoE^{-/-}$ or C57BL/6 recipients.

2.4 Preparation of tissue for multiphoton laser scanner microscopy (MPLSM)

Twenty-four hours after transfer mice were euthanised with CO_2 and quickly perfused with 20 ml chilled PBS via cardiac puncture, cutting the right atrium and injecting PBS in through the left ventricle, in order to remove blood contamination from the vascular tissue. The abdominal aorta, comprising the A. renalis and the diaphragmatic muscle and the popliteal lymph node (pLN) were excised under a dissecting microscope, transferred into RPMI at room temperature and bound using Vetbond (3M, UK) onto a plastic coverslip as previously described [340]. The coverslip was then adhered with grease to the bottom of the imaging chamber which was continuously supplied with warmed (37^{o}C) and gassed (95% O_2, 5% CO_2) RPMI before and throughout the period of microscopy. Before MPLSM imaging, the excised section of vessel in the imaging chamber was imaged using epifluorescence in order to identify areas with significant red cell accumulation. These sites were then imaged using the MPLSM as potential ATLO sites.

2.5 Multiphoton imaging of ATLO region

Due to the extended nature of this study the imaging of the ATLO region was carried out on two multiphoton microscope rigs. The initial microscopes excitiation source was a titanium sapphire Chameleon laser system (Coherent Laser Group). The beam was routed into a Radiance 2000MP laser scanning system (Bio-Rad Laboratories). The output laser beam from the scan head was aligned through an E600-FN upright microscope (Nikon). The objective lens used for all imaging on this system were a CFi-60 Nikon Fluor 40X/0.8 NA water-dipping objective lens or a Nikon Fluor 10X/0.8 NA water immersion objective. The sample was excited at 830 nm, 210fs pulse (approx.) and 75 MHz frequency.

Fluorescence passed through an E625SP blocking filter (Chroma Technologies) and was detected with a multi-cathode photomultiplier tube (S20 PMT) as part of the Radiance 2000MP system. A custom built filter block was used to separate fluorescence at 500-550 nm, which separated green dyes/autofluorescence from the higher wavelengths of red labelled cells.

The second microscope was a Zeiss 7MP multiphoton system (Carl Zeiss) with a Chameleon tunable laser (Coherent). Objectives used on this system for imaging were Zeiss 10X/0.3 NA air and 20X/1.0 NA water immersion lenses (Carl Zeiss). Fluorescence emission was collected at <375 nm (autofluorescence), 500-550 (green dyes) and 600-680 nm (red dyes)

2.6 Image acquisition and analysis

Once the potential ATLO region had been identified, a time series of z-stack images were obtained to allow subsequent 4D tracking of the labelled lymphocytes. Depending on the size and shape of the ATLO, its anatomical location in the vessel and cell density, the imaged area was adjusted (from 180 µm x 180 µm to 362 µm x 362 µm), the z step was 1.2 µm, to give a total depth of 16-36 stacks. For image analysis, Volocity 5 software (Improvision, UK) was used.

The number of cells per imaged area was calculated after the location (centroid) of individual cells within each three-dimensional image stack was determined by intensity threshold-based object detection. Elastic fibres were manually tracked by the operator. Objects were tracked for at least nine time points. Image analysis of cells in the pLN was performed as previously described [341-343]. Measurements of cell behaviours the velocity, track length, displacement (straight line distance from start to finish of track) and meandering index (displacement/length, a measure of deviation from the straight line with an index of 1 being a perfect straight

line; the smaller the value of the meandering index, the greater the meandering of the track) were calculated for each labelled cell.

Tissue Drift Correction

An artifact of real time imaging of entire excised vessels in perfusion chamber that cannot be avoided is the drifting of the imaged tissue, mainly due to flow of medium causing movement of the semi-attached vessel wall. Correction for tissue drift was carried out using custom made software (SULSA, UK). Briefly, elastic fibres, visualized by autofluorescence, were used as reference static objects. For each time point, the average displacement of the centres of mass of elastic fibres was calculated, and the movement (assumed to be artifactual instead of real) was subtracted from the displacement of all tracked cells [344] These corrected tracks were then used for quantification of cell dynamics.

2.7 Synthesis of murine interleukin 10 gene and insertion into pShuttle plasmid

The sequence for murine IL-10 was obtained through NCBI PubMed's "Gene" and "Protein" database searches with the accession number of NM 010548.2 (NP 034678.1), confirmed as murine IL-10 in previous literature [345]. The protein sequence for murine IL-10 was sent to GeneArt (Life Technologies, Germany) along with the sequence for 5' and 3' restriction enzyme sites to allow for sub-cloning of the gene into the relevant shuttle plasmids, which were also sent to GeneArt. For insertion into the pShuttle-CMV plasmid, the restriction sites XhoI (5') and HindIII (3') were chosen while PvuI (5') and XhoI (3') were chosen for insertion into pShuttle-IRES-hrGFP-1. The presence of these restriction site sequences in murine IL-10 was checked using CLC Sequence Viewer 6 (CLC Bio, Denmark). Plasmid suspensions were stored in a PCR eppendorf tube which was sealed with

parafilm (Pechiney Plastic Packaging Company, USA), enclosed in a 1.5 ml Eppendorf tube which was also sealed in Parafilm and sent in a padded parcel to GeneArt. pShuttle plasmids were then returned via post in a lyophilised state containing the IL-10 sequence.

2.8 Plasmid linearisation

pShuttle CMV, pShuttle-IRES-hrGFP-1 and pShuttle-IRES-hrGFP-1 IL-10 plasmids were all linearised using the restriction enzyme Pme I (New England Biolabs, USA) as described in the accompanying protocol. Briefly, 10 µg of plasmid DNA was incubated with 20 µl NEBuffer 4 (New England Biolabs, USA), 100 µg/ml Bovine Serum Albumin (New England Biolabs, USA), 3 µl of Pme I, double de-ionised water to make the total reaction volume 200 µl and incubated at 37^{o}C for 1 hour using a PCR machine. pShuttle CMV IL-10 was linearised using the EcoRI enzyme (Promega USA), 10 µg of DNA being incubated with 20 µl of 10X Buffer H (Promega, USA), 100 µg/ml BSA (Promega, USA), 3 µl of EcoRI and dH_20 to make the final volume 200 µl and incubated at 37^{o}C for 1 hr using a PCR machine. Following linearisation, DNA was treated with Calf Intestinal Phosphatase (CIP, Promega, USA), 1 µl for 1 hr at 37^{o}C, to dephosphorylate the 5'end of the linearised DNA, inhibiting DNA recirculation. For larger amounts of DNA, the reagents were scaled up as appropriate.

For linearisation of recombinant pShuttle/Ad-Easy plasmids, Pac I (New England Biolabs, USA) was used. 24 µg of recombinant plasmid DNA was incubated with 10 µl NEBuffer 1 (New England Biolabs, USA), 100 µg/ml BSA (New England Biolabs, USA), 3 µl Pac I and dH_20 to make the final volume 100 µl. Plasmid/enzyme mixtures were incubated at 37^{o}C overnight in a PCR machine.

Success of enzymatic digestion was assessed by adding the digestion mix to Crystal 5x DNA Loading Buffer (Bioline, UK) and double de-ionised water and run on a 1% agarose gel (Sigma, UK), 100 V for 60 mins. A molecular ladder was also run with the samples (Hyperladder I. Bioline, UK). Gels were then imaged in an X-ray light box. Non-linearised plasmids appear as a double banded smear whereas linearised plasmids are a singular bar located further down the gel compared to non-linearised.

2.9 Purification of linearised plasmids

After confirmation of linearisation has been carried out, the remainder of the plasmid digest was loaded along with loading dye onto a 0.8% agarose gel, 100 V for 1 hr. A molecular ladder was also run with the samples. Gels were placed on a UV light box to visualise the linearised bands and the bands were cut from the gel using a scalpel and kept at -20^{o}C until used. Excised gels were then run through the NucleoSpin Gel Extraction kit (Macherey-Nagel, Germany). Briefly, excised gels were weighed and dissolved in Buffer NT1 in a 1.5 ml Eppendorf, 50^{o}C for 10 mins, vortexing every 2 mins. The samples were then loaded into a Nucle0Spin Extract Spin Column and spun at 8000 x g for 1 min, with flowthrough discarded. Buffer NT3 was added to the column which was spun at 11000 x g for 1 min, again with flowthrough being discarded. Further NT3 buffer was added and the column spun at 11000 x g for 2 mins, discarding flowthrough. The column was then placed in a 1.5 ml Eppendorf tube and 25 µl of Buffer NE was added and incubated for 1 minute before spinning at 11000 x g for 1 minute, this step was repeated twice to recover maximum DNA levels. DNA output was quantified by using UV spectrophotometry.

2.10 Co-transfection of linearised pshuttle plasmid with AdEasy plasmid into BJ5183 cells

Aliquots of BJ5183 electroporation competent cells (Agilent Technologies, UK) were thawed on ice and transferred into pre-chilled microcentrifuge tubes along with either linearised pShuttle CMV, pShuttle CMV IL-10, pShuttle-IRES-hrGFP-1 or pShuttle-IRES-hrGFP-1 IL-10 plasmids, along with pAdEasy-1 supercoiled vector. Linearised pShuttle plasmids were also added without addition of pAdEasy-1 plasmid to control for background colony growth contributed by the shuttle vector alone. After mixing, the cell/plasmid cocktail was transferred into a pre-chilled electroporation cuvette and run through an electroporator with the following settings: 200 Ω, 2.5 kV, 25 μF. After pulsing the samples, sterile LB broth (see buffers and media section) was added to the cuvette to resuspend the cells. Transformed cells were then placed in a Falcon tube (Corning, UK) and incubated for 1 hr at 37^{o}C while being shaken. After incubation, dilutions of each transformation were plated onto LB-Kanamycin plates. These plates were then incubated overnight at 37^{o}C.

2.11 Screening for recombinant plasmid colonies

After 18 hours incubation (37^{o}C), the bacterial plates were examined by eye for possible recombinant colonies. Colonies appeared as 2 distinct sizes, large and small. Due to the success of homologous recombination between the linearised plasmid and pAdEasy-1 plasmid, this increase in genetic sequence needing copied before cell division can occur, results in smaller sized colonies, with the larger representing unsuccessful homologous recombination. All small colonies observed on the plates were picked off the plate using a sterile pipette tip, transferred onto a patch plate (LB-Kan) and incubated at 37^{o}C overnight. Individual colonies were taken from the patch plate and incubated in LB broth overnight with the

produced plasmid being liberated using a MiniPrep kit (Qiagen,UK), see miniprep protocol. Plasmids from each colony were then tested for recombination by digesting them with PacI, added to loading dye and run on a 0.8% agarose gel for 1 hr at 100 V, a recombinant plasmid showing a band at around 30kb and a band at 4.5 or 3kb whereas non-recombinant plasmids would not. Once recombination had been confirmed, colonies were recovered from the patch plate and stored on Protect Storage Beads (Technical Service Consultants Ltd., UK) at -80^{o}C.

2.12 Transfection of recombinant plasmids into XL10 Gold cells

Ultracompetent XL10 Gold cells (Agilent Technologies, UK) were thawed from -80^{o}C on ice and 100 µl of cells were aliquoted into pre-chilled 15 ml tubes. 4 µl of the ß-mercaptoethanol mix provided with the XL10 Gold cells, and the mixture shaken gently before incubation on ice for 10 minutes. Recombinant plasmid was added to the cell mix and swirled gently before a further 30 mins incubation on ice. The cell/plasmid mix was then heat pulsed in a pre-warmed water bath of 42^{o}C for 30 secs and immediately placed on ice for 2 minutes. To this, pre-warmed (42^{o}C) NZY+ broth (see 2.35.1) was added to the cells and incubated for 1 hr at 37^{o}C with shaking. Each transformation reaction was plated onto LB-kanamycin plates and the plates were incubated at 37^{o}C overnight. One colony was picked from each transformation group and grown in LB broth, following which a MaxiPrep (Qiagen, UK) was carried out to obtain large amounts of the recombinant plasmid. Recombinant adenovirus plasmid was digested with PacI with the cut plasmid run on a 0.8% agarose gel to double check for linearisation. The rest of the digested plasmid was run through the Nucleospin PCR Clean Up kit in order to remove all traces of enzyme and buffer etc. Purified digested plasmid was resuspended in double de-ionised water at -20^{o}C until use for transfection into HEK 293 cells.

2.13 Sequencing of viral plasmids

For sequencing of recombinant plasmids the Dundee University based DNA Sequencing Services was used. Recombinant plasmid DNA was resuspended at in dH20. In addition 32 picomoles in dH_20 of the relevant pShuttle primers were also sent. Samples were sealed in a PCR tube wrapped in parafilm which was then contained within a 1.5 ml Eppendorf, also wrapped in parafilm and sent via post.

2.14 HEK 293 cell transfection using Fugene 6

Transfection of HEK 293 cells was carried out as per the protocol [346]. Briefly, $1x10^6$ HEK 293 cells were plated onto cell culture petri dishes. When ~50% confluency was observed, Opti-MEM media (Invitrogen, UK) was incubated with FuGene 6 (Roche, UK) for 5 mins at room temperature. Digested recombinant plasmid was added to this and incubated for a further 15 mins at room temperature. This mixture was then added in a drop-wise fashion to the dish of HEK 293 cells and left on as per the protocol. Plates including no plasmid but with FuGene 6 and a GFP expressing plasmid (pmax GFP, Lonza, Swizerland) were also included as a positive and negative control for transfection, which were read at 48 hrs for GFP expression. Cytopathic effect (CPE) was subsequently monitored in the coming days, once ~60% CPE was observed, cells were detached from the plates using pipetting. Cells were then spun at 300 x g for 5 mins to create a pellet, washed in PBS (Invitrogen, UK) and re-spun. Pellets were resuspended in sterile PBS and underwent 4 rounds of freeze-thaw, between -80^{o}C and 37^{o}C to lyse the cells. Cells were then spun at 12000 x g for 10 mins with the supernatant (crude virus) taken and stored at -80^{o}C.

2.15 GFP and IL-10 expression levels in HEK 293 packaging cell line during virus production

A positive control plasmid (pmaxGFP) was used during the transfection of the HEK 293 packaging cell line and the success of the transfection was observed via FACS and fluorescent imaging (data not shown).

Before the HEK 293 cells were lysed for the collection of virus, the media was taken for mIL-10 ELISA and the cells imaged using fluorescent imaging. ELISA results (data not shown) showed that mIIL-10 was only found in the flasks containing IL-10 producing viruses (Ad IL-10 and Ad GFP IL-10). Figure 1A shows that fluorescent GFP was only found in the Ad GFP and Ad GFP IL-10 flasks and not in the Ad IL-10 flasks. This showed that during production, the Ad GFP, Ad GFP IL-10 and Ad IL-10 viruses were all producing the appropriate transgene. Figure 1B is a representative brightfield image.

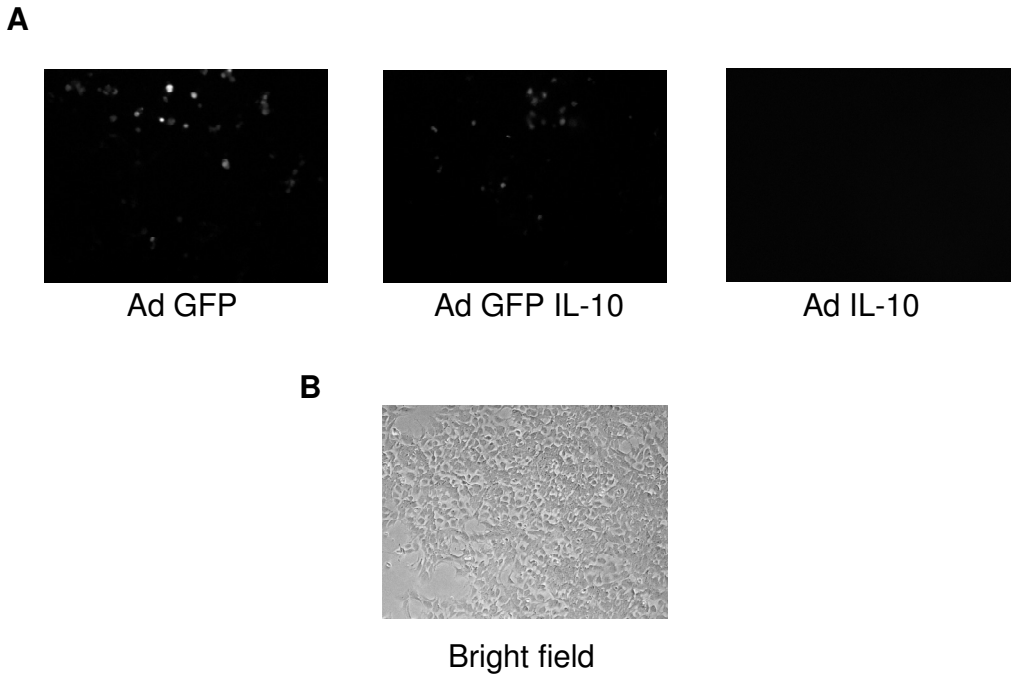

Figure 1: HeLa transduction with Ad GFP, Ad IL-10 and Ad GFP IL-10. The presence of GFP was assessed at this pre-harvest stage, with GFP expression evident from fluorescent imaging of Ad GFP and Ad GFP IL-10 producing flasks but not Ad IL-10 (A). B shows a representative bright field image.

2.16 Creation of viral seed stocks

The crude virus product from Fugene 6 transduction (see previous) was added along with fresh media to 1 x T150 flask at 70% confluency per virus. Once signs of CPE are visible, cells were detached from the T150 flask by incubation with citric saline (see media and buffers section) for 5 min at 37^{o}C followed by gentle bashing to detach remaining cells. Cells were then spun at 300 x g for 5 mins to form a pellet, which was resuspended in 1 ml sterile PBS and transferred to a 1.5 ml Eppendorf. To this Arklome P (Sigma, UK) was added and the mixture shaken well and centrifuged for 5 mins at 14000rpm. As much of the top layer was taken using a pipette, taking care not to disturb the cell debris layer, and was aliquoted into aliquots for storage at -80^{o}C until used.

2.17 Detection of GFP expressing cells using fluorescent imaging

Cells to be imaged were imaged in their respective culture flasks (T150) using a Nikon Eclipse TS100 inverted microscope (Nikon, UK) combined with a FAST 1394 camera (QImaging, Canada) and Image-Pro Plus software (MediaCybernetics, USA), with the excitatory light coming from a mercury vapour lamp (Zeiss, Germany). The mercury lamp was allowed to warm up for 30 mins before imaging the cells. The exposure for the camera was set at 1 s to allow for focusing and 8 s for image acquisition.

2.18 Virus production and purification

A single preparation for one adenovirus uses 25 x T150 flasks of HEK 293 cells. The general protocol for cell splitting is as follows, the DMEM media was removed from a T150 at ~70% confluency (1 flask splits into 5) and cells were washed with sterile PBS. Citric saline was added to the flask and incubated for 5 min at 37^{o}C. The flask is then agitated to remove all cells which were then resuspended in DMEM (all cells in other flasks were resuspended in this same 5 ml of media. Cells were then placed in a Falcon tube and centrifuged at 350 x g for 5 min. Cells were then reuspended in an appropriate volume for aliquoting into 5 new flasks, pre-filled with fresh DMEM media. To infect the 25 flasks, viral seed stock was added to fresh DMEM media which was then used to replace the media in 24 of the flasks, with one flask being kept as a control flask and not receive any virus. Cells were then incubated for 3-10 days until CPE was observed. To collect infected cells, flasks were agitated which detached the majority of cells, adherent cells were removed with pipetting. Cells were transferred into Falcon tubes and centrifuged for 10 min and the supernatant removed completely with pipetting. Cells were resuspended in sterile PBS, collecting the pellet from all Falcon tubes. To this an equal volume of Arklome P was added and the mixture shaken. This was then spun at 3000rpm for 10 min after which the top layer was removed without disturbing the cell debris layer. This crude virus was then frozen at -80^{o}C until purification.

Viral constructs were purified on a Caesium Chloride gradient. Ultracentrifuge tubes (Beckman and Coulter, USA) were sterilised by rinsing with 70% ethanol followed by sterile dH_20, at the same time as the crude virus was thawed on ice. The gradient for the first spin was made as follows, CsCl density 1.45 (see 2.35.1) was pipetted into the sterile ultracentrifuge tube followed by CsCl density 1.32 added in a drop-wise fashion to prevent mixing, which is then followed by 40% glycerol also added drop-wise. The crude adenovirus was then layered on top of these

drop-wise. Sterile PBS was added drop-wise to take the volume to the top of the ultracentrifuge tubes. Tubes were then centrifuged at 35000rpm at 16^{o}C for 1.5 hrs with deceleration set to zero, acceleration to maximum. On completion, a distinct white virus layer was seen with immature components above it. Figure 2, shows the banding observed after spinning the viral products on a double Caesium Chloride gradient. The tube was held in place using a retort stand and a 5 ml syringe with a green 21G needle is used to puncture the side of the tube and the immature portion was removed. Leaving the first syringe in place, a second syringe was inserted into the tube just below the white viral layer and tilted up at an angle to remove the pure virus. A second group of ultracentrifuge tubes were prepared with the following gradient, 1.34 density CsCl, the purified virus dripped on top of this CsCl and sterile PBS added drip-wise to fill the ultracentrifuge to the very top. Tubes were then centrifuged at 35000rpm at 16^{o}C for 18 hours, following which the viral band was taken as described previously. Slide-A-Lyzer cassettes (Thermo Scientific, USA) were pre-soaked in a large beaker with 1 x TE buffer (see media and buffers section) 5 min before the addition of the purified virus. The virus was introduced to the cassette using a plastic syringe and green 21G needle, marking which port had been used. The air was removed from the cassette and soaked in the TE buffer for 2 hr under gentle stirring. 1 x TE buffer was replaced with a fresh TE buffer and the cassette soaked for a further 2 hours. 1 x TE buffer was replaced with 0.5 x TE buffer and 10% glycerol, and the cassette soaked over night. Virus was then removed from the cassette and aliquoted.

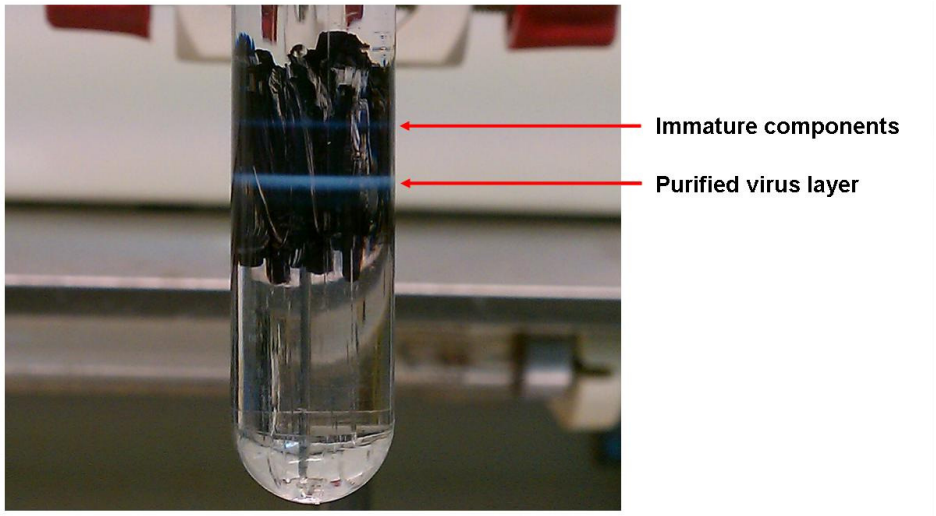

Figure 2: A representative image of the purification banding achieved from the CsCl purification. A black pen is used to colour in the rear of the tube to allow easy viewing of the viral bands. The top band is composed of immature viral components while the lower down band represents the fully formed Adenovirus, which is removed via syringe.

2.19 Total viral particle titre, BCA and NanoSight

The total viral particle count of an adenoviral preparation was calculated using a micro BCA protein assay (Thermo Scientific, USA) as was standard practice in Professor Baker's lab. Viral particle counts were also assessed using a new NanoSight system, but ultimately the count given by the micro BCA assay was the number we used. Standards were constructed as per the protocol with BSA and PBS and 150 µl alliquoted into a flat bottomed 96-well plate. For samples virus was diluted in PBS. To these, freshly prepared BCA working solution was added and incubated for 2 hr at 37^{o}C. Both standards and samples were prepared in duplicate. Following incubation the plate was cooled and absorption read on a plate reader. The following calculation was carried out to find total viral particle number.

Standard µg/ml	Actual protein (µg)/well (**A**)	Abs - blank value (**B**) **A/B**
0.5	0.075	
1	0.15	
2.5	0.375	
5	0.75	
10	1.5	
20	3	
40	6	
200	30	

All A/B values were then averaged for one value. The two readings for each sample were then averaged, the blank subtracted, multiplied by the averaged A/B value and divided for the number of µl in the sample. The three numbers from this was then averaged and multiplied by 1000 which gives the total protein present in µg/ml. For viral particles/ml, this value was multiplied by 4 x 10^{9}.

The NanoSight LM10 microscope along with Nanoparticle Tracking Analysis (NTA) software version 2.1 (NanoSight Ltd., UK) was used to analyse the viral particle concentration. Virus stock to be analysed was diluted 1 in 1000 (1 µl in 999 µl) PBS. A syringe was used to take up the diluted virus and connected to the leur attachment on the imaging cradle and the virus solution was inserted into the cradle. Viral particles were first observed using the eyepiece of the microscope in order to find the correct region in the laser path to see the viral particles. The shutter was then closed on the microscope and the microscope refocused so that the viral particles were in focus through the attached camera and software. The gain and exposure of the camera were adjusted so that only low level saturation was observed. Movies were recorded for 60 sec at polydispersity and concentration set to medium. Further adjustments to gain were made if required and the autotracking feature was used to target the particles for tracking, with alterations made to the blur setting in order to have one track point per particle, following which the movie was analysed.

Infectious particle titering and testing for replication deficiency

To calculate what number of the total viral particles were infectious (plaque forming units, pfu), the following protocol was followed. The cells from 1 fully confluent T150 flask of HEK 293 cells were harvested, resuspended in media and this suspension diluted in fresh media (see 2.35.1). These cells were then added to a flat bottomed 96-well plate, leaving blank the 1st and 12th column, and incubated at 37°C overnight. The media was then removed from these cells and the following serial dilutions and plate layout followed, adding the virus one line at a time to prevent the cells drying out.

Numbers denote 10 to the power of *

	2	2	2	2	2	4	4	4	4	4	
	6	6	6	6	6	6	6	6	6	6	
	7	7	7	7	7	7	7	7	7	7	
	8	8	8	8	8	8	8	8	8	8	
	9	9	9	9	9	9	9	9	9	9	
	10	10	10	10	10	10	10	10	10	10	
	11	11	11	11	11	11	11	11	11	11	
	C	C	C	C	C	C	C	C	C	C	

The viral media was removed after 24 hours and replaced with 250 µl of fresh media. At 8-10 days the plate was then studied for the presence of plaques. Wells which contained signs of budding (plaque formation) were marked and used in the following calculation described in detai [347]. The number of plaque containing wells was fit into the following equation.

The proportionate distance =

$$\frac{\text{\% positive above 50 \% - 50 \%}}{\text{\% positive above 50 \% - \% positive below 50 \%}}$$

and log ID_{50} (tissue culture infectivity dose 50) =

log dilution above 50 % + (proportionate distance x -1) x dilution factor

1 $TCID_{50}$ (tissue culture infectivity dose 50) = 0.7 pfu

In order to assess whether the vectors are capable of replication in cells other than the HEK293 packaging cell line, the same dilutions and plate layout were followed as above, however with HeLa cells replacing HEK 293.

2.20 Adenoviral transduction of HeLa cells

$3x10^5$ HeLa cells were plated per well of 6-well plates 24 hours before infection, in HeLa growth media. A range of virus concentrations from 0 to 10000 vp/cell were used in triplicate, of both the GFP and IL-10 expressing adenoviruses. The media was removed and replaced with 2 mls of serum free media (growth media without FCS) containing the viruses, and incubated for 3 hr at 37°C. After incubation, the media was replaced with fresh growth media and incubated for 48 hr at 37°C. The media was then taken for IL-10 ELISA and the cells removed from the wells using a cell scraper for FACS analysis of GFP expression.

2.21 Miniprep maxiprep

Plasmid production and purification were carried out as per the Mini or Maxi plasmid purification kits (Qiagen, UK). Briefly, for Mini Preps, a single colony of transformed plasmid containing E.Coli is used to inoculate a starter culture of LB broth containing the appropriate antibiotic. This was then incubated for approximately 8 hrs at 37^{o}C with vigorous shaking and the lid taped loosely to the vessel. The number of cultures inoculated was typically 12, if more plasmid was required, a Maxi Kit was used. Cells were then harvested by centrifugation at 6000 x g for 15 min and the supernatant removed. Pellets were resuspended in Buffer A1 and transferred to Eppendorf tubes, to which Buffer A2 is added, the mixture gently inverted 6-8 times and incubated at room temperature for 5 min, which lyses the cells. Buffer A3 is added to cease the reaction and precipitate the lysate, the tube was inverted 6-8 times. Tubes were then centrifuged at 11000 x g in a microcentrifuge for 5 min or until supernatant is clear and the supernatant containing the plasmid DNA is removed without disturbing the cell debris. The supernatant was decanted into a collection tube and spun for 1 minute at 11000 x g to bind the DNA to the silicon membrane. The collection tube was replaced with a fresh tube and Buffer A4 was added before spinning for 1 minute at 11000 x g, washing the DNA. The collection tube was emptied and replaced and the tube spun without addition of buffer for 2 min at 11000 x g which dries the silicon membrane. The plasmid DNA was eluted by addition of 50 µl of Buffer AE and the column placed in a fresh 1.5 ml eppendorf in order to collect the DNA after a 1 min spin at 11000 x g.

For Maxi Prep preparations the following protocol was followed. As before a 5 ml starter culture was inoculated from a single colony. This starter culture is then used to inoculate LB broth containing the appropriate antibiotic, which was then incubated with shaking at 37^{o}C for 18 hr. Cells were harvested by centrifugation at 6000 x g for 15 mins at 4^{o}C. The pellet

was then resuspended in Buffer P1 to which Buffer P2 was added and mixed thoroughly and incubated for 5 mins at room temperature. After incubation, pre-chilled Buffer P3 was added, mixed thoroughly, and incubated on ice for 20 mins. The mixture was then centrifuged at 20000 x g for 30 minutes at 4^{o}C following which the supernatant containing the plasmid DNA was removed promptly. The supernatant was then spun again at 20000 x g for 15 minutes at 4^{o}C after which the supernatant was taken promptly. Before the supernatant was run through a collection column, the column (QIAGEN-tip 500) was pre-equilibrated by running Buffer QBT through it first. The supernatant was applied to the column and allowed to enter the resin by gravity flow. The column was then washed with Buffer QC. DNA was eluted from the columns via the addition of Buffer QF and precipitated by addition of room temperature isopropanol. This was mixed and centrifuged immediately at 15000 x g for 30 mins at 4^{o}C, the supernatant was carefully removed. The remaining DNA pellet was washed with room temperature 70% ethanol and centrifuged at 15000 x g for 10 min. The ethanol was removed and the pellet air dried for 10 min following which the DNA was resuspended in TE buffer and frozen until used.

2.22 Enzyme-linked immunosorbent assay (ELISA)

For both IFN-γ and IL-10 ELISA, Ready-SET-Go ELISA kits were used (eBioscience) and the included protocols followed. To summarize, 96-well microtitre plate (Costar) were coated with antigen or capture antibody in coating buffer (composition refer to the appendix) (100 µl per well), overnight at 4^{o}C. Plates were washed with ELISA wash buffer (x3) (for composition refer to the appendix), and non specific binding was blocked by incubation with blocking reagent (room temperature, 1 hr). Following this, the plates were washed with wash buffer, and the media samples/standards were added (50 µl/well) and incubated for 2 hrs at room temperature. After incubation, plates were washed with wash buffer (x4)

and were incubated with the detection antibody 100 µl per well, diluted in dilution buffer for 1hr at room temperature. Plates were washed (x4) with wash buffer and horse-radish-peroxidise (HRP)-conjugated streptavidin (100 µl/well, diluted in dilution buffer) was added for 30 minutes at room temperature. Plates were then washed (x4) with wash buffer and incubated with 100 µl/well substrate solution for 15 minutes at room temp. The reaction was terminated by the addition of 10% H_2SO_4 and the absorption was determined at OD_{450} using an ELISA plate reader (Molecular Devices).

2.23 Preparation of a single cell suspension from lymph node and spleen

Mice were euthanized by CO_2 asphyxiation and various lymph nodes (LNs) (cervical, inguinal, auxiliary, brachial, mesenteric) and/or spleen were extracted in RPMI complete media (for composition see appendix). Single cell suspensions were prepared by passing them through a 40 µm cell strainer (BD Biosciences) into RPMI complete media using the plunger of a sterile 2 ml syringe (BD Biosciences). Cell suspensions were washed with complete RPMI media and centrifuged at 400 x g for 5 mins at 4^{o}C. When using the spleen, the pellet was resuspended into 2-5 ml of red blood cell (RBC) lysis buffer (ebioscience) and cells were incubated for 5min on ice. 20-40 ml of complete RPMI media was added and the cells were centrifuged (400 x g, 5 mins, 4^{o}C) and resuspended in complete RPMI media. Cells were counted using a haemocytometer with non-viable cells excluded on the basis of trypan blue staining.

2.24 Flow cytometric analysis

Lymph nodes (LNs), spleens and/or livers were made into a single cell suspension as described previously. For surface staining, cells were placed in 6 ml polypropylene FACS tubes, washed with 2 mls of FACS buffer (see buffers section) per tube and centrifuged for 5 minutes at 400 x g. Cells were resuspended in 50 µl of FcR blocking buffer (see buffers section) and incubated at 4-8^{o}C for 15 minutes. Antibodies for surface labelling were diluted in FcR blocking buffer in a concentration from 1-5 µg/ml (1 in 100 dilution) and 50 µl was added to the cells and incubated for 30 minutes at 4-8^{o}C in the dark. Cells were then washed with 2 ml of FACS buffer per tube and centrifuged for 5 minutes at 400 x g. For labelling cell viability, Ethidium Monoazide Bromide (EMA) was used. A 1 in 45,000 dilution was made in PBS, with 800 µl being added per sample. Cells were incubated for 10 mins at room temperature in the dark followed by 10 mins at room temp in front of a bright light. Cells were then washed as described previously. Data were acquired on a FACSCalibur (BD, UK) using Cell Quest Pro software and analysed with FlowJo software (Treestar, USA).

2.25 CD4+ magnetic-activated cell sorting (MACS)

Mice were euthanized by CO_2 asphyxiation and various lymph nodes (cervical, inguinal, auxiliary, brachial, mesenteric) and/or spleen were extracted in RPMI complete media. The CD4+ T cell isolation kit from Miltenyi Biotec (#130-095-248) was used and the manufacturer's instructions were followed. In detail, spleen and LNs were made to single cell suspension as described in 2.24. The cells were then centrifuged (300 x g, 10 min, 4^{o}C), resuspended in 40 µl of MACS buffer (for composition refer to the appendix) per 10^7 cells and 10 µl of antibody cocktail per 10^7 cells and incubated for 10 mins at 4-8^{o}C. According to the manufacturer, the antibodies of the cocktail were directed against CD8a, CD11b, CD11c,

CD19, CD45R (B220), CD49b (DX5), CD105, MHC-class II and Ter-119 (an erythroid cell marker). This incubation was followed by the addition of 30 µl of MACS buffer per 10^7 cells to and 20 µl of anti-biotin labelled magnetic beads per 10^7 cells to the cell suspension and incubation for 15 min at 4-8^oC. Cells were then washed with MACS buffer (30-40 ml), centrifuged (300 x g, 10 min, 4^oC) and resuspended for cell sorting in the appropriate volume of MACS buffer (500 µl per 10^8 cells). LS columns (Miltenyi Biotec) were fitted to a magnet (Miltenyi Biotec), primed with 3 ml of MACS buffer and the cells were applied onto them (up to $2x10^9$ per column). Columns were washed 4 times with 3 ml of MACS buffer and used as a source of antigen presentation cells for the Th1 polarisations. The cells in the positive and negative fractions were counted using a haemocytometer (Hawksley, UK) and trypan blue (Sigma) for non-viable cell exclusion. Cells were washed and resuspended in complete RPMI until further use. In the case of the positive fractions as a source of APCs, cells were treated with mitomycin C (50 µg/ml, Sigma, UK) for 60 mins at 37^oC, 5% CO_2 and were then washed twice with complete media.

2.26 Th1 polarisation

Th1 polarisation was based on the protocol used by Maffia et al. [348]. In detail, MACS sorted CD4+ T cells from DO11.10 mice at a concentration of $5x10^5$ cells/ml were co-cultured with mitomycin C treated MACS positive fraction at a concentration of $5x10^6$ cells/ml in complete RPMI media in the presence of 0.5 µg/ml $OVA_{323-339}$ (Cambridge Biosciences) and the following cytokines and neutralising antibodies: IL-12 (10 ng/ml, RnD Systems), anti-IL-4 (clone 30340, 2 µg/ml, RnD Systems) [349, 350]. Cells were cultured in round bottomed 96 well plates (Costar, UK) for 3 days at 37^oC, 5% CO_2. The phenotype of the polarised cells was assessed by enzyme linked immunosorbent assay (ELISA) of the culture supernatants. In the case of viral transduction of Th1 cells, polarising media was replaced at day 3 with

complete RPMI and incubated for a further 24 hours at 37°C, 5% CO_2, before further use.

2.27 Nucleofection™ of CD4+ T cells

CD4+ T cells were isolated from the lymph node and spleen as previously described (see 2.24), with lymph node and spleen CD4+ cells being kept separate. The Nucleofection™ was carried out as described in the Amaxa, "Optimized Protocol for T cells isolated from C57BL/6 & BALB/c mice" protocol. Briefly, after cell isolation, cells were counted, centrifuged at 90 x g for 10 min and resuspended in the Mouse T cell Nucleofector Solution, at a concentration of $5x10^6$ CD4+ T cells per 100 µl at room temperature. The cell suspensions were then combined with 2.5 µg of pmaxGFP Vector (Amaxa/Lonza, UK), or not (control), and the suspensions transferred into an electroporation cuvette, making sure there are no bubbles and that the cell/DNA suspension remains in the nucleofector solution no longer than 15 min. The cuvette was placed into the Nucleofector device and the Program X-001 was selected. After the program finished, 500 µl of pre-incubated (37°C 5% CO_2) supplemented culture media (see 2.35.1) was added directly to the cuvette, and the total suspension transferred into 1.5 ml pre-incubated (37°C, 5% CO_2) supplemented culture media in a 24 well plate. Cells were then incubated (37°C 5% CO_2) for 48 hr, after which cells were then collected for FACS.

2.28 Lentiviral transduction of C57BL/6 CD4+ T cells

CD4+ T cells were isolated from the lymph nodes and spleen as previously described (see 2.24). The transduction protocol was based on a protocol by Gilham et al. [351]. Briefly, isolated cells were then counted, centrifuged 350 x g 5 mins, and resuspended in complete RPMI containing 25 mM HEPES

(Sigma, UK), 5 µg/ml anti-CD28 and 100 U/ml IL-2 (R&D Systems, UK). Cells were plated at $5x10^4$ per well in a 96 well round bottomed plate, 150 µl per well, which had previously been coated with anti-CD3 (BD Bioscience,UK),incubated overnight at 4°C with 1 µg/ml anti-CD3 in 100 µl PBS. Lentivirus was then added in an additional 50 µl of complete RPMI containing 25 mM HEPES bringing the total volume to 200 µl. The cells and virus were then spinoculated (1200 x g for 90 mins at room temperature) and returned to normal incubation (37°C, 5% CO_2) for 5 days, after which cells were labelled with ethidium monoazide bromide (EMA, Molecular Probes, UK) and CD4 APC (see 2.25 and 2.35.2).

2.29 Generation of bone marrow derived dendritic cells

DCs were generated from bone marrow (of BALB/c mice) as previously described [352]. Bone marrow was flushed out from the femur and tibia of BALB/c mice using a syringe filled with complete RPMI media. Cells were passed through nitex mesh (Cadisch & Sons Ltd. London, UK) to filter any bone particles and tissue and were washed in complete RPMI, centrifuged and counted. Bone marrow cells were plated at a concentration of $1x10^6$cells/well in 6 well plates (Costar) in DC culture media (see appendix for composition). Fresh DC culture media was added at days 3 and 6 with DCs being used on day 7 of the preparation.

2.30 Adenoviral transduction of CD4+ T cells

CD4+ T cells were isolated as described in Materials and Methods (CD4+ Magnetic-Activated Cell Sorting MACS). Where indicated, after MACS separation cells were also polarised to a Th1 phenotype also described in

Materials and Methods (Th1 Polarisation). Adenoviral transduction of T cells was based on a protocol developed by Hurez et al. [296]. In detail, following CD4 isolation, cells were plated in round bottomed 96 well plates (Costar, UK) at a density of $1x10^5$/well in 100 µl of DMEM containing 10 mM HEPES. Virus addition was based on viral particles per cell (vp/cell) and was added to the plated out cells in a further 100 µl of DMEM HEPES per well bringing the total per well to 200 µl. Cells were incubated for 30 mins at 37°C 5% CO_2 with agitation every 10 mins. Following incubation, the plates were spun in a centrifuge at 350 x g for 5 mins to promote pellet formation in the well. Viral media was then aspirated using a pipette and replaced with 200 µl of activation media for 4 hours incubation at 37°C, 5% CO_2. Activation media consisted of complete RPMI with 50 ng/ml phorbol 12-myristate 13-acetate (PMA) and 500 ng/ml Ionomycin (Sigma, UK). In the case where activation was instead carried out using anti-CD3 and anti-CD28 stimulation, cells were transferred to an activation plate which had been coated with anti-CD3 (incubated overnight at 4°C with 1 µg/ml anti-CD3 in 100 µl PBS) and reususpended in 200 µl of complete RPMI containing 5 µg/ml anti-CD28 and incubated for 18 hrs as used in Hurez et al. [296]. Cells were then centrifuged at 350 x g for 5 mins and the media aspirated. Cells were then resuspended in complete RPMI and incubated at 37°C 5% CO_2 for 48 hours, after which either FACS analysis or ELISA were carried out to assess transgene expression levels. In experiments involving non-transduced cells, the same protocol was carried out, only omitting the addition of virus.

2.31 Adoptive transfer of transduced CD4+ T cells

Following transduction (Materials and Methods, Adenoviral Transduction of CD4 T cells), cells were collected from the 96 well plates and the wells washed with PBS to collect any residual cells. Cells were then washed with PBS once and counted, then spun and washed again. Cells were

resuspended in PBS and kept on ice until transfer. Cells were resuspended so that $2x10^6$ GFP+ cells would be in each transfer into the mice. The % transduction achieved in previous data at the 24 hour time point was used in order to judge of how many cells needed to be transferred to achieve $2x10^6$ GFP+ cells, the total transfer number being $3.2x10^6$ cells. $3.2x10^6$ non-transduced were transferred into the non-transduced cell group. Mice were pre-heated in a warming box prior to transfers to induce vasodilation. 1 ml plastic syringes with 25G needles were used for the transfer into either of the veins located on the tail.

2.32 Activation of bone marrow derived dendritic cells

Following the generation of DCs as previously in Methods, on day 7, the plates were spun and the media replaced with fresh DC media (see media and buffers). Along with the addition of fresh media, LPS (Sigma, UK) was added at 1 µg/ml, IL-10 containing media was added for a final IL-10 concentration of 10 ng/ml and anti-IL-10 (R and D Systems, UK) added at 5 µg/ml [353], depending on the experimental group, giving a final volume of 2 mls per well. Cells were then incubated (37^oC, 5% CO_2) for 18 hr and harvested for FACS by carefully scraping them from the wells using a cell scraper, resuspended in FACS buffer and labelled for CD11c APC (BD Bioscience, UK) and MHC II FITC (I-A/I-E) (eBioscience, UK).

2.33 Statistics

Data were analysed using the GraphPad Prism® software. To test if the means of two samples are different, the Student's t-test or Mann-Whitney test was used, to compare the means of two or more samples, one-way

analysis of variance (ANOVA) was used, when the interaction of two independent variables were tested, a two-way ANOVA was employed. A value of $p<0.05$ was considered significant.

Appendix

2.33.1 Media and Buffers

Phosphate Buffered Saline

(PBS) 1x 1000ml

NaCl	8g	Sigma
KCl	0.2g	Sigma
Na_2HPO_4	1.44g	Sigma
KH_2PO_4	0.24g	Sigma

Fc Receptor Blocking

Buffer

Supernatant from 2.4G2

Hybridoma cultures

Mouse Serum	10%	Biosera
NaN_3	0.01%	Sigma

FACS Buffer

PBS	1x	
FCS Invitrogen	2%	GIBCO,
NaN_3	0.1%	Sigma

MACS Buffer

PBS Invitrogen	1x, pH7.2	GIBCO,
FCS Invitrogen	2%	GIBCO,
EDTA	2mM	Sigma

Roswell Park Memorial Institute (RPMI) complete Media

RPMI-1640 Invitrogen	1x	GIBCO,
FCS Invitrogen	10%	GIBCO,
Penicillin Invitrogen	10,000U/ml	GIBCO,
Streptomycin Invitrogen	10,000µg/ml	GIBCO,
L-Glutamine Invitrogen	200mM	GIBCO,

Dendritic Cell Inducing

Culture Media

RPMI	1x	GIBCO, Invitrogen
Supernatant from the X65 GM-CSF producing cell line	10%	
FCS	10%	GIBCO, Invitrogen
Penicillin	10,000U/ml	GIBCO, Invitrogen
Streptomycin	10,000µg/ml	GIBCO, Invitrogen
L-Glutamine	200mM	GIBCO, Invitrogen

T cell transduction Media (adenovirus)

Dulbecco's Modified Eagle Medium (DMEM)	1x	GIBCO, Invitrogen
HEPES Buffer	10mM	Sigma

T cell Transduction Media (lentivirus)

RPMI Invitrogen	1x	GIBCO,
FCS Invitrogen	10%	GIBCO,
Penicillin Invitrogen	10,000U/ml	GIBCO,
Streptomycin Invitrogen	10,000µg/ml	GIBCO,
L-Glutamine Invitrogen	200mM	GIBCO,
HEPES Buffer	25mM	Sigma

10x Citric Saline

Distilled Water	500ml	Sigma
KCl	50g	Sigma
Sodium Citrate	22g	Sigma

TD Buffer 10x (pH7.4)

Distilled Water	1000ml	
NaCl	80g	Sigma
KCl	3.8g	Sigma
Na_2HPO_4	2.5g	Sigma
Tris Base	30g	Sigma

TE Buffer 10x (pH8)

Distilled Water	1000ml	
Tris-HCl	12.1g	Sigma
EDTA	3.72g	Sigma

Caesium Chloride Gradients

1.25g/ml

CsCl	18.08g	Sigma
TD Buffer 1x	50ml	

1.40g/ml

CsCl	31.1g	Sigma
TD buffer 1x	50ml	

1.34g/ml

CsCl	25.6g	Sigma
TD buffer 1x	50ml	

HEK293, 293T and HeLa Growth Media

DMEM	500ml	GIBCO, Invitrogen
Penicillin	10,000U/ml	GIBCO, Invitrogen
Streptomycin	10,000µg/ml	GIBCO, Invitrogen
FCS	50ml	GIBCO, Invitrogen
Sodium Pyruvate	5ml	Sigma

LB Broth

Distilled Water	1000ml	
LB Broth	20g	Sigma

NZY+ Broth

De-ionised Water	1000ml	
Casein Hydrolysate	10g	Sigma
Yeast Extract	5g	Sigma
NaCl	5g	Sigma
MgCl2 1M (added before use)	12.5ml	Sigma
MgSO4 1M (added before use)	12.5ml	Sigma
Glucose 20% (added before use)	20ml	Sigma

ELISA Wash Buffer

PBS	1x	
Tween	0.05%	Sigma

ELISA Blocking Buffer

PBS	1x	
FCS	10%	GIBCO, Invitrogen

ELISA Dilution buffer

PBS	1x	
FCS	0.2%	GIBCO, Invitrogen
Tween	0.05%	Sigma

2.33.2 Antibodies

Target	Antibody Name	Isotype	Provider
CD4	anti-CD4-APC, Clone GK1.5	Rat IgG2b, κ	eBioscience
DO11.10	anti-DO11.10 TCR-PE, Clone KJ1-26	Mouse IgG2a, κ	eBioscience
MHC II	anti-MHC II (I-A/I-E), Clone M5/114.15.2	Rat IgG2b, κ	eBioscience
CD11c	anti-CD11c-APC, Clone HL3	Hamster IgG1, λ2	BD Bioscience
CD3	anti-CD3e NA/LE, Clone 145-2c11	Hamster IgG1, κ	BD Bioscience
CD28	anti-CD28 NA/LE, Clone 37.51	Hamster IgG2, λ1	BD Bioscience

Chapter 3: Real time imaging of leukocyte dynamics in ApoE$^{-/-}$ mouse aortic tertiary lymphoid organs

3.1 Aims and rationale

In this chapter, *ex vivo* multi photon laser scanning microscopy (MPLSM) was used to promote new insights into the behaviour of leukocytes within the arterial tertiary lymphoid organ (ATLO) of aged (80-90 weeks) $ApoE^{-/-}$ mice. Achieving a greater understanding of where, when and how the cellular interactions that regulate the immune response in atherosclerosis is fundamental to developing effective therapeutic interventions in the future. Thus far however, a number of technical limitations have prohibited real time quantitative imaging of individual immune cells within the intact atherosclerotic vessel. Here, multiphoton laser scanning microscopy (MPLSM) is used for real time imaging at cellular resolution and quantitative analysis of labelled adoptively transferred leukocytes in the adventitia of $ApoE^{-/-}$ mice aorta and ATLO region, which is implicated in late stages in atherosclerosis.

3.2 Introduction

Atherosclerosis can in broad terms be defined as a progressive thickening and hardening of the walls of arteries due to the absorption and accumulation of fatty deposits, with plaque formation occurring between the tunica media and tunica intima. Due to evidence at the time, lipids were thought to be the key cause of this pathology pre-1970 [46], this then moved onto focus on the proliferation of smooth muscle cells and growth factors in the 1970's and 80's, however in the last decade an appreciation of the prominent role the immune response play has developed. Although evidence supports the involvement of the immune response in a systemic nature towards hyperlipidemia, a considerable amount of recent data suggests that a highly local immune response developing within the vessel wall itself may be of key importance [40, 49-51].

During both the early and late stages of atherosclerosis in mouse models, there is accelerated leukocyte recruitment into the arterial wall, with the majority of lymphocytes residing the adventitia of the arteries [40, 51]. A unique phenomenon found in the very late stages of disease progression is the development of fully structured adventitial aortic tertiary lymphoid organs (ATLOs), containing B cell zones, germinal centres, plasma cells, T cell zones as well as high endothelial venules (HEVs) [49, 50]. Aggregations of leukocytes within the adventitia were first reported in the 1970's by Gerrity et al. [57] but these conglomerates of cells were only first termed part of the vascular-associated lymphoid tissues (VALTs) in a review by Wick et al. in 1997 [279]. Within these ATLOs are proliferating leukocytes and CD138+ plasma cells [291] which could indicate a locally generated immune response, possibly directly linked to the plaque on the interior of the vessel. Although the internal structure of the ATLO has been revealed through detailed immunohistochemistry, the actual role that the ATLO plays is still unclear, in particular, if it is detrimental or beneficial in the

context of the pathology. To shed light on the workings of the ATLO in the context of a non-fixed, non-sectioned vessel, (MPLSM) can be utilised.

In the last decade, MPLSM has allowed real time *in vivo* imaging and analysis of individual immune cell interactions in the context of the tissue being studied, and offers insight into the dynamics of the developing immune response [341, 343, 354]. Study of these dynamics can give us great insight into cell to cell interactions, such as the migration and interaction of T and B cells [355], the activation state of the immune system [356] and even the study of parasite motility [357] in infections. Although it is known that the structure and composition of the ATLO is remarkably similar to that of a peripheral lymph node, it is indefinite if the cells inside it behave like those found in the periphery and consequently, further study may help elucidate its role in pathology.

In recent years, protocols have been established that allow structural [167, 358-362] and functional [363, 364] MPLSM imaging of intact large vessels. Few studies have used intravital imaging of exposed arteries, primarily because of its sensitivity to sample movement due to blood flow and respiration movement [365]. Motion artefacts could be avoided by blocking the blood flow [170] or by accelerated image acquisition triggered on cardiac and respiratory activity, at the cost of reduced image quality [168]. The latter approach enables imaging of a stable area of interest over time but comes at the cost of reduced time resolution and reduced image quality [365].

Yet, for quantification of immune cell recruitment in the vessel wall *in vivo* MPLSM is more difficult for several reasons including the small field of view. Thus so far, application of MPLSM has only been utilised in a few laboratories, mainly for imaging neutrophils or total leukocytes adhering to the carotid artery of $ApoE^{-/-}$ mice [170, 366]. In addition, MPLSM has been used for 3-dimensional *ex vivo* imaging of leukocyte recruitment into the

adventitia of ApoE$^{-/-}$ mice [51], for static imaging of CD11b-positive foam cells in atherosclerotic plaque of ApoE$^{-/-}$ mice mounted arteries [169] and elegantly for 3D revealing of EGFP+ DCs in close contact with CD4+ T cells in the carotid artery bifurcation and the aortic root of hypercholesterolemic mice [70].

To date, however, none of the above mentioned methods are suitable for studying dynamics and behaviour of inflammatory cells recruited into the vessel wall.

In this chapter, a viable protocol is presented for the MPLSM real time imaging of adoptively transferred leukocytes in the adventitial region of intact ApoE$^{-/-}$ mouse arteries, including the associated ATLO regions. Individual cell tracks are then analysed and their movement dynamics quantified. This is the first application of MPLSM in this way, representing a new and powerful tool to dissect the immune systems interactions directly in the context of the atherosclerotic vessel.

3.3 Results

3.3.1 Adoptively transferred labelled leukocytes, migrate and reside in the adventitia at the ATLO region of aged ApoE$^{-/-}$ mice in larger numbers than in aged C57BL/6 control mice

It has been previously shown through highly detailed histology and immunofluorescent labelling, that the preferential site for ATLO formation is located in the abdominal region of the aortic tree [50]. Therefore the aortic trees were dissected as shown in Figure 1, taking the section from between the renal artery and diaphragmatic muscle. Vessels were cleaned of any fat and also lymph nodes located on the peripheral of the vessel to prevent possible contamination. Due to the difficulty in visualising the ATLO with the naked eye, vessels were first imaged using epifluorescence and areas with high levels of red cell accumulation were then imaged and analysed using the 2-photon microscope. Several areas scanned in aged C57BL/6 mice showed no leukocytes or rarely more than 1 to 2 cells per imaging volume, these cells all being found in the adventitial layer of the vessel Figure 2A. As expected, several red labelled transferred cells could be found in the adventitia of aged ApoE$^{-/-}$ mice with preferential accumulation regions identified as the site of ATLO formation (Figure 2B). To quantify the number of cells in each imaging volume, cell counts were normalised for the volume of the field and averaged for each mouse. As shown in Figure 2C, the mean leukocyte density was significantly (P<0.001) higher in ApoE$^{-/-}$ mice (9.09 ± 1.32 thousand/mm^3, n=8) compared to the C57BL/6 wild type mice (0.83 ± 0.27 thousand/mm^3, n=11). It is worth noting that the actual density of labelled transferred cells in the aorta is greater than these numbers suggest as the volumes in the C57BL/6 mice containing no fluorescent cells were not imaged and so excluded.

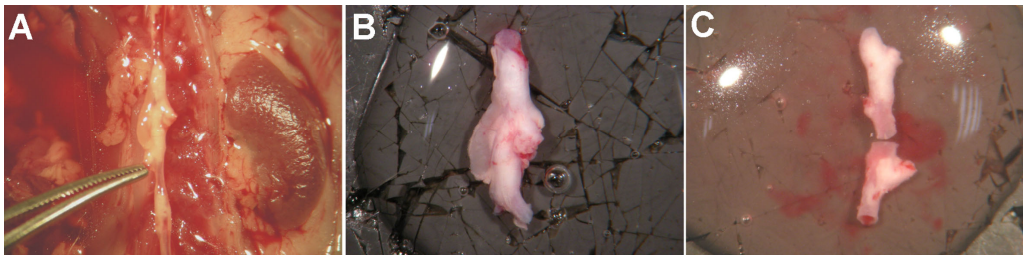

Figure 1: Representative images of the dissection of the ATLO region of aortic tree. 24 hours post-transfer, the region between the diaphragmatic muscle and renal artery (A), was excised under a dissecting microscope with all the fat from around the vessel removed (B). The para-aortic LN was then separated from the artery (C) and the cleaned vessel imaged as described.

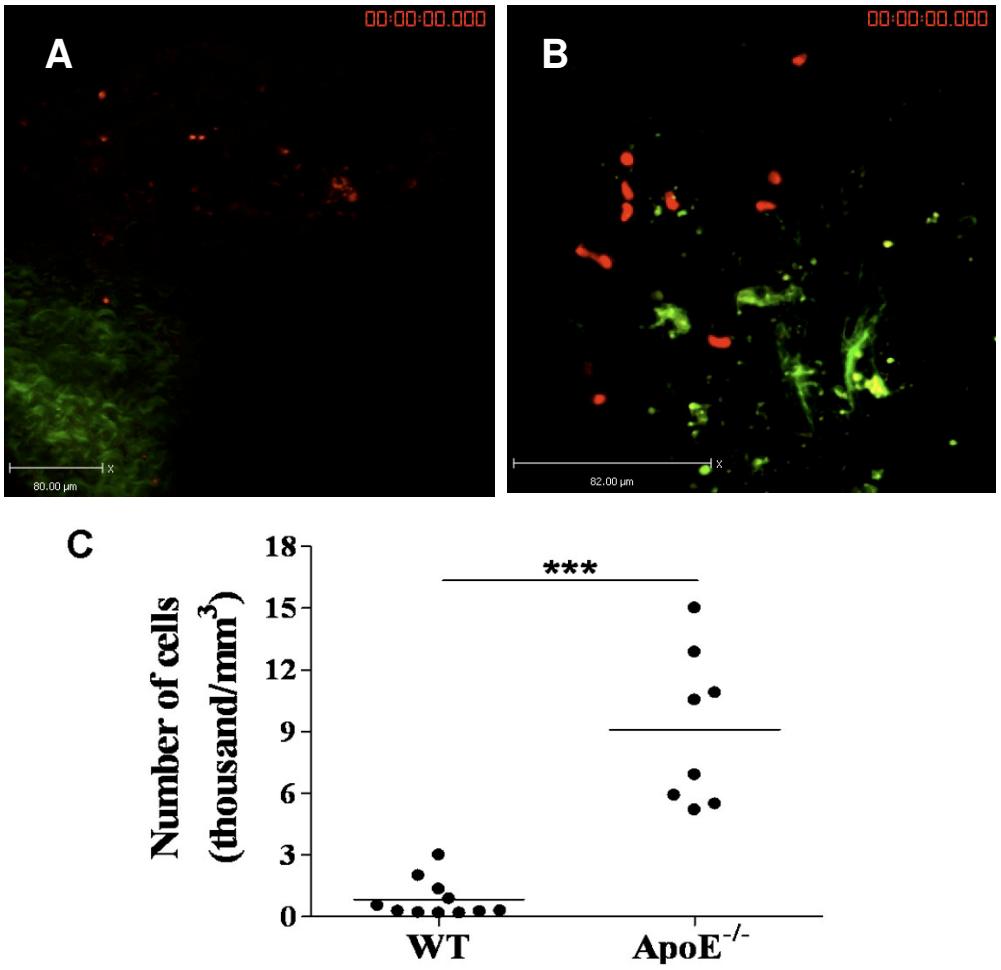

Figure 2: Total number of labelled leukocytes present in the ATLO region of aged WT and ApoE$^{-/-}$ mice. At 24 h after transfer, few leukocytes were seen in the adventitia of the C57BL/6 mice (A), whereas many more red labelled leukocytes were observed in the aortic adventitia/ATLO of aged ApoE$^{-/-}$ mice (B). Elastin fibres in the media were clearly visible due to autofluorescence. (C) Numbers of leukocytes observed in the assessed volume in 8 ApoE$^{-/-}$ mice *vs* 11 C57BL/6 mice. Individual data points represent average value per mouse; horizontal bars indicate mean. ***P<0.001.

3.3.2 Labelled cells in the ATLO region of aged ApoE$^{-/-}$ mice showed higher motility, velocity, displacement and meandering index than labelled cells seen in the aged C57BL/6 mice

A great deal of information can be ascertained through the study of immune cell dynamics, looking at parameters such as how fast the cells move, how far they travel and what their path of migration is [367] [344]. We therefore used the tracking software Volocity, to plot the tracks of each of the red labelled cells. From these tracks a range of parameters, associated with immune cell behaviour were measured. Examples of these tracks can be seen in Figure 3 A and B, showing the cells at the beginning of their track and 40 minutes later respectively. To counter the inevitable tissue drift, drift correction software was used. Points of clearly defined autofluorescent elastic lamina were used as static reference points and the movement (Figure 3C and D) subtracted from the tracks of the labelled cells. Representative 3-dimensional plots of the track of a single cell before (Figure 3E) and after the drift correction (Figure 3F).

Leukocytes in the ATLO region of an aged ApoE$^{-/-}$ mice showed clearly enhanced dynamics compared to WT animals (Figure 4). With the exception of 1 animal in the 11 that were analysed, the few leukocytes imaged in the C57BL/6 mice were almost stationary with an average velocity of <2 μm/min, with cell movement generally confined to a radius of ~10 μm. In contrast, leukocytes found in the ATLO region of the ApoE$^{-/-}$ mice, moved quickly with an average speed of 3.59 ± 0.14 μm/min with cells moving over 100 μm found in all 8 mice. In addition to significantly increased track velocity (Figure 4), cells in the ApoE$^{-/-}$ ATLO region showed significantly increased displacement (Figure 4) and a higher meandering index (Figure 4) compared to cells imaged in the C57BL/6 mice. Transferred labelled cells were compared in the pLNs between ApoE$^{-/-}$ and C57BL/6 mice (Figure 5). There was no statistical difference between track length, track velocity or displacement between the groups.

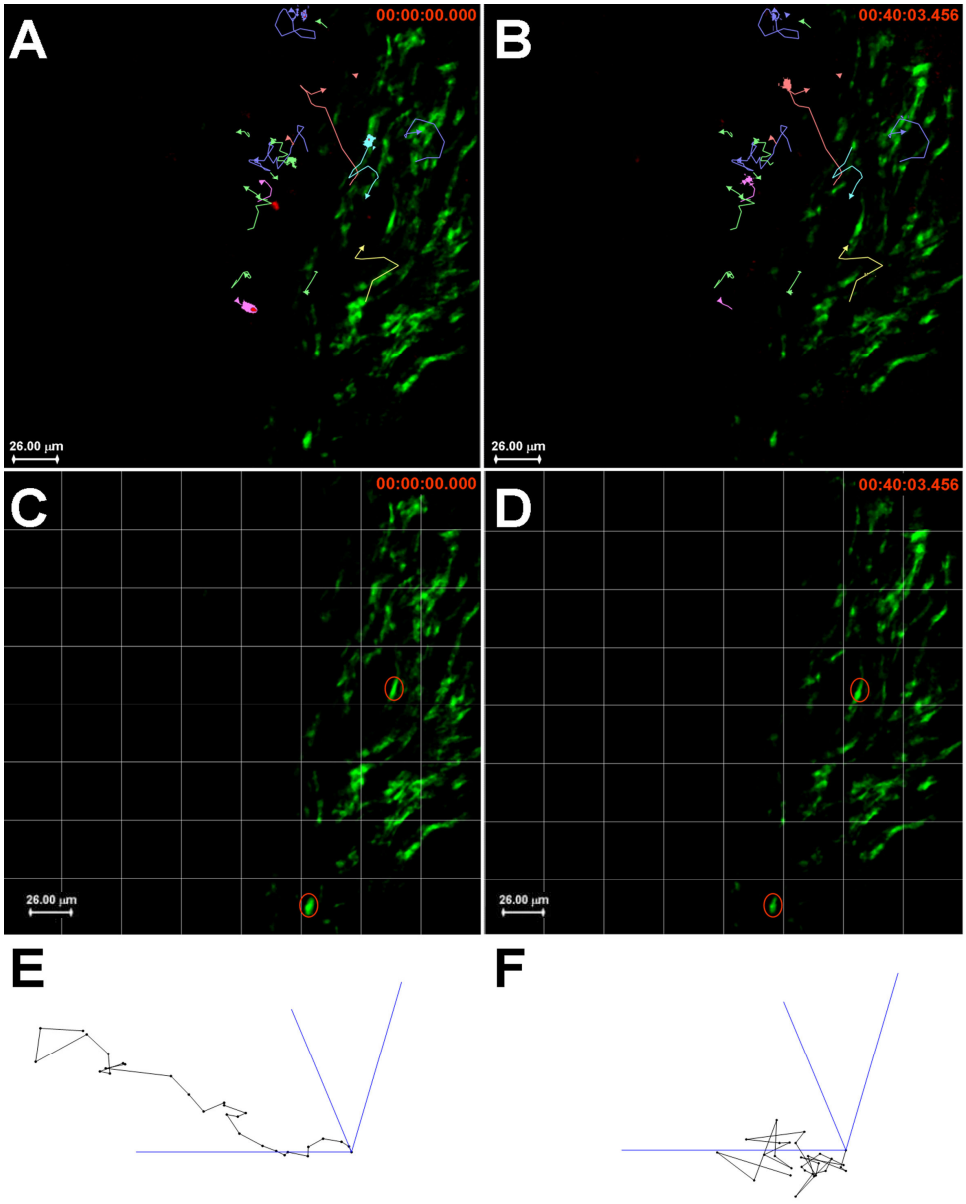

Figure 3: Representative tracks of labelled leukocytes in the vessel wall with and without drift correction. (A,B) Movements of cells in the ATLO. Successive positions of the cells in (B) were joined by coloured lines and images at 2 time points (0 and 40 min) are shown. For quantitative analysis of cells dynamics correction for tissue drift was carried out using elastic fibres (green autofluorescence) as reference objects (C and D; images at 2 time points 0 and 40 min). The average displacement of the centres of mass of elastic fibres was calculated for each time point, and subtracted from the movement of all tracked cells. (E,F) Representative 3-dimensional plots of the track of a single cell before (E) and after (F) correction for tissue drift.

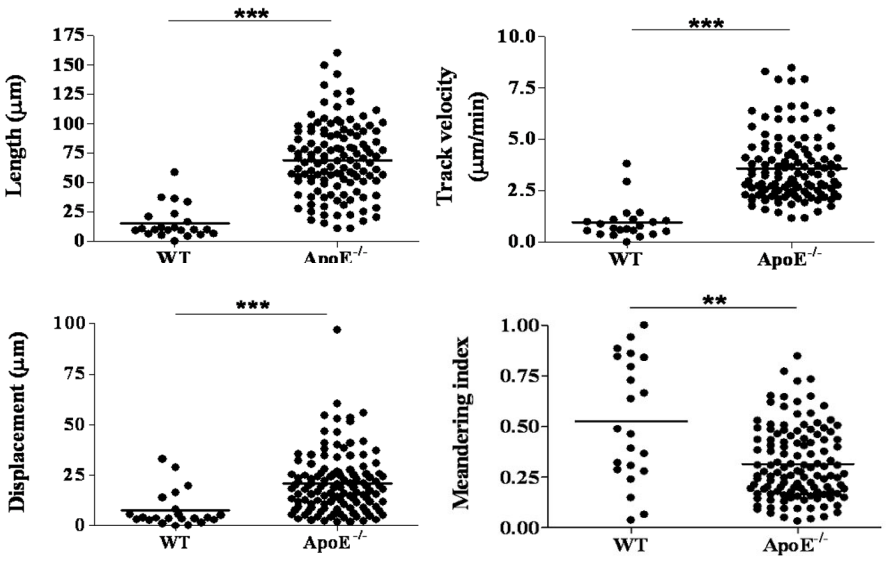

Figure 4: Track parameters of labelled leukocytes in the ATLO region of aged WT and ApoE$^{-/-}$ mice. Quantitative analysis of leukocyte dynamics, correction for tissue drift was carried using custom made software (see Methods). Cells in the ATLO exhibited significantly greater length, track velocity, and displacement compared with cells in the adventitia of WT mice. Results are expressed per single cell from a total of 8 ApoE$^{-/-}$ *vs* 11 C57BL/6 mice analyzed. Horizontal bars denote mean. ***P*<0.01; ****P*<0.001.

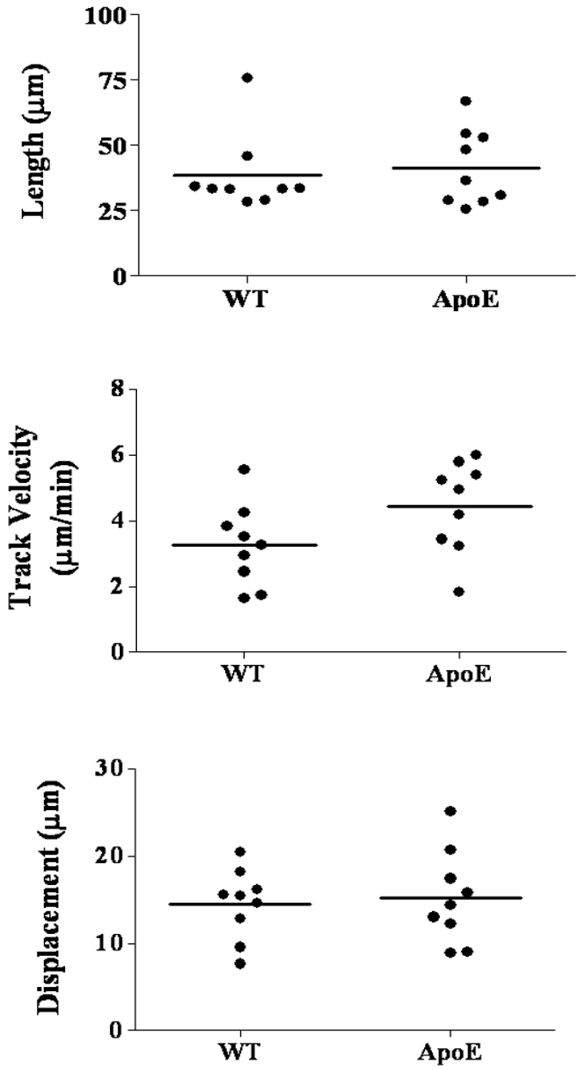

Figure 5: Track parameters of labelled leukocytes in the peripheral lymph nodes of aged WT and ApoE$^{-/-}$ mice. Cells in the pLN of ApoE$^{-/-}$ mice exhibited similar length, track velocity, and displacement compared with cells in the pLN of WT mice. Individual data points represent average value per mouse; horizontal bars denote mean.

3.3.3 Track velocity and displacement of labelled cells within the ATLO region of aged ApoE$^{-/-}$ mice were similar to labelled cells in the pLN

To observe if transferred cells behaved in a similar manner between the ATLO region and a peripheral lymph node, dynamics of transferred labelled cells were compared between the ATLO region and pLN within the same mouse. No statistical difference was seen in either track velocity or displacement (Figure 6 B,C) however, a difference was seen in both track length and meandering index (Figure 6 A,D).

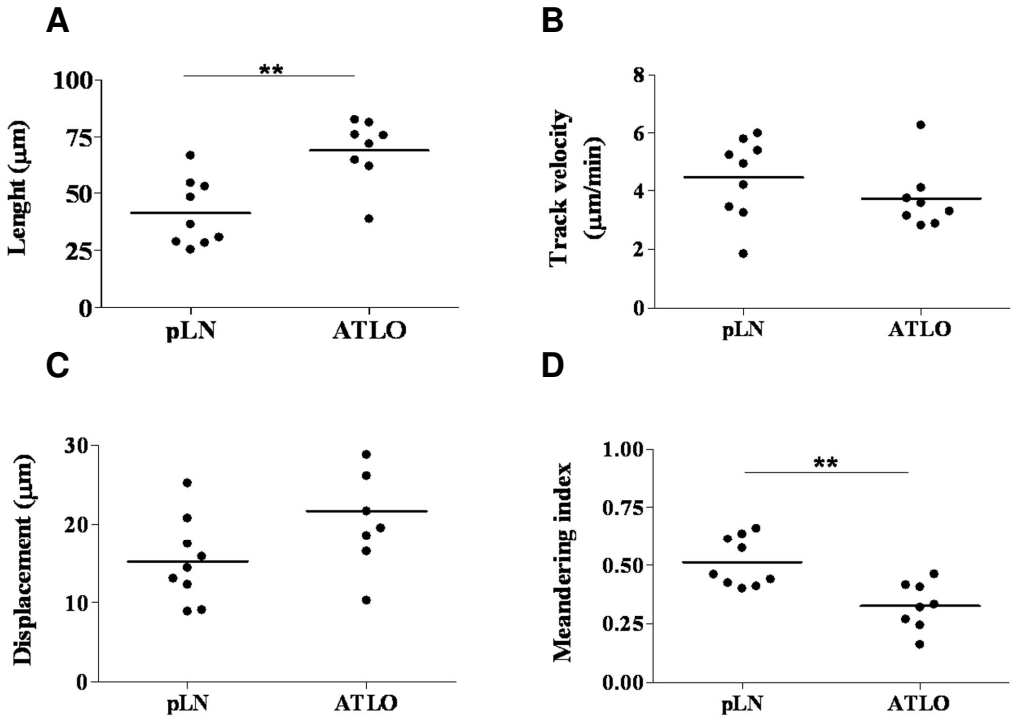

Figure 6: Quantitative analysis of red labelled leukocyte dynamics in the ATLO *vs* pLN (popliteal). Cells in the ATLO exhibited similar dynamics, track velocity, displacement (B,C) to leukocytes in the lymph node of the same mice. Cells in the ATLO covered longer mean path length (A) and showed a higher meandering (D) compared to leukocytes in the pLN. Individual data points represent average value per mouse; horizontal bars denote mean. $^{**}P<0.01$

3.4 Discussion

In this chapter, the dynamics of adoptively transferred CMTPX labelled leukocytes have been studied in the adventitial and ATLO regions of both aged ApoE$^{-/-}$ and Wild Type C57BL/6 mice, using multiphoton laser-scanning microscopy. It was found that an accumulation of the labelled leukocytes was found only in the ApoE$^{-/-}$ mice with little or none being found in the adventitia of wild type C57BL/6 mice. The cells found in the ApoE$^{-/-}$ mice displayed higher velocity, track length and displacement than the few labelled cells found in the wild type mice and there was no difference in any of the movement parameters when comparing the peripheral lymph node of the wild type and the ApoE$^{-/-}$ mice. Lastly, no statistical difference was seen with track velocity and cell displacement between the peripheral lymph node and ATLO region of ApoE$^{-/-}$ mice however a difference was seen in the track length and meandering index.

As described in previous work [50, 291], the region between the diaphragmatic muscle and renal artery is the preferential region for tertiary lymphoid organ formation. As the ATLO itself is not discernable with the naked eye, this preferential area was first scanned using epifluorescence and areas showing high densities of red cells were then imaged using the 2 photon system. As hypothesised, a significantly larger number of labelled cells were observed in the ATLO region of ApoE$^{-/-}$ mice compared to the same region in the wild type mice. It is worth noting that as regions with no fluorescent cells were not imaged and that far less cells were in the aortas of C57BL/6 mice, the volumes used for normalisation between the groups would have been quite different. This implies that the number of fluorescent cells per mm^3 in the wild type group were perhaps actually lower than this data suggests. This correlates with the histological study of ATLOs by Andreas Habenicht's group [50, 291] which also utilised an adoptive transfer approach using labelled leukocytes. It was established that after only 3 hrs, labelled cells were detectable in all ATLO

compartments with a particular preference for the ATLOs T cell compartment.

An early problem we encountered when imaging the vessel was tissue drift, due to the workings of the perfusion chamber that was used. Custom software developed by Dr Francis Burton (SULSA, UK), overcame this issue by effectively subtracting any movement due to drift from each cell track, thereby only leaving the true data for analysis. This system for counteracting sample drift could be used in the MPLSM tracking of moving cells in many different settings and has proven an essential tool in our study.

Using these corrected tracks, it was observed that the majority of labelled cells imaged in the wild type mice appeared to be stationary, as defined by Miller et al. [354] as a speed of <2 μm/min. These cells therefore also had a very small displacement value, owing to their lack of motility in the vessel wall, this lack of overall motility being represented in Figure 4. This was in contrast to the behaviour expressed by the labelled cells found in the ATLO region of the aged ApoE$^{-/-}$ mice, which showed higher velocity, longer track lengths, higher displacement and a larger meandering index. This significant difference in motility of the labelled cells found within the ATLO region of ApoE$^{-/-}$ mice, compared to the wild type mice, clearly indicates that the cells in the ApoE$^{-/-}$ mice are part of some activity or function that is not present in wild type mice. This, taken along with our data showing a significant accumulation of cells in the vessel wall of ApoE$^{-/-}$ mice permits us to assume that it is indeed the ATLO we have imaged and that our methods in locating, imaging and tracking the cells within the organ are effective.

In order to rule out that this difference in cell behaviour was in some way due to the chronic hypercholesterolemia or some other aspect present systemically in the ApoE$^{-/-}$ mice, the cellular dynamics were compared

between the pLNs of wild type and ApoE$^{-/-}$ mice. It was found that no difference was recorded in any of the parameters measured between the two groups, therefore indicating that the increase seen in cellular motility was specific to the ATLO region of the vessel.

Lastly, as was shown by Grabner et al. [50], the ATLO is structurally similar to a peripheral lymph node, containing similar cells and compartmentalisation e.g. T cell zones, germinal centres etc. suggesting that it may function as an "on-site" lymph node. We therefore wanted to compare the behaviour of labelled cells between the ATLO region and peripheral (popliteal) lymph node of ApoE$^{-/-}$ mice in order to observe if there were similarities between the two sites. It was found that the dynamics of cells found in the pLNs were analogous to those of the labelled cells within the ATLO. It should be noted that here we measured the mean cell velocity in the pLNs as around 4.45 ± 0.46 μm/min, which is slightly slower when comparing to data reported in the literature [354], where T cells were shown to have a mean velocity of ~10 μm/min and B cells of ~6 μm/min. In the literature, cells with speeds of <2 μm/min were define as stationary and excluded by their analysis. In contrast, we have analysed all the cells visualized in order to get a fuller picture of cellular dynamics in this unexplored environment. Interestingly, cells analysed in the ATLO covered significantly longer path lengths and also had a higher meandering index than those found in the pLNs. Although the other parameters of cell velocity and displacement showed no statistical difference between groups, these parameter differences of how far each cell travels and to what degree it deviates from a direct path, may indicate that the cells are interacting with unseen elements of the ATLO environment. These diverse patterns of behaviour suggest that the reticular fibre network could be different in the ATLO versus the secondary lymph node, perhaps less organised and refined.

In conclusion, this is the first application of MPLSM for quantitative real time imaging of arterial wall inflammation at the cellular level and has proven to be an effective tool to study the immune interactions in the context of the intact atherosclerotic wall. This live imaging of the vessel will provide key insight into the dynamic and complex range of immunological events, cellular and molecular, that occur in all stages of atherosclerosis. Research just published by Ekaterina Koltsova et al. [368] has taken the imaging of immune interactions within the vessel wall a step further. In this paper it was shown that CD4 T cells were capable of interacting with labelled APCs within explanted aortas, but that this only occurred in the presence of the cognate antigen for the T cells, therefore showing that antigen presentation to T cells in the vessel wall results in local T cell activation. In combination with the extensive and ever expanding range of target specific fluorescent markers as well as genetically modified mice, MPLSM of the aortic wall could open a vast array of options for studying the immune response, not just in atherosclerosis but for other cases of vascular pathology also. This is also the first instance of MPLSM of the relatively undefined ATLO. The data has shown a distinct accumulation of transferred labelled cells only in the aorta of aged $ApoE^{-/-}$ mice and that the cells present within these regions behave in a similar way to cells found in the peripheral lymph nodes. Whether these structures are beneficial or harmful is not entirely clear at this early stage of study, however it is important that we do not rely on our knowledge of immune interactions in the well defined secondary lymphoid organs, as the response generated in these tertiary organs develops in a completely different microenvironment, surrounded by inflammatory cells, damaged tissue and defective lymphatic drainage and as such exhibit altered characteristics [369]. Elucidating the mechanisms occurring within these tertiary structures will be crucial for understanding their role and for either inducing or preventing their contribution to a range of pathologies [370-372], including its role in atherosclerosis.

To summarize:

- A higher number of transferred leukocytes migrate and reside in the adventitia at the ATLO region of aged ApoE$^{-/-}$ mice than in aged C57BL/6 mice

- The transferred cells in the ATLO region of aged ApoE$^{-/-}$ mice showed increased motility compared to those found in the aorta adventitia of aged C57BL/6 mice

- Labelled cells in the peripheral lymph nodes of both mouse groups have comparable motility kinetics, indicating that the difference in cell behaviour observed in the ATLO region of aged ApoE$^{-/-}$ mice was due to the ATLO and no a systemic aspect of the animal model

- The transferred cells found in the ATLO region of aged ApoE$^{-/-}$ mice behaved in a similar way to transferred found in the peripheral lymph node of the same mouse indicating that cells in the ATLO act in a similar fashion to those in the peripheral lymph nodes.

Chapter 4: Production and testing of GFP and murine IL-10 expressing adenovirus

4.1 Aims and rationale

In this chapter, four different adenoviral vectors were constructed for further use in the transduction of murine CD4+ T cells. The four vectors consisted of an empty vector, a GFP only, an IL-10 only and also a dual expressing GFP and IL-10 vector. The dual expression vector would allow both detection of the cells location and the release of the therapeutic cytokine, a vector not described in the literature to date. The newly produced vectors were tested at the production stage and also post-production in an easily transducible cell line to assess transgene expression before finally being tested in murine CD4+ T cells. The protocol from the Ad-Easy kit from Agilent Technologies was followed to produce the vectors.

4.1.1 Production of Ad GFP, Ad GFP IL-10, Ad IL-10 and Ad empty recombinant plasmids

The sequence for murine IL-10 was ascertained as described in the methods, the sequence for is documented in Figure 1C. In order for GeneArt to synthesis the IL-10 and then sub-clone it into the 2 different pShuttle vectors (pShuttle CMV and pShuttle-IRES-hrGFP), appropriate restriction sites were chosen from the multiple cloning site (MCS), as displayed in Figure 1A and B and incorporated into the appropriate ends of the murine IL-10 sequence. The pShuttle plasmids were returned from GeneArt with sequencing analysis showing the presence of murine IL-10 in both pShuttle plasmids, shown in Figure 2 and Figure 3. In order for the pShuttle plasmids to undergo homologous recombination within the BJ5183 bacterial cell line, they first needed to be linearised using the protocol recommended restriction enzyme PmeI, pShuttle CMV for an empty vector, pShuttle CMV IL-10 for an IL-10 only vector, pShuttle IRES hrGFP for a GFP only vector and pShuttle IRES hrGFP IL-10 for a GFP and IL-10 producing vector. Linearisation of pShuttle CMV IL-10 with PmeI was problematic and so an alternative restriction enzyme, EcoRI, was used resulting in successful linearisation. Following the transfection of the BJ5183 cells with the linearised pShuttle plasmids and AdEasy plasmid, individual colonies of the cells were screened for correct recombination, this being shown by banding at ~30 kb and ~4.5 kb. A representative image of a plate with mixed colony sizes is shown in Figure 4A, the smallest colonies (example indicated in red) represented possible recombinant plasmid colonies and were picked based on size. A range of colonies were screened, an example of a positively identified recombinant colony indicated by a red box in Figure 4B. After several rounds of screening, recombinant plasmids were found for each of the pShuttle plasmids (Figure 4C), which were then grown and used for transfection of the HEK 293 packaging cell line.

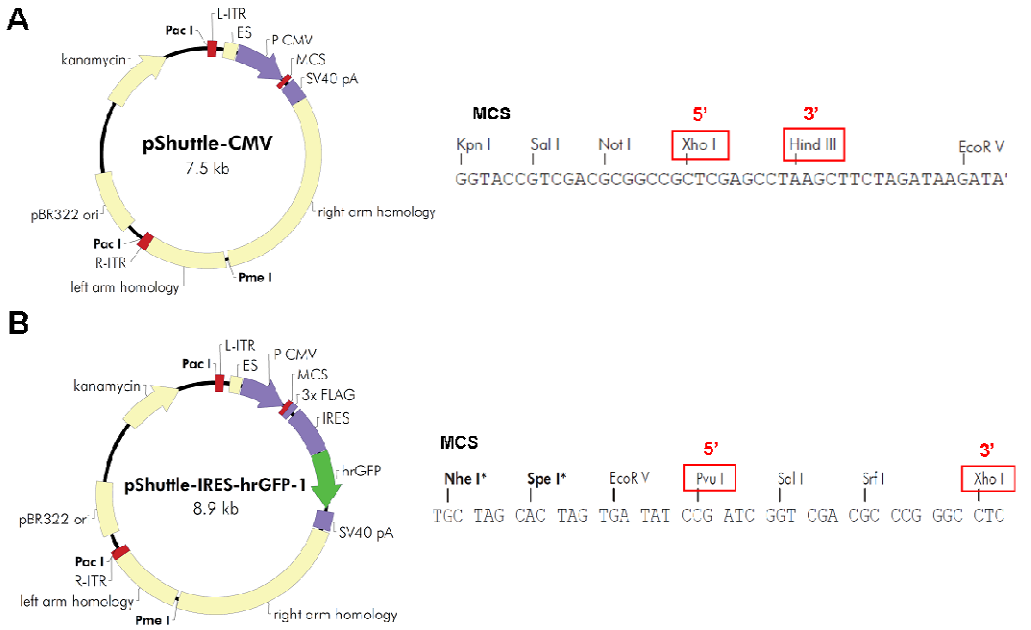

C

```
  1 ATGCCAGGAA GCGCACTACT ATGCTGCCTA CTACTACTAA CAGGAATGAG AATAAGCAGA GGACAATACA GCAGAGAAGA
 81 CAACAACTGC ACACACTTCC CAGTAGGACA AAGCCACATG CTACTAGAAC TAAGAACAGC ATTCAGCCAA GTAAAAACAT
161 TCTTCCAAAC AAAAGACCAA CTAGACAACA TACTACTAAC AGACAGCCTA ATGCAAGACT TCAAAGGATA CCTAGGATGC
241 CAAGCACTAA GCGAAATGAT ACAATTCTAC CTAGTAGAAG TAATGCCACA AGCAGAAAAA CACGGACCAG AAATAAAAGA
321 ACACCTAAAC AGCCTAGGAG AAAAACTAAA AACACTAAGA ATGAGACTAA GAAGATGCCA CAGATTCCTA CCATGCGAAA
401 ACAAAAGCAA AGCAGTAGAA CAAGTAAAAA GCGACTTCAA CAAACTACAA GACCAAGGAG TATACAAAGC AATGAACGAA
481 TTCGACATAT TCATAAACTG CATAGAAGCA TACATGATGA TAAAAATGAA AAGCTAA
```

Figure 1: Plasmid maps and multiple cloning sites (MCS). The CMV promoter only plasmid, pShuttle-CMV (A) and CMV promoter with GFP expression plasmid, pShuttle-IRES-hrGFP-1 (B). The highlighted restriction sites in the MCS represent those chosen to be added at the respective ends of the synthesised murine interleukin 10 (mIL-10). The nucleotide sequence of mIL-10 can be seen in C.

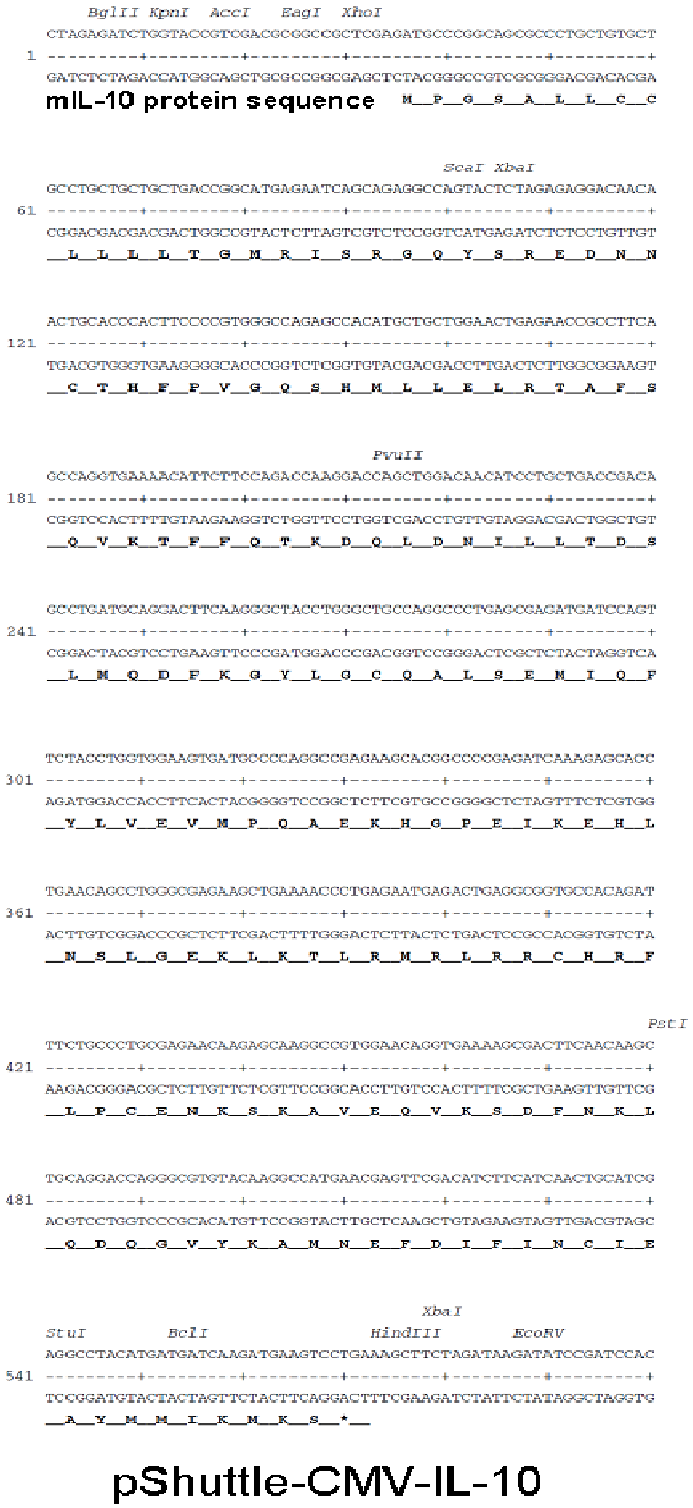

Figure 2: Sequencing of the pShuttle-CMV-IL-10 plasmid following mIL-10 insertion by GeneArt. The protein sequence for mIL-10 is indicated below the nucleotide sequence, indicating its presence in the plasmid.

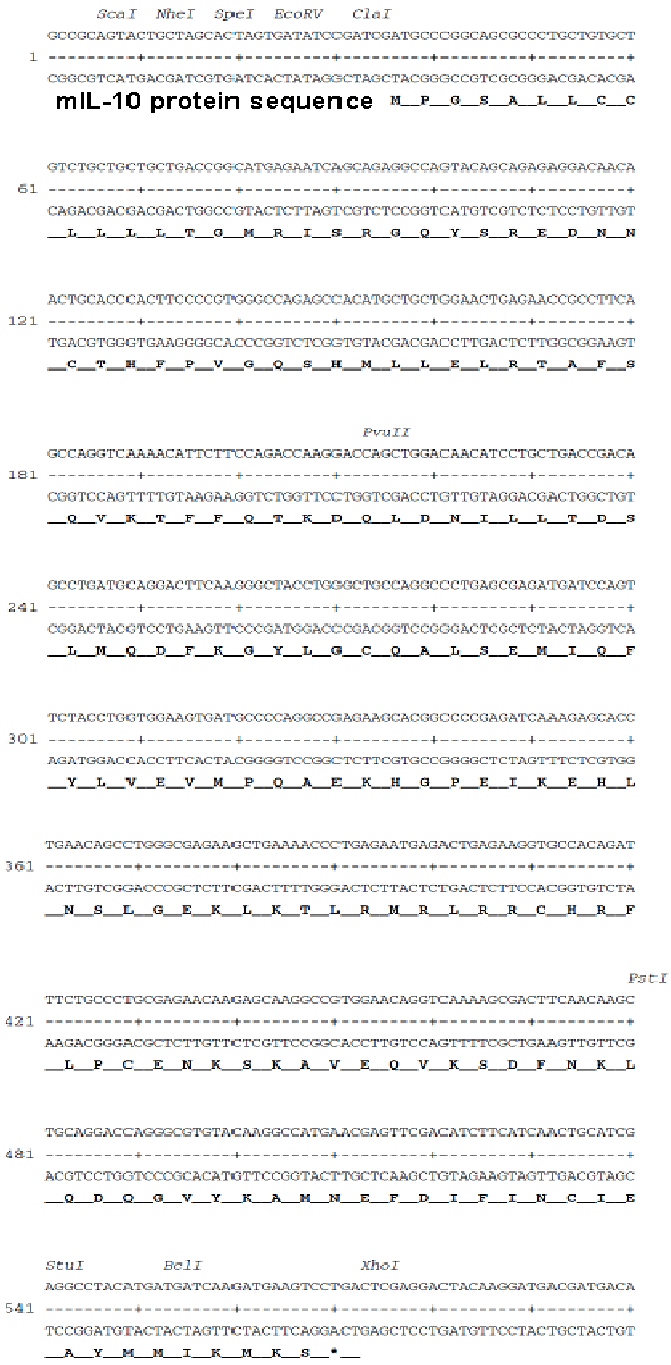

pShuttle-IRES-hrGFP-1-IL-10

Figure 3: Sequencing of the pShuttle-IRES-hrGFP-1-IL-10 plasmid following mIL-10 insertion by GeneArt. The protein sequence for mIL-10 is indicated below the nucleotide sequence, indicating its presence in the plasmid.

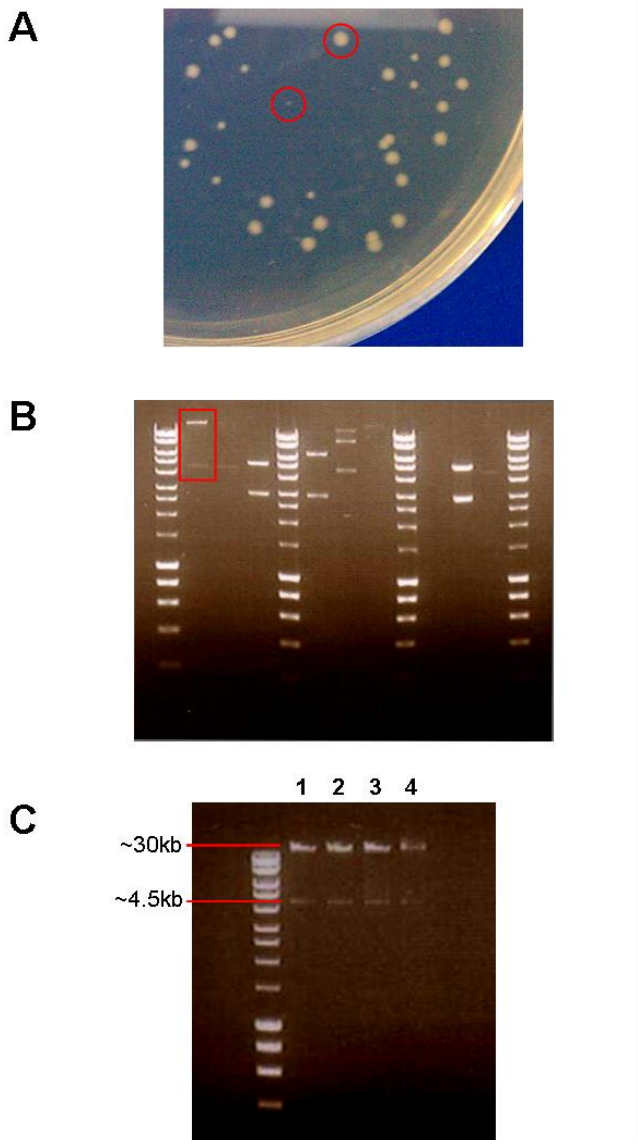

Figure 4: Screening and linearisation of recombinant pShuttle/AdEasy plasmids. A representative image of large and tiny colonies (red circles) used for recombinant plasmid screening compared to a large colony (A). A representative image of electrophoresis carried out on a number of tiny colonies, the isolated plasmid DNA having been digested with Pac I. The highlighted column indicates the presence of recombinant plasmid in that particular colony (B). Recombinant plasmids were found for all pShuttle plasmids 1-pShuttle-CMV, 2- pShuttle-CMV-IL-10, 3- pShuttle-IRES-hrGFP-1, 4- pShuttle-IRES-hrGFP-1-IL-10 (C).

4.1.2 Ad empty virus dropped due to presence of IL-10 in recombinant pShuttle/AdEasy plasmid

Following the production of the four pShuttle and AdEasy recombinant plasmids, samples of each were sent to Dundee University for sequencing. Figure 5 shows the presence of the mIL-10 sequence in the pShuttle-CMV plasmid which should contain no mIL-10 and was therefore not used further. Figure 6 shows the presence of mIL-10 in the pShuttle-CMV-IL-10 plasmid. Figure 7 shows low levels of random correlation between the sequences but does not indicate the presence of IL-10 in the pShuttle-IRES-hrGFP-1 plasmid whereas Figure 8 does. All apart from the pShuttle empty plasmid were then used to create the vectors.

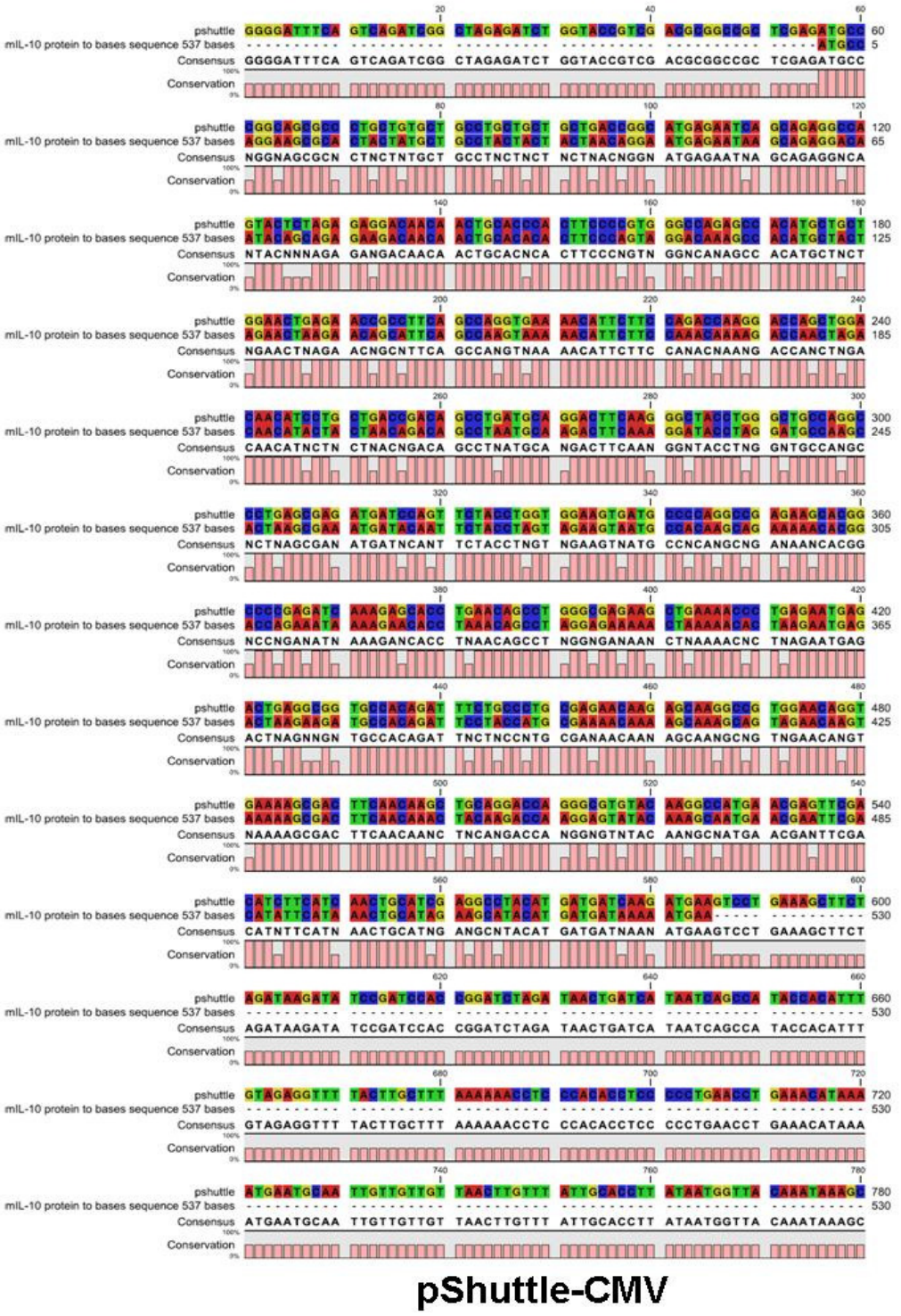

Figure 5: MCS sequencing of recombinant pShuttle/AdEasy plasmid. The high levels of nucleotide conservation indicate the presence of IL-10 in the pShuttle-CMV plasmid.

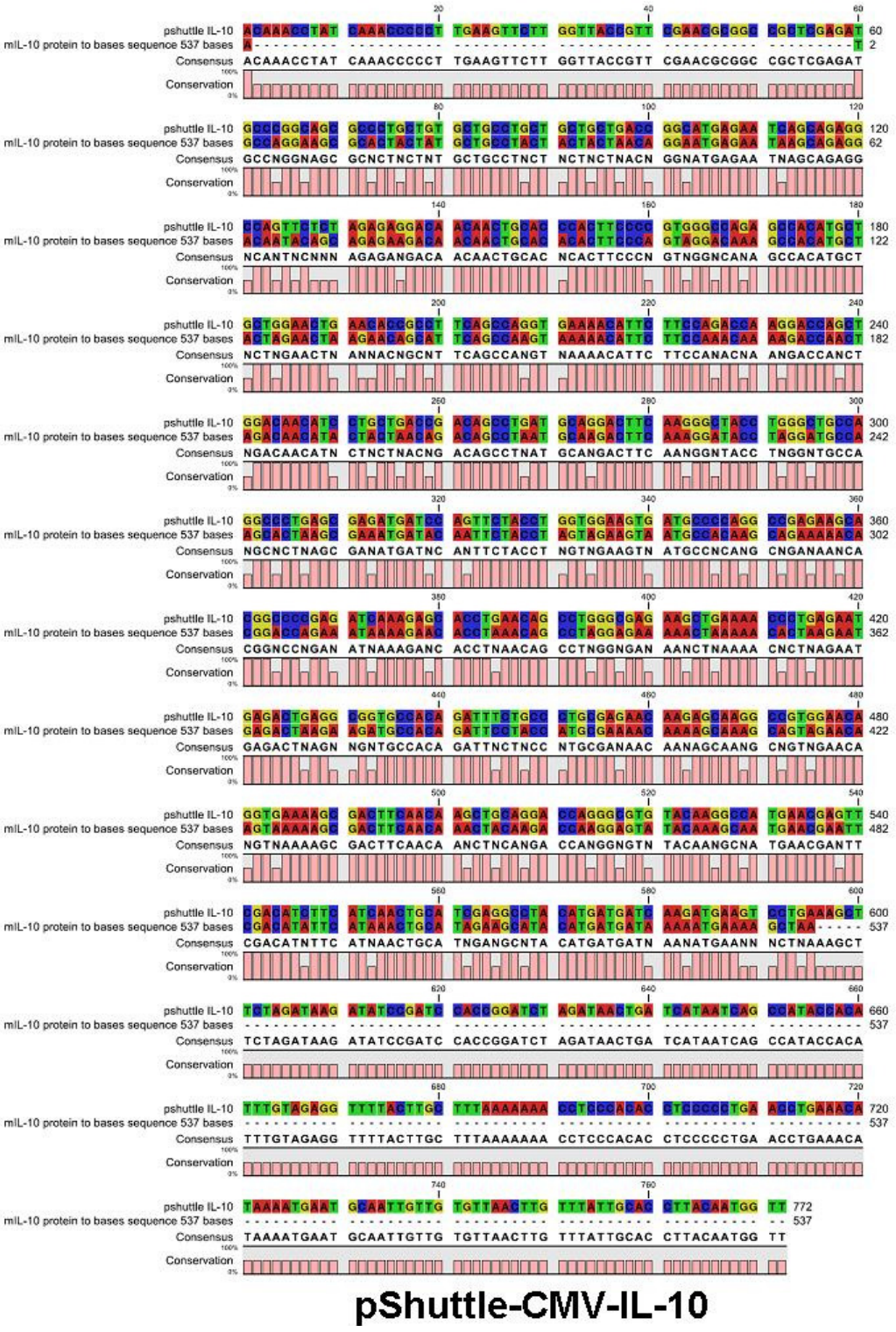

Figure 6: MCS sequencing of recombinant pShuttle/AdEasy plasmid. The high levels of nucleotide conservation indicate the presence of IL-10 in the pShuttle-CMV-IL-10 plasmid.

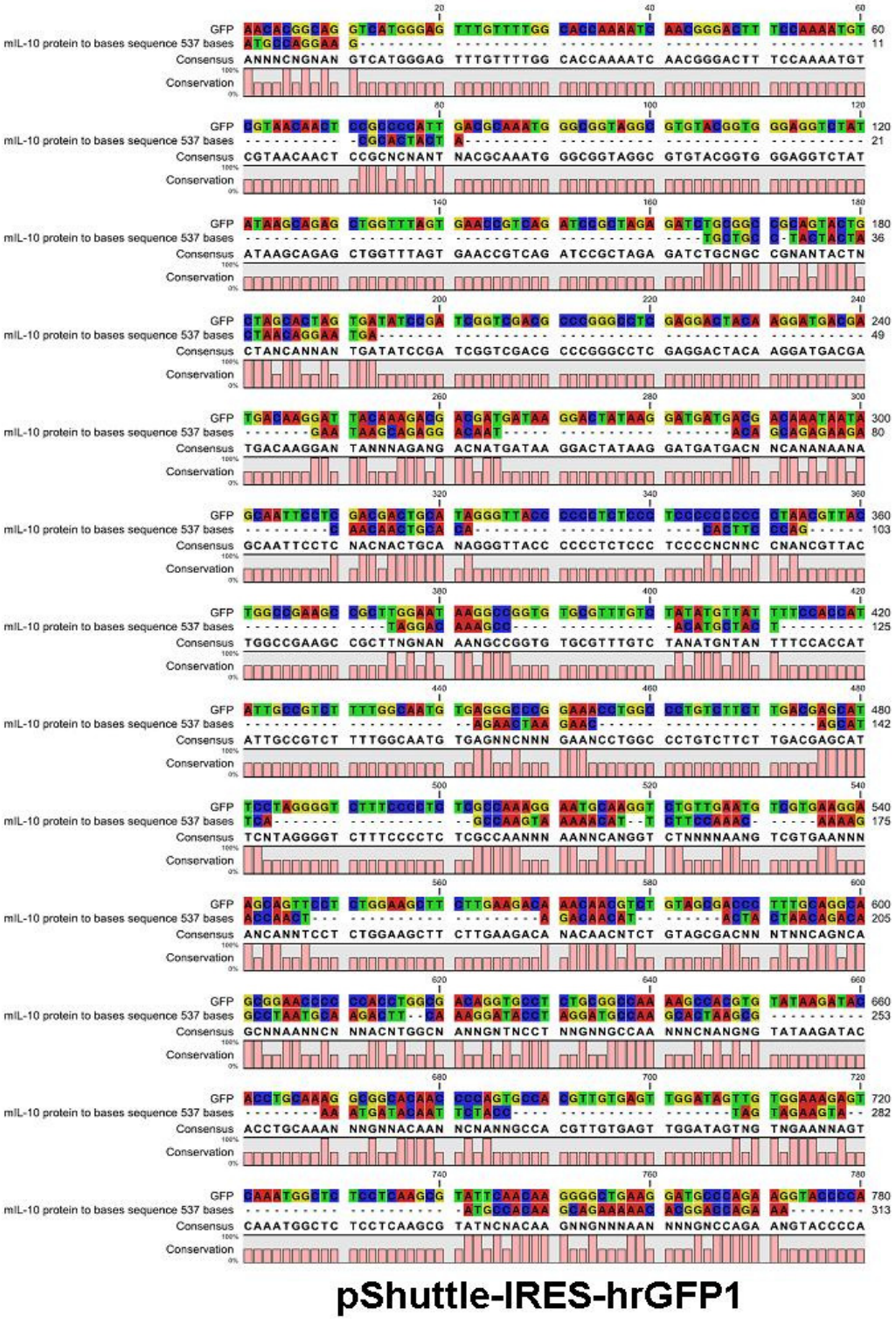

Figure 7: MCS sequencing of recombinant pShuttle/AdEasy plasmid. Low and erratic levels of nucleotide conservation indicate no IL-10 presence in the pShuttle-IRES-hrGFP1 plasmid.

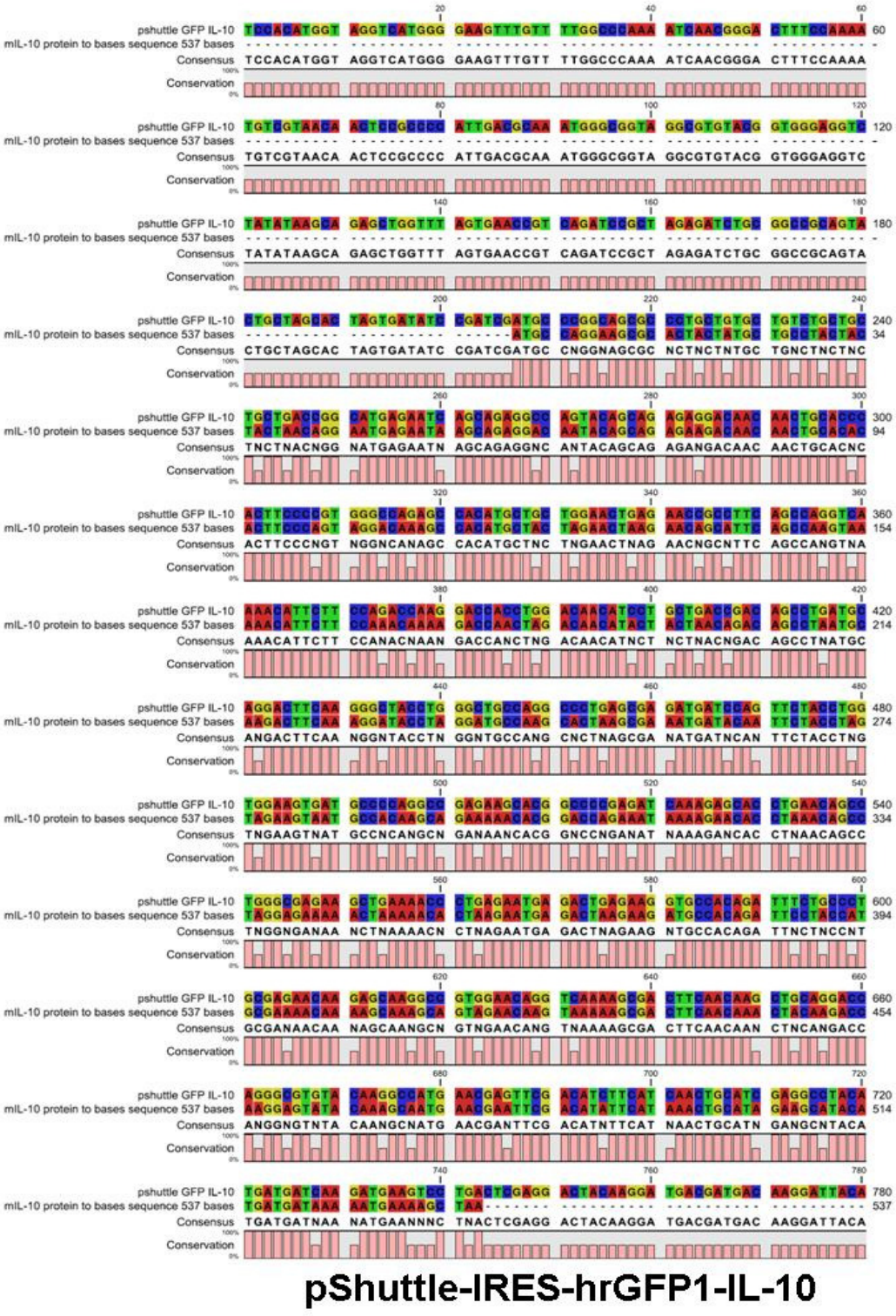

Figure 8: MCS sequencing of recombinant pShuttle/AdEasy plasmid. The high levels of nucleotide conservation indicate the presence of IL-10 in the pShuttle-IRES-hrGFP1-IL-10 plasmid.

4.1.3 The plaque forming unit (PFU) to viral particle (VP) ratio indicates mIL-10 has a negative affect on HEK 293 cells during production

As the efficiency and success of virus production can differ greatly from vector to vector and also from preparation to preparation of the same virus, it is important to know the quality of vector that is being produced. The total viral particle counts for each vector are displayed in Table 1 as are the total PFU however, a useful comparison is the ratio of how many of the VP produced are capable of infection, the pfu:vp ratio. From the data shown in Table 1C, it can be seen that the ratio for the Ad IL-10 vector preparations is several fold higher than the ratio for the Ad GFP preparations. Such a large ratio indicates that the overall efficiency of the preparation for the IL-10 vectors is probably low, producing only 1 infectious unit per 45-75,000 VP.

A

NanoSight	***1st production***	***2nd production***
Ad IL-10	9.64 x 10^{11}vp/ml	6.05 x 10^{10}vp/ml
Ad GFP	3.52 x 10^{11}vp/ml	4.18 x 10^{11}vp/ml
Ad GFP IL-10	1.208 x 10^{12}vp/ml	N/A

B

µBCA Assay	***1st production***	***2nd production***
Ad IL-10	2.176 x 10^{12}vp/ml	7.9 x 10^{11}vp/ml
Ad GFP	1 x 10^{12}vp/ml	2.03 x 10^{12}vp/ml
Ad GFP IL-10	1.62 x 10^{12}vp/ml	N/A

C

PFU Assay	***1st production***	***VP:PFU ratio***	***2nd production***	***VP:PFU ratio***
Ad IL-10	1.2 x 10^{8}pfu/ml	**45979:1**	1.05 x 10^{7}pfu/ml	**75238:1**
Ad GFP	3.59 x 10^{9}pfu/ml	**452:1**	1.49 x 10^{10}pfu/ml	**136:1**

Table 1: Titration results for the total viral particles (VP) and plaque forming units (PFU) of the viral vectors produced. A, shows the VP concentrations of the 3 viruses using the newly acquired NanoSight system B, shows the VP concentrations using the lab standard micro bicinchoninic acid (µBCA) assay. The number of functional viral particles, plaque forming units (PFU), is shown in C, with the ratio of PFU per VP also shown.

4.1.4 Transduction of HeLa cells demonstrates the ability of Ad GFP and Ad IL-10 but not of Ad GFP IL-10

In order to test whether the viruses produced could produce their respective transgenes, HeLa cells were transduced with the vectors due to their known susceptibility to adenoviral transduction [373-375]. Figure 9A depicts the IL-10 levels quantified in the media of Ad IL-10 transduced HeLa cells, with significant levels being observed at 2500 vp/cell and maximum levels reaching ~450 ng/ml. Figure 9B shows mIL-10 levels found in the media from HeLa cells transduced with Ad GFP IL-10, showing substantially reduced levels of IL-10 being produced, with a maximum of just under 3 ng/ml produced. The ability of both Ad GFP and Ad GFP IL-10 to produce detectable GFP was also examined. It was observed that Ad GFP IL-10 also produced reduced GFP levels in comparison to Ad GFP (Fig 9C). Taken together, the data indicates that the Ad GFP IL-10 vector produces very little of the transgene in the HeLa cell line.

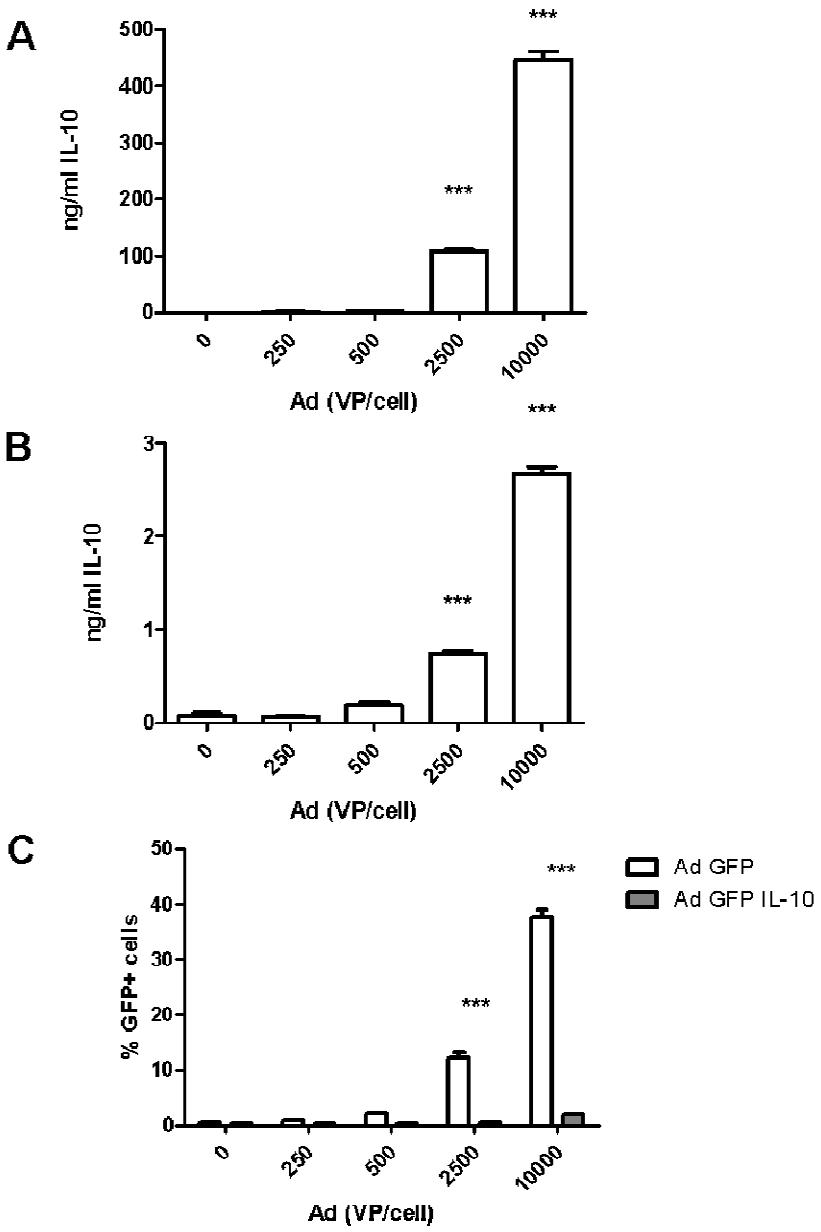

Figure 9: HeLa cells transduced with Ad GFP, Ad IL-10 and Ad GFP IL-10. High levels of mIL-10 were detected in the media of HeLa cells transduced with the Ad IL-10 vector (A). Over a 150 fold decrease in mIL-10 was observed in the HeLa cells transduced with the Ad GFP IL-10 vector compared to Ad IL-10 (B). GFP expression was observed in cells transduced with Ad GFP however no significant GFP levels were observed when using the Ad GFP IL-10 vector (C). Bars denote mean ± SEM, n=3, ***$P<0.001$ vs 0 VP/cell.

4.1.5 Transduction of murine CD4 T cells confirms poor transgene production with Ad GFP IL-10 vector

To further examine if the lack of transgene expression by Ad GFP IL-10, CD4 T cells were transduced with the vector. In Figure 10A it was observed that a significant decrease in GFP expression was found in Ad GFP IL-10 transduced T cells compared to those transduced with Ad GFP, with no statistically significant GFP levels being detected. Variable IL-10 levels were also found through the range of viral concentrations, with 2 groups indicating a significant increase in IL-10 levels over the negative control group however, the overall inconsistency in the data indicates that there were no virus dependent increase in the levels of IL-10 produced by T cells transduced by Ad GFP IL-10 vector (Figure 10B). Taken together with previous HeLa transduction data, it has been shown that the Ad GFP IL-10 vector is not capable of efficient transgene production and was not taken forward into other experiments.

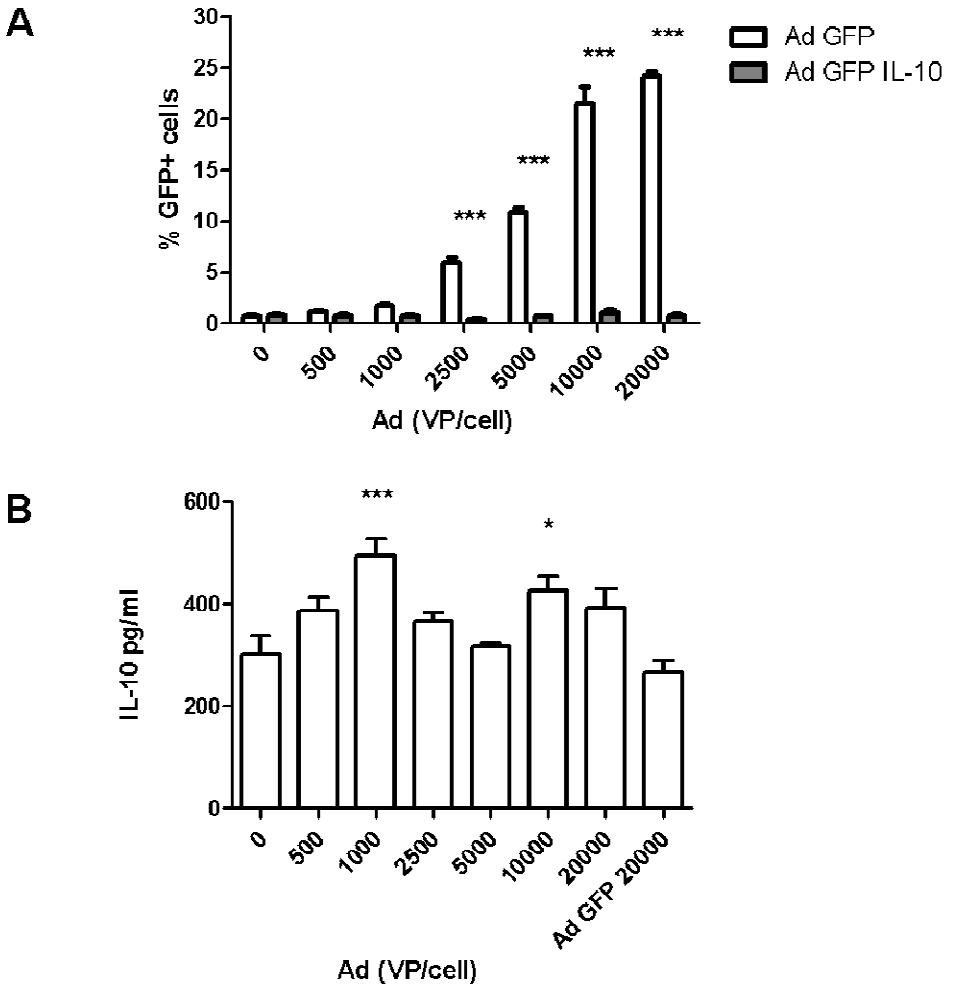

Figure 10: Quantification of CD4 T cells transduced with the Ad GFP IL-10 vector. No significant levels of GFP expression were observed in cells transduced with the Ad GFP IL-10 vector at any viral concentration (A). mIL-10 levels, in the media from T cells transduced with the Ad GFP IL-10 vector were inconsistent and showed no increase in mIL-10 with increasing virus concentration (B). Bars denote mean ± SEM, n=3, *$P<0.05$, ***$P>0.001$ *vs* 0 VP/cell.

4.2 Discussion

In this chapter, the production of adenoviral vectors expressing either GFP or murine IL-10 using the AdEasy system were documented. The original experimental plan had involved the production of Ad GFP, Ad empty, Ad IL-10 and Ad GFP IL-10 vectors, however technical problems which arose during production hindered the production of all 4 vectors. It was found after sequencing of the recombinant plasmids that the pShuttle plasmid which should have contained no mIL-10 sequence, did, and was subsequently dropped from further production. It was also found that during initial testing of the vectors on the HeLa cell line, that the Ad GFP IL-10 vector produced very little GFP and IL-10 in comparison to the other Ad GFP and Ad IL-10 vectors. This inability to produce functional levels of either transgene was confirmed upon transduction of murine CD4+ hCAR DO11.10 T cells, and was therefore not used in further experiments. Upon comparing the production efficiency of the remaining Ad GFP and Ad IL-10 vectors, it was clear that the IL-10 being produced by the HEK 293 cells (due to the constitutive CMV promoter in the vector) during vector production, was affecting their growth and ability to produce functional VP, a problem that may need to be rectified if this IL-10 vector were to be used again.

In our initial experimental plans, we had planned to use all four vectors, Ad empty, Ad GFP, Ad IL-10 and Ad GFP IL-10. The murine IL-10 was synthesised and sub-cloned into the various pShuttle vectors by GeneArt, which was shown in sequencing of the retuned plasmids (Figures 2 and 3). Digestion problems were encountered with the pShuttle IL-10 plasmid at the linearisation stage using the restriction enzyme PmeI however this was overcome by using an alternative restriction enzyme found within the plasmid that was not present anywhere else in the plasmid. As described in the methods, the linearised pShuttle plasmids were co-transformed into BJ5183 cells along with the AdEasy plasmid which contained the backbone

genes of the adenoviral vector. Within these cells homologous recombination between the two plasmids occurs due to regions with a high level of homology located on both plasmids. As a fully formed recombinant plasmid will be significantly larger than a plasmid which has not undergone correct homologous recombination, the overall division of the bacteria containing these recombinant plasmids will take longer, resulting in a smaller sized colony. This meant that during the screening process for colonies which contained recombinant plasmids, only the smallest found on each plate were taken, grown and the plasmid digested for screening. As the antibiotic resistance gene is located on the pShuttle plasmids, the larger colonies also observed on the plates represent uncut or recirculised pShuttle plasmids. Subsequently these confirmed recombinant plasmids were then amplified in number in XL10 Gold cells, suited for large plasmid/cosmid production, the plasmids linearised and transfected into HEK 293 cells from which the fully formed vectors were produced.

Unfortunately after all the selected recombinant plasmids had been sequenced for the presence of the IL-10 sequence (Figures 5 to 8), it was found that the plasmid designated as “empty” contained the murine IL-10 gene. The most likely explanation for this insertion is probably due to contamination at a step in the preparation of the recombinant plasmids, due to dealing with a large number of DNA constructs all of which were progressing at different rates. It was decided at this point to return to the initial pShuttle plasmid stage and create another recombinant “empty” plasmid, however due to time constraints encountered later on, this plasmid was effectively dropped with the Ad GFP plasmid taking over as a control vector for the IL-10 secreting vectors, Ad IL-10 and Ad GFP IL-10.

As an early indicator of the vector progress, just before the HEK 293 cells were harvested for lysis and subsequent virus recovery, the media and cells were checked for the presence of the IL-10 and GFP transgenes respectably. All flasks at this stage indicated that the vectors were

producing their respectful transgenes, with Ad GFP showing only GFP, Ad IL-10 only IL-10 and Ad GFP IL-10 showing both GFP and IL-10 expression, although these levels were not quantified. Additionally, before using the viruses in T cell experiments, we wanted to test the vectors ability to infect a cell type known to be easily transduced by the vectors and again check that the appropriate transgene products were produced. HeLa cells were chosen due to their documented ease of transduction [373-375], they are also used to test replication deficiency in adenoviruses (see 2.21). Both the Ad GFP and Ad IL-10 produced detectable levels of GFP in the HeLa cells and large amounts of IL-10 in the media respectfully, however it was found that the Ad GFP IL-10 vector produced approximately 100 fold less IL-10 in comparison to the Ad IL-10 vector, and the % GFP+ cells were also very low in comparison to the Ad GFP transduction levels. As the ability of the Ad GFP IL-10 vector to produce GFP had previously been observed in the HEK 293 cells, it would be reasonable to use this % GFP+ as an indicator of the vectors ability to transduce the cells. Therefore as the % transduction was very low with this vector, that would also explain the lower levels of IL-10 found in the media. Although a pfu plate (see methods) was not carried out for this particular vector to compare against vp levels, as the same number of vp/cell were used on the HeLa cells it may be fair to assume that the number of pfu were lower than found with the other two vectors, which would result in a lower number of infectious particles being present per cell and therefore evoke lower transduction levels. This lack of either IL-10 or GFP production was also observed in Ad GFP IL-10 transduced CD4 T cells, showing significantly lower transduction levels and no significant IL-10 levels at all. Due to time constraints it was decided at this stage that, although a novel dual expressing vector which could provide interesting data, the Ad GFP IL-10 vector be discontinued and the remainder of the experiments carried out using the validated Ad GFP and Ad IL-10 vectors with Ad GFP acting as the control virus.

With regards to the PFU *vs* total viral particle mentioned previously, it was observed that the ratio of infectious VP to total VP from the Ad IL-10 virus preparations were extremely high i.e. the number of infectious units per preparation was very low. Although not quantified, the levels of IL-10 found in the media of the HEK293 cells during production was very high and it was assumed that it is this high levels of secreted IL-10 that is affecting the viral production. It was observed that the HEK 293 cells took longer to grow and to reach the CPE stage in flasks containing the Ad IL-10 and Ad GFP IL-10 vectors, showing that the IL-10 levels produced had a direct affect on the cells division rate and proliferation. The fact that the efficiency of the cells to produce functioning VP was also affected suggests that as well as affecting growth, the IL-10 had some form of deleterious effect on the viral replication cycle. There have been well documented incidents of cell toxicity due to hypercytokineamia [376] a.k.a. “cytokine storm”, most famously the phase one clinical trial TGN1412 [377], where high levels of cytokines induced cell death in multiple organs. At present, there is no literature indicating the presence of an IL-10 receptor on the surface of HEK 293 cells nor evidence of the affects of IL-10 directly on *in vitro* cell lines. Reported anti-tumor growth affects of IL-10 are not related to it’s interaction with the tumor cells, rather that it acts as an anti-angiogenic factor [378] for the cancer cells which in our case could not be a factor in the suppression of HEK 293 growth and function. It has been shown however, that the production of adenoviral vectors by HEK 203 cells under hyperosmotic conditions can decrease the cell growth and viral output from these cells [379]. It may be the case that the high levels of IL-10 create this hyperosmotic condition and therefore explain our stunted production of the IL-10 containing vectors only.

Methods in which to circumvent this toxicity issue could include the neutralisation of the IL-10 in the media by the addition of neutralising IL-10 antibodies or proteins; however this is relatively impractical due to the extremely high cost of using neutralising antibodies in the quantity that

would be required. A more cost effective method would be to change the promoter from the constitutively activated cytomegalovirus (CMV) promoter to one which is either inducible [380] or specific to the target CD4 T cell, such as CD3 [381], therefore either allowing advanced control over transgene expression and avoiding transgene product secretion during adenoviral production.

To summarize:

- We have produced GFP and IL-10 encoding adenoviral vectors capable of transducing murine CD4+ T cells

- Due to unforeseen issues the original vectors of Ad Empty, Ad IL-10, Ad GFP and Ad GFP IL-10 were reduced to Ad GFP and Ad IL-10

- The constitutive expression of IL-10 during virus production appeared to have a deleterious effect on the cell line and resulted in a lower output of functional VP of IL-10 producing vectors

- Remaining Ad GFP and Ad IL-10 used in all further experiments.

Chapter 5: Optimisation of CD4+ T cell transduction

5.1 Aims and rationale

In this chapter, a range of experiments were carried out in order to optimise CD4+ T cell transduction for adoptive transfer experiments into recipient mice, using either a GFP or IL-10 encoding adenovirus. Both flow cytometry and ELISA were used in order to determine the % transduction of T cells, the level of IL-10 produced by the transduced T cells and also the viability of the cells post-transduction. Areas of research in this chapter include, the affects of Th1 polarisation and the addition of blood coagulation factor 10 (FX) on transduction levels of hCAR DO11.10 CD4+ T cells (BALB/c) and testing the functionality of the murine IL-10 produced by Ad IL-10 transduced cells. As the intended recipient mouse for these cells was the $ApoE^{-/-}$ model, which is on a C57BL/6 background and as the hCAR DO11.10 mice are of a BALB/c background, a number of methods were tried in order to over come this. These included using Nucleofection™ and use of lentivirus vectors to transduce C57BL/6 CD4+ T cells and also using imported hCAR OT-I mice on a C57BL/6 background. It is important to note that the GFP virus used in these optimisation experiments was not the vector produced in chapter 4 and was instead a vector being produced in Prof. Baker's lab. The experiments in chapters 4 and 5 are not necessarily in chronological order as production of the vectors was undertaken alongside transduction optimisation.

5.2 Introduction

As mentioned earlier in chapter 1, atherosclerosis is a disease which was traditionally thought to simply be the accumulation of fatty deposits in the vessel walls which, after time, occludes the vessel causing pathology. Work carried out in the last few decades however, has revealed that there is an underlying inflammatory aspect of the pathology locally in the vessel wall, in which a host of immune cells migrate to and reside [48]. Taking advantage of this migration and using the cells as "Trojan horses" may provide an effective and inflammation-specific means of delivering therapeutic molecules directly to the source of the pathology, thereby having a significant local effect on pathology while avoiding non-specific delivery of the therapeutic. This approach has proven promising in arthritis, [382] experimental autoimmune encephalomyelitis [383] and with a lot of research being undertaken in directing cells to sites of cancer growth [384], but this has never before been applied to the treatment of vascular pathology.

CD4+ T cells were selected as the candidate cell type for several reasons. T cells have been shown to be present in the vascular wall at the very early stages, during the progression of atherosclerosis and also at the very late stages of the disease, having involvement in the formation and functionality of arterial tertiary lymphoid organs (ATLO) [40, 51]. Upon quantification of the cellular composition of the plaque, it was found that T cells make up the majority of cells, surprisingly outnumbering macrophages, the cell type most commonly associated with the atherosclerotic plaque [40]. In addition to being a persistent presence, T cells have also been shown to have a significant role in the disease development. The addition of CD4+ cells into immunodeficient scid/scid $ApoE^{-/-}$ mice reversed the decrease in fatty streak formation reported in these immunodeficient mice and increased pathology past levels seen in immunocompetent $ApoE^{-/-}$ mice [5], the same effect being observed in

scid/scid ApoE$^{-/-}$mice which received OxLDL specific CD4+ T cells [258]. These results demonstrate the importance of CD4+ T cells in atherosclerosis and also why they have the potential to be ideal “Trojan horses”.

As our approach required the general suppression of the vessel based inflammation, a well known and well documented anti-inflammatory cytokine was chosen, interleukin 10 (IL-10). It’s general effects include the down-regulation of the expression of pro-inflammatory cytokines [317], MHC class II molecules and also co-stimulatory molecules [385]. In the context of atherosclerosis, significant increases in lipid accumulation, immune cell infiltration, MMP levels, lesion size and markers of systemic coagulation result in IL-10 KO mice, with some of these being reversed upon administration of IL-10 [80, 97, 336]. From a more cellular approach, over expression of IL-10 by either T cells or macrophages in atherosclerotic mice after a bone marrow transplant of modified cells, has resulted in a decrease in lesion size, necrotic core, cholesterol accumulation, apoptosis and promoted a switch to a Th2 based response [96, 337]. These results suggest that, if IL-10 is secreted from the modified transferred T cells, it may have a measurable affect on the pathology of atherosclerosis.

An issue raised early on in this project was that the transgenic mouse strain required for adenoviral transduction, the hCAR mouse strain, was on a BALB/c genetic background (hCAR DO11.10 mice), whereas our animal model of atherosclerosis, the ApoE$^{-/-}$ mouse strain was of a C57BL/6 genetic background. Due to the different backgrounds, the transferred cells would be recognised as non-self, the consequence of which would be deletion and rapid clearance by the host’s immune response. This occurs much in the same way as in transplant rejection, with the transferred T cells expressing proteins on their surface foreign to the recipient, to which the innate and adoptive immune systems generate a response to [386]. In an attempt to overcome this obstacle and allow transfer of modified cells into ApoE$^{-/-}$ recipients, several approaches were tried.

The Nucleofection™ system from Amaxa/Lonza (UK), presented the opportunity to avoid having to use the transgenic hCAR mouse strain and instead directly transfect C57BL/6 CD4+ T cells. The Nucleofection™ system is based on electroporation, whereby a current is briefly applied across the surface of the cell creating small pores, through which genetic material, in this case plasmid DNA, can pass through and be expressed. This system has found success in the transfection of T cells from rabbit [387], pig [315], rat [388] and also mouse [388, 389], with the Nucleofection™ protocol stating that transfection levels of around 35% may be reached in CD4+ cells.

A further alternative approach which would allow the direct transduction of C57BL/6 cells is the use of a lentivirus vector expressing the vesicular stomatitis virus (VSV-G) envelope. The G protein of this envelope binds through electrostatic interactions with the phospholipids of the target cells membrane, therefore bestowing the ability for the lentivirus to gain entry into most cell types [390]. Lentiviral transduction of T cells also brings with it the added benefit of transfer of the transgene to each daughter cell post division, as the nature of a retrovirus like lentivirus is that it incorporates itself into the genome of the target cell. Due to this integration, lentiviral vectors require the cell to be dividing in order for transcription of the genes to occur [391], which is a problem when dealing with CD4+ T cells which do not have a consistent proliferative turnover. Some success has been made in transducing both human [392] and murine CD4+ T cells [303, 393] by inducing cell proliferation or using the T cell survival cytokines interleukin 7 (IL-7) and interleukin 2 (IL-2) [351]. It has also been shown that transduction is possible of T cells whereby the immunological activity of the cell is not affected [394]. In this chapter we used the protocol of Gilham at al [351] and an SFFV-GFP virus to carry out transduction.

A final method of circumventing the issue of the BALBc hCAR mice was to breed, or locate hCAR mice on a C57BL/6 background. Due to time constraints and the numbers of mice that would be required to carry out a

transfer experiment, breeding our BALB/c hCAR mice strain onto a C57BL/6 background was not feasible. We therefore searched for C57BL/6 mice expressing the hCAR molecule on CD4+ T cells and were able to import breeding pairs from Professor Kristin Hogquist's group based in the University of Minnesota. Although these mice were hCAR OT-I cells, whereby the T cell receptor (TCR) of the CD8 T cells is specific for the ovalbumin peptide fragment (257-264), this was of no consequence to the work we intended to carry out.

In this chapter, the optimisation of hCAR DO11.10 (BABL/c) CD4+ T cells was carried out, including looking at the effects of Th1 polarisation and the addition of coagulation factor X (FX) had on transduction levels. It is important to note that the GFP expressing adenovirus was not the virus produced in chapter 4 and was instead one already produced in Prof. Baker's lab. Alternate methods of introducing genetic information into non hCAR expressing C57BL/6 CD4+ T cells was also carried out by means of the Nucleofection™ system and lentiviral vector. Finally transduction optimisation was carried out on the imported hCAR OT-I mice (C57BL/6) in order to allow for transfer of modified cells into an $ApoE^{-/-}$ recipient. hCAR DO11.10 refers to the transgenic hCAR expressing BALB/c mice, BALB/c mice refers to wild type BALB/c control mice, C57BL/6 refers to wild type mice and hCAR OT-I refers to the transgenic C57BL/6 mice.

5.3 Results

5.3.1 Transduction of CD4+ T cells with a GFP expressing adenovirus reaches ~80%, 48 hours post-transduction

In order to validate the protocol for T cell transduction detailed by Hurez et al. [296] and also the validity of our hCAR DO11.10 (BALB/c) mouse strain, initial optimisation experiments were carried out using a range of adenovirus concentrations based on total VP per cell. CD4+ T cells were first isolated from single cell suspensions of total lymph node and spleen leukocytes, incubated with the adenovirus and then activated using PMA (50 ng/ml) and Ionomycin (500 ng/ml) for 4 hours before being washed and incubated in complete RPMI. Cells were labelled with the viability stain ethidium monoazide bromide (EMA) and CD4+, with cells being gated on the viable population (EMA negative) followed by CD4+ *vs* GFP. BALB/c mice were used as a control to demonstrate transduction levels due to the hCAR molecule on our hCAR DO11.10 mice strain.

Figure 1A is a representative FACS plot of the gating strategy used for analysing GFP expression in hCAR DO11.10 (BALB/c) CD4+ T cells, this was also used in all following experiments. At 24 hours post-transduction, statistically significant levels of GFP expression were observed at all viral concentrations in the hCAR DO11.10 group. The % of viable CD4+GFP+ cells ranged from just under 40% at 500 vp/cell to ~80% at 20,000 vp/cell. Small but statistically insignificant levels of transduction were observed in the BALB/c CD4+ cells at the higher virus concentrations (Figure 1B). The peak % of GFP+ cells remained relatively the same, just over 80%, at 48 hours post-transduction however this peak was reached at a lower viral concentration, 2500 vp/cell as opposed to 10,000 vp/cell (Figure 1C). The transduction levels in the BALB/c T cells also increased between 24 and 48 hr after transduction.

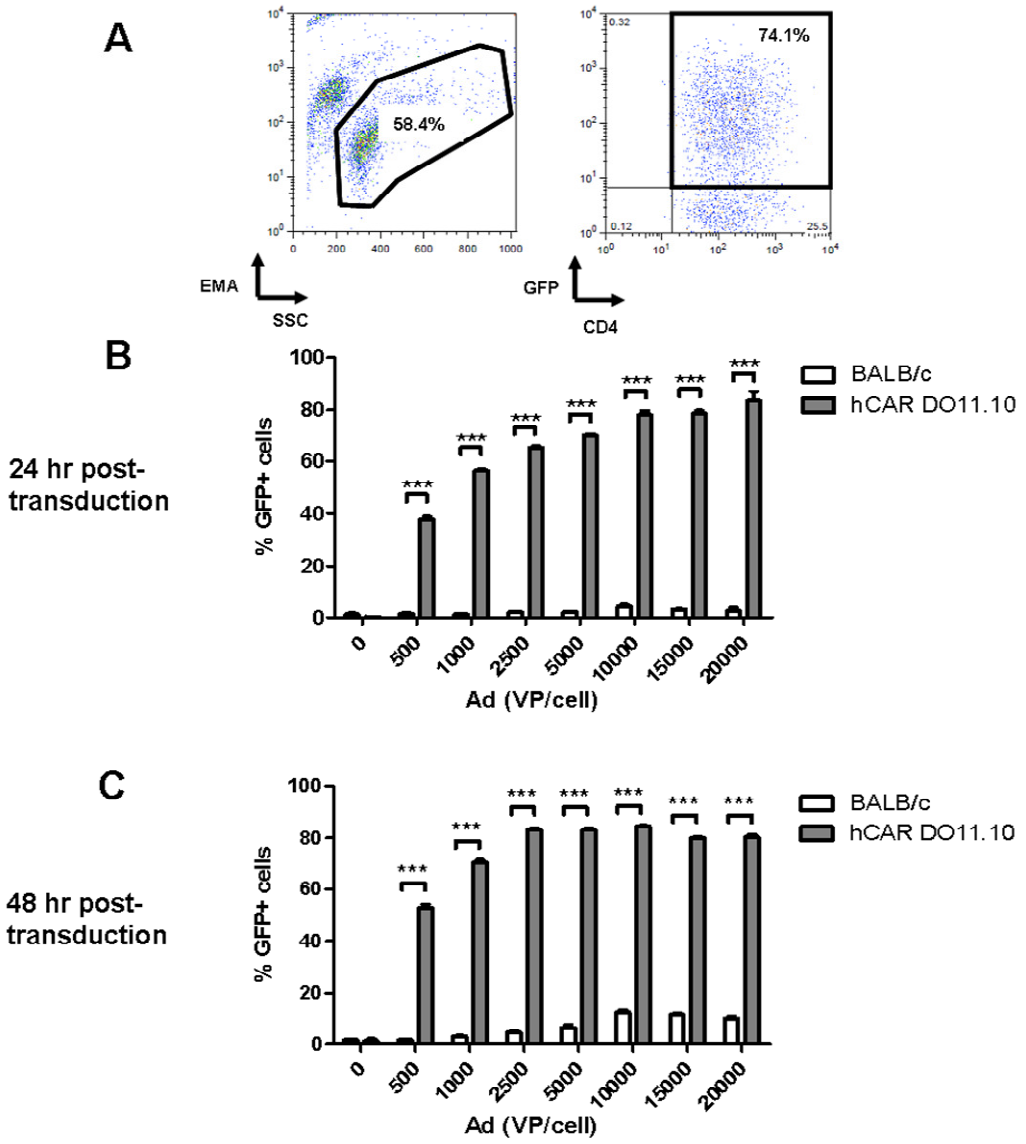

Figure 1: %CD4+ GFP+ cells at 24 and 48 hrs post transduction. Representative FACS plot indicating gating strategy for assessing CD4+ T cell transduction levels. Gated on EMA negative fraction and the GFP *vs* CD4+ (A). Significant transduction levels were observed at 500 vp/cell at 24 hrs in hCAR DO11.10 cells. Up to ~80% transduction levels were reached at 20,000 vp/cell in hCAR DO11.10 cells. Very low levels of transduction were observed in the wild type BALB/c mice (B). At 48 hrs, transduction levels at all VP were increased, peaking at 84% at 10,000 vp/cell in hCAR DO11.10 cells. Transduction levels of BALB/c cells was also increased (C). (B,C) were both repeated with analogous results obtained. Results are expressed as mean ± SEM, n=3 per group, ****P<0.001*.

5.3.2 Polarisation of T cells to a Th1 phenotype increased transduction levels and transgene production

Atherosclerosis is generally defined as a Th1 based inflammatory response [6], with the majority of CD4+ T cells present being of Th1 phenotype [6, 48]. This particular phenotype may be of importance for the migration and residing of T cells in the vessel wall at sites of plaque formation and so was identified as a possible option for later adoptive transfer experiments. CD4+ cells were isolated as before but underwent 3 days of Th1 polarisation before viral incubation and activation. Labelling and gating strategy were the same as the previous experiments with the addition of GFP MFI also being considered. 48 hours was chosen as the incubation period as it is known to be the time where adenovirus transgene expression peaks.

Figure 2A shows the %GFP+ cells in non-polarised and Th1 polarised cells of both the hCAR DO11.10 and BALB/c mice strains. A significant increase in transduction is seen in the Th1 polarised hCAR DO11.10 cells at 500 vp/cell, 1000 vp/cell and 2500 vp/cell with the remaining concentration of 5000 vp/cell not significant but also trending an increase in %GFP+. This Th1 polarisation based increase was also observed in the BALB/c cells, with significant increases in %GFP+ cells being seen at all viral concentrations. Interestingly, there was also a significant increase in the MFI of GFP in the GFP+ Th1 cells, which was observed at all viral concentrations (Figure 2B).

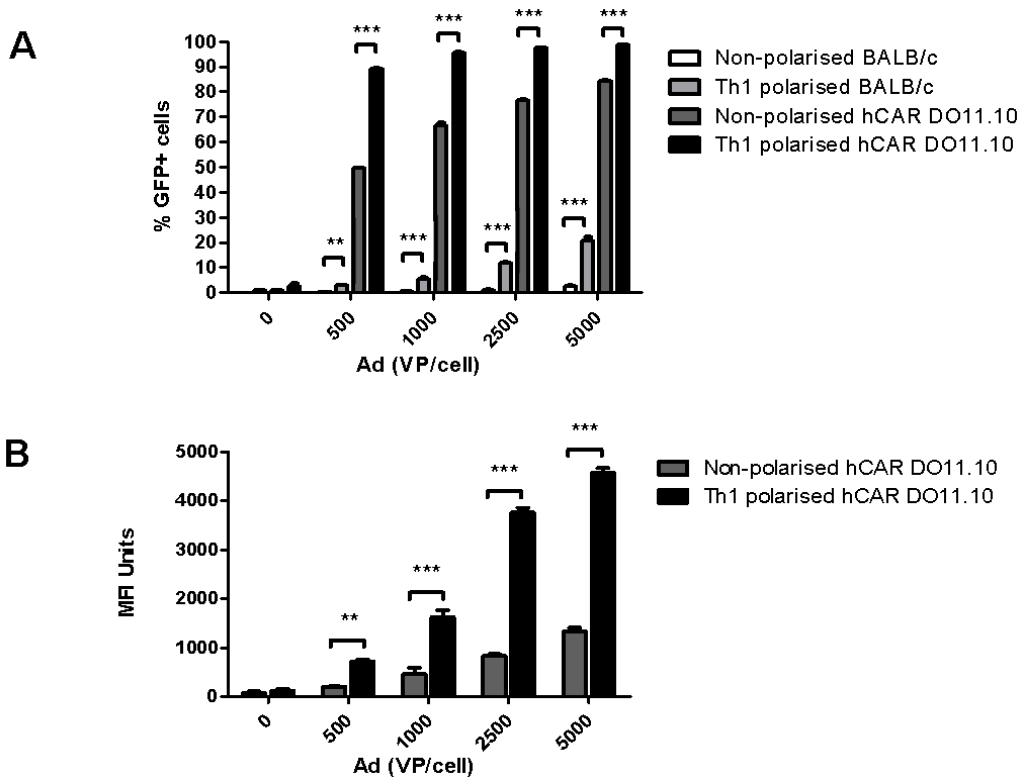

Figure 2: GFP expression at 48 hours in non-polarised and Th1 polarised hCAR DO11.10 cells. A significant increase in transduction levels was seen at 500 vp/cell and 1000 vp/cell. A significant increase was also seen at all VPs in the BALB/c group (A). Significant differences were seen in the MFI of GFP+ cells at all VPs (B). The experiment was repeated with analogous results obtained. Results expressed as mean ± SEM, n=3, ***P<0.01*, ****P<0.001*.

5.3.3 Coagulation factor 10 (FX) decreases CD4+ T cell transduction in both non-polarised and Th1 polarised cells but only decreases transgene expression in Th1 cells

It is well known that coagulation factor 10 (FX) is capable of binding to the hexon region of the adenovirus and retargets the vector for heparan sulphate proteoglycans (HSPGs) in the liver [395, 396]. It has also been shown that HSPGs are expressed on T cells [397-399] and so the ability of FX to bind and therefore modify CD4+ T cell transduction was investigated. Th1 or non-polarised hCAR DO11.10 T cells were incubated in the presence and absence of FX during viral incubation with %GFP+ and GFP MFI being assessed at 48 hr.

In Figure 3A, it can be seen that the addition of FX causes a significant decrease in the number of GFP positive cells at all but 20,000 vp/cell, however the MFI levels of the GFP+ cells were not affected (Figure 3B). This same decrease in transduction levels was observed in Th1 cells (Figure 3C) however in these Th1 cells, a large decrease in GFP MFI was found (Figure 4D). GFP MFI levels in the Th1 cells treated with FX were reduced to approximately the same levels as was seen in the non-polarised cells.

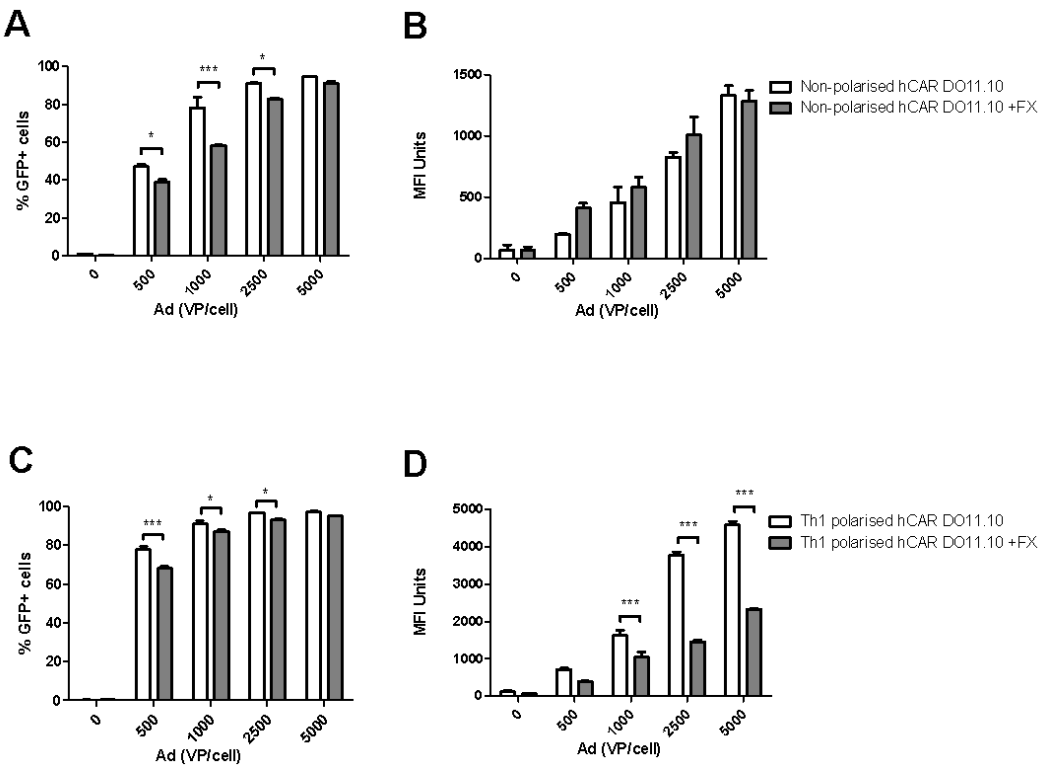

Figure 3: GFP expression of non-polarised and Th1 polarised hCAR DO11.10 cells with and without the addition of coagulation factor X (FX). A significant decrease in %GFP+ was seen at all VPs excluding 20,000 vp/cell, in non-polarised hCAR DO11.10 cells (A). No significant difference was seen in the MFI between non-polarised cells with and without FX (B). A significant decrease in %GFP was also observed at all VPs excluding 20,000 vp/cell in Th1 polarised cells (C). A significant decrease in GFP MFI was seen in the FX treated group (D). The experiment was repeated with analogous results obtained. Results expressed as mean ± SEM, n=3, **P<0.05*, ****P<0.001*.

5.3.4 CD4+ T cells transduced with an IL-10 expressing adenovirus, produce biologically active murine IL-10

In the production stages of the IL-10 encoding adenovirus, we had shown that substantial amounts of murine interleukin 10 (IL-10) were produced by both the HEK 293 packaging cell line and also HeLa cells (exceeding maximal detection limit of ELISA >4 μg/ml). A vital element of our adoptive immunotherapy approach is that the transferred cells produce the therapeutic molecule and that this molecule is capable of having an effect on the inflammatory environment. It was therefore imperative that hCAR DO11.10 CD4+ T cells were able to produce murine IL-10 post-transduction and also that this murine IL-10 was biologically active, being able to suppress elements of an immune response. CD4+ T cells were transduced as discussed previously and a murine IL-10 ELISA carried out on the culture media 48 hours post-transduction. Previous evidence suggested DCs would be a good candidate on which to test the activity of IL-10 due to its range of effects on these cells [400, 401]. As a substantial amount of IL-10 would be required for these experiments it was more feasible to use media from Ad IL-10 transduced HeLa cells as a source of viral IL-10, due to the large amounts produced by the cell line. DCs were activated using LPS 1 μg/ml in the presence or absence of the IL-10 containing media and the levels of MHC II on the DCs were analysed via flow cytometry 18 hrs after activation.

At 48 hrs post transduction with the Ad IL-10 virus, CD4+ T cells showed significant production of IL-10 at the lowest VP of 500 vp/cell. This production peaked at around 4000 pg/ml at 10,000 vp/cell (Figure 4A). Figure 4B shows that the addition of murine IL-10 with LPS, significantly reduces the MHC II levels in comparison to LPS alone. Interestingly, recombinant IL-10 was not able to significant decrease MHC II levels whereas the viral IL-10 could, at the same concentration. Addition of anti-IL-10 negated the affects of IL-10 on MHC II levels. Interestingly, the

addition of viral IL-10 and anti- IL-10 on their own increased MHC II levels above baseline levels.

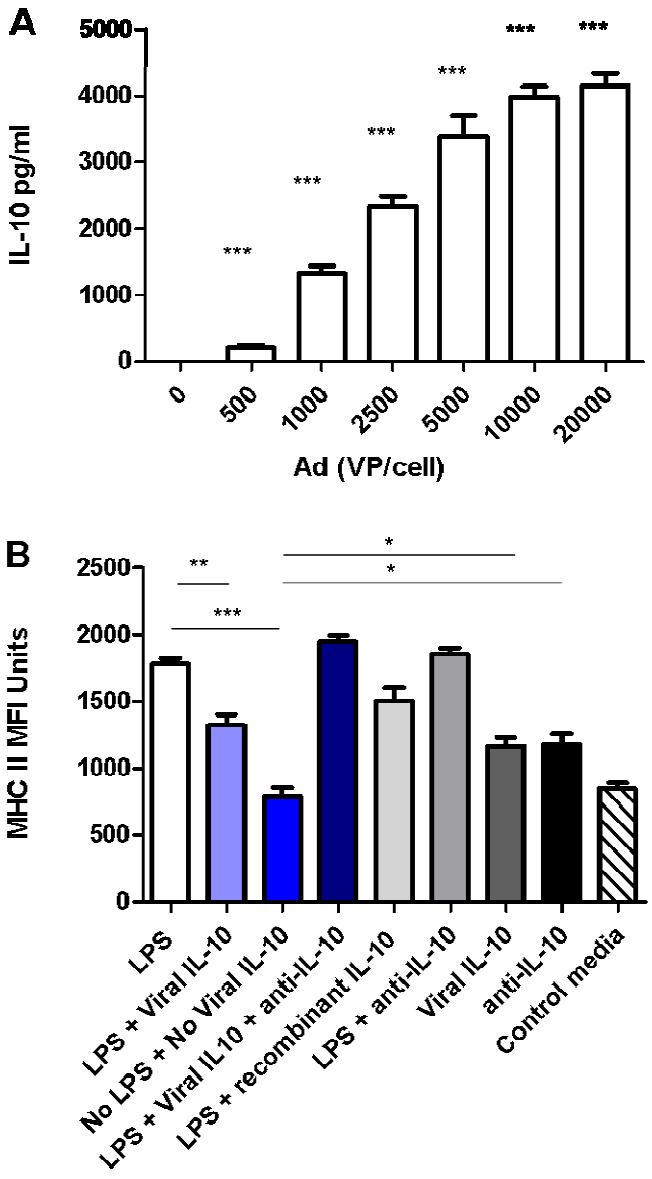

Figure 4: Transduction of hCAR DO11.10 CD4+ T cells with an IL-10 adenovirus and MHC II levels on DCs after activation with LPS in the presence of this IL-10. Significant levels of IL-10 were produced by T cells from the lowest VP of 500 and peaked at ~4000 pg/ml at 20,000 vp/cell (A). A significant decrease in MHC II levels was seen between LPS *vs* LPS with viral IL-10 group. No statistical difference was seen between LPS *vs* LPS, Viral IL-10 and anti-IL10 groups. No statistical difference was seen between LPS with viral IL-10 and LPS and recombinant IL-10 groups (B). Bars represent mean ± SEM, samples run in triplicate. *$P<0.05$, **$P<0.01$, ***$P<0.001$. A repeat experiment showed analogous results.

5.3.5 Th1 cells do not produce larger amounts of IL-10 than non-polarised CD4+ cells. The IFN-γ produced by these cells is unaffected by the increasing IL-10 they produce

As it was found in previous experiments that the GFP levels produced by hCAR DO11.10 Th1 cells transduced with an Ad GFP were significantly increased over non-polarised cells, it was hypothesised that this increase in transgene expression may also apply to IL-10 if Th1 cells were transduced with an IL-10 adenovirus. In addition, as these cells would now be producing IL-10, it was unknown if these Th1 cells would continue to produce their canonical cytokine, IFN-γ. A rare population of CD4+ T cells which produce both IL-10 and IFN-γ are found in some chronic inflammatory conditions [402] and so it was possible that IFN-γ production may be unaffected. Both Th1 polarised and non-polarised CD4+ T cells were transduced with an Ad IL-10 vector and IL-10 and IFN-γ ELISA carried out on the media 48 hrs after transduction.

Although IL-10 levels peaked at around 6000 pg/ml at 20,000 vp/ml which was higher than seen in previous experiments with non-polarised cells, the comparison at 10,000 vp/ml of IL-10 levels revealed no statistical difference between amounts produced in polarised and non-polarised cells (Figure 5A). It was found that although the level of IL-10 produced by transduced Th1 cells increased, the IFN-γ produced by these cells remained relatively constant with no statistically significance found between viral concentrations (Figure 5B).

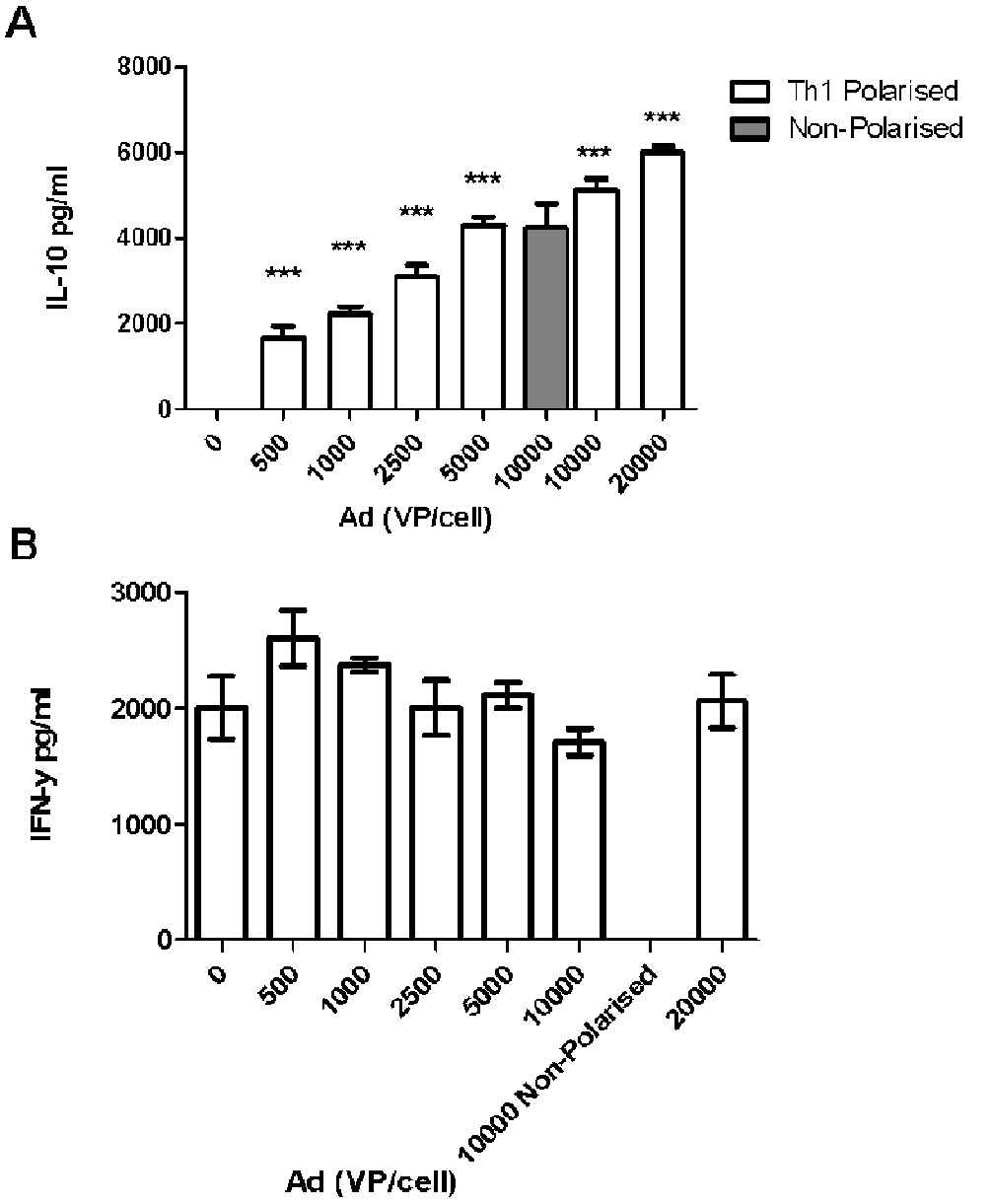

Figure 5: IL-10 levels from non-polarised and Th1 polarised hCAR DO11.10 cells post Ad IL-10 transduction and the IFN-γ from those Th1 cells. Significant IL-10 was again detected at all VP. No significant difference in IL-10 was detected between non-polarised cells and Th1 cells at 10,000 vp/cell (A). IFN-γ levels remained constant in the Th1 polarised group despite increasing IL-10 levels. No statistical difference was found (B). Results are expressed as mean ± SEM, n=3. ****P<0.001*

5.3.6 C57BL/6 CD4+ T cells were unable to be transfected using the Nucleofection™system

The murine model of atherosclerosis in our laboratories is the ApoE$^{-/-}$ mouse. A deletion of the ApoE gene results in normal mouse development but a serum cholesterol level 5 times that of a normal mouse which in turn induces spontaneous atherosclerotic lesion development. In an effort to work around the issue of different model backgrounds (hCAR BALB/c, ApoE$^{-/-}$ C57BL/6), the introduction of plasmid DNA may be achieved via electroporation, thereby removing the need for the hCAR strain and allowing direct transfection of C57BL/6 CD4+ cells. According to the protocol, different transfection levels are seen in cells derived from the lymph node and spleen therefore CD4+ cells from both were transfected separately with GFP expression being assessed 48 hrs later.

Figure 6 shows that in all samples the majority of cells were killed by the Nucleofection™ process as shown by the low number of cells falling into the lymphocyte gate, leaving on average just under 1% of lymphocytes. Of these remaining cells, only a very low number expressed GFP. Figure 4 is a representative plot of each group (n=3), there was no statistically significant production of GFP in any group.

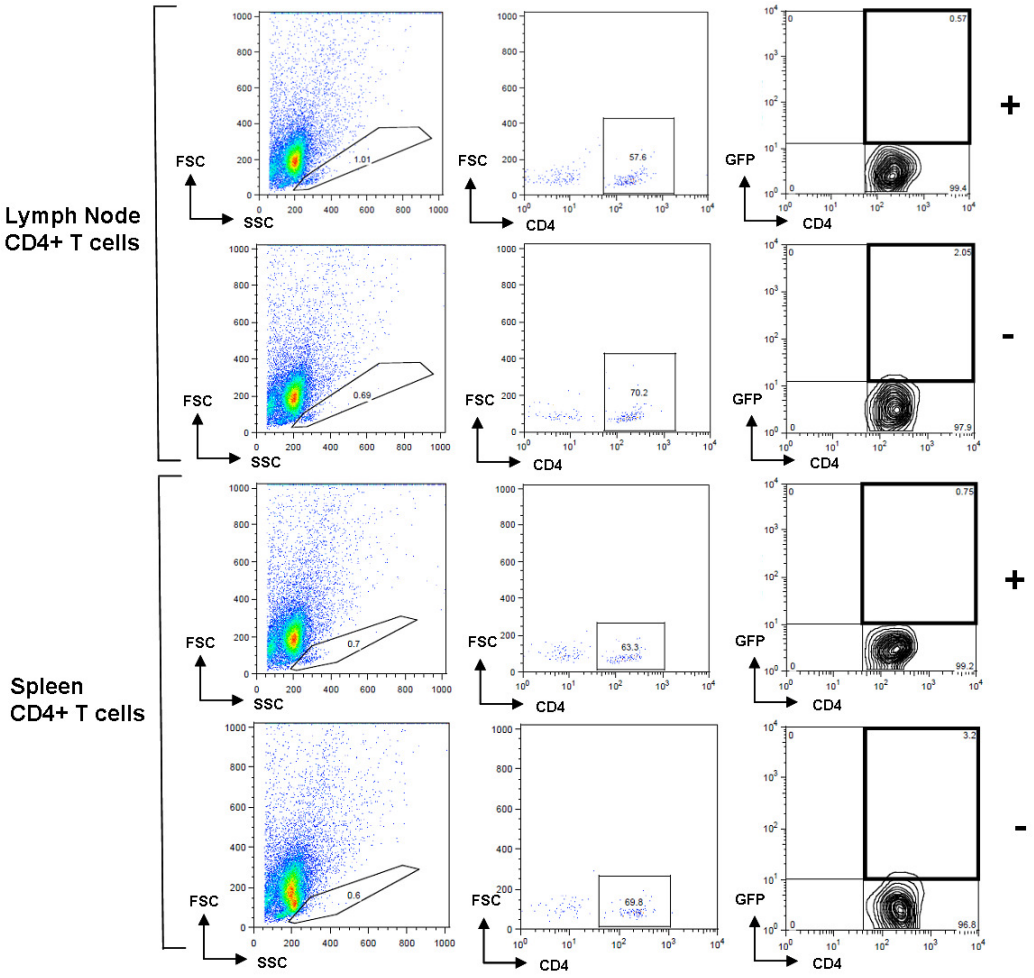

Figure 6: Representative FACS plot of the Nucleofection™ of either lymph node or spleen derived C57BL/6 CD4+ T cells with (+) and without (-) GFP expressing plasmid (pmaxGFP). Cells were gated on lymphocytes, CD4+, CD4+ GFP+. Only a very small proportion of lymphocytes survived the electroporation. No statistically significant levels of GFP expression were seen in either lymph node or spleen derived CD4+ T cells. Horizontal plot groups are representative of 3 mice per group.

5.3.7 C57BL/6 CD4+ T cells were unable to be transduced by a GFP expressing lentivirus

As discussed before, an alternate method of delivery for our therapeutic gene into T cells was needed in order to overcome genetic background issues related to the hCAR DO11.10 and ApoE$^{-/-}$ mouse strains. Using a lentiviral vector engineered to express the vesicular stomatitis virus (VSV-G) envelope allows the transduction of C57BL/6 CD4+ T cells as it does not require a specific receptor (e.g.hCAR) in order to enter the cell [390]. An additional advantage of using a lentiviral vector lies in its ability to incorporate itself into the genome of the host cell, therefore if the cell proliferates, every daughter cell will contain the inserted transgene which would allow sustained expression. C57BL/6 CD4+ T cells were incubated with a range of GFP expressing lentivirus following a protocol by [351]. GFP expression was check 72 hrs post-transduction, the peak time for lentiviral transgene expression.

Figure 7 shows representative plots of the viral concentrations used, each group being n=3. It was found that no GFP expression was observed at any of the MOIs of lentivirus used.

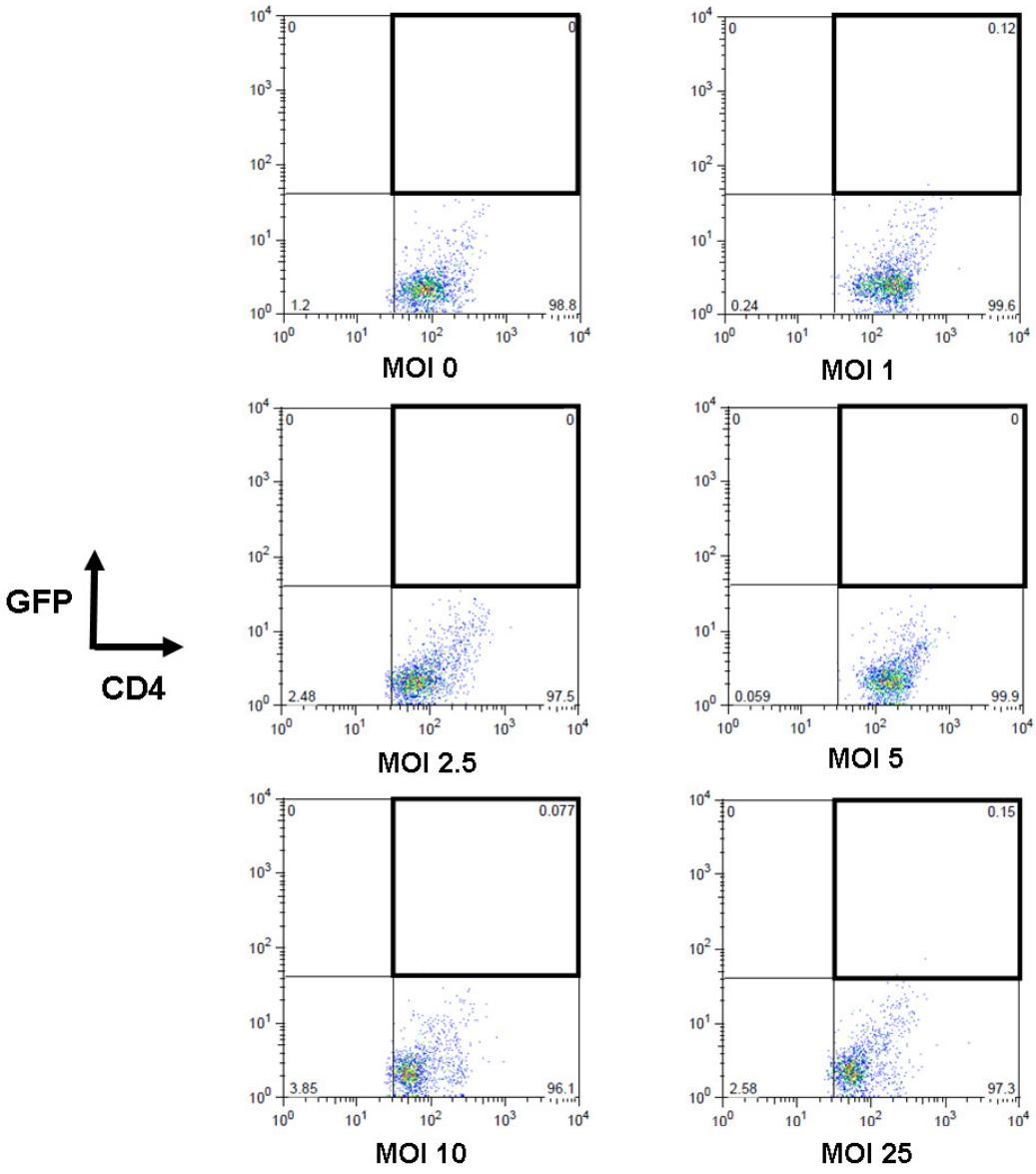

Figure 7: Representative FACS plot of C57BL/6 CD4+ T cells transduced with a GFP expressing lentivirus. Cells were first gated on lymphocyte population determined by size and granularity, then CD4+ *vs* GFP. No statistically significant GFP expression was observed at any of the MOIs of lentivirus used. Plots are representative of n=3 mice.

5.3.8 hCAR OT-I cells exhibit poorer transduction levels and cell viability after transduction with Ad GFP and Ad IL-10

hCAR mice on a C57BL/6 background (hCAR OT-I) were found and imported from Professor Kristin Hogquist's group, with the hope of using these cells for transfer into $ApoE^{-/-}$ recipients. As the transduction of these cells may be different from the data obtained in the hCAR DO11.10 mice and the fact that the future transfer experiments would be based on transduction data obtained here, it was imperative that these new hCAR OT-I C57BL/6 CD4+ cells be tested with a concentration range of the IL-10 adenovirus, and the control GFP virus, in order to find the optimal viral concentration for maximal transduced cell output. CD4+ T cells were isolated from both hCAR OT-I (C57BL/6) and hCAR DO11.10 (BALB/c) mice and transduced with a range of both Ad IL-10 and its control Ad GFP virus at a range of concentrations and FACS analysis and IL-10 ELISA carried out 48 hrs post-transduction.

In Figure 8A, it is shown that there is a significantly lower amount of IL-10 produced from the hCAR OT-I CD4+ cells than the hCAR DO11.10 cells at all the viral concentration used. When looking at the viability of the cells, it was found that the hCAR OT-I cells exhibited significantly higher levels of cells death when compared to the hCAR DO11.10 cells (Figure 8B). Again we observe that a significantly lower amount of transgene expression when the hCAR OT-I CD4+ cells are transduced with an Ad GFP (Figure 8C) when compared to hCAR DO11.10 cells with the same significant increase in cell death (Figure 8D).

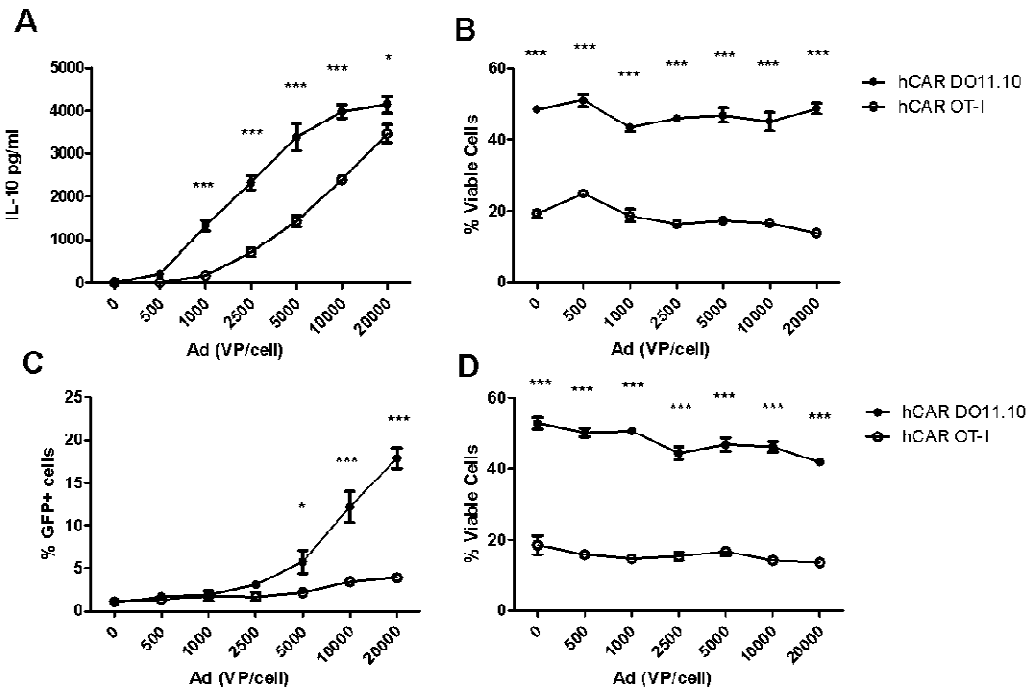

Figure 8: A comparison of Ad GFP and Ad IL-10 transduced hCAR DO11.10 (BALB/c) and hCAR OT-I (C57BL/6) CD4+ T cells. A significantly lower amount of IL-10 was produced by hCAR OT-I cells at most VPs after transduction with Ad IL-10 (A), the viability of these cells was also significantly lower than the hCAR DO11.10 cells (B). hCAR OT-I cells showed significantly lower transduction levels than hCAR DO11.10 after transduction with Ad GFP, only producing significant levels of GFP at 10,000 vp/cell and 20,000 vp/cell (C), again a consistently lower viability was observed in the hCAR OT-I cells (D). Points denote mean ± SEM, n=3, *$P<0.051$ ***$P<0.001$

5.3.9 Poor hCAR OT-I CD4+ cell viability is not related to C57BL/6 background and have a tendency to die over hCAR DO11.10 CD4+ cells.

In order to further investigate the significant cell death observed only in the hCAR OT-I C57BL/6 CD4+ cells, the same experiment was carried out but this time using wild type (wt) C57BL/6 CD4+ T cells. If cell viability is also low in the wt group, the cells death may be attributable to the genetic background of the mice. In addition, hCAR OT-I and wt CD4+ T cells were incubated after isolation, with no viral transduction or activation, for 48 hrs in order to observe the natural cell survival with no stimulus. The activation method was also altered from PMA/Ionomycin to anti-CD3 anti-CD28 stimulation with double serum complete RPMI incubation media, as it was thought this may be a less harsh method of activating the cells which may in turn result in higher cell viability.

Similar IL-10 levels were found in the media at 48 hrs in comparison to the previous experiment from the hCAR OT-I cells with low levels produced by wt T cells (Figure 9A). Cell death was significantly higher in the hCAR OT-I CD4+ T cells than it was in the wt CD4+ T cell group, with similar viability levels of ~15-25% as seen in the previous experiment (Figure 9B). Transduction using the Ad GFP was more successful in this experiment, with a peak of ~18% observed at 20,000vp/cell (Figure 9C) in hCAR OT-I CD4+ cells, however the same significantly higher level of cell death was found in the hCAR OT-I cells compared to the wt group.

After 48 hrs of incubation, no transduction, the hCAR OT-I CD4+ T cells were found to, again, have significantly increased cell death over wt CD4+ cells (Figure 10A). Altering the activation to anti-CD3 anti-CD28 with incubation media containing 20% FCS was found to be ineffective at raising the hCAR OT-I cell viability above the 15-20% observed in previous experiments (Figure 10B).

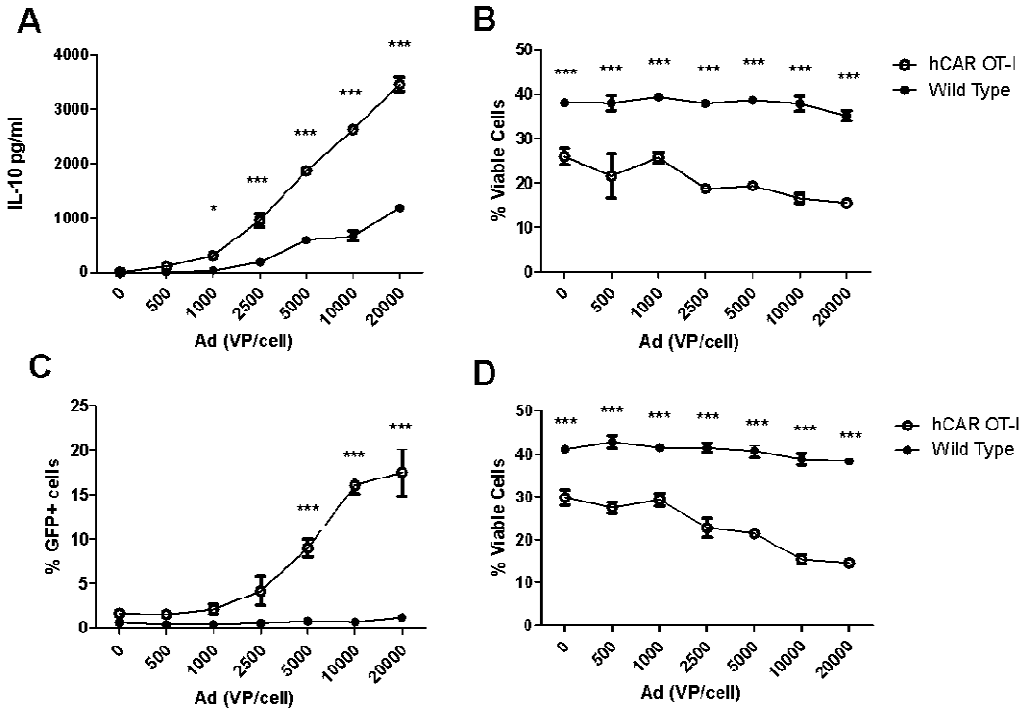

Figure 9: A comparison of Ad GFP and Ad IL-10 transduced hCAR OT-I and wt CD4+ T cells. As expected a higher amount of IL-10 was produced by the hCAR OT-I cells than wt cells post Ad IL-10 transduction (A), with the viability of the hCAR OT-I cells being significantly lower than that of wt CD4+ cells (B). Up to ~18% transduction was seen in the hCAR OT-I mice after Ad GFP transduction (C) with the viability once again being significantly lower than that of the wt CD4+ cells (D). Points represent mean ± SEM, n=3, *$P<0.05$ ***$P<0.001$.

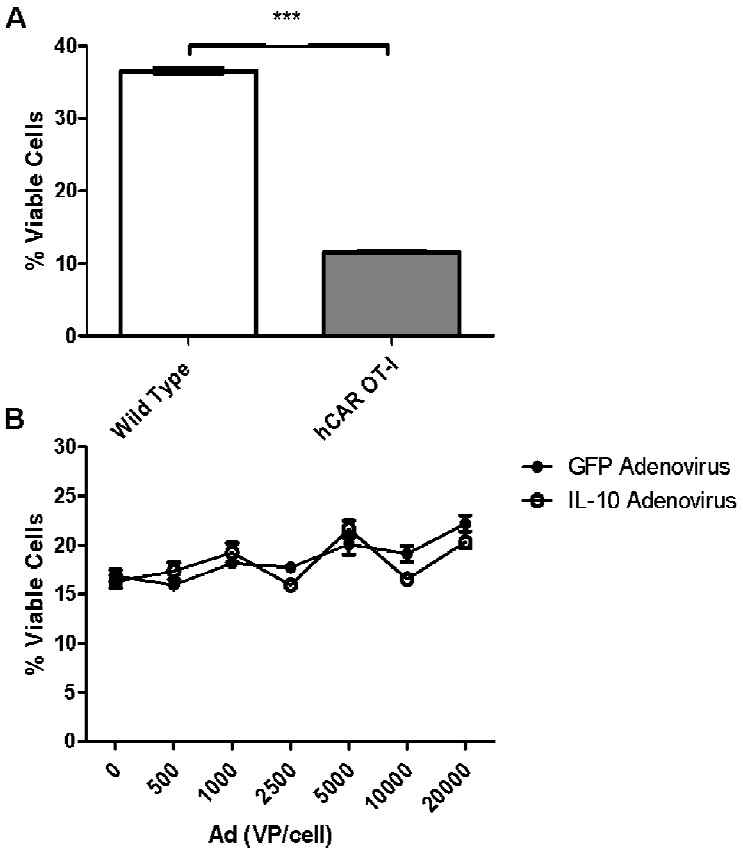

Figure 10: Cell viability of hCAR OT-I and wt T cells after 48 hours incubation. Viability of hCAR OT-I T cells after using anti-CD3/CD28 activation in place of PMA/Ionomycin. After only incubation, a significant decrease in viability can be seen in the hCAR OT-I group compared to wt CD4+ cells (A). The same low levels of viability of hCAR OT-I CD4+ T cells were observed when using anti-CD3/CD28 activation as in the previous experiments using PMA/Ionomycin (B). Bars represent mean ± SEM, n=3. ****P<0.001*

5.4 Discussion

In this chapter, optimisation of the transduction and transfection of CD4+ T cells for future transfer into an animal model of atherosclerosis was attempted. A range of techniques were used including adenoviral vectors, lentiviral vectors and Nucleofection™ with the inclusion of Th1 polarisation and the addition of blood coagulation factor 10 (FX). Using a GFP expressing adenovirus we found that peak transduction levels were reached at a viral particle to cell ratio of 5000 vp/cell at 48 hrs post-transduction. Polarisation of CD4+ T cells to a Th1 phenotype induced a slight increase in transduction levels and showed to bring about a large increase in the amount of GFP produced within the cells. A decrease in transduction was observed in both Th1 polarised and non-polarised CD4+ cells after the addition of FX at the time of virus addition however a significant decrease in GFP levels within the cells was only seen in Th1 cells. Biologically active IL-10 was successfully produced from T cells transduced by an IL-10 expressing adenovirus, the IL-10 being capable of suppressing MHC II upregulation on LPS stimulated DCs. The same increase in transgene expression of GFP observed in Th1 cells was not seen here as IL-10 levels remained the same as in non-polarised cells. In IL-10 producing Th1 cells IFN-γ levels remained constant. Both the Nucleofection™ and lentiviral approaches to CD4+ T cells transduction were unsuccessful, with the Nucleofection™ killing the majority of the CD4+ T cells used. The imported hCAR OT-I mice exhibited lower levels of transduction than their BABL/c counterparts, displaying high levels of cell mortality. This affect was not observed in C57BL/6 mice and under normal incubation conditions, the hCAR OT-I CD4+ T cells showed a tendency to die. Altering the activation method in the transduction protocol to an alternative manner had no effect on these low viability levels.

Although the majority of optimisation work had been carried out previously by Hurez et al. [296] it was practical for us to carry out a level of

optimisation with our hCAR DO11.10 mice strain and vectors. The majority of initial work was carried out using a GFP expressing adenovirus serotype 5 (not the vector produced in chapter 4 but one already in production in Prof. Baker's lab), which proved a reliable tool for our work. Upon using a range of virus concentrations with the CD4+ hCAR cells, a maximal transduction level of around 80% was reached at the higher viral concentrations (10-20,000 vp/cell) after 24 hrs post-transduction. After 48 hrs post-transduction 80% of transduction was reached but at a lower concentration of 5000 vp/cell, matching levels in previous literature [296]. This maximum transduction of 80% could indicate that not all of the CD4+ T cells from the hCAR DO11.10 transgenic mouse expressed the hCAR molecule on their surface. As screening of these animals was conducted using PCR rather than FACS analysis, mice were deemed hCAR positive based on the presence of the hCAR gene rather than surface expression. The increase in transduction between 24 and 48 hrs is consistent with previous literature indicating that peak adenoviral transgene expression is reached at 2 days post-transduction [403, 404], and so for all other adenoviral experiments, transgene expression was recorded after 48 hrs. Interestingly, the BALB/c control mice also showed a low level of transduction despite lacking the hCAR receptor, an affect also observed to an extent in previous literature [405]. T cells naturally express very low levels of $\alpha_v\beta_3$ and $\alpha_v\beta_5$, integrins thought to be essential along with the CAR molecule for adenoviral transduction. Previous work has shown however, that activation of T lymphocytes with a stimulus such as phorbol myristate acetate (PMA), upregulates these surface integrins and allows low levels of CAR independent adenoviral transduction [406]. It is likely that this integrin based transduction accounts for the low levels of transduction seen in the BALB/c cells.

As discussed earlier, the majority of immune cells in the aortic wall at the site of a plaque are T cells [50], the majority of which being of a Th1 phenotype [6, 48]. This polarisation may have some positive affect on the

migration and residing of these cells at this site, so with this in mind, transduction of Th1 cells was investigated. A small increase in transduction levels was observed in Th1 cells, this being more evident at the lower virus concentrations, with transduction reaching into the 90% and above, higher than levels obtained in Hurez et al. [296]. It is worth noting that the transduction of non-polarised cells was also slightly higher than in previous experiments however a significant increase was still observed in the Th1 group. This slight increase may be attributable to the increase in CAR independent uptake, discussed previously [150], as transduction levels observed in the Th1 BALB/c group were also higher than non-polarised BALB/c cells. Although not stated in the literature, it may be that Th1 cells express higher levels of these $\alpha_v\beta_3$ and $\alpha_v\beta_5$ integrins, or alternatively that the levels are higher due to the two rounds of activation they have under gone, one for Th1 polarisation and a second for viral transduction. An even more interesting finding was that the MFI of GFP in the GFP+ cells, which gives a measurement of the amount of GFP present within the cells, was significantly higher in the Th1 groups than non-polarised. This data implies that the adenovirus is producing higher levels of the transgene (GFP) in the Th1 cells, a phenomenon also observed by Hurez et al. [296]. This increase may be related to multiple factors associated with Th1 cells and also the protocol used in this research. The fact that Th1 cells produce higher levels of IFN-γ mRNA than non-Th1 cells [407] may allow the vector access to more abundant and sustained transcriptional machinery, therefore creating larger amounts of GFP. Alternatively, in our method, the polarisation process involves activation through the TCR, this means that the activation of the cells at the time of viral incubation is the second round of activation and the resulting proliferation could therefore involve a memory cell response of some sort. As it is now generally accepted that naïve and memory CD4 T cells proliferate at a similar rate [408], it is unlikely that this increase in GFP is related to cellular proliferation. It may be more likely that, as memory cells have a higher and more rapid level of transcription post-activation [409], related in part to increased NF-κB

controlled cytokine production [410], that this is in some way taken advantage of by the viral vector, therefore creating the higher levels of GFP transgene. As mentioned, one of the main motives for using Th1 polarised cells, was due to their superior accumulation at the site of plaque formation, an element we may have wished to take advantage of for adoptive transfers. However due to our inability to use $ApoE^{-/-}$ mice as recipients for these cells (discussed in later chapters), the use of Th1 cells for future adoptive transfer was discontinued.

HSPGs, further divided into syndecans and glypicans, are cell surface molecules which bind extracellular proteins to form signalling complexes, can also immobilise proteins for internalisation by the cell and enable cells to snare a wide variety of extracellular molecules [411]. It is well known that HSPGs are expressed on a wide variety of adhesive cells [412] but there is also literature indicating that proteoglycans are also present on the surface of T cells [397-399]. Due to the retargeting properties coagulation factor 10 (FX) has on adenoviral vectors for these HSPGs [395, 396], we investigated if the addition of FX during viral incubation with a GFP expressing adenovirus would have a positive effect on transduction. We found that the addition of FX actually had a negative effect on transduction levels, inducing a significant reduction in both non-polarised and Th1 cells. If the correct HSPG is not displayed on the surface of the T cells, this reduction in GFP expression may be due to a form of steric hindrance brought on by the binding of FX to the viral capsid, the lack of HSPG possibly inhibiting the rapid entry into the T cell [413].

To our surprise, the GFP levels produced by the cells was decreased in Th1 cells, with MFI levels returning to those seen in the non-polarised cells. An effect at the transcriptional level could imply an effect on the translocation to the nucleus perhaps through an effect on molecules of the cytoskeleton. The cytoplasmic motor dynein plays a critical role in the transport of the post-endosomal adenovirus to the nucleus of the

transduced cell. The binding of the adenovirus to the dynein molecule is through the hexon region of the virus capsid [414, 415] (the same site as FX), therefore the binding of FX could affect dynein binding and therefore the translocation of the virus to the nucleus, indeed it has been shown that if hexon/dynein binding is inhibited, transport of adenoviral vectors is affected [416]. As a result, FX was not used in any further transduction experiments.

The concept behind this project was to use the natural homing properties of T cells, for sites of inflammation, so that they could infiltrate the inflamed vascular tissue and release a therapeutic molecule into the surrounding tissue, inhibiting the inflammatory process. The therapeutic molecule we chose for this task was interleukin 10 (IL-10) a well known anti-inflammatory cytokine with a proven record in inhibiting the pathological symptoms of atherosclerosis [80, 96, 97, 336, 337]. An adenovirus encoding the murine IL-10 gene was produced and, as with the GFP encoding virus used previously, a range of virus concentrations were used on the T cells to assess its viability. We found that even at the lowest concentration of virus used, significant levels of IL-10 were detectable in the culture media after 48 hours. In addition to knowing that the viral IL-10 was detectable by the anti-mouse IL-10 antibody of the ELISA kit, we needed to know if it was functional. Owing to its effects on DCs [400, 401], this cell type was chosen to be our functionality assay. The viral IL-10 was capable of inhibiting the upregulation of MHC II in response to LPS stimulation, to the same extent as that seen with recombinant murine IL-10 purchased from a supplier. When the IL-10 was neutralised using an anti-IL-10 antibody at the time of DC activation, the MHC II levels were the same as in the group which received LPS only, therefore showing that it was categorically the viral IL-10 causing this downregulation of DC MHC II levels. From this data we can summarize that as DCs play such a crucial role in the development and perpetuation of an immune response, that if IL-10-transduced T cells were transferred into an $ApoE^{-/-}$ recipient mouse they

would suppress the local and systemic response and therefore pathology. Unfortunately, due to a low viral output and low quality in terms of functional VP during production (discussed in chapter 4), using this IL-10 vector in future transfer experiments has been impractical.

As our previous data showed, polarisation to a Th1 phenotype increased the levels of GFP produced after transduction by a GFP encoding adenovirus. If this was also the case with Th1 cells transduced with our IL-10 adenovirus, although deemed unfeasible for this project, it could be of significant interest for future research into immunotherapy research. To our surprise we found that Th1 cells transduced with our IL-10 adenovirus did not produce higher levels of IL-10 compared to non-polarised cells, this may indicate that although higher levels of IL-10 may have been produced, elements involved in the secretion of the cytokine may not be functioning at a high enough rate for proper secretion, this could be assessed in the future by comparing intracellular IL-10 levels in Th1 and non-polarised cells. An additional aspect of IL-10 transduction we wanted to investigate was its possible affects on the transduced cells ability to produce its natural cytokines, in this case using Th1 cells. As IL-10 and IFN-γ are only produced simultaneously by a small subset of T cells present in cases of non-clearing chronic inflammation [402], it was unknown if, with increasing levels of IL-10 being produced by the Th1 cells, whether their ability to produce IFN-γ would be altered. Although slightly variable, we found that there was no statistical difference in IFN-γ levels at any of the increasing virus concentrations used. Hurez et al. [296] had previously looked at the effects of purely transduction on Th1 cells showing it had no effect, we have shown that although cells are producing increasing amounts of an immunologically suppressive cytokine, that it has no autocrinological affects on the host cells normal cytokine profile.

In an attempt to circumvent the issue of not being able to use the BALB/c hCAR DO11.10 for transfer into a C57BL/6 ApoE$^{-/-}$ recipient we employed

the use of both the Nucleofection™ system (kindly loaned by Prof. Andrew Waters, University of Glasgow) and a Lentiviral vector to allow direct incorporation into C57BL/6 CD4+ T cells, avoiding the need for transgenic mice. Although success in using the Nucleofection™ system had previously been reported in T cells [315, 387-389], our findings were that the electroporation process was too harsh on our C57BL/6 T cells, killing the majority of cells and only leaving a very small viable population. This technique was repeated twice with the same high cell mortality so this approach was abandoned in favour of trying a lentiviral approach. Basing our protocol on that of Gilham et al. [351] we used a range of virus concentrations (multiplicity of infection-MOI), but found no significant GFP expression at any of the concentrations used. It is worth noting here that we used only IL-2 and not IL-7 in this protocol, however even with this missing low levels of transduction should have been visible. This lack of transduction may be due to the activity of endogenous restriction factors APOBEC3G/F and TRIM5α which are endogenous anti-viral molecules found within most cells. APOBEC3G/F are cytidine deaminases which convert viral cytidine residues to uracil, these mutations then leading to the inactivation or viral replication. The TRIM5α molecule tags the virus for proteosomal degradation before any significant levels of virus replication can occur [417]. Both of these factors represent a robust method by which infected cells can protect themselves from retroviral infection [418], including CD4+ T cells [419]. Additionally, the vector we used in these experiments had the promoter of the spleen focus forming virus (SFFV) which was shown by Gilham et al. [351] to have the lowest transduction efficiency of a range of promoters they tested.

As the adenoviral transduction of T cells had proven successful, we would ideally have liked to use this approach in transducing cells before transfer into $ApoE^{-/-}$ recipient mice. Luckily we were able to locate and import hCAR mice on a C57BL/6 background (hCAR OT-I) from Professor Kristin Hogquist in Minnesota which should have enabled us to proceed as planned.

Unfortunately we found that transduction levels with both the IL-10 and its control GFP virus proved to be significantly lower than those obtained in the hCAR DO11.10 cells, producing lower levels of IL-10 and variable levels of GFP. An unusual result that was found with these cells was that they had a constant and significantly higher level of cell mortality when compared to their BABL/c counterparts, this being observed in both Ad GFP and Ad IL-10 transduced cells. In order to rule out that this mortality wasn't related to the C57BL/6 background, hCAR OT-I cells were then compared to C57BL/6 wt CD4+ cells. In this comparison, cell death was significantly higher in the hCAR OT-I cells than wt, again for both vectors. Cells that were isolated for this experiment (CD4+ isolation) but not used in the transduction stage were incubated under standard incubation conditions in complete RPMI for 48 hours. It was found that the number of viable cells after this time was much lower in the hCAR OT-I group therefore indicating that hCAR OT-I CD4+ cells have a lower survival ability or have a natural tendancy to die over normal CD4+ T cells. Altering the protocol to replace the activation method with a TCR based technique and the inclusion of double serum incubation media, had no affect on this low viability count. Unfortunately there are no current publications using these mice and so this hCAR and background-independent mortality is difficult to explain. Members from Prof. Hogquist's group have only used the CD8 cells from this moue strain and not CD4+ and so have not encountered this issue. Generally in OT-I transgenic mice, CD4+ cell counts are very low in comparison to the number of CD8 cells in the mouse [420] due to the thymic TCR selection process, although how this would affect the cells out of the donor is not clear. These findings have therefore meant that using the $ApoE^{-/-}$ mouse as a recipient for our genetically modified T cells would not be a feasible option and would instead need to be replaced with a BALB/c alternative.

To conclude, we have shown that the modification of CD4+ T cells was most successful using an adenoviral vector in comparison to Nucleofection™ or a lentiviral approach. We have demonstrated that polarisation to a Th1

phenotype appears to have an affect on the level of transgene produced within the cell and also increases transduction levels slightly, whereas FX has a deleterious affect on these aspects. Most importantly we have shown that T cells can be transduced with an IL-10 encoding vector with the cells going on to secrete this cytokine and that it is also biologically active, with no affects on the transduced cells ability to produce it's natural cytokine profile, indicating it would not alter its normal inflammatory related function. Unfortunately, transduction of hCAR mice of a C57BL/6 background proved ineffective due to unknown issues with cell viability which will compel us to alter our recipient animal model for these genetically modified cells. Although we found it to be ineffective at transducing CD4+ T cells, the lentiviral approach could be promising if more time and optimisation could be carried out. It has already been shown that with the correct cytokine and TCR stimulation, CD4+ T cells can be transduced to a reasonable level using either the EF1 or PGK promoter (~60%) [351] with the added advantage that every daughter cell of a proliferating transduced T cell would also carry the inserted therapeutic gene, rendering it a powerful tool in relation to T cell expansion *in vivo*.

To summarize:

- Transduction of CD4+ T cells was successful with transduction reaching up to 80%

- The polarisation of the T cells to the Th1 phenotype pre-transduction increased transduction % and the amount of transgene produced in the cells

- The addition of blood coagulation factor 10 decreased the transduction levels of both non-polarised and Th1 CD4+ T cells, most likely due to a form of steric hindrance

- The IL-10 produced by transduced cells was shown to be biologically active

- Unlike with GFP production, Th1 cells do not produce larger amounts of IL-10

- The main pro-inflammatory cytokine produced by Th1 cells was not affected by the anti-inflammatory IL-10 the cells were producing

- Nucleofection was unsuccessful in transfecting C57BL/6 CD4 T cells as was lentivirus, which would have allowed direct transfer of the T cells in $ApoE^{-/-}$ recipients

- The hCAR OT-I mice imported to allow transduction and transfer into $ApoE^{-/-}$ mice were poor at being transduced and exhibited poor viability which was not related to their C57BL/6 background.

Chapter 6: Migration of adenovirus transduced CD4 T cells post-transfer into BALB/c recipient

6.1 Aims and rationale

In this chapter, fluorescent activated cell sorting (FACS) was used to track the migration of adoptively transferred CD4 T cells, transduced with a GFP expressing adenovirus, in BALB/c recipient mice. There has been relatively little research into the transduction of CD4 T cells using adenoviral vectors, some of which having studied what affects this transduction has on the ability of cells to act and behave in a typical CD4 manner. As the overall concept for this transduction of T cells would be to use them as an inflammation-specific immunotherapy. It is therefore important to know that the cells will act identically to non-transduced cells in their migration patterns. Therefore, transduced hCAR DO11.10 (BALB/c) cell migration was compared to non-transduced in naïve BALB/c mice. Here the lymph nodes, spleen and liver of BALB/c mice that either received AdGFP-transduced CD4 T cells or non-transduced CD4 T cells, were strained and FACS analysis carried out to look for the presence of GFP positive CD4 T cells at 24 hrs and 72 hrs post-transfer.

6.2 Introduction

Although current approaches for treating atherosclerosis, both clinical and experimental, are proving to be effective treatments (see chapter 1.11), none address the chronic inflammation directly present at lesion sites. This lack of site-specific treatment is in part related to the lack of effective site targeting and it is important to emphasise that at this time it is not possible to effectively target the vascular wall. Previous research using transduced T cells have shown promise in other pathologies [382, 383], but none have been applied to the field of atherosclerosis. In this chapter we investigate whether immune cells transduced with a viral vector will, after adoptive transfer into a mouse recipient, migrate in a similar way to non-transduced immune cells, thereby offering a novel approach to delivery of a therapeutic molecule specifically to the site of inflammation, thus avoiding the non-specific systemic affects encountered with the current therapies.

Naïve CD4+ T cells re-circulate through the secondary lymphoid organs of the body (lymph nodes, spleen, mucous based lymphoid structures) [421] until they come into contact with an APC (dendritic cell), presenting antigen specific for a particular naïve T cell, which interrupts this recirculation process. Following antigen presentation in these secondary lymphoid organs, T cells upregulated CD69 which binds and inactivates $S1P_{1,}$ (a molecule which allows the efflux of T cells from a lymphoid organ) therefore retaining the T cells within the lymphoid organ [422]. T cells release growth factors, divide, and undergo polarisation to specific subsets best equipped for the task they are preparing for [423, 424], all of which peaks at around 1 week after encountering the presented antigen [425, 426]. As numbers peak, the CD4+ T cells regain $S1P_1$ and leave the lymphoid organ, moving into the blood. Linked to this activation process is the expression of new adhesion molecules which allow the T cells to move into non-lymphoid tissues and carry out their role [427], with evidence

indicating that molecules related to the initial APC location and subsequent uptake of antigen, customise these adhesion molecules allowing tissue specific homing of the T cells [427, 428].

This natural ability of immune cells to migrate to sites of inflammation renders them ideal candidates as a site specific delivery vehicle. If re-programmed using a viral vector, such as adenovirus, these cells could act as "Trojan Horses", infiltrating tissues and also lymphoid tissues to release their therapeutic molecules that were encoded by the vector.

CD4 T cells were selected as the candidate cell type for several reasons. T cells have been shown to be present in the vascular wall at the very early stages, during the progression of atherosclerosis and also at the very late stages of the disease, having involvement in the formation and functionality of arterial tertiary lymphoid organs (ATLO) [40, 51]. Upon quantification of the cellular composition of the plaque, it was found that T cells make up the majority of cells, surprisingly outnumbering macrophages, the cell type most commonly associated with the atherosclerotic plaque [40]. In addition to being a persistent presence, T cells have also been shown to have a significant role in the disease development. The addition of CD4 cells into immunodeficient scid/scid $ApoE^{-/-}$ mice reversed the decrease in fatty streak formation those reported in these immunodeficient mice and also increased pathology past levels seen in immunocompetent $ApoE^{-/-}$ mice [5], this same effect being observed in scid/scid $ApoE^{-/-}$mice which received OxLDL specific CD4 T cells [258]. In addition, if the T cells present are altered to a Th2 phenotype instead of the typical Th1 found in atherosclerosis, pathology is reduced [6]. As well as their location and importance, T cells were also documented as being readily transducible using adenovirus (serotype 5), the protocol for which was optimised and published by Casey Weaver's group [296]. There is evidence for lentiviral vectors [351] and also Nucleofection™ [389] being able to introduce genetic information into T cells however we found that

both of these methods were unsuccessful (see chapter 5). Most importantly our approach requires that the T cells are capable of homing to the atherosclerotic plaque and lymphoid tissues in order for the therapeutic molecule to be effective. This has already been shown by Maffia et al. [51] and in chapter 3 of this thesis, where labelled leukocytes were able to home the vessel wall in both early and late stages of atherosclerosis in $ApoE^{-/-}$ mice. What is unknown however is if the transduction of the T cells has any effect on their migrational behaviour. Unfortunately, due to the issues encountered in using the hCAR OT-I mice (C57BL/6 background), discussed in the chapter 5, we were unable to use $ApoE^{-/-}$ mice as recipients. In this chapter, transduced hCAR DO11.10 CD4 T cells (BALB/c background) were instead transferred into BALB/c recipients and the migrational behaviour of the cells compared to that of non-transduced cells. Additionally, due to production problems encountered with the IL-10 expressing adenovirus (see chapter 5), not enough virus was available for transfer experiments and so a GFP expressing adenovirus was used. In this chapter, CD4 T cells transduced with a GFP expressing adenovirus, are transferred into BALB/c recipient mice. At 24 hours and 72 hours post transfer FACS analysis is carried out on the peripheral lymph nodes, spleen and liver of each animal and the migration of the cells is analysed and compared to that of non-transduced CD4 T cells.

6.3 Results

6.3.1 Adoptively transferred Ad GFP transduced hCAR DO11.10 CD4 T cells can be found in the peripheral lymph nodes, spleen and low variable numbers in the liver, at 24 and 72 hours post transfer into BALB/c recipient

In order to assess whether the approach of using transduced cells was optimal, the migration of these transduced cells must be studied to observe how they behave *in vivo*. Due to the lack of an inflammatory model and hCAR expressing CD4 cells on a C57BL/6 background, which would allow transfer into an $ApoE^{-/-}$ recipient, cells were instead transferred into a normal BALB/c recipient and their migration kinetics compared to non-transduced DO11.10 CD4 T cells. Cells were either transduced or not transduced with Ad GFP and at 24 and 72 hrs post-transfer into BALB/c recipients, the lymph nodes, spleen and liver were removed as described in the Methods.

After gating on CD4+, KJ1.26+ and then KJ1.26/GFP, a distinct GFP+ population was seen at 24 hrs in both the GFP cell recipient mice's peripheral lymph nodes (Fig 1), the spleen (Fig 2) but only in one of the liver samples (Fig 3). A very small percentage of GFP+ cells were seen in mice which received no transduced cells (Fig 1, 2, 3), however, this is attributable to "gating" on such a small population. This GFP+ population was also seen after 72 hrs with the organs again showing distinct GFP+ cells in the lymph node (Fig 4) the spleen (Fig 5) and a variable population seen in the liver (Fig 6). This data was confirmed in a repeat experiment, displayed in Figures 7, 8 9. No GFP+ cells were observed in the liver of this repeat (Fig 9), emphasising the variability of migration of transduced GFP+ T cells to this organ.

The migration of GFP+ cells to the lymph node is also clearly shown by looking at the total GFP+ cells in each organ. Figure 10 shows a GFP

population of approx. 400 cells in the lymph node at 24 hrs compared to approximately 25 GFP+ cells in the mice that received no GFP+ cells. Higher numbers were seen in the spleen, around 9000 cells at 24 hrs. In the liver, one of the mice that received transduced cells showed a population of approx. 263 cells with the other mouse showing no population at all.

At 72 hrs post transfer (Fig 11) the number of cells in the GFP+ population increased several fold, ranging from $8.23x10^3$ to $1.2x10^4$ in the peripheral lymph nodes, compared to the approximate 400 observed at 24 hrs. This increase in cell number was also seen in the spleen, the numbers present at 24 hrs being approx. 9000 ranging from $1.13x10^5$ to $1.43x10^5$. A very low GFP+ population was observed in the liver of both the GFP transduced cell recipients with numbers of 75 and 10 observed.

The repeat of this experiment, assessing at the 72 hr time point (Fig 12), again showed higher numbers than were seen at the 24 hr time point. Numbers present in the lymph nodes were 5500 and 4400 and in the spleen, 5.42×10^4 and 3.34×10^4. The number of GFP cells found in the liver was again low and variable with 35 in one mouse and 160 seen in the second mouse that received transduced cells. Due to the difficulty in gating on an organ composed of so much connective tissue, high background levels of GFP expression were detected even in the mice which did not receive GFP+ cells. The liver cell number counts were therefore omitted from this experiment.

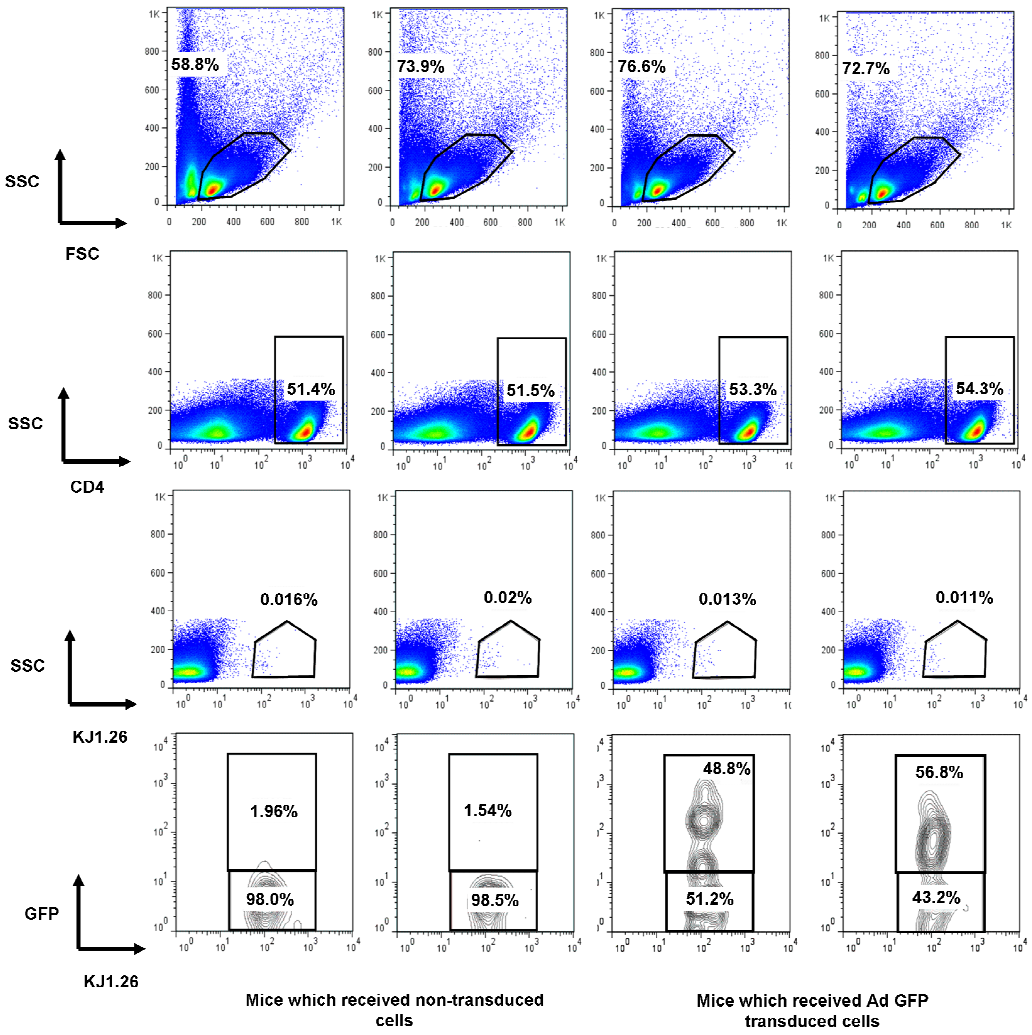

Figure 1: FACS plots showing GFP+ cells in peripheral lymph nodes, 24 hrs post-transfer. Ad GFP-transduced, or non-transduced, hCAR DO11.10 CD4+ T cells were transferred into BALB/c recipients. After 24 hrs the inguinal, brachial, axillary and 2 x superficial cervical lymph nodes were taken and strained through a nitex cell strainer and washed with FACS Buffer. Cells were labelled with CD4 APC and KJ1.26 PE. Lymphocytes were identified based on the FSC and SSC profile and were gated on CD4 expression and then KJ1.26 and GFP. Plots for each mouse were analysed and the data represented in later figures.

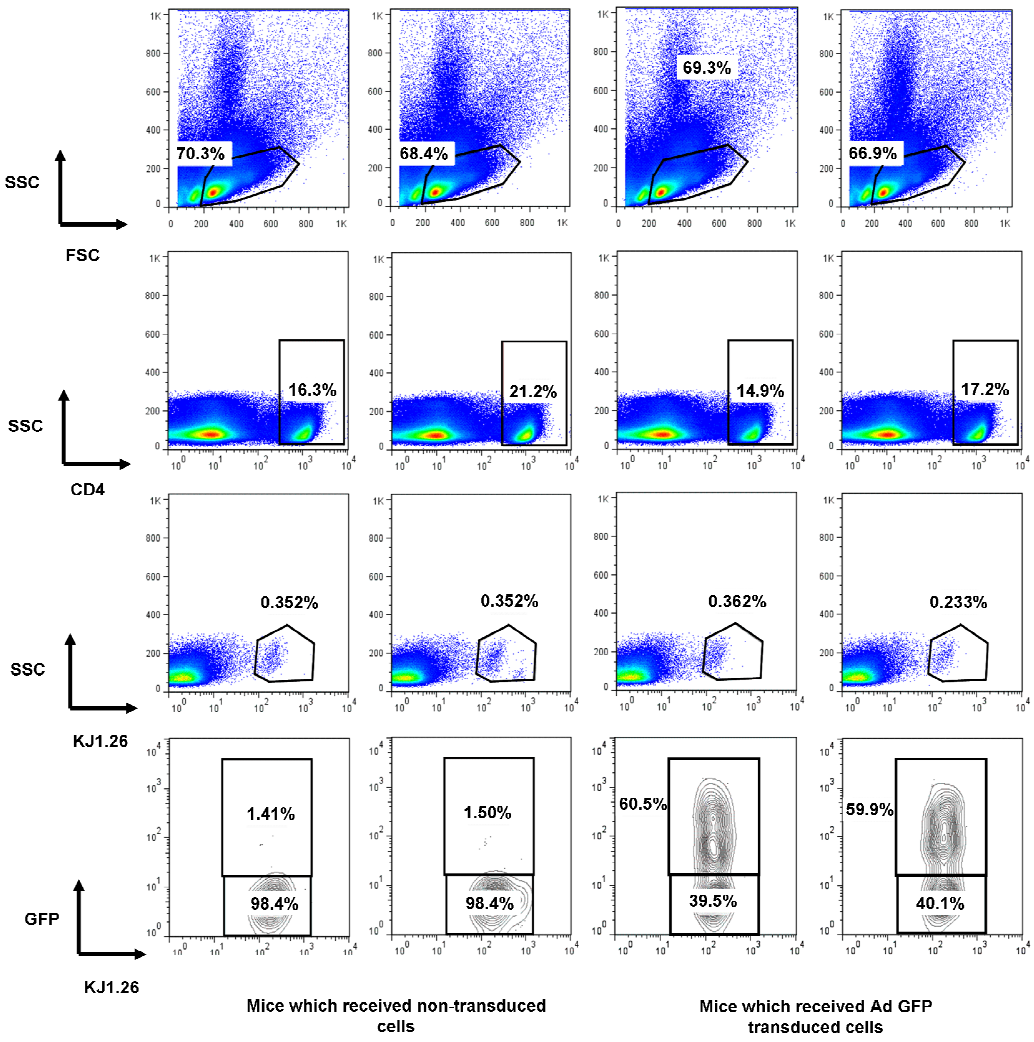

Figure 2: FACS plots showing GFP+ cells in spleen, 24 hrs post-transfer. Ad GFP transduced, or non-transduced, hCAR DO11.10 CD4+ T cells were transferred into BALB/c recipients. After 24 hrs the spleen was taken, strained through a nitex cell strainer, treated with RBC lysis solution and washed with FACS Buffer. Cells were labelled with CD4 APC and KJ1.26 PE. Lymphocytes were identified based on the FSC and SSC profile and were gated on CD4 expression and then KJ1.26 and GFP.

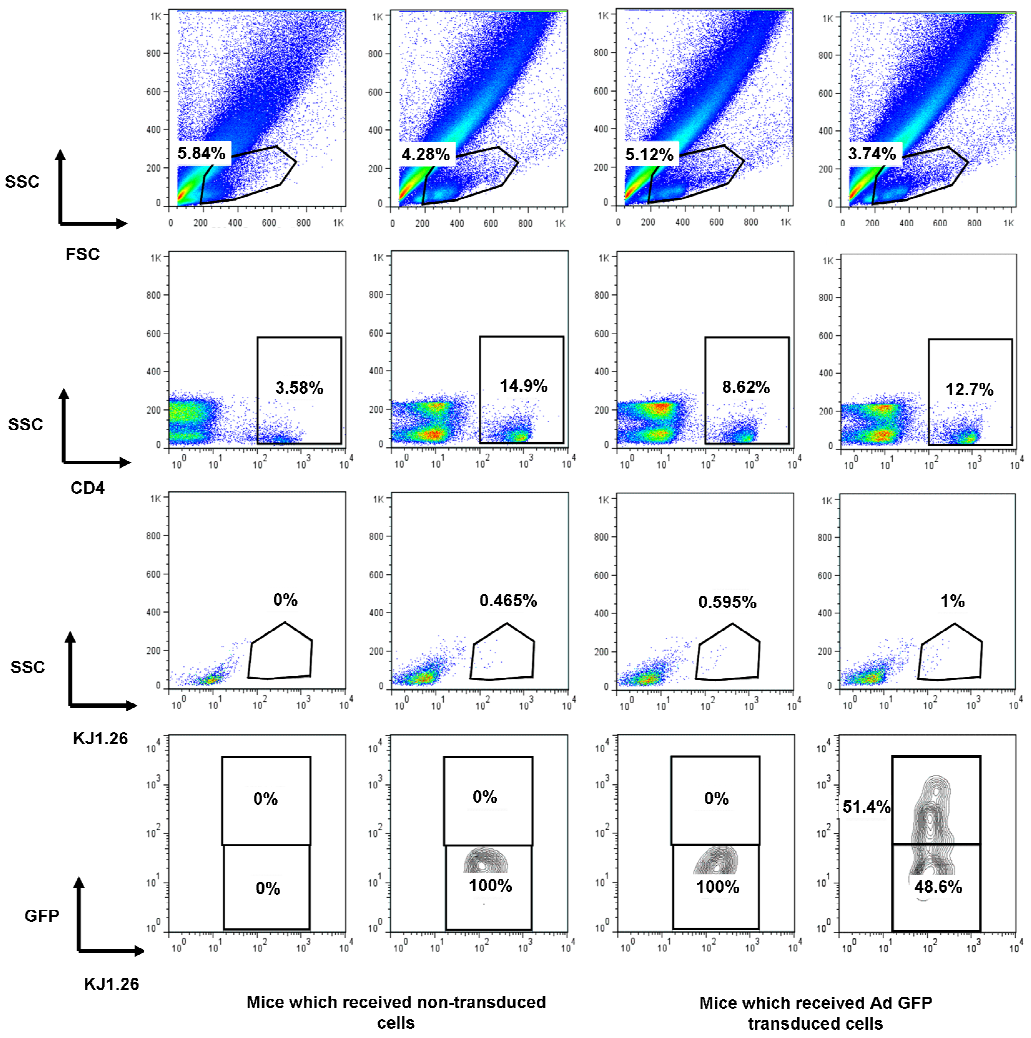

Figure 3: FACS plots showing GFP+ cells in the liver, 24 hrs post-transfer. Ad GFP transduced, or non-transduced, hCAR DO11.10 CD4+ T cells were transferred into BALB/c recipients. After 24 hrs the larger left lobe of the liver was taken, strained through a nitex cell strainer, treated with RBC lysis solution and washed with FACS Buffer. Cells were labelled with CD4 APC and KJ1.26 PE. Lymphocytes were identified based on the FSC and SSC profile and were gated on CD4 expression and then KJ1.26 and GFP.

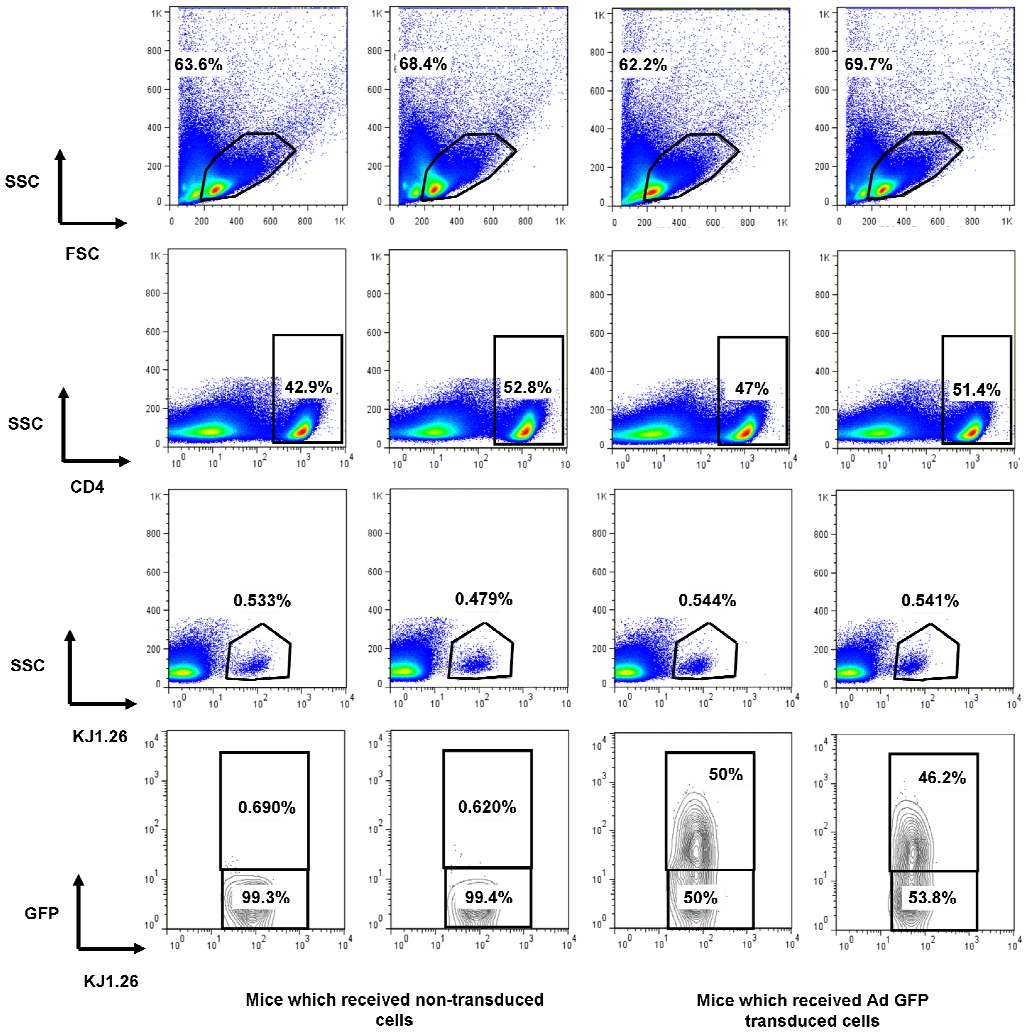

Figure 4: FACS plots showing GFP+ cells in peripheral lymph nodes, 72 hrs post-transfer. Ad GFP transduced, or non-transduced, hCAR DO11.10 CD4+ T cells were transferred into BALB/c recipients. After 72 hrs the inguinal, brachial, axillary and 2 x superficial cervical lymph nodes were taken and mashed through a nitex cell strainer and washed with FACS Buffer. Cells were labelled with CD4 APC and KJ1.26 PE. Lymphocytes were identified based on the FSC and SSC profile and were gated on CD4 expression and then KJ1.26 and GFP.

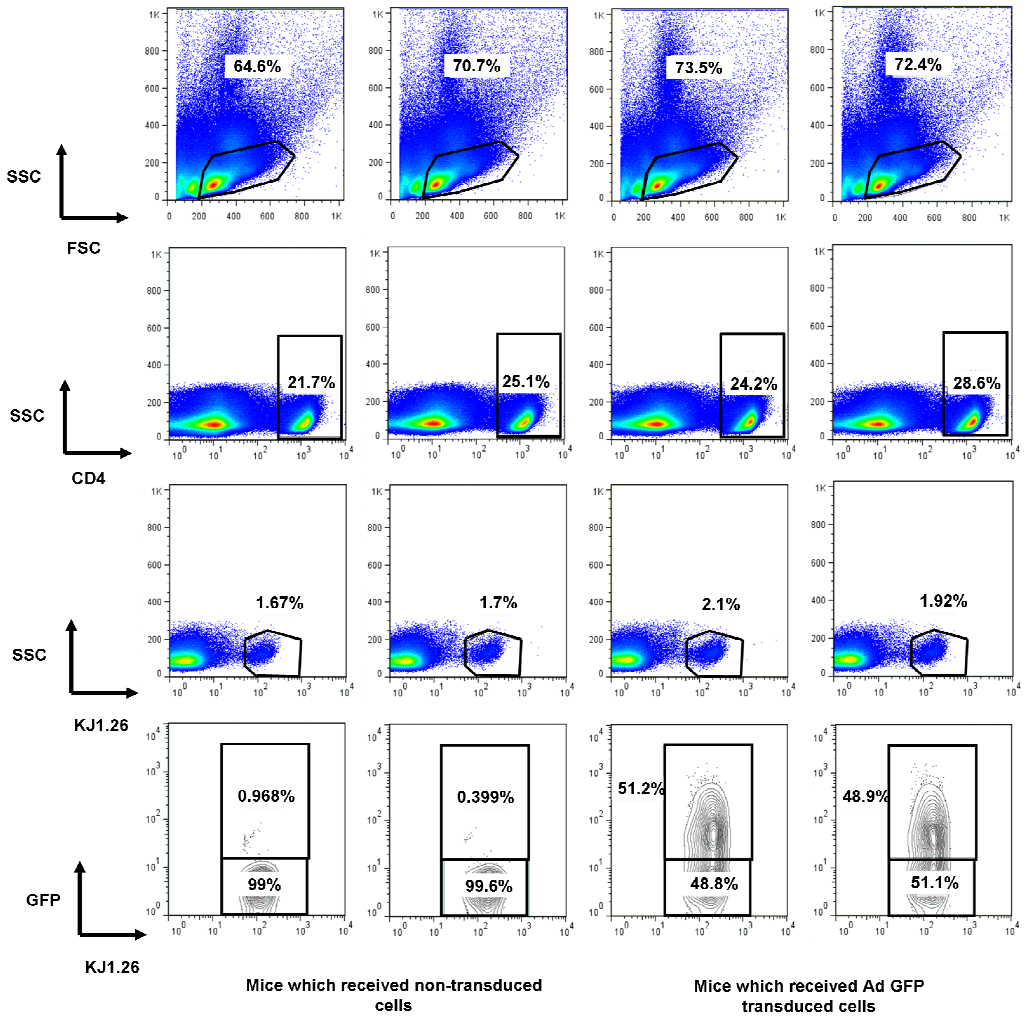

Figure 5: FACS plots showing GFP+ cells in spleen, 72 hrs post-transfer. Ad GFP transduced, or non-transduced, hCAR DO11.10 CD4+ T cells were transferred into BALB/c recipients. After 72 hrs the spleen was taken, strained through a nitex cell strainer, treated with RBC lysis solution and washed with FACS Buffer. Cells were labelled with CD4 APC and KJ1.26 PE. Lymphocytes were identified based on the FSC and SSC profile and were gated on CD4 expression and then KJ1.26 and GFP.

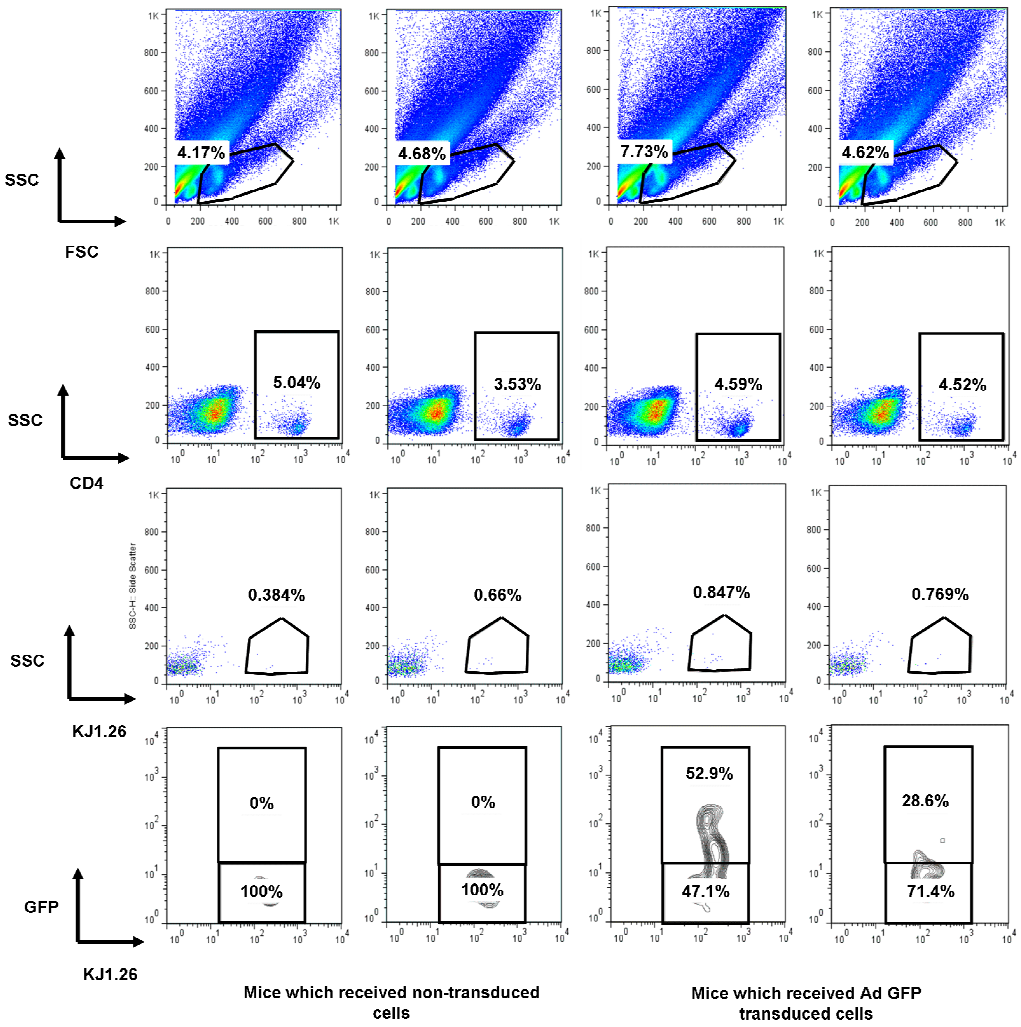

Figure 6: FACS plots showing GFP+ cells in the liver, 72 hrs post-transfer. Ad GFP transduced, or non-transduced, hCAR DO11.10 CD4+ T cells were transferred into BALB/c recipients. After 72 hrs the larger left lobe of the liver was taken, strained through a nitex cell strainer, treated with RBC lysis solution and washed with FACS Buffer. Cells were labelled with CD4 APC and KJ1.26 PE. Lymphocytes were identified based on the FSC and SSC profile and were gated on CD4 expression and then KJ1.26 and GFP.

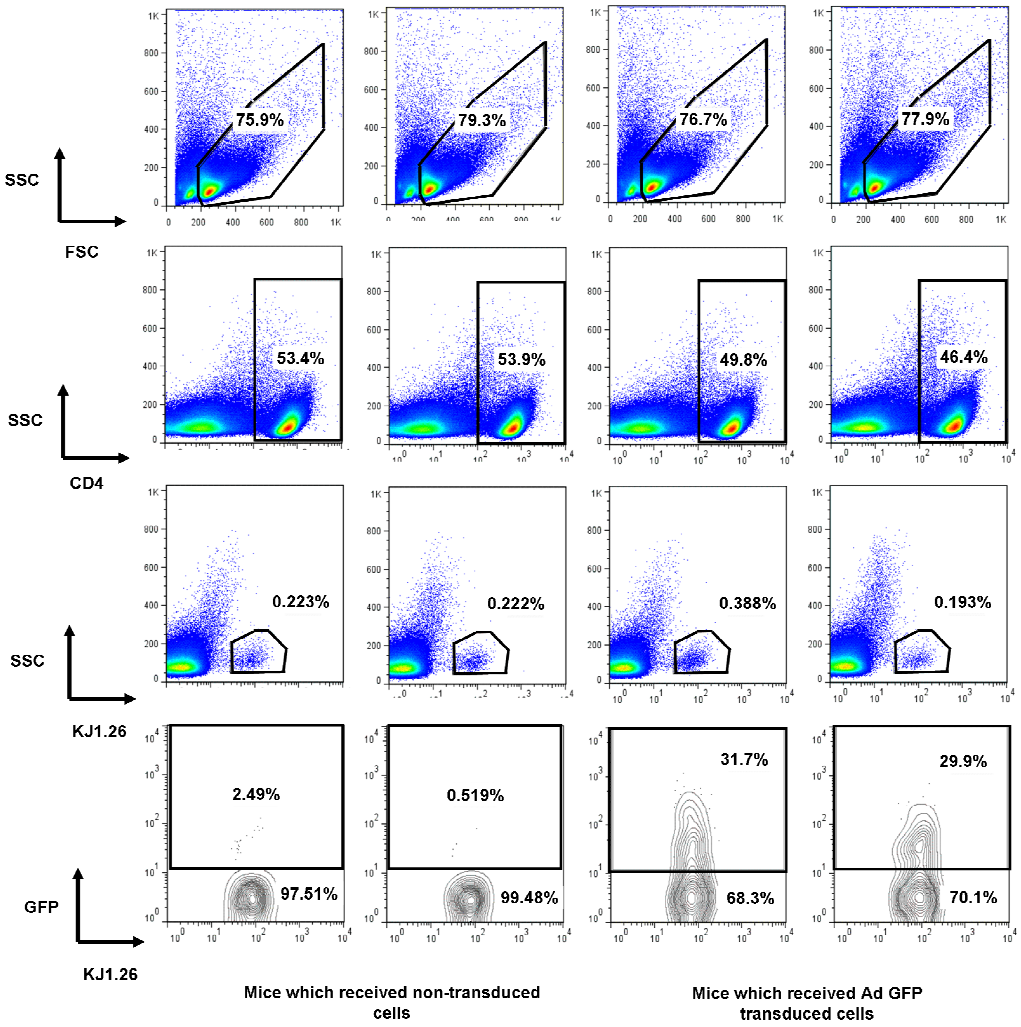

Figure 7: FACS plots showing GFP+ cells in peripheral lymph nodes, 72 hrs post-transfer. Ad GFP transduced, or non-transduced, hCAR DO11.10 CD4+ T cells were transferred into BALB/c recipients. After 72 hrs the inguinal, brachial, axillary and 2 x superficial cervical lymph nodes were taken and strained through a nitex cell strainer and washed with FACS Buffer. Cells were labelled with CD4 APC and KJ1.26 PE. Lymphocytes were identified based on the FSC and SSC profile and were gated on CD4 expression and then KJ1.26 and GFP.

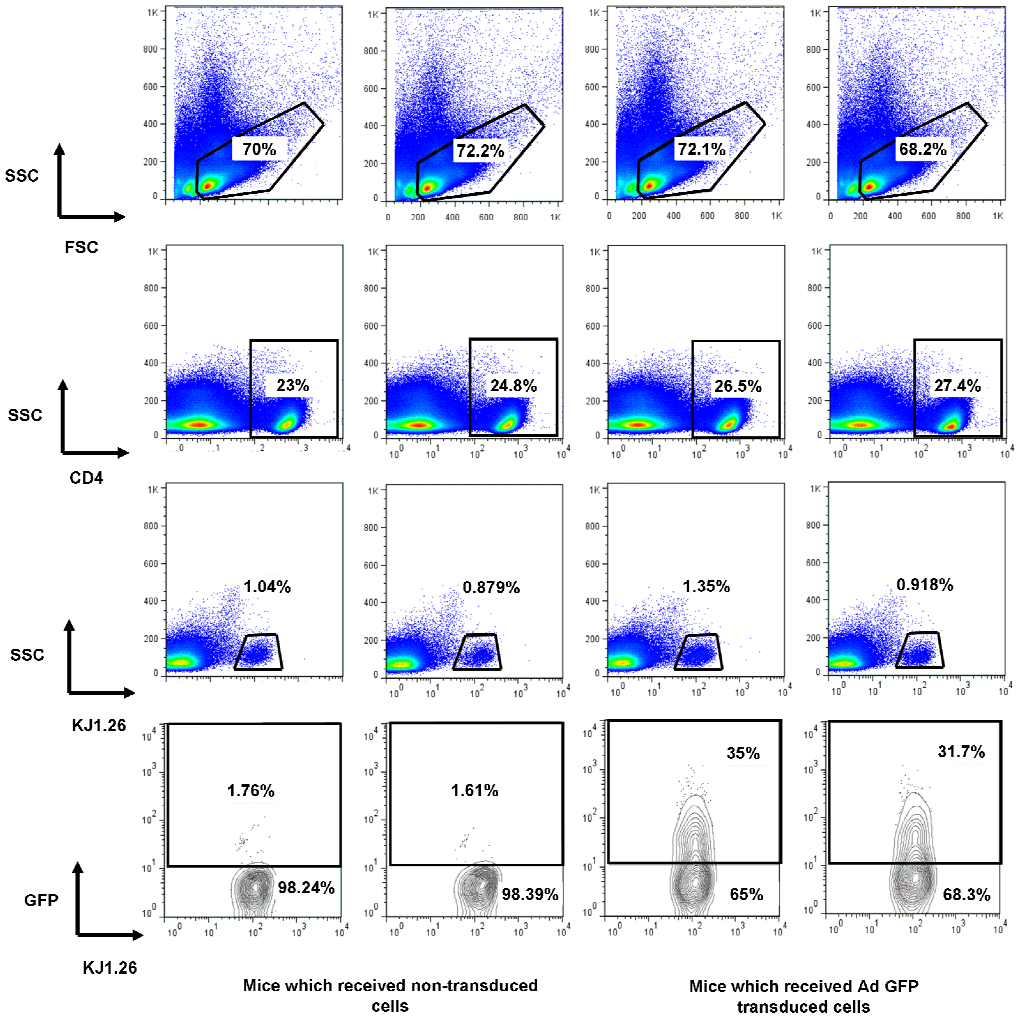

Figure 8: FACS plots showing GFP+ cells in spleen, 72 hrs post-transfer. Ad GFP transduced, or non-transduced, hCAR DO11.10 CD4+ T cells were transferred into BALB/c recipients. After 72 hrs the spleen was taken, strained through a nitex cell strainer, treated with RBC lysis solution and washed with FACS Buffer. Cells were labelled with CD4 APC and KJ1.26 PE. Lymphocytes were identified based on the FSC and SSC profile and were gated on CD4 expression and then KJ1.26 and GFP.

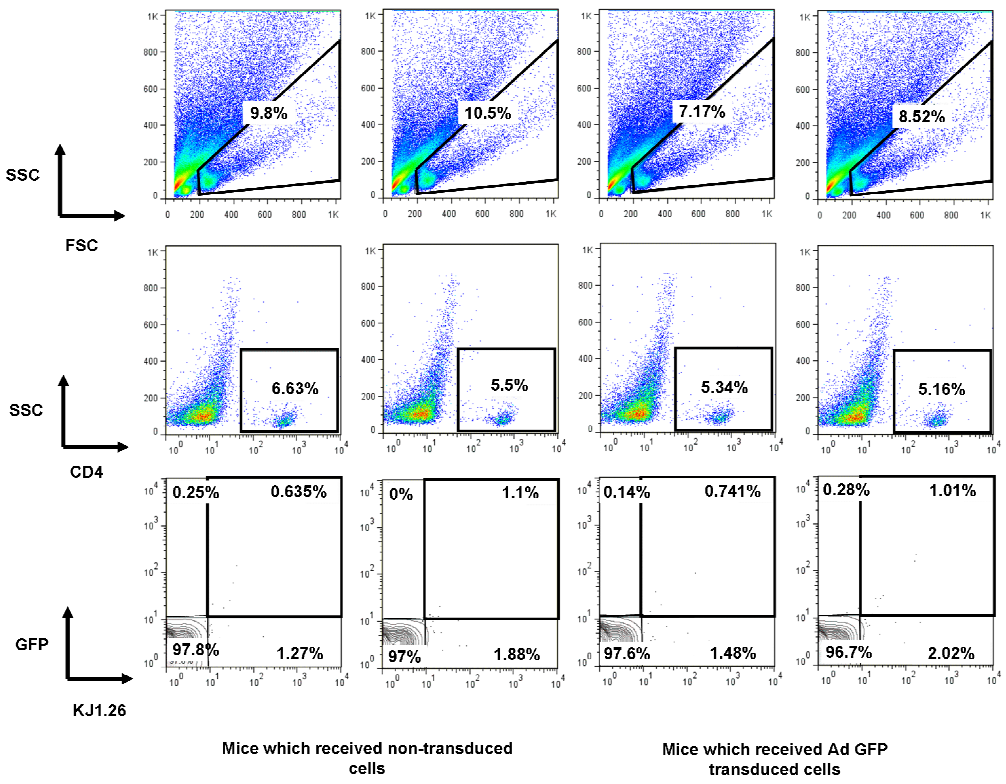

Figure 9: FACS plots showing GFP+ cells in the liver, 72 hrs post-transfer. Ad GFP transduced, or non-transduced, hCAR DO11.10 CD4+ T cells were transferred into BALB/c recipients. After 72 hrs the larger left lobe of the liver was taken, strained through a nitex cell strainer, treated with RBC lysis solution and washed with FACS Buffer. Cells were labelled with CD4 APC and KJ1.26 PE. Lymphocytes were identified based on the FSC and SSC profile and were gated on CD4 expression and then KJ1.26 and GFP.

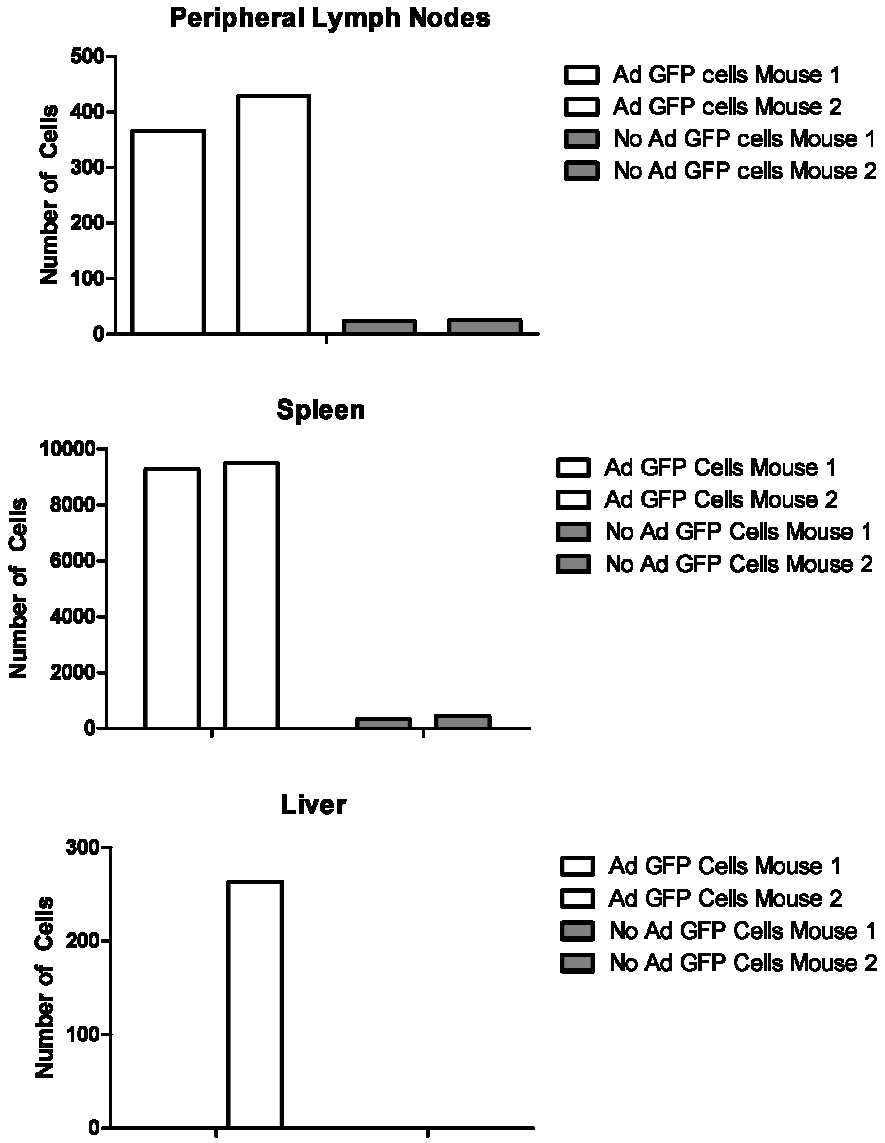

Figure 10: Total numbers of CD4+ KJ1.26+ GFP+ cells in each mouse at 24 hrs post-transfer. Ad GFP transduced, or non-transduced, hCAR DO11.10 CD4+ T cells were transferred into BALB/c recipients. After 24 hrs the peripheral lymph nodes, spleen and liver were taken and strained through a nitex cell strainer, treated with RBC lysis solution and washed with FACS Buffer. Cells were labelled with CD4 APC and KJ1.26 PE. Lymphocytes were identified based on the FSC and SSC profile and were gated on CD4 expression and then KJ1.26 and GFP.

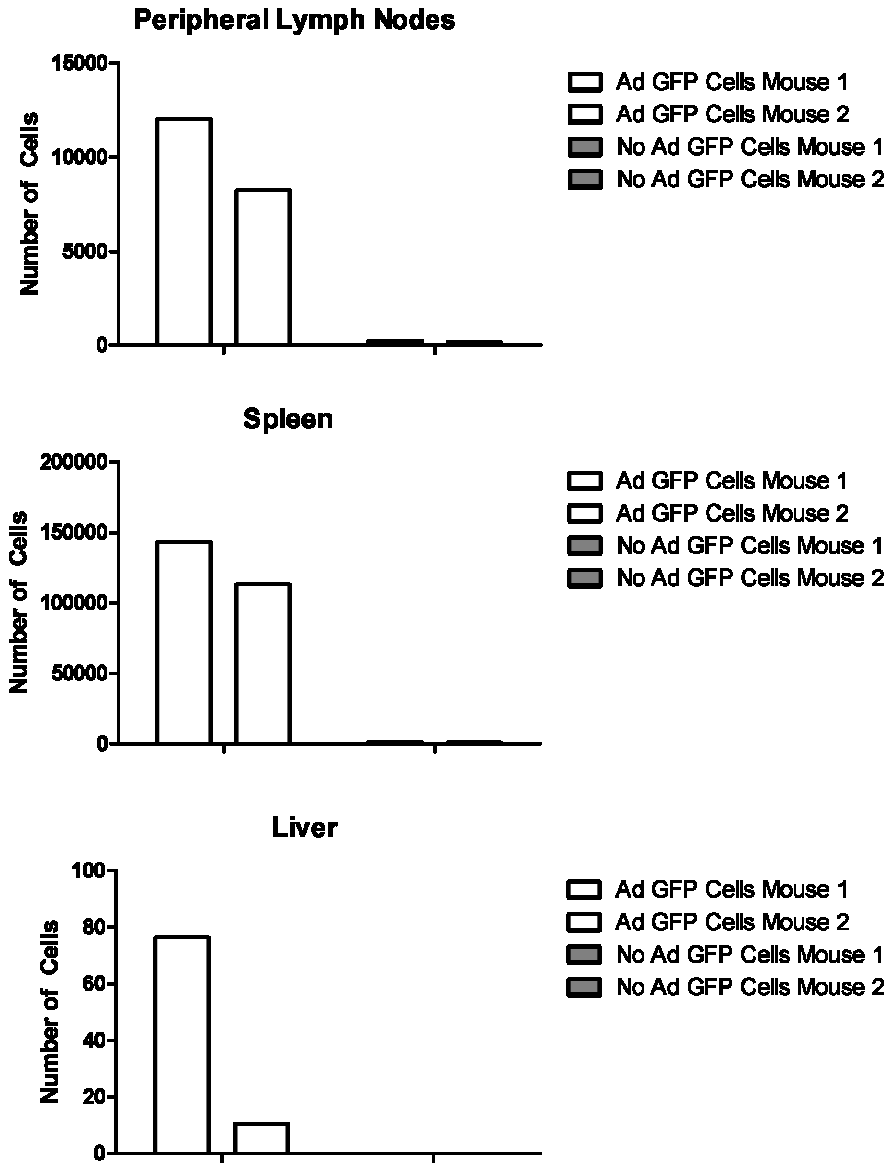

Figure 11: Total numbers of CD4+ KJ1.26+ GFP+ cells in each mouse at 72 hrs post-transfer. Ad GFP transduced, or non-transduced, hCAR DO11.10 CD4+ T cells were transferred into BALB/c recipients. After 72 hrs the peripheral lymph nodes, spleen and liver were taken and strained through a nitex cell strainer, treated with RBC lysis solution and washed with FACS Buffer. Cells were labelled with CD4 APC and KJ1.26 PE. Lymphocytes were identified based on the FSC and SSC profile and were gated on CD4 expression and then KJ1.26 and GFP.

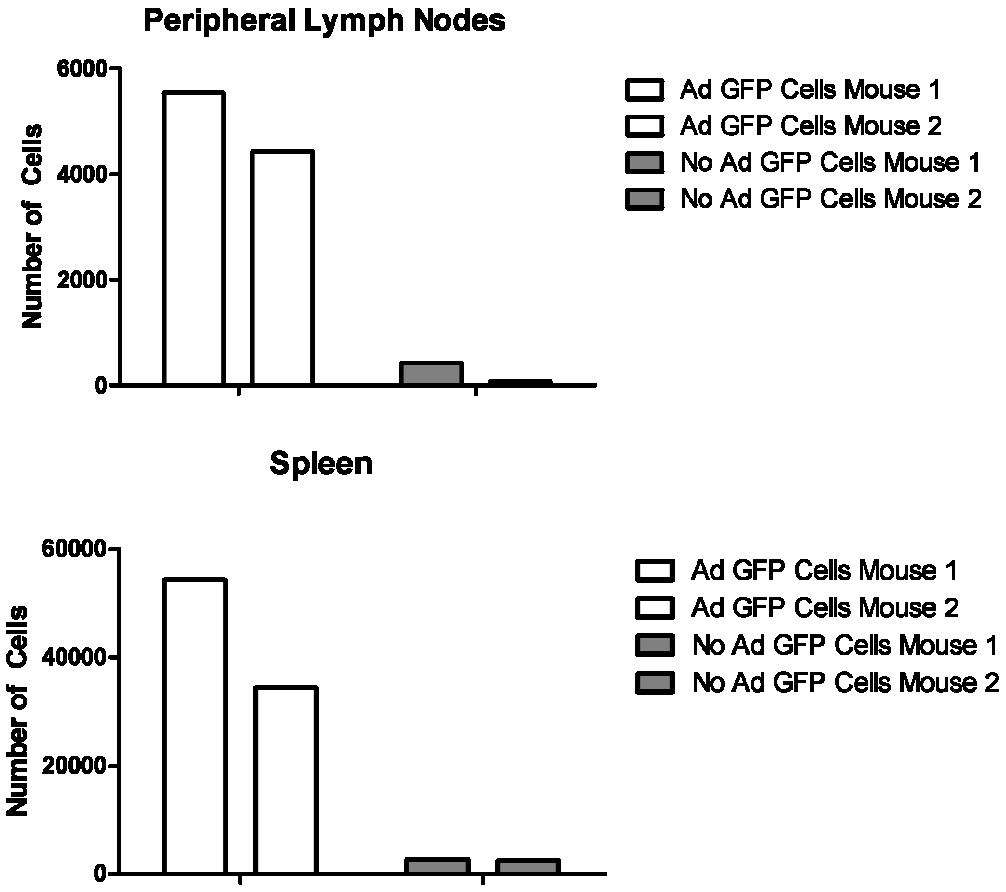

Figure 12: Total numbers of CD4+ KJ1.26+ GFP+ cells in each mouse at 72 hrs post-transfer. Ad GFP transduced, or non-transduced, hCAR DO11.10 CD4+ T cells were transferred into BALB/c recipients. After 72 hrs the peripheral lymph nodes, spleen and liver were taken and strained through a nitex cell strainer, treated with RBC lysis solution and washed with FACS Buffer. Cells were labelled with CD4 APC and KJ1.26 PE. Lymphocytes were identified based on the FSC and SSC profile and were gated on CD4 expression and then KJ1.26 and GFP.

6.3.2 Ad GFP transduced hCAR DO11.10 CD4 T cells migrate to the peripheral lymph nodes and spleen, and reside there in similar numbers as non-transduced DO11.10 CD4 T cells

In order to observe if transduced cell migration was comparable to non-transduced cells, the total number of KJ1.26+ cells was evaluated. Figure 13 shows the total KJ1.26+ cells in the lymph nodes, spleen and liver at 24 hrs. It was observed that a larger number of KJ+ cells were observed in the lymph nodes and spleen of mice which received the non-transduced cells. ~750 cells in the lymph nodes of transduced cell recipient group compared to 1150 and 1600 in the non-transduced cell recipients and ~1.55 x 10^4 in the spleens of GFP cell recipient compared to 2.2 x10^4 and 2.8 x 10^4 in the non-GFP cell recipient group. The liver showed variable results with one of the GFP recipient mice showing no KJ1.26+ cells present with the other showing a population of ~500. Non-transduced cell recipient mice showed the presence of 178 and 157 KJ1.26+ cells, respectively.

Figure 14 shows KJ1.26+ cells present at 72 hours. As seen at 24 hours, a slightly larger number of KJ1.26+ cells could be detected the lymph nodes of the non-GFP recipient mice, 3.3x10^4 and 2.77x10^4 compared to the 2.4x10^4 and 1.78x10^4 seen in the GFP cell recipient mice. This trend was not seen in the spleen however, with higher numbers present in the GFP cell recipient mice (2.8x10^5 and 2.3x10^5 *vs* 1.15x10^5 and 1.72x10^5 in non-GFP cell recipient mice). Higher levels of KJ1.26+ cells were observed in only one of the GFP cell recipient mice while the other contained a population similar to that found in the non-transduced group (144 compared to 36, 33 and 39 cells).

In the experimental repeat looking at 72 hours post transfer, more consistency between groups was observed (Fig 15). There was no notable difference between KJ1.26+ numbers in either the transduced cell recipient of non-transduced cell recipient mice (1.75x10^4 and 1.48x10^4 *vs* 1.68x10^4

and $1.36x10^4$). This consistency was also observed in the spleen with all but one mouse showing near identical population numbers ($1.55x10^5$ and $1.08x10^5$ *vs* $1.52x10^5$ and $1.53x10^5$). Relatively similar population levels were seen in the liver; with no group showing a distinct tendency for KJ1.26+ cell accumulation over the other (102 and 465 *vs* 297 and 1030).

When comparing the KJ1.26+ cell number in each organ between the two groups, it is worth noting that, although variable at 24 hours and 72 hours in the first experiment, the difference in cell number between the groups was relatively small. Figure 16 shows the CD4+ KJ1.26+ populations as a %, which again shows the relatively small difference between the two groups.

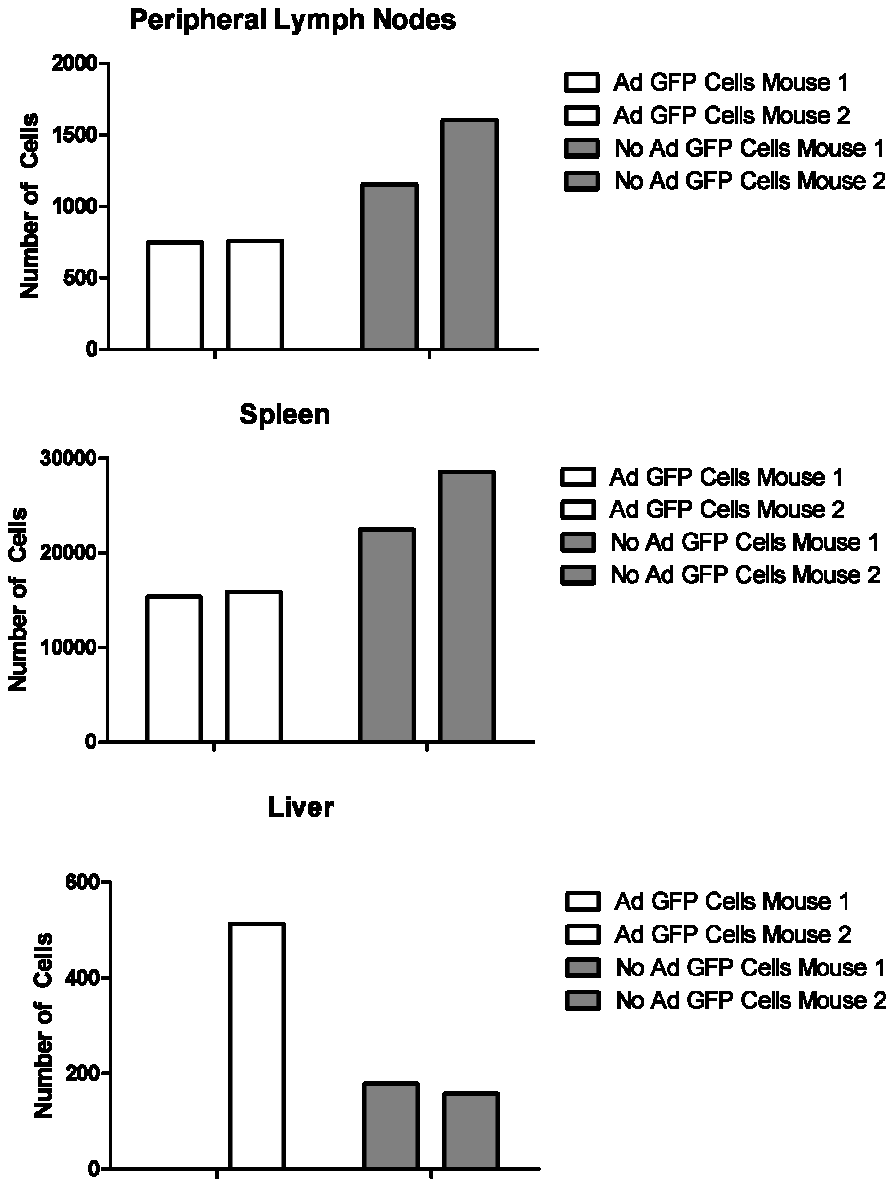

Figure 13: Total numbers of CD4+ KJ1.26+ cells in each mouse at 24 hrs post-transfer. Ad GFP transduced, or non-transduced, hCAR DO11.10 CD4+ T cells were transferred into BALB/c recipients. After 24 hrs the peripheral lymph nodes, spleen and liver were taken and strained through a nitex cell strainer, treated with RBC lysis solution and washed with FACS Buffer. Cells were labelled with CD4 APC and KJ1.26 PE. Lymphocytes were identified based on the FSC and SSC profile and were gated on CD4 expression and then KJ1.26.

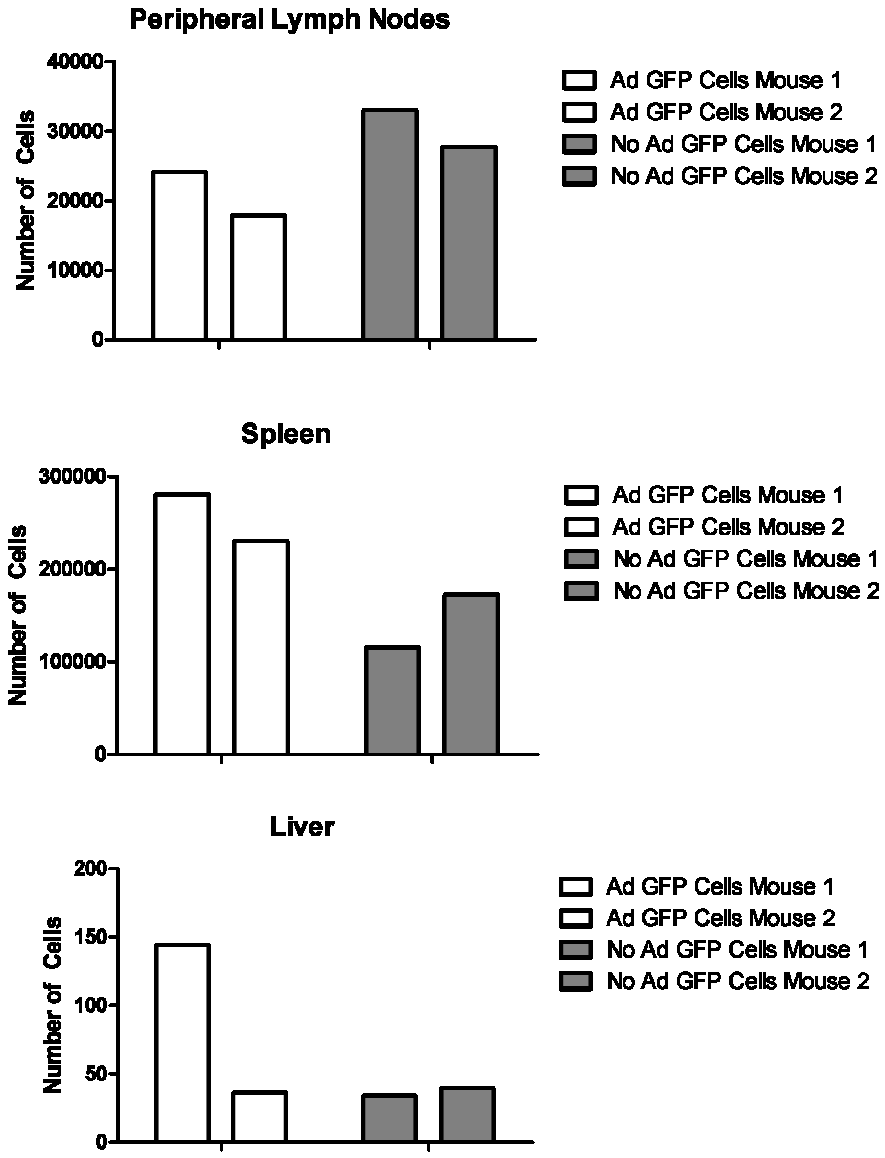

Figure 14: Total numbers of CD4+ KJ1.26+ cells in each mouse at 72 hrs post-transfer. Ad GFP transduced, or non-transduced, hCAR DO11.10 CD4+ T cells were transferred into BALB/c recipients. After 72 hrs the peripheral lymph nodes, spleen and liver were taken and strained through a nitex cell strainer, treated with RBC lysis solution and washed with FACS Buffer. Cells were labelled with CD4 APC and KJ1.26 PE. Lymphocytes were identified based on the FSC and SSC profile and were gated on CD4 expression and then KJ1.26.

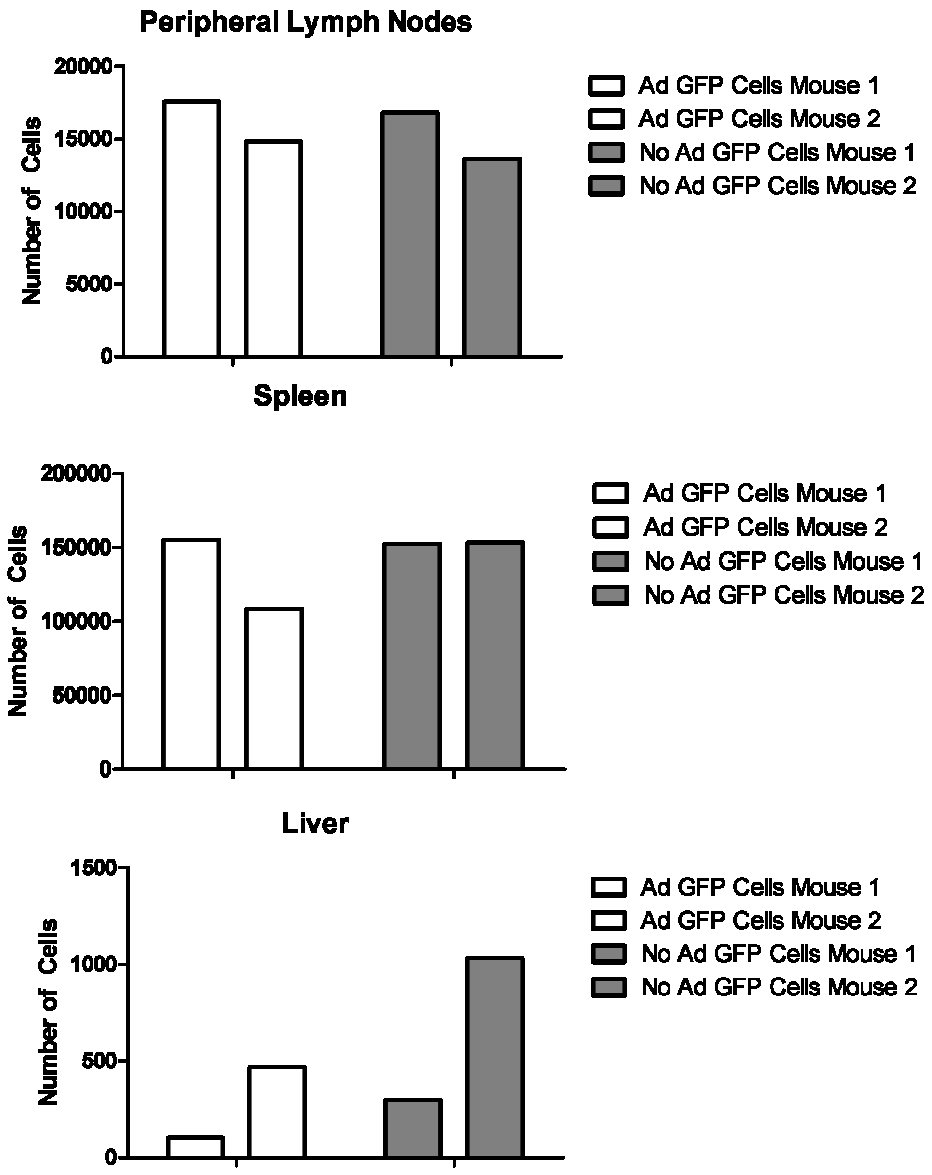

Figure 15: Total numbers of CD4+ KJ1.26+ cells in each mouse at 72 hrs post-transfer. Ad GFP transduced, or non-transduced, hCAR DO11.10 CD4+ T cells were transferred into BALB/c recipients. After 72 hrs the peripheral lymph nodes, spleen and liver were taken and strained through a nitex cell strainer, treated with RBC lysis solution and washed with FACS Buffer. Cells were labelled with CD4 APC and KJ1.26 PE. Lymphocytes were identified based on the FSC and SSC profile and were gated on CD4 expression and then KJ1.26.

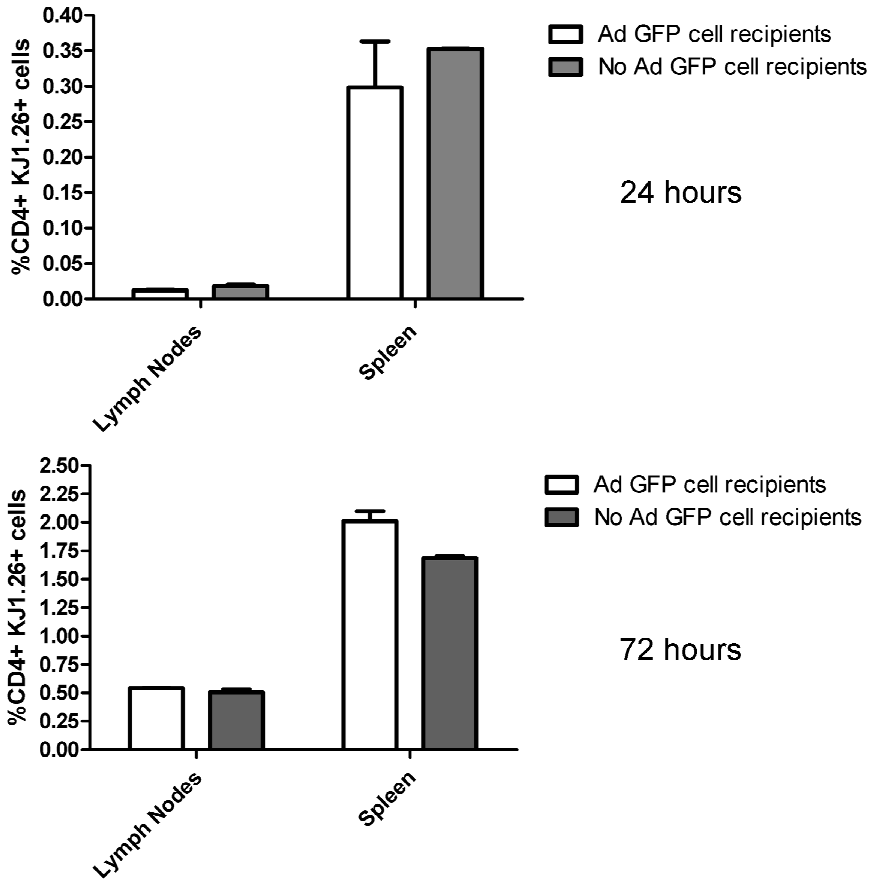

Figure 16: % CD4+ KJ1.26+ present in mice at 24 and 72 hour time points of the first experiment. FACS analysis of total KJ1.26+ cells in the lymph node and spleen of mice which received GFP cells and those that did not. Lymphocytes were gated using FSC and SSC profiles and then CD4+ KJ1.26+. Data represent mean ± SEM (n=2)

6.3.3 Adoptively transferred Ad GFP transduced hCAR DO11.10 cells survive at comparable levels to non-transduced cells in recipient mice, 72 hours post transfer

A possible issue that may arise due to the cells being infected with a virus is that the cells once transferred may be cleared by the host's immune system due to their expressing of viral peptides on MHC I molecules. This would limit the application of these cells as a useful therapy and may be harmful to the recipient. The ratio (shown as a percentage) of GFP+ cells to GFP- cells was compared before cell transfer, at 24 hrs and 72 hrs in each organ to ascertain if the percentage of GFP+ cells altered through the time points. The number of cells and quantity of virus to use in order to have $2x10^6$ GFP+ cells for the transfers was based on previous optimisation experiments. As in previous experiments cells were gated on 7-AAD negative population (viable cells) followed by GFP+. The % viable and % GFP in the cell population pre-transfer were nearly exactly what were predicted. The FACS plot of cells pre-transfer can be seen in Figure 17. As can be seen in the bar chart, the % of GFP+ remains relatively constant in both the peripheral lymph nodes and spleen from before transfer through to 72 hrs. Figure 18 shows that in the repeat the % transduction was lower than expected, 36.9%, however as before the % of GFP+ cells was relatively similar to the % GFP+ cells pre-transfer. As the previous data showed that the transferred cells are proliferating in the recipient, the consistent % of GFP+ cells implies that the GFP+ cells and GFP- cells are proliferating/dying at comparable rates to one another. This survival is also demonstrated in Figures 13, 14 and 15 which show the number of total KJ1.26 cells being relatively similar in both experimental groups.

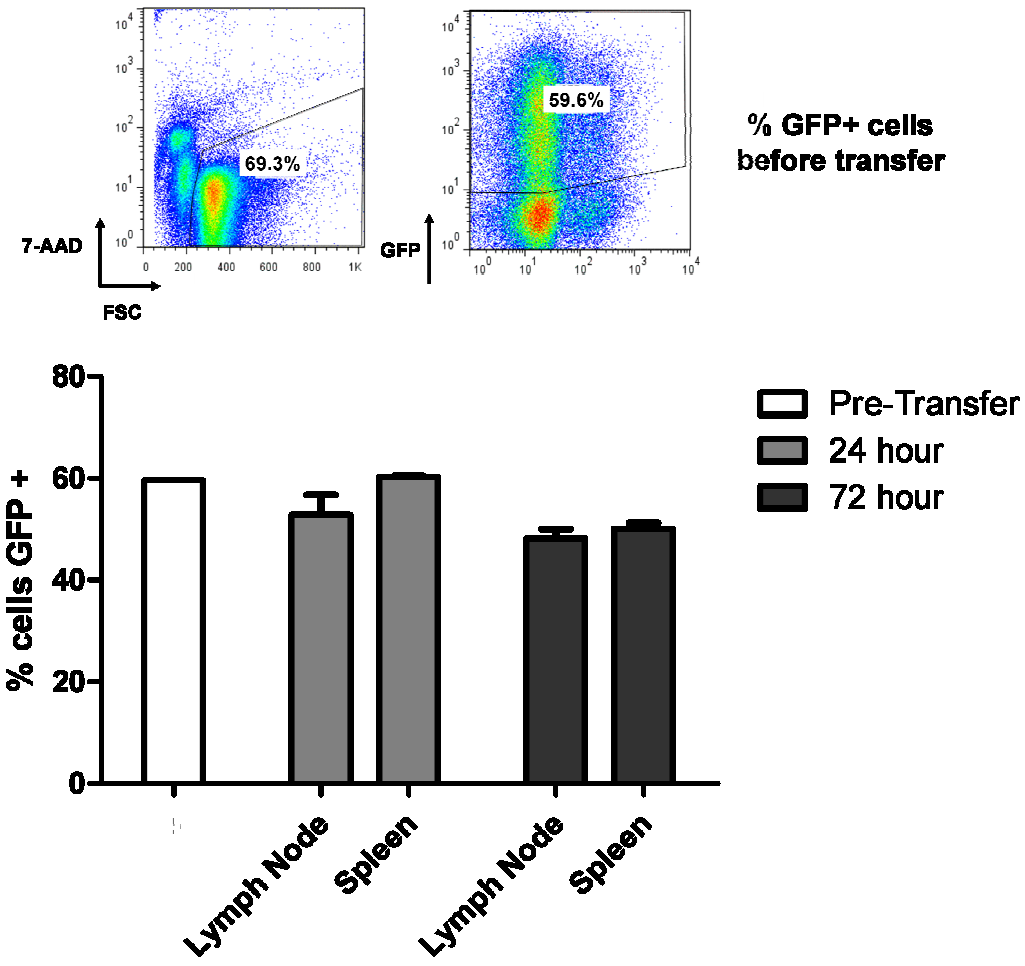

Figure 17: % GFP+ cells present before transfer and at 24 and 72 hours in peripheral lymph nodes and spleen. FACS analysis of the pooled Ad GFP transduced T cells before adoptive transfer into recipient mice. Cells were labelled with 7-AAD to indicate viable non-labelled cells and then gated on the GFP+ population, % GFP+ at each time-point was derived as described in the previous figures. Data indicates there was no decline in % GFP+ cells present in each organ over 72 hours. Data represent mean ± SEM (n=2 excluding the pre-transfer group n=1).

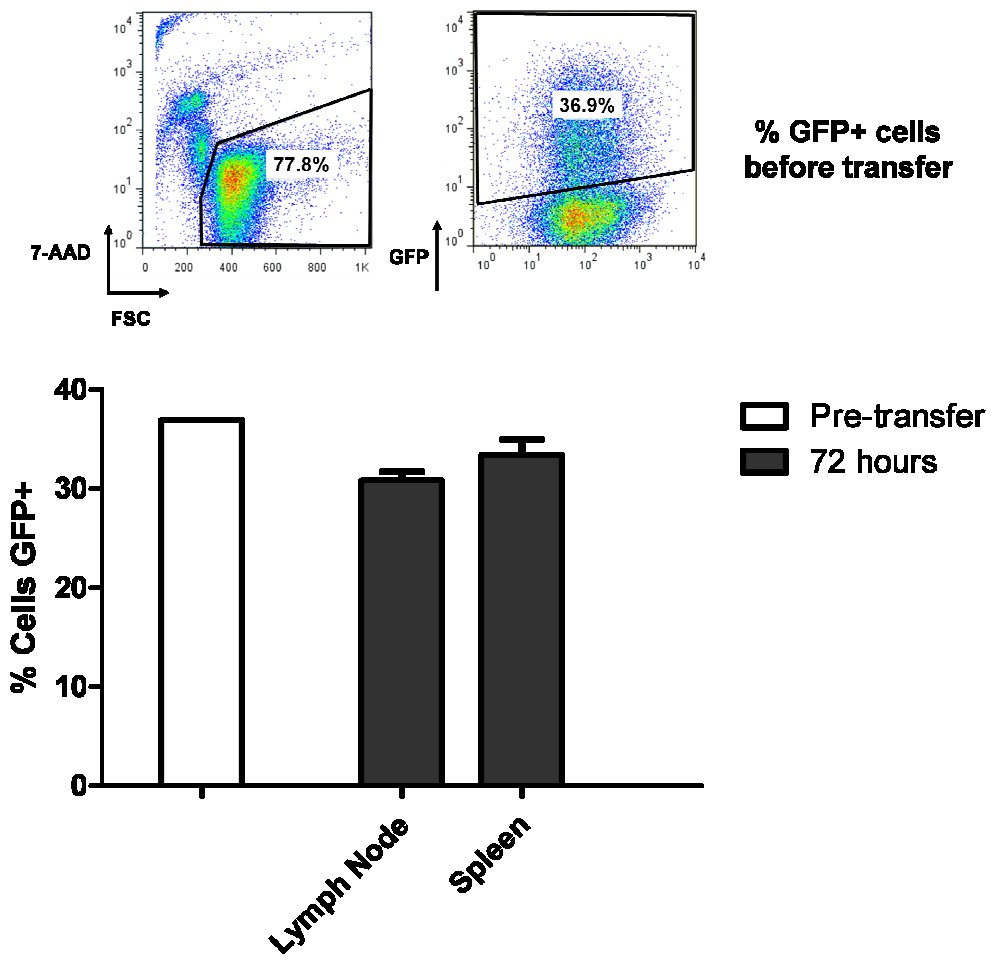

Figure 18: % GFP+ cells present before transfer and at 72 hours in peripheral lymph nodes and spleen. FACS analysis of the pooled Ad GFP transduced T cells before adoptive transfer into recipient mice. Cells were labelled with 7-AAD to indicate viability percentages and then gate on the GFP+ population, % GFP+ at each time-point was derived as described in the previous figures. Data indicates there was no decline in % GFP+ cells present in each organ over 72 hours. Data represent mean ±SEM (n=2 except for pre-transfer group n=1).

6.4 Discussion

In this chapter, hCAR DO11.10 CD4 T cells were transduced using a GFP expressing adenovirus, and then adoptively transferred into BALB/c recipient mice. These cells were then tracked using flow cytometry in the peripheral lymph nodes, spleen and liver after organ harvest, and their migrational kinetics compared to non-transduced cells. It was found that these transduced GFP CD4 cells were easily detectable using flow cytometry, with populations being found in the lymph nodes and spleen, with very low levels if any being identified in the liver. Transduced cells also migrated and resided in these organs at similar levels to non-transduced cells. Finally, these transduced cells rate of survival was also very similar to the transferred non-transduced cells.

Due to the issues faced in the previous chapter with using the hCAR OT-I C57BL/6 mice, our initial plan of tracking the transduced CD4 T cells in $ApoE^{-/-}$ recipients was no longer be an option. Additionally, the problems faced obtaining a high titre of functional IL-10 adenovirus, resulted in a return to using the GFP expressing adenovirus used in the initial optimisation experiments. As shown previously, adoptively transferred leukocytes can home to the aortic tree wall in $ApoE^{-/-}$ recipient mice [50, 51]. We also know that following adoptive transfer, immune cells will equilibrate mainly in the lymph nodes and spleen of the recipient mice after around 24 hours [429], and home to sites of inflammation [429]. 24 hr and 72 hr time points were chosen in order to give us as much reliable information as possible given the limited amount of adenovirus we had.

At both 24 and 72 hr time points, a clear population of CD4+KJ1.26+GFP+ cells could be seen in the lymph nodes, spleen and in some cases liver of the mice which received the transduced cells, therefore showing that transduced cells do migrate to the predicted locations, and that they are easily distinguishable from resident cells. The low percentages of GFP+ cells observed in the mice which did not receive transduced cells can be

attributed to gating inaccuracies, some autofluorescence was observed when gating on CD4 *vs* KJ1.26 which was counteracted as much as possible in the gating. Between the 24 hr and 72 hr time point a distinct proliferation occurred in the GFP+ population, as was also found in the KJ1.26+ population, with numbers rising around 14 fold. The transferred cells did express the DO11.10 T cell receptor specific for OVA, however no OVA was present within the recipient mice in order to induce clonal expansion. It was therefore assumed that this proliferation was instead due to the continued proliferation after the phorbol 12-myristate 13-acetate and ionomycin stimulation carried out as part of the transduction protocol. Consistent of this notion, the literature indicates that this proliferation may continue up to day 5 post stimulation [430].

In order to elucidate whether transduced cells migrate in similar numbers to the same location, the total KJ1.26+ cells were compared between mice that received the transduced cells and those which didn't. We found that total KJ1.26+ levels seen in both groups did show some variance but were of a similar number in the first transfer experiment, in both the lymph nodes and spleen at 24 and 72 hours, with the same variability in the liver. The repeat of this experiment revealed almost similar KJ1.26+ population at 72 hours in both groups, with cell number being almost identical. This similarity in population numbers between groups was further illustrated when looking at the population as % CD4+ KJ1.26+ cells rather than total number, where it can again be seen to be very similar between groups. The comparable KJ1.26+ populations in the mice which received or not transduced, indicates that the transduced CD4 cells migrate post-transfer in a similar manner to the non-transduced CD4 cells in a non-inflamed recipient context. It could therefore be assumed that these cells would also behave as normal CD4 T cells would in an inflammatory context, homing to the site of inflammation (e.g. aorta), however it is not possible to definitively verify this without the use of a mouse model of atherosclerosis. Due to the lack of transduction of the C57Bl/6 hCAR cells, using $ApoE^{-/-}$

mice as recipients was unfeasible. The logical follow up experiment to those discussed would be to use an alternative inflammatory model in order to show definitively, transduced cell behaviour in this setting. The effectiveness of virally-transduced cells used as an adoptive immunotherapy has been demonstrated in both rheumatoid arthritis [382] and also experimental autoimmune encephalomyelitis (EAE) [383], with both describing the effects as site specific. Importantly, these papers utilise T cells with a TCR specific for the disease type. TCR engineering has proven to be an effective method of targeting T cells to non-lymphoid tissues [431], having found success in rheumatoid arthritis [432] and especially in the field of cancer immunotherapies [384, 433]. The fact that these immunotherapies have shown to be effective in other inflammatory models shows promise for the effectiveness of this approach in atherosclerosis. The addition of TCR manipulation, while inherently tricky in atherosclerosis due to the unknown immunogen(s), may be an area in the future this research could expand into, therefore offering unparalleled tissue specificity compared to any current therapies.

A possible setback with transferring transduced cells was that these cells may be deleted as they contained viral proteins, thus limiting the length of time the cells would be viable in the recipient. As the transduction of CD4 cells with the GFP adenovirus did not reach 100%, along with the $2x10^6$ GFP+ transferred in were $6x10^5$ GFP- cells. We assessed the consistency of the % GFP+ cells found in each organ at the different time points, if the % decreased it meant that the GFP+ cells were dying or being deleted at a faster rate than the non-transduced GFP- cells. We found that the % GFP+ remained relatively constant when compared to the % GFP+ cells at the time of transfer, in the lymph nodes and spleen up to 72 hours. This data taken with the our findings that the total KJ1.26+ populations were similar between the two groups at 24 and 72 hours, indicates that the virally transduced CD4 T cells are likely to be surviving in the recipient host in the same manner as non-transduced CD4 T cells. This lack of deletion may

indicate that utilising the T cells as a delivery vehicle, to some extent, conceals the virus from the immune system.

To conclude, we have shown that CD4 T cells transduced with a GFP expressing adenovirus can be transferred and tracked in multiple organs using flow cytometry, up to 72 hours post transfer. These transduced cells also migrate to, and reside in, the peripheral lymph nodes and spleen in similar numbers to non-transduced cells and also have the same survival ability of non-transduced cells, indicating a lack of immune recognition towards the virus within the infected cells. Using the T cell as a delivery method not only takes advantage of the useful homing capabilities of this cell type in treating an inflammatory condition [50, 51, 382, 383, 432], but also combats two major issues faced when using viral vector treatments at present, organ toxicity and an inflammatory response/clearance [226, 395]. Unfortunately due to experimental limitations, we were unable to observe transduced cell behaviour in an atherosclerosis context however, our work has shown that virally modified cells behave in a similar way to non-modified cells under non-inflamed conditions. This data taken with our previous work [50, 51], shown in chapter 3, suggests that if these modified cells were to be transferred into and $ApoE^{-/-}$ mouse, they would home the vessel wall where they would release their therapeutic potential. Further work is required to fully realise the potential of this approach, however our data along with current literature, advocates that this could be a viable immunotherapeutic approach.

To summarize:

- Transferred transduced cells could be found using FACS in the lymph nodes, spleen and, in some mice, liver of BALB/c recipient mice at 72 hours post transfer

- These transduced cells also migrate to these areas in similar numbers as non-transduced T cells

- Extremely low or no transduced cells were found in the liver of recipient mice, indicating an avoidance of liver toxicity

- The transduced cells migrate and survive the same as non-transduced cells in a non-inflamed context.

Chapter 7: Conclusions-future perspectives

As highlighted in chapter 1, atherosclerosis is characterised by a progressive thickening and hardening of the arterial wall due to the accumulation of fatty deposits such as cholesterol. In the past three decades it has been accepted that, in addition to this accumulation, atherosclerosis is an inflammatory disease [2], due to the chronic inflammatory response found at sites of plaque formation, and the significant role immune cells play in the pathology. It is a pathology which will soon become the biggest cause of death worldwide however no single therapy has been able to make a significant impact in these mortality rates. Current therapies e.g. Statins, anti-hypertensives, represent a systemic approach to treating the disease however, none of them offer site specific treatment of the atherogenesis. This thesis aimed to investigate whether T-cells, moving to the inflamed vascular wall, could be ideal candidates for targeted delivery of therapeutic genes/agents, which would have been inserted into the T cell via viral vector; thus creating a site-specific delivery method for the treatment of atherosclerosis.

The first question that was posed in this thesis was related to the migration and movement characteristics of transferred labelled leukocytes in the arterial tertiary lymphoid organ (ATLO) of aged $ApoE^{-/-}$ mice. The ATLO is a unique phenomenon found in the very late stages of disease progression, the end result being a fully structured adventitial lymphoid organ, consisting of all the major compartments found in the secondary lymphoid organs. Although the internal structure of the ATLO has been revealed [50], it has not been elucidated whether the ATLO is detrimental or beneficial in the context of the pathology. In order to shed some light on the workings of the ATLO *in vivo*, leukocytes were fluorescently labelled and transferred into aged mice which have developed these tertiary lymphoid organs. The cells were then imaged via multi-photon laser scanning microscopy (MPLSM) and their movement dynamics measured. It was found that a significantly larger number of labelled cells were observed in the ATLO region of the aged $ApoE^{-/-}$ mice compared to the aged wild type mice which correlated

with the histological studies by Andreas Habenicht's group [50, 291], showing that the ATLO region could be reliably located using the MPLSM approach. Upon studying the tracks made by these labelled cells located in the vessel wall, it was observed that cells in the $ApoE^{-/-}$ mice moved with a high velocity, longer track lengths, higher displacement and higher meandering index in comparison to labelled cells in the wild type mice adventitia. This difference in motility between the two groups clearly indicates that the cells in the $ApoE^{-/-}$ mice are involved in some activity that is not present in the wild type mice. The possibility that some other systemic aspect present in the $ApoE^{-/-}$ mice could be affecting the cells behaviour was ruled out from comparison of cellular dynamics in the pLNs of $ApoE^{-/-}$ and wild type mice. It was observed that the dynamics measured of the labelled cells were the same, therefore showing that the cellular behaviour observed previously was specific to the ALTO region of the vessel. Our final observation was that the cells imaged in the ATLO region showed similar dynamics to those imaged in the peripheral lymph nodes of the same mouse. This indicates that similar processes are underway in both organs which further aids in the elucidation of the role of the ATLO in advanced atherosclerosis. This data showed the viability of MPLSM as a novel tool for the imaging of cells with the ATLO and also gave insight into the workings of the ATLO. In addition it showed that transferred immune cells will home to key sites of atherosclerosis even in the very late stages of the pathology, further supporting the main goals of this thesis.

Chapter 4 of this thesis related to the production of the viral vectors which were to be used in the transduction of T cells. Here, the AdEasy adenoviral kit was used to produce a GFP, IL-10 and GFP IL-10 which would have allowed dual expression of both GFP and IL-10 from the T cells. Due to errors in the early production stages, only the GFP, IL-10 and GFP IL-10 producing vectors were brought to the experimental stage. It was here that we found that, although already shown to produce both transgenes in the packaging cell line, the GFP IL-10 expressing adenovirus seemed unable to

transduce either HeLa or CD4+ T cells efficiently. Due to the limited amount of time available, this vector was not used further and instead the remainder of the work was carried out using the IL-10 and GFP producing vectors, which had both been shown to produce their respective transgenes effectively in HeLa and CD4+ T cells. When at the vector production stage, it was noticed that the HEK 293 flasks which contained the IL-10 and GFP IL-10 producing vectors, cells grew slower and took longer to reach the CPE stage. In addition, when undertaking quality control (QC) for the vectors, it was observed that the number of plaque forming units (PFU), that is the number of VP which are in fact functional, was very low for the IL-10 producing vectors. These observations taken with the very high levels of IL-10 present in the HEK 293 media, imply that the IL-10 may be involved in the inhibition of cell proliferation, most likely due to the extreme concentrations present in the media. The fact that the efficiency of the cells to produce functioning VP was also affected suggests that as well as affecting growth, the IL-10 had some form of deleterious affect on the viral replication cycle. The most effective method for circumventing this transgene based cell toxicity would be to modify the promoter, from the constitutive cytomegalovirus (CMV) used here, to either a T cell specific or inducible promoter, thereby eradicating transgene production at the production stage. This would be taken intro consideration if further IL-10 or cytokine based vectors were to be produced in the future.

Following on from the production of the vectors, the next chapter in this thesis, chapter 5, related to the use of these vectors in the transduction of CD4+ T cells. As the viral production was being undertaken at the same time as some of the initial experiments optimisation here, an alternative GFP expressing vector was utilised. Using this vector, we found that the optimal concentration of virus to use with non-polarised CD4+ T cells was around 5000 viral particles per cell (vp/cell), giving around 80% transduction in viable cells at 48 hr, correlating with previous literature [296]. Due to the large presence of Th1 polarised CD4+ T cells within the

inflamed aortic wall and the possible positive effects this may have on the migration and residing of the cells, we then transduced Th1 polarised cells using the protocol previously described in this thesis. It was observed that higher levels of transduction were observed in the Th1 cells (~90%) and also when studying the mean fluorescent intensity (MFI) of the transduced cells, that more of the transgene (GFP) was produced. A lack of current literature on CD4+ T cell transduction leads us to assume that the increase in transduction levels in Th1 cells could be related to increased CAR independent uptake [150], perhaps through higher levels of $\alpha_v\beta_3$ and $\alpha_v\beta_5$ integrin expression, or that it may be due to the extra round of T cell activation that they receive.

HSPGs are cell surface molecules which bind to, among other things, blood coagulation factor 10 (FX) which has been shown to have re-targeting properties on adenoviral vectors [6, 395]. As T cells express proteoglycans on their surface [397-399] it was supposed that FX could enhance T cell transduction. Counter to our theory, the addition of FX along with the GFP expressing adenovirus actually lowered overall transduction levels of both Th1 and non-polarised CD4+ T cells. In addition it also decreased the MFI of GFP, but only in Th1 cells, negating the MFI increase due to polarisation. An important aspect to test was the T cells ability to produce biologically active interleukin-10 (IL-10) following transduction with our IL-10 adenovirus. In the previous chapter we found that detectable IL-10 was produced by the T cells at a range of viral concentrations. In order to show that it was biologically active we chose a simple test involving dendritic cells, due to their susceptibility to the activities of IL-10 [400, 401]. It was shown that the virally produced IL-10 significantly inhibited the upregulation of the MHC II molecules post lipopolysaccharides stimulation of the DCs. It could be extrapolated that as the IL-10 was proven functionally active, that if produced at the site of plaque formation, it would also bestow its anti-inflammatory activities on other aspects of the pathology [48, 97, 98, 317, 327, 331, 337], including those on DCs.

Unfortunately due to issues encountered in the production of the IL-10 vector regarding pfu/vp levels, (discussed earlier and also in chapter 4) there was not enough virus available to transduce the required number of CD4+ T cells for use in an adoptive transfer experiment. At this point it was decided that any further adoptive transfer experiments would instead use the GFP expressing vector, thereby still showing that they could migrate to areas of inflammation.

One of the major issues faced in this project was that the hCAR mice used for cell transduction and the recipient $ApoE^{-/-}$ mice were of different genetic backgrounds, hCAR being BALBc and $ApoE^{-/-}$ being C57BL/6. This would mean that if the transduced cells were transferred into the $ApoE^{-/-}$ recipient mice, the cells would be treated as a foreign pathogen and deleted. In order to overcome this, a number of different techniques were tried. The Nucleofection™ system by Amaxa was suggested as a possible non-viral alternative. As it is based on electroporation and requires the presence of no specific receptor, this would allow the direct modification of C57BL/6 CD4+ T cells which could then be directly transferred into the $ApoE^{-/-}$ mice. Unfortunately we found that nearly all the cells used were killed by this process with those surviving expressing no GFP. Along the same vein of transducing C57BL/6 CD4+ cells, we also tried using a lentiviral vector. This approach would allow direct transduction due to the lack of requirement for a specific membrane receptor and would also have the advantage of integration into the cell genome, therefore sustaining the transgene expression but again we found no significant production of GFP in the T cells. Time constraints stopped us from pursuing alternative lentiviral vector constructs however with time this may prove a valuable approach, which will be discussed later. One final approach attempted in order to circumvent this transfer issue was to use C57BL/6 hCAR mice. C57BL/6 hCAR OT-I mice were located and gifted to us from Kristin Hogquist's group, these mice expressing hCAR on CD4+ T cells and also the OVA specific TCR on CD8 cells, although in our case this was irrelevant. Oddly

we found that the transduction of these hCAR OT-I CD4+ T cells was significantly lower than the normal hCAR mice, with both the GFP and IL-10 expressing vectors. An observation made early on was that these hCAR OT-I cells seemed to have a significantly higher mortality rate than their hCAR counterparts. Upon further investigation it was ascertained that this high cell death was not related to the C57BL/6 background of the cells and instead was due to some inherent lack of survival of these CD4+ cells from the hCAR OT-I mouse line. The low transduction levels combined with the high death rate, made using this mouse line for donor cells unfeasible. When considering both the successes and problems faced in this chapter, it was decided that only the GFP expressing vector be chosen for use in the forthcoming adoptive transfer experiments, and that wild type BALBc mice would be the recipients. Although this would not allow for us to study the effect of IL-10 transduced cells on the pathology, it would allow us to study the migration of these transduced cells and compare them to non-transduced.

The final chapter of this thesis looked at the transfer of Ad GFP-transduced non-polarised T cells into BALBc recipient mice, and their kinetics at 24 hr and 72 hr post-transfer compared to non-transduced cells. The cells were tracked using flow cytometry in the peripheral lymph nodes, spleen and liver after enzymatic digest. Clear GFP+ CD4+ T cell populations were detectable in the lymph nodes, spleen and in some cases the liver of the transduced cell recipient mice at 24 and 72 hour time points. This showed us that the transduced cells do migrate to the locations to which normal CD4+ T cells migrate and reside. A rise in the transferred CD4+ T cell number was observed in both groups and it was deduced that this increase in population number was due to continued proliferation from the PMA and Ionomycin stimulation undertaken as part of the transduction protocol [430]. In order to elucidate whether the transduced cells migrated to these sites in the same manner as non-transduced cells, the total number of the transferred cells was compared. We found that similar cell numbers of

transferred cells were found in both the spleen and lymph nodes at 24 and 72 hr time points in both groups, therefore showing that, although altered with the adenoviral vector, the migration kinetics are the same as normal non-transduced CD4+ T cells.

In addition to studying the migration of these transduced cells, the ability of these cells to reside in these organs was also assessed. As these cells contain viral proteins, it is possible that these proteins may be recognised by the immune system of the recipient mouse and deleted. It may also be the case that due to the transduction protocol, the cells may not survive to the same extent as normal T cells post transfer. The consistency of GFP+ cell survival was assessed at the two time points. We found that the % of cells that were GFP+ remained relatively constant when compared to the % GFP+ at the time of transfer in the lymph node and spleens. This therefore meant that the GFP+ and GFP- cells transferred into the recipient mice were surviving at the same rate as each other. This lack of deletion could indicate that premature death or eradication may not be an issue faced when using this approach.

A key observation in these transfer experiments was that extremely little or no transduced cells were found in the livers of the recipient mice. Current adenoviral gene therapy approaches are plagued with targeting issues, the most prominent of which being redirection towards the liver, due to binding with blood coagulation factor 10 (FX) [396]. This binding results in re-targetting of the vector towards HSPGs found in the liver which, in turn can result in liver toxicity [221, 294, 395, 396], therefore limiting their usage. This approach whereby the vector is, to an extent, hidden within the T cell, avoids this issue and bypasses a significant safety risk.

Taken together, the findings indicate that virally modified CD4+ T cells will migrate and reside in the same manner as normal non-transduced cells.

Therefore, although we were unable to study these cells in an inflammatory context, it could be assumed that, as normal immune cells and CD4+ cells migrate to the inflamed artery wall [51] (chapter 3), the virally modified cells would also migrate to the inflamed artery wall.

To conclude, at present only systemic therapy approaches are currently in use to treat atherosclerosis. Our approach was to take advantage of the unique homing capabilities of immune cells, modify them with a genetic vector and use them as "Trojan Horses", injecting them into mice with atherosclerosis, where they should infiltrate the inflamed arterial wall and release their newly encoded therapeutic molecule. This thesis has shed light into the possible roles of immune cells in the ATLO of advanced atherogenesis and provided a reliable and repeatable protocol for the study of this organ using MPLSM. Most importantly, we have also shown that transferred immune cells will migrate to the inflamed vessel wall and areas of therapeutic importance. We have shed light on issues faced when producing cytokine based vectors and other genetic approaches but most importantly we have shown that once transduced by our vector, that CD4+ T cells are capable of producing biologically active IL-10. In addition, we showed that virally modified CD4+ T cells have similar migration and survival characteristics as non-transduced CD4+ T cells in a non-inflamed model. Taken together, these findings indicate that, if used in an inflammatory atherogenic context, these cells should migrate to the atherosclerotic vessel walls and release the functional IL-10. Although this method could prove effective, there are a number of ways this approach could be modified and improved in future research.

Further increasing the tissue specificity and how long the transferred cells reside at the required site would be one area where modification to our approach could be made. Due to the possibly potent nature of the therapeutic molecules that could be inserted into the T cell, a vessel wall only approach may be favourable, for instance, the IL-10 released by

modified T cells which have migrated to the lymph nodes could have a suppressive effect on the generation of other immune responses not related to atherosclerosis. Success has been found in using the knowledge that, after expansion, antigen specific T cells will migrate to the inflamed tissue in order to aid in the elimination of the antigen/pathogen they are specific for. Work by Nakajima et al. [382] showed that lentiviral modified antigen specific (collagen) CD4 T cells accumulated in the inflamed paws of mice with rheumatoid arthritis and also showed that similarly modified CD4 T cells not specific for collagen, had no effect on pathology. Similar success in increased targeting and persistence were also found in work on metastatic cancer [434] and also in experimental allergic encephalomyelitis [383, 435]. Modification of T cell receptors (TCRs) in order to create clones specific for a particular antigen have also shown promise in increasing specificity of T cell migration. Here the TCR α and ß genes are identified from sites of pathology and used to create targeted T cells for modification and adoptive transfer, showing promise in the treatment of RA [432]. An alternative method which also uses the concept of antigen specificity is in the use of chimeric antigen receptors (CAR). These man made receptors mainly consist of a single chain variable fragment (scFv) coupled to a T cell signalling domain. CARs have several advantages in that they do not need HLA/MHC presentation in order to activate (especially useful with some cancers), can be directed to any cell surface protein present on the desired target and that more than one follow up intracellular signalling event can be linked to the external scFV molecule [431]. These CARs have been shown to be able to alter both the specificity and function of the modified T cells, having found main success in the treatment of cancers [384, 433], basing the scFV region on TCR genes specific for cancer molecules [436]. These CARs are created using transduction with a lentiviral vector, however Hilde Almåsbak and colleagues have shown that this modification can instead be done using electroporation of mRNA encoding the CAR genes, therefore avoiding any issues of insertional mutagenesis. In addition to this they showed the effectiveness of incorporating chemokines receptor genes

along with the CAR, thereby modifying migration [437]. All of these methods could increase the migration specificity for our modified transferred cells to the vessel wall however, as mentioned previously, a common issue in developing a vaccine or molecule specific immunotherapy for atherosclerosis is that the particular pathological antigen(s) are not known. These techniques could however be tried with the many that are thought to be indicated such as oxLDL, heat shock proteins and various bacterial antigens, as only one may be required to create enough cell persistence in order for the transgene to be more effective.

Although viral modification of T cells is a powerful tool in the creation of effective cellular therapies, the possible oncogenic events due to vector/transgene integration into the cell present themselves as a problem. In addition to this, unforeseen pathological effects from transgene expression combined with the relative lack of control over a therapy once delivered has fuelled interest in developing means by which the cells could be ablated safely if needed. To date the majority of work in this field has been on T cells due to their proven efficacy in the treatment of viral infections and cancer [438-441]. Several different genes have been used in various studies as a suicide gene such as herpes simplex virus-1 derived thymidine kinase (HSV-TK) [442, 443] and *E.coli* derived cytosine deaminase [444] and CD20 [445] however these have proven to be inefficient at cell ablation, immunogenic or have too broad an effect, deleting non-target cells. Work by Straathof et al. [446] have engineered an efficient suicide system using the initiator caspase, caspase 9, which was coupled to the extracellular FK506 binding protein (FKBP), a receptor for the immunosuppressant FK-506/Tacrolimus. This approach reached up to 99% cell clearance, avoided immunogenicity due to the human gene products and has no effect on T cell function, allowing them to act unhindered until deletion is required. Further to this concept of incorporating suicide genes, Martin Pule and colleagues [447] have constructed a remarkably compact suicide and marker gene which could be

integrated into a range of plasmids e.g. for virus production or non-viral gene delivery. The 136 amino acid gene incorporates two shorted CD20 binding sites, to which the monoclonal anti-CD20 antibody Rituximab can bind. Currently in clinical use as an anti-B cell therapy for autoimmune diseases and lymphomas etc., binding of Rituximab induces antibody-dependant cell cytotoxicity (ADCC) and complement based cell destruction, therefore killing the cells it has bound to. These CD20 sites flank a single CD34 epitope which allows for cell sorting using the cliniMACS system which utilises antibodies specific for CD34. This combination allows for cell sorting based on CD34 expression and also Rituximab based cell destruction. In addition, due to the small size of this suicide/marker gene, it can also be easily co-expressed with the before mentioned CARs, therefore allowing selection, detection, suicide control and targeting of these modified therapeutic T cells.

In conclusion, this thesis provided a novel protocol for the multiphoton imaging of labelled leukocytes within the tertiary lymphoid organs of aged $ApoE^{-/-}$ mice, and also shown that adoptively transferred lymphocytes are able to migrate to the inflamed vessel wall even at this very late stage in the pathology. The production of a murine IL-10 and GFP expressing adenovirus and the unforeseen issues which arose during this process have been discussed, following which CD4+ T cell transduction was optimised and T cells were shown to produce biologically active murine IL-10. Finally, virally modified CD4+ T cells were shown *in vivo* to migrate and survive comparably to non-modified T cells and also avoid the liver, indicating that, if used in an inflammatory atherosclerotic context, they would migrate as normal T cells do into the inflamed vessel wall, avoiding any liver toxicity. This combined with the IL-10 they would produce, indicates that this could be a feasible approach to a tissue specific anti-atherogenic immunotherapy.

References

1. Kita, T., et al., *The role of atherogenic low density lipoproteins (LDL) in the pathogenesis of atherosclerosis.* Ann N Y Acad Sci, 1990. **598**: p. 188-93.
2. Libby, P., *Inflammation in atherosclerosis.* Nature, 2002. **420**(6917): p. 868-74.
3. Kakkar, R. and R.T. Lee, *The IL-33/ST2 pathway: therapeutic target and novel biomarker.* Nat Rev Drug Discov, 2008. **7**(10): p. 827-40.
4. Niessner, A., J.J. Goronzy, and C.M. Weyand, *Immune-mediated mechanisms in atherosclerosis: prevention and treatment of clinical manifestations.* Curr Pharm Des, 2007. **13**(36): p. 3701-10.
5. Zhou, X., et al., *Transfer of CD4(+) T cells aggravates atherosclerosis in immunodeficient apolipoprotein E knockout mice.* Circulation, 2000. **102**(24): p. 2919-22.
6. Buono, C., et al., *T-bet deficiency reduces atherosclerosis and alters plaque antigen-specific immune responses.* Proc Natl Acad Sci U S A, 2005. **102**(5): p. 1596-601.
7. Stary, H.C., et al., *A definition of advanced types of atherosclerotic lesions and a histological classification of atherosclerosis. A report from the Committee on Vascular Lesions of the Council on Arteriosclerosis, American Heart Association.* Arterioscler Thromb Vasc Biol, 1995. **15**(9): p. 1512-31.
8. Falk, E., P.K. Shah, and V. Fuster, *Coronary plaque disruption.* Circulation, 1995. **92**(3): p. 657-71.
9. Tabas, I., K.J. Williams, and J. Boren, *Subendothelial lipoprotein retention as the initiating process in atherosclerosis: update and therapeutic implications.* Circulation, 2007. **116**(16): p. 1832-44.
10. Skalen, K., et al., *Subendothelial retention of atherogenic lipoproteins in early atherosclerosis.* Nature, 2002. **417**(6890): p. 750-4.
11. Yamamoto, S., *Mammalian lipoxygenases: molecular structures and functions.* Biochim Biophys Acta, 1992. **1128**(2-3): p. 117-31.
12. Peiser, L., S. Mukhopadhyay, and S. Gordon, *Scavenger receptors in innate immunity.* Curr Opin Immunol, 2002. **14**(1): p. 123-8.
13. Stary, H.C., et al., *A definition of initial, fatty streak, and intermediate lesions of atherosclerosis. A report from the Committee on Vascular Lesions of the Council on Arteriosclerosis, American Heart Association.* Circulation, 1994. **89**(5): p. 2462-78.
14. Jonasson, L., et al., *Regional accumulations of T cells, macrophages, and smooth muscle cells in the human atherosclerotic plaque.* Arteriosclerosis, 1986. **6**(2): p. 131-8.
15. Moore, K.J., et al., *Loss of receptor-mediated lipid uptake via scavenger receptor A or CD36 pathways does not ameliorate atherosclerosis in hyperlipidemic mice.* J Clin Invest, 2005. **115**(8): p. 2192-201.

16. Chen, H., et al., *EPA and DHA attenuate ox-LDL-induced expression of adhesion molecules in human coronary artery endothelial cells via protein kinase B pathway.* J Mol Cell Cardiol, 2003. **35**(7): p. 769-75.
17. Chen, H., et al., *Cytokine-induced cell surface expression of adhesion molecules in vascular endothelial cells in vitro.* J Tongji Med Univ, 2001. **21**(1): p. 68-71.
18. Cybulsky, M.I. and M.A. Gimbrone, Jr., *Endothelial expression of a mononuclear leukocyte adhesion molecule during atherogenesis.* Science, 1991. **251**(4995): p. 788-91.
19. Pradhan, S. and B. Sumpio, *Molecular and biological effects of hemodynamics on vascular cells.* Front Biosci, 2004. **9**: p. 3276-85.
20. Kol, A., et al., *Cutting edge: heat shock protein (HSP) 60 activates the innate immune response: CD14 is an essential receptor for HSP60 activation of mononuclear cells.* J Immunol, 2000. **164**(1): p. 13-7.
21. Chang, M.K., et al., *Apoptotic cells with oxidation-specific epitopes are immunogenic and proinflammatory.* J Exp Med, 2004. **200**(11): p. 1359-70.
22. Millette, E., et al., *Platelet-derived growth factor-BB-induced human smooth muscle cell proliferation depends on basic FGF release and FGFR-1 activation.* Circ Res, 2005. **96**(2): p. 172-9.
23. Gupta, S., et al., *IFN-gamma potentiates atherosclerosis in ApoE knock-out mice.* J Clin Invest, 1997. **99**(11): p. 2752-61.
24. Kovanen, P.T., *Atheroma formation: defective control in the intimal round-trip of cholesterol.* Eur Heart J, 1990. **11 Suppl E**: p. 238-46.
25. Getz, G.S. and C.A. Reardon, *Animal models of atherosclerosis.* Arterioscler Thromb Vasc Biol. **32**(5): p. 1104-15.
26. Skold, B.H., R. Getty, and F.K. Ramsey, *Spontaneous atherosclerosis in the arterial system of aging swine.* Am J Vet Res, 1966. **27**(116): p. 257-73.
27. Reiser, R., M.F. Sorrels, and M.C. Williams, *Influence of high levels of dietary fats and cholesterol on atherosclerosis and lipid distribution in swine.* Circ Res, 1959. **7**: p. 833-46.
28. Koskinas, K.C., et al., *Natural history of experimental coronary atherosclerosis and vascular remodeling in relation to endothelial shear stress: a serial, in vivo intravascular ultrasound study.* Circulation. **121**(19): p. 2092-101.
29. Gerrity, R.G., et al., *Endothelial cell morphology in areas of in vivo Evans blue uptake in the aorta of young pigs. II. Ultrastructure of the intima in areas of differing permeability to proteins.* Am J Pathol, 1977. **89**(2): p. 313-34.
30. Davies, P.F., *Hemodynamic shear stress and the endothelium in cardiovascular pathophysiology.* Nat Clin Pract Cardiovasc Med, 2009. **6**(1): p. 16-26.
31. Bocan, T.M., et al., *The relationship between the degree of dietary-induced hypercholesterolemia in the rabbit and atherosclerotic lesion formation.* Atherosclerosis, 1993. **102**(1): p. 9-22.

32. Shiomi, M. and T. Ito, *The Watanabe heritable hyperlipidemic (WHHL) rabbit, its characteristics and history of development: a tribute to the late Dr. Yoshio Watanabe*. Atherosclerosis, 2009. **207**(1): p. 1-7.
33. Kritchevsky, D., *Herman Award Lecture, 1992: lipid nutrition--a personal perspective*. Am J Clin Nutr, 1992. **56**(4): p. 730-4.
34. Wolfe, M.S., et al., *Dietary polyunsaturated fat decreases coronary artery atherosclerosis in a pediatric-aged population of African green monkeys*. Arterioscler Thromb, 1994. **14**(4): p. 587-97.
35. Vesselinovitch, D., et al., *Atherosclerosis in the rhesus monkey fed three food fats*. Atherosclerosis, 1974. **20**(2): p. 303-21.
36. Davis, H.R., D. Vesselinovitch, and R.W. Wissler, *Histochemical detection and quantification of macrophages in rhesus and cynomolgus monkey atherosclerotic lesions*. J Histochem Cytochem, 1984. **32**(12): p. 1319-27.
37. Mott, G.E., et al., *Dietary cholesterol and type of fat differentially affect cholesterol metabolism and atherosclerosis in baboons*. J Nutr, 1992. **122**(7): p. 1397-406.
38. Meir, K.S. and E. Leitersdorf, *Atherosclerosis in the apolipoprotein-E-deficient mouse: a decade of progress*. Arterioscler Thromb Vasc Biol, 2004. **24**(6): p. 1006-14.
39. Nakashima, Y., et al., *ApoE-deficient mice develop lesions of all phases of atherosclerosis throughout the arterial tree*. Arterioscler Thromb, 1994. **14**(1): p. 133-40.
40. Galkina, E., et al., *Lymphocyte recruitment into the aortic wall before and during development of atherosclerosis is partially L-selectin dependent*. J Exp Med, 2006. **203**(5): p. 1273-82.
41. Dansky, H.M., et al., *T and B lymphocytes play a minor role in atherosclerotic plaque formation in the apolipoprotein E-deficient mouse*. Proc Natl Acad Sci U S A, 1997. **94**(9): p. 4642-6.
42. Getz, G.S. and C.A. Reardon, *Apoprotein E as a lipid transport and signaling protein in the blood, liver, and artery wall*. J Lipid Res, 2009. **50 Suppl**: p. S156-61.
43. Barcat, D., et al., *Combined hyperlipidemia/hyperalphalipoproteinemia associated with premature spontaneous atherosclerosis in mice lacking hepatic lipase and low density lipoprotein receptor*. Atherosclerosis, 2006. **188**(2): p. 347-55.
44. Teupser, D., A.D. Persky, and J.L. Breslow, *Induction of atherosclerosis by low-fat, semisynthetic diets in LDL receptor-deficient C57BL/6J and FVB/NJ mice: comparison of lesions of the aortic root, brachiocephalic artery, and whole aorta (en face measurement)*. Arterioscler Thromb Vasc Biol, 2003. **23**(10): p. 1907-13.
45. Braun, A., et al., *Loss of SR-BI expression leads to the early onset of occlusive atherosclerotic coronary artery disease, spontaneous myocardial infarctions, severe cardiac dysfunction, and premature*

death in apolipoprotein E-deficient mice. Circ Res, 2002. **90**(3): p. 270-6.
46. Ross, R. and L. Harker, *Hyperlipidemia and atherosclerosis*. Science, 1976. **193**(4258): p. 1094-100.
47. Wick, G., M. Knoflach, and Q. Xu, *Autoimmune and inflammatory mechanisms in atherosclerosis*. Annu Rev Immunol, 2004. **22**: p. 361-403.
48. Galkina, E. and K. Ley, *Immune and inflammatory mechanisms of atherosclerosis (*)*. Annu Rev Immunol, 2009. **27**: p. 165-97.
49. Houtkamp, M.A., et al., *Adventitial infiltrates associated with advanced atherosclerotic plaques: structural organization suggests generation of local humoral immune responses*. J Pathol, 2001. **193**(2): p. 263-9.
50. Grabner, R., et al., *Lymphotoxin beta receptor signaling promotes tertiary lymphoid organogenesis in the aorta adventitia of aged ApoE$^{-/-}$ mice*. J Exp Med, 2009. **206**(1): p. 233-48.
51. Maffia, P., et al., *Images in cardiovascular medicine. Multiphoton microscopy for 3-dimensional imaging of lymphocyte recruitment into apolipoprotein-E-deficient mouse carotid artery*. Circulation, 2007. **115**(11): p. e326-8.
52. Chomarat, P., et al., *TNF skews monocyte differentiation from macrophages to dendritic cells*. J Immunol, 2003. **171**(5): p. 2262-9.
53. Galkina, E. and K. Ley, *Vascular adhesion molecules in atherosclerosis*. Arterioscler Thromb Vasc Biol, 2007. **27**(11): p. 2292-301.
54. Missiou, A., et al., *Tumor necrosis factor receptor-associated factor 1 (TRAF1) deficiency attenuates atherosclerosis in mice by impairing monocyte recruitment to the vessel wall*. Circulation. **121**(18): p. 2033-44.
55. Shah, Z., et al., *Long-term dipeptidyl-peptidase 4 inhibition reduces atherosclerosis and inflammation via effects on monocyte recruitment and chemotaxis*. Circulation. **124**(21): p. 2338-49.
56. Potteaux, S., et al., *Suppressed monocyte recruitment drives macrophage removal from atherosclerotic plaques of Apoe$^{-/-}$ mice during disease regression*. J Clin Invest. **121**(5): p. 2025-36.
57. Gerrity, R.G., et al., *Dietary induced atherogenesis in swine. Morphology of the intima in prelesion stages*. Am J Pathol, 1979. **95**(3): p. 775-92.
58. Werling, D. and T.W. Jungi, *TOLL-like receptors linking innate and adaptive immune response*. Vet Immunol Immunopathol, 2003. **91**(1): p. 1-12.
59. Yvan-Charvet, L., et al., *Combined deficiency of ABCA1 and ABCG1 promotes foam cell accumulation and accelerates atherosclerosis in mice*. J Clin Invest, 2007. **117**(12): p. 3900-8.
60. Zhao, B., et al., *Macrophage-specific transgenic expression of cholesteryl ester hydrolase significantly reduces atherosclerosis and lesion necrosis in Ldlr mice*. J Clin Invest, 2007. **117**(10): p. 2983-92.

61. Khallou-Laschet, J., et al., *Macrophage plasticity in experimental atherosclerosis.* PLoS One. **5**(1): p. e8852.
62. Boyle, J.J., et al., *Human blood-derived macrophages induce apoptosis in human plaque-derived vascular smooth muscle cells by Fas-ligand/Fas interactions.* Arterioscler Thromb Vasc Biol, 2001. **21**(9): p. 1402-7.
63. Edwards, I.J., W.D. Wagner, and R.T. Owens, *Macrophage secretory products selectively stimulate dermatan sulfate proteoglycan production in cultured arterial smooth muscle cells.* Am J Pathol, 1990. **136**(3): p. 609-21.
64. Hutter, R., et al., *Caspase-3 and tissue factor expression in lipid-rich plaque macrophages: evidence for apoptosis as link between inflammation and atherothrombosis.* Circulation, 2004. **109**(16): p. 2001-8.
65. Stoneman, V., et al., *Monocyte/macrophage suppression in CD11b diphtheria toxin receptor transgenic mice differentially affects atherogenesis and established plaques.* Circ Res, 2007. **100**(6): p. 884-93.
66. Jongstra-Bilen, J., et al., *Low-grade chronic inflammation in regions of the normal mouse arterial intima predisposed to atherosclerosis.* J Exp Med, 2006. **203**(9): p. 2073-83.
67. Bobryshev, Y.V. and R.S. Lord, *Mapping of vascular dendritic cells in atherosclerotic arteries suggests their involvement in local immune-inflammatory reactions.* Cardiovasc Res, 1998. **37**(3): p. 799-810.
68. Yilmaz, A., et al., *Emergence of dendritic cells in rupture-prone regions of vulnerable carotid plaques.* Atherosclerosis, 2004. **176**(1): p. 101-10.
69. Ranjit, S., et al., *Differentiation of dendritic cells in monocyte cultures isolated from patients with unstable angina.* Int J Cardiol, 2004. **97**(3): p. 551-5.
70. Weber, C., et al., *CCL17-expressing dendritic cells drive atherosclerosis by restraining regulatory T cell homeostasis in mice.* J Clin Invest. **121**(7): p. 2898-910.
71. Kawahara, I., et al., *The expression of vascular dendritic cells in human atherosclerotic carotid plaques.* Hum Pathol, 2007. **38**(9): p. 1378-85.
72. Gautier, E.L., et al., *Conventional dendritic cells at the crossroads between immunity and cholesterol homeostasis in atherosclerosis.* Circulation, 2009. **119**(17): p. 2367-75.
73. Paulson, K.E., et al., *Resident intimal dendritic cells accumulate lipid and contribute to the initiation of atherosclerosis.* Circ Res. **106**(2): p. 383-90.
74. Jeziorska, M., C. McCollum, and D.E. Woolley, *Mast cell distribution, activation, and phenotype in atherosclerotic lesions of human carotid arteries.* J Pathol, 1997. **182**(1): p. 115-22.
75. Bot, I., et al., *Perivascular mast cells promote atherogenesis and induce plaque destabilization in apolipoprotein E-deficient mice.* Circulation, 2007. **115**(19): p. 2516-25.

76. Sun, J., et al., *Mast cells promote atherosclerosis by releasing proinflammatory cytokines.* Nat Med, 2007. **13**(6): p. 719-24.
77. Tupin, E., et al., *CD1d-dependent activation of NKT cells aggravates atherosclerosis.* J Exp Med, 2004. **199**(3): p. 417-22.
78. Nakai, Y., et al., *Natural killer T cells accelerate atherogenesis in mice.* Blood, 2004. **104**(7): p. 2051-9.
79. Rogers, A. and G. Major, *The quantitative risks of mesothelioma and lung cancer in relation to asbestos exposure: the Wittenoom data.* Ann Occup Hyg, 2002. **46**(1): p. 127-8; author reply 128-9.
80. Caligiuri, G., et al., *Protective immunity against atherosclerosis carried by B cells of hypercholesterolemic mice.* J Clin Invest, 2002. **109**(6): p. 745-53.
81. Montecino-Rodriguez, E. and K. Dorshkind, *New perspectives in B-1 B cell development and function.* Trends Immunol, 2006. **27**(9): p. 428-33.
82. Binder, C.J., et al., *The role of natural antibodies in atherogenesis.* J Lipid Res, 2005. **46**(7): p. 1353-63.
83. Klingenberg, R., et al., *Intranasal immunization with an apolipoprotein B-100 fusion protein induces antigen-specific regulatory T cells and reduces atherosclerosis.* Arterioscler Thromb Vasc Biol, 2010. **30**(5): p. 946-52.
84. Sage, A.P., et al., *BAFF Receptor Deficiency Reduces the Development of Atherosclerosis in Mice--Brief Report.* Arterioscler Thromb Vasc Biol. **32**(7): p. 1573-6.
85. Ait-Oufella, H., et al., *B cell depletion reduces the development of atherosclerosis in mice.* J Exp Med. **207**(8): p. 1579-87.
86. Locksley, R.M., N. Killeen, and M.J. Lenardo, *The TNF and TNF receptor superfamilies: integrating mammalian biology.* Cell, 2001. **104**(4): p. 487-501.
87. Ohta, H., et al., *Disruption of tumor necrosis factor-alpha gene diminishes the development of atherosclerosis in ApoE-deficient mice.* Atherosclerosis, 2005. **180**(1): p. 11-7.
88. Canault, M., et al., *Progression of atherosclerosis in ApoE-deficient mice that express distinct molecular forms of TNF-alpha.* J Pathol, 2008. **214**(5): p. 574-83.
89. Lee, T.S., et al., *The role of interleukin 12 in the development of atherosclerosis in ApoE-deficient mice.* Arterioscler Thromb Vasc Biol, 1999. **19**(3): p. 734-42.
90. Davenport, P. and P.G. Tipping, *The role of interleukin-4 and interleukin-12 in the progression of atherosclerosis in apolipoprotein E-deficient mice.* Am J Pathol, 2003. **163**(3): p. 1117-25.
91. Schroder, K., et al., *Interferon-gamma: an overview of signals, mechanisms and functions.* J Leukoc Biol, 2004. **75**(2): p. 163-89.
92. Whitman, S.C., et al., *Exogenous interferon-gamma enhances atherosclerosis in apolipoprotein $E^{-/-}$ mice.* Am J Pathol, 2000. **157**(6): p. 1819-24.

93. Koga, M., et al., *Inhibition of progression and stabilization of plaques by postnatal interferon-gamma function blocking in ApoE-knockout mice.* Circ Res, 2007. **101**(4): p. 348-56.
94. King, V.L., L.A. Cassis, and A. Daugherty, *Interleukin-4 does not influence development of hypercholesterolemia or angiotensin II-induced atherosclerotic lesions in mice.* Am J Pathol, 2007. **171**(6): p. 2040-7.
95. Miller, A.M., et al., *IL-33 reduces the development of atherosclerosis.* J Exp Med, 2008. **205**(2): p. 339-46.
96. Pinderski, L.J., et al., *Overexpression of interleukin-10 by activated T lymphocytes inhibits atherosclerosis in LDL receptor-deficient Mice by altering lymphocyte and macrophage phenotypes.* Circ Res, 2002. **90**(10): p. 1064-71.
97. Mallat, Z., et al., *Protective role of interleukin-10 in atherosclerosis.* Circ Res, 1999. **85**(8): p. e17-24.
98. Von Der Thusen, J.H., et al., *Attenuation of atherogenesis by systemic and local adenovirus-mediated gene transfer of interleukin-10 in LDLr$^{-/-}$ mice.* FASEB J, 2001. **15**(14): p. 2730-2.
99. Nadig, S.N., et al., *In vivo prevention of transplant arteriosclerosis by ex vivo-expanded human regulatory T cells.* Nat Med.
100. Nelken, N.A., et al., *Monocyte chemoattractant protein-1 in human atheromatous plaques.* J Clin Invest, 1991. **88**(4): p. 1121-7.
101. Yla-Herttuala, S., et al., *Expression of monocyte chemoattractant protein 1 in macrophage-rich areas of human and rabbit atherosclerotic lesions.* Proc Natl Acad Sci U S A, 1991. **88**(12): p. 5252-6.
102. Yu, X., et al., *Elevated expression of monocyte chemoattractant protein 1 by vascular smooth muscle cells in hypercholesterolemic primates.* Proc Natl Acad Sci U S A, 1992. **89**(15): p. 6953-7.
103. Boring, L., et al., *Decreased lesion formation in CCR2$^{-/-}$ mice reveals a role for chemokines in the initiation of atherosclerosis.* Nature, 1998. **394**(6696): p. 894-7.
104. Gu, L., et al., *Absence of monocyte chemoattractant protein-1 reduces atherosclerosis in low density lipoprotein receptor-deficient mice.* Mol Cell, 1998. **2**(2): p. 275-81.
105. Gosling, J., et al., *MCP-1 deficiency reduces susceptibility to atherosclerosis in mice that overexpress human apolipoprotein B.* J Clin Invest, 1999. **103**(6): p. 773-8.
106. Ni, W., et al., *New anti-monocyte chemoattractant protein-1 gene therapy attenuates atherosclerosis in apolipoprotein E-knockout mice.* Circulation, 2001. **103**(16): p. 2096-101.
107. Inoue, S., et al., *Anti-monocyte chemoattractant protein-1 gene therapy limits progression and destabilization of established atherosclerosis in apolipoprotein E-knockout mice.* Circulation, 2002. **106**(21): p. 2700-6.
108. Aiello, R.J., et al., *Monocyte chemoattractant protein-1 accelerates atherosclerosis in apolipoprotein E-deficient mice.* Arterioscler Thromb Vasc Biol, 1999. **19**(6): p. 1518-25.

109. Martinovic, I., et al., *Elevated monocyte chemoattractant protein-1 serum levels in patients at risk for coronary artery disease.* Circ J, 2005. **69**(12): p. 1484-9.
110. Schecter, A.D., et al., *Human vascular smooth muscle cells possess functional CCR5.* J Biol Chem, 2000. **275**(8): p. 5466-71.
111. von Hundelshausen, P., et al., *RANTES deposition by platelets triggers monocyte arrest on inflamed and atherosclerotic endothelium.* Circulation, 2001. **103**(13): p. 1772-7.
112. Veillard, N.R., et al., *Differential expression patterns of proinflammatory and antiinflammatory mediators during atherogenesis in mice.* Arterioscler Thromb Vasc Biol, 2004. **24**(12): p. 2339-44.
113. Weber, C., A. Schober, and A. Zernecke, *Chemokines: key regulators of mononuclear cell recruitment in atherosclerotic vascular disease.* Arterioscler Thromb Vasc Biol, 2004. **24**(11): p. 1997-2008.
114. Szalai, C., et al., *Involvement of polymorphisms in the chemokine system in the susceptibility for coronary artery disease (CAD). Coincidence of elevated Lp(a) and MCP-1 -2518 G/G genotype in CAD patients.* Atherosclerosis, 2001. **158**(1): p. 233-9.
115. Gonzalez, P., et al., *Genetic variation at the chemokine receptors CCR5/CCR2 in myocardial infarction.* Genes Immun, 2001. **2**(4): p. 191-5.
116. Veillard, N.R., et al., *Antagonism of RANTES receptors reduces atherosclerotic plaque formation in mice.* Circ Res, 2004. **94**(2): p. 253-61.
117. Potteaux, S., et al., *Role of bone marrow-derived CC-chemokine receptor 5 in the development of atherosclerosis of low-density lipoprotein receptor knockout mice.* Arterioscler Thromb Vasc Biol, 2006. **26**(8): p. 1858-63.
118. Braunersreuther, V., et al., *Ccr5 but not Ccr1 deficiency reduces development of diet-induced atherosclerosis in mice.* Arterioscler Thromb Vasc Biol, 2007. **27**(2): p. 373-9.
119. Flanagan, K., et al., *The lymphoid chemokine CCL21 costimulates naive T cell expansion and Th1 polarization of non-regulatory CD4+ T cells.* Cell Immunol, 2004. **231**(1-2): p. 75-84.
120. Marsland, B.J., et al., *CCL19 and CCL21 induce a potent proinflammatory differentiation program in licensed dendritic cells.* Immunity, 2005. **22**(4): p. 493-505.
121. Damas, J.K., et al., *Enhanced expression of the homeostatic chemokines CCL19 and CCL21 in clinical and experimental atherosclerosis: possible pathogenic role in plaque destabilization.* Arterioscler Thromb Vasc Biol, 2007. **27**(3): p. 614-20.
122. Trogan, E., et al., *Laser capture microdissection analysis of gene expression in macrophages from atherosclerotic lesions of apolipoprotein E-deficient mice.* Proc Natl Acad Sci U S A, 2002. **99**(4): p. 2234-9.
123. Trogan, E., et al., *Gene expression changes in foam cells and the role of chemokine receptor CCR7 during atherosclerosis regression*

in ApoE-deficient mice. Proc Natl Acad Sci U S A, 2006. **103**(10): p. 3781-6.
124. Terkeltaub, R., et al., *Oxidized LDL induces monocytic cell expression of interleukin-8, a chemokine with T-lymphocyte chemotactic activity.* Arterioscler Thromb, 1994. **14**(1): p. 47-53.
125. Apostolopoulos, J., P. Davenport, and P.G. Tipping, *Interleukin-8 production by macrophages from atheromatous plaques.* Arterioscler Thromb Vasc Biol, 1996. **16**(8): p. 1007-12.
126. Boisvert, W.A., et al., *A leukocyte homologue of the IL-8 receptor CXCR-2 mediates the accumulation of macrophages in atherosclerotic lesions of LDL receptor-deficient mice.* J Clin Invest, 1998. **101**(2): p. 353-63.
127. Boisvert, W.A., et al., *Up-regulated expression of the CXCR2 ligand KC/GRO-alpha in atherosclerotic lesions plays a central role in macrophage accumulation and lesion progression.* Am J Pathol, 2006. **168**(4): p. 1385-95.
128. Visse, R. and H. Nagase, *Matrix metalloproteinases and tissue inhibitors of metalloproteinases: structure, function, and biochemistry.* Circ Res, 2003. **92**(8): p. 827-39.
129. Galis, Z.S. and J.J. Khatri, *Matrix metalloproteinases in vascular remodeling and atherogenesis: the good, the bad, and the ugly.* Circ Res, 2002. **90**(3): p. 251-62.
130. Galis, Z.S., et al., *Increased expression of matrix metalloproteinases and matrix degrading activity in vulnerable regions of human atherosclerotic plaques.* J Clin Invest, 1994. **94**(6): p. 2493-503.
131. de Nooijer, R., et al., *Lesional overexpression of matrix metalloproteinase-9 promotes intraplaque hemorrhage in advanced lesions but not at earlier stages of atherogenesis.* Arterioscler Thromb Vasc Biol, 2006. **26**(2): p. 340-6.
132. Webster, N.L. and S.M. Crowe, *Matrix metalloproteinases, their production by monocytes and macrophages and their potential role in HIV-related diseases.* J Leukoc Biol, 2006. **80**(5): p. 1052-66.
133. Raffetto, J.D. and R.A. Khalil, *Matrix metalloproteinases and their inhibitors in vascular remodeling and vascular disease.* Biochem Pharmacol, 2008. **75**(2): p. 346-59.
134. Fernandez-Catalan, C., et al., *Crystal structure of the complex formed by the membrane type 1-matrix metalloproteinase with the tissue inhibitor of metalloproteinases-2, the soluble progelatinase A receptor.* EMBO J, 1998. **17**(17): p. 5238-48.
135. Johnson, J.L., et al., *Suppression of atherosclerotic plaque progression and instability by tissue inhibitor of metalloproteinase-2: involvement of macrophage migration and apoptosis.* Circulation, 2006. **113**(20): p. 2435-44.
136. Zacchigna, S., et al., *AAV-mediated gene transfer of tissue inhibitor of metalloproteinases-1 inhibits vascular tumor growth and angiogenesis in vivo.* Cancer Gene Ther, 2004. **11**(1): p. 73-80.

137. Baker, A.H., D.R. Edwards, and G. Murphy, *Metalloproteinase inhibitors: biological actions and therapeutic opportunities.* J Cell Sci, 2002. **115**(Pt 19): p. 3719-27.
138. Rundhaug, J.E., *Matrix metalloproteinases and angiogenesis.* J Cell Mol Med, 2005. **9**(2): p. 267-85.
139. Bailie, M.B., et al., *Leukotriene-deficient mice manifest enhanced lethality from Klebsiella pneumonia in association with decreased alveolar macrophage phagocytic and bactericidal activities.* J Immunol, 1996. **157**(12): p. 5221-4.
140. Mancuso, P., et al., *5-Lipoxygenase reaction products modulate alveolar macrophage phagocytosis of Klebsiella pneumoniae.* Infect Immun, 1998. **66**(11): p. 5140-6.
141. Mehrabian, M., et al., *Identification of 5-lipoxygenase as a major gene contributing to atherosclerosis susceptibility in mice.* Circ Res, 2002. **91**(2): p. 120-6.
142. Cyrus, T., et al., *Disruption of the 12/15-lipoxygenase gene diminishes atherosclerosis in apo E-deficient mice.* J Clin Invest, 1999. **103**(11): p. 1597-604.
143. Reilly, K.B., et al., *12/15-Lipoxygenase activity mediates inflammatory monocyte/endothelial interactions and atherosclerosis in vivo.* J Biol Chem, 2004. **279**(10): p. 9440-50.
144. Huo, Y., et al., *Critical role of macrophage 12/15-lipoxygenase for atherosclerosis in apolipoprotein E-deficient mice.* Circulation, 2004. **110**(14): p. 2024-31.
145. Serhan, C.N., N. Chiang, and T.E. Van Dyke, *Resolving inflammation: dual anti-inflammatory and pro-resolution lipid mediators.* Nat Rev Immunol, 2008. **8**(5): p. 349-61.
146. Ishikawa, K., et al., *Induction of heme oxygenase-1 inhibits the monocyte transmigration induced by mildly oxidized LDL.* J Clin Invest, 1997. **100**(5): p. 1209-16.
147. Yet, S.F., et al., *Absence of heme oxygenase-1 exacerbates atherosclerotic lesion formation and vascular remodeling.* FASEB J, 2003. **17**(12): p. 1759-61.
148. Orozco, L.D., et al., *Heme oxygenase-1 expression in macrophages plays a beneficial role in atherosclerosis.* Circ Res, 2007. **100**(12): p. 1703-11.
149. Deguchi, J.O., et al., *Inflammation in atherosclerosis: visualizing matrix metalloproteinase action in macrophages in vivo.* Circulation, 2006. **114**(1): p. 55-62.
150. Chen, J., et al., *In vivo imaging of proteolytic activity in atherosclerosis.* Circulation, 2002. **105**(23): p. 2766-71.
151. Jaffer, F.A., et al., *Optical visualization of cathepsin K activity in atherosclerosis with a novel, protease-activatable fluorescence sensor.* Circulation, 2007. **115**(17): p. 2292-8.
152. Jaffer, F.A., et al., *Real-time catheter molecular sensing of inflammation in proteolytically active atherosclerosis.* Circulation, 2008. **118**(18): p. 1802-9.

153. Yabushita, H., et al., *Characterization of human atherosclerosis by optical coherence tomography.* Circulation, 2002. **106**(13): p. 1640-5.
154. Kircher, M.F., et al., *Noninvasive in vivo imaging of monocyte trafficking to atherosclerotic lesions.* Circulation, 2008. **117**(3): p. 388-95.
155. Tawakol, A., et al., *In vivo 18F-fluorodeoxyglucose positron emission tomography imaging provides a noninvasive measure of carotid plaque inflammation in patients.* J Am Coll Cardiol, 2006. **48**(9): p. 1818-24.
156. Aime, S., et al., *Insights into the use of paramagnetic Gd(III) complexes in MR-molecular imaging investigations.* J Magn Reson Imaging, 2002. **16**(4): p. 394-406.
157. Kooi, M.E., et al., *Accumulation of ultrasmall superparamagnetic particles of iron oxide in human atherosclerotic plaques can be detected by in vivo magnetic resonance imaging.* Circulation, 2003. **107**(19): p. 2453-8.
158. Naruko, T., et al., *Increased expression and plasma levels of myeloperoxidase are closely related to the presence of angiographically-detected complex lesion morphology in unstable angina.* Heart. **96**(21): p. 1716-22.
159. Demos, S.M., et al., *In vivo targeting of acoustically reflective liposomes for intravascular and transvascular ultrasonic enhancement.* J Am Coll Cardiol, 1999. **33**(3): p. 867-75.
160. Hamilton, A.J., et al., *Intravascular ultrasound molecular imaging of atheroma components in vivo.* J Am Coll Cardiol, 2004. **43**(3): p. 453-60.
161. Leong-Poi, H., et al., *Noninvasive assessment of angiogenesis by ultrasound and microbubbles targeted to alpha(v)-integrins.* Circulation, 2003. **107**(3): p. 455-60.
162. Andreasson, A.C., M. Abt, and A.C. Jonsson-Rylander, *Confocal scanning laser microscopy measurements of atherosclerotic lesions in mice aorta. A fast evaluation method for volume determinations.* Atherosclerosis, 2005. **179**(1): p. 35-42.
163. Taatjes, D.J., et al., *Improved quantitative characterization of atherosclerotic plaque composition with immunohistochemistry, confocal fluorescence microscopy, and computer-assisted image analysis.* Histochem Cell Biol, 2000. **113**(3): p. 161-73.
164. Wadsworth, M.P., et al., *Delineation of the evolution of compositional changes in atheroma.* Histochem Cell Biol, 2002. **118**(1): p. 59-68.
165. Cefalu, W.T., et al., *Effects of insulin sensitizers on plaque vulnerability associated with elevated lipid content in atheroma in ApoE-knockout mice.* Acta Diabetol, 2004. **41**(1): p. 25-31.
166. Denk, W., J.H. Strickler, and W.W. Webb, *Two-photon laser scanning fluorescence microscopy.* Science, 1990. **248**(4951): p. 73-6.

167. van Zandvoort, M., et al., *Two-photon microscopy for imaging of the (atherosclerotic) vascular wall: a proof of concept study.* J Vasc Res, 2004. **41**(1): p. 54-63.
168. Megens, R.T., et al., *In vivo high-resolution structural imaging of large arteries in small rodents using two-photon laser scanning microscopy.* J Biomed Opt. **15**(1): p. 011108.
169. Megens, R.T., et al., *Two-photon microscopy on vital carotid arteries: imaging the relationship between collagen and inflammatory cells in atherosclerotic plaques.* J Biomed Opt, 2008. **13**(4): p. 044022.
170. Yu, W., et al., *In vivo imaging of atherosclerotic plaques in apolipoprotein E deficient mice using nonlinear microscopy.* J Biomed Opt, 2007. **12**(5): p. 054008.
171. von Hundelshausen, P. and C. Weber, *Platelets as immune cells: bridging inflammation and cardiovascular disease.* Circ Res, 2007. **100**(1): p. 27-40.
172. Wallentin, L., et al., *Ticagrelor versus clopidogrel in patients with acute coronary syndromes.* N Engl J Med, 2009. **361**(11): p. 1045-57.
173. Patrono, C., et al., *Clinical pharmacology of platelet cyclooxygenase inhibition.* Circulation, 1985. **72**(6): p. 1177-84.
174. Lewis, H.D., Jr., et al., *Protective effects of aspirin against acute myocardial infarction and death in men with unstable angina. Results of a Veterans Administration Cooperative Study.* N Engl J Med, 1983. **309**(7): p. 396-403.
175. Dorsam, R.T. and S.P. Kunapuli, *Central role of the P2Y12 receptor in platelet activation.* J Clin Invest, 2004. **113**(3): p. 340-5.
176. Dangelmaier, C., et al., *Potentiation of thromboxane A2-induced platelet secretion by Gi signaling through the phosphoinositide-3 kinase pathway.* Thromb Haemost, 2001. **85**(2): p. 341-8.
177. Kauffenstein, G., et al., *The P2Y(12) receptor induces platelet aggregation through weak activation of the alpha(IIb)beta(3) integrin--a phosphoinositide 3-kinase-dependent mechanism.* FEBS Lett, 2001. **505**(2): p. 281-90.
178. Quinton, T.M., et al., *Protein kinase C- and calcium-regulated pathways independently synergize with Gi pathways in agonist-induced fibrinogen receptor activation.* Biochem J, 2002. **368**(Pt 2): p. 535-43.
179. Dorsam, R.T., et al., *Coordinated signaling through both G12/13 and G(i) pathways is sufficient to activate GPIIb/IIIa in human platelets.* J Biol Chem, 2002. **277**(49): p. 47588-95.
180. Nieswandt, B., et al., *Costimulation of Gi- and G12/G13-mediated signaling pathways induces integrin alpha IIbbeta 3 activation in platelets.* J Biol Chem, 2002. **277**(42): p. 39493-8.
181. Sipahi, I., et al., *Beta-blockers and progression of coronary atherosclerosis: pooled analysis of 4 intravascular ultrasonography trials.* Ann Intern Med, 2007. **147**(1): p. 10-8.

182. Holmer, S.R., et al., *Beta adrenergic blockers lower renin in patients treated with ACE inhibitors and diuretics.* Heart, 1998. **80**(1): p. 45-8.
183. Yusuf, S., et al., *Telmisartan, ramipril, or both in patients at high risk for vascular events.* N Engl J Med, 2008. **358**(15): p. 1547-59.
184. Golomb, B.A. and M.A. Evans, *Statin adverse effects : a review of the literature and evidence for a mitochondrial mechanism.* Am J Cardiovasc Drugs, 2008. **8**(6): p. 373-418.
185. Wilson, S.H., et al., *Simvastatin preserves coronary endothelial function in hypercholesterolemia in the absence of lipid lowering.* Arterioscler Thromb Vasc Biol, 2001. **21**(1): p. 122-8.
186. Bonetti, P.O., et al., *Simvastatin preserves myocardial perfusion and coronary microvascular permeability in experimental hypercholesterolemia independent of lipid lowering.* J Am Coll Cardiol, 2002. **40**(3): p. 546-54.
187. Anderson, T.J., et al., *The effect of cholesterol-lowering and antioxidant therapy on endothelium-dependent coronary vasomotion.* N Engl J Med, 1995. **332**(8): p. 488-93.
188. Treasure, C.B., et al., *Beneficial effects of cholesterol-lowering therapy on the coronary endothelium in patients with coronary artery disease.* N Engl J Med, 1995. **332**(8): p. 481-7.
189. Gimbrone, M.A., Jr., *Vascular endothelium, hemodynamic forces, and atherogenesis.* Am J Pathol, 1999. **155**(1): p. 1-5.
190. Aikawa, M., et al., *An HMG-CoA reductase inhibitor, cerivastatin, suppresses growth of macrophages expressing matrix metalloproteinases and tissue factor in vivo and in vitro.* Circulation, 2001. **103**(2): p. 276-83.
191. Crisby, M., et al., *Pravastatin treatment increases collagen content and decreases lipid content, inflammation, metalloproteinases, and cell death in human carotid plaques: implications for plaque stabilization.* Circulation, 2001. **103**(7): p. 926-33.
192. Fukumoto, Y., et al., *Statins alter smooth muscle cell accumulation and collagen content in established atheroma of watanabe heritable hyperlipidemic rabbits.* Circulation, 2001. **103**(7): p. 993-9.
193. Trocha, M., et al., *Effect of simvastatin on nitric oxide synthases (eNOS, iNOS) and arginine and its derivatives (ADMA, SDMA) in ischemia/reperfusion injury in rat liver.* Pharmacol Rep. **62**(2): p. 343-51.
194. Esmon, C.T., *Inflammation and thrombosis.* J Thromb Haemost, 2003. **1**(7): p. 1343-8.
195. Kobashigawa, J.A., et al., *Effect of pravastatin on outcomes after cardiac transplantation.* N Engl J Med, 1995. **333**(10): p. 621-7.
196. Wenke, K., et al., *Simvastatin reduces graft vessel disease and mortality after heart transplantation: a four-year randomized trial.* Circulation, 1997. **96**(5): p. 1398-402.
197. Katznelson, S., et al., *The effect of pravastatin on acute rejection after kidney transplantation--a pilot study.* Transplantation, 1996. **61**(10): p. 1469-74.

198. Kwak, B., et al., *Statins as a newly recognized type of immunomodulator*. Nat Med, 2000. **6**(12): p. 1399-402.
199. Bustos, C., et al., *HMG-CoA reductase inhibition by atorvastatin reduces neointimal inflammation in a rabbit model of atherosclerosis*. J Am Coll Cardiol, 1998. **32**(7): p. 2057-64.
200. Romano, M., et al., *Inhibition of monocyte chemotactic protein-1 synthesis by statins*. Lab Invest, 2000. **80**(7): p. 1095-100.
201. Diomede, L., et al., *In vivo anti-inflammatory effect of statins is mediated by nonsterol mevalonate products*. Arterioscler Thromb Vasc Biol, 2001. **21**(8): p. 1327-32.
202. Ito, T., et al., *Regulation of interleukin-8 expression by HMG-CoA reductase inhibitors in human vascular smooth muscle cells*. Atherosclerosis, 2002. **165**(1): p. 51-5.
203. Weitz-Schmidt, G., et al., *Statins selectively inhibit leukocyte function antigen-1 by binding to a novel regulatory integrin site*. Nat Med, 2001. **7**(6): p. 687-92.
204. Chen, Z., et al., *Simvastatin reduces neointimal thickening in low-density lipoprotein receptor-deficient mice after experimental angioplasty without changing plasma lipids*. Circulation, 2002. **106**(1): p. 20-3.
205. Youssef, S., et al., *The HMG-CoA reductase inhibitor, atorvastatin, promotes a Th2 bias and reverses paralysis in central nervous system autoimmune disease*. Nature, 2002. **420**(6911): p. 78-84.
206. Rosenson, R.S., C.C. Tangney, and L.C. Casey, *Inhibition of proinflammatory cytokine production by pravastatin*. Lancet, 1999. **353**(9157): p. 983-4.
207. Navab, M., et al., *Structure and function of HDL mimetics*. Arterioscler Thromb Vasc Biol. **30**(2): p. 164-8.
208. Tardif, J.C., *Emerging high-density lipoprotein infusion therapies: fulfilling the promise of epidemiology?* J Clin Lipidol. **4**(5): p. 399-404.
209. Nissen, S.E., et al., *Effect of recombinant ApoA-I Milano on coronary atherosclerosis in patients with acute coronary syndromes: a randomized controlled trial*. JAMA, 2003. **290**(17): p. 2292-300.
210. Vuorio, T., S. Jauhiainen, and S. Yla-Herttuala, *Pro- and anti-angiogenic therapy and atherosclerosis with special emphasis on vascular endothelial growth factors*. Expert Opin Biol Ther. **12**(1): p. 79-92.
211. Van-Assche, T., et al., *Gene therapy targeting inflammation in atherosclerosis*. Curr Pharm Des. **17**(37): p. 4210-23.
212. Baumgartner, I., et al., *Constitutive expression of phVEGF165 after intramuscular gene transfer promotes collateral vessel development in patients with critical limb ischemia*. Circulation, 1998. **97**(12): p. 1114-23.
213. Vale, P.R., et al., *Randomized, single-blind, placebo-controlled pilot study of catheter-based myocardial gene transfer for therapeutic angiogenesis using left ventricular electromechanical*

mapping in patients with chronic myocardial ischemia. Circulation, 2001. **103**(17): p. 2138-43.
214. Asahara, T., et al., *Accelerated restitution of endothelial integrity and endothelium-dependent function after phVEGF165 gene transfer.* Circulation, 1996. **94**(12): p. 3291-302.
215. Tsurumi, Y., et al., *Direct intramuscular gene transfer of naked DNA encoding vascular endothelial growth factor augments collateral development and tissue perfusion.* Circulation, 1996. **94**(12): p. 3281-90.
216. Lee, R.J., et al., *VEGF gene delivery to myocardium: deleterious effects of unregulated expression.* Circulation, 2000. **102**(8): p. 898-901.
217. Celletti, F.L., et al., *Vascular endothelial growth factor enhances atherosclerotic plaque progression.* Nat Med, 2001. **7**(4): p. 425-9.
218. French, B.A., et al., *Percutaneous transluminal in vivo gene transfer by recombinant adenovirus in normal porcine coronary arteries, atherosclerotic arteries, and two models of coronary restenosis.* Circulation, 1994. **90**(5): p. 2402-13.
219. Hajjar, R.J., et al., *Modulation of ventricular function through gene transfer in vivo.* Proc Natl Acad Sci U S A, 1998. **95**(9): p. 5251-6.
220. Lemarchand, P., et al., *In vivo gene transfer and expression in normal uninjured blood vessels using replication-deficient recombinant adenovirus vectors.* Circ Res, 1993. **72**(5): p. 1132-8.
221. Shayakhmetov, D.M., et al., *Analysis of adenovirus sequestration in the liver, transduction of hepatic cells, and innate toxicity after injection of fiber-modified vectors.* J Virol, 2004. **78**(10): p. 5368-81.
222. Work, L.M., et al., *Vascular bed-targeted in vivo gene delivery using tropism-modified adeno-associated viruses.* Mol Ther, 2006. **13**(4): p. 683-93.
223. Havenga, M.J., et al., *Improved adenovirus vectors for infection of cardiovascular tissues.* J Virol, 2001. **75**(7): p. 3335-42.
224. Havenga, M.J., et al., *Exploiting the natural diversity in adenovirus tropism for therapy and prevention of disease.* J Virol, 2002. **76**(9): p. 4612-20.
225. Nicklin, S.A., et al., *Selective targeting of gene transfer to vascular endothelial cells by use of peptides isolated by phage display.* Circulation, 2000. **102**(2): p. 231-7.
226. Jooss, K. and N. Chirmule, *Immunity to adenovirus and adeno-associated viral vectors: implications for gene therapy.* Gene Ther, 2003. **10**(11): p. 955-63.
227. Palinski, W., et al., *Low density lipoprotein undergoes oxidative modification in vivo.* Proc Natl Acad Sci U S A, 1989. **86**(4): p. 1372-6.
228. Palinski, W., E. Miller, and J.L. Witztum, *Immunization of low density lipoprotein (LDL) receptor-deficient rabbits with homologous malondialdehyde-modified LDL reduces atherogenesis.* Proc Natl Acad Sci U S A, 1995. **92**(3): p. 821-5.

229. Ameli, S., et al., *Effect of immunization with homologous LDL and oxidized LDL on early atherosclerosis in hypercholesterolemic rabbits.* Arterioscler Thromb Vasc Biol, 1996. **16**(8): p. 1074-9.
230. Freigang, S., et al., *Immunization of LDL receptor-deficient mice with homologous malondialdehyde-modified and native LDL reduces progression of atherosclerosis by mechanisms other than induction of high titers of antibodies to oxidative neoepitopes.* Arterioscler Thromb Vasc Biol, 1998. **18**(12): p. 1972-82.
231. Zhou, X., et al., *LDL immunization induces T-cell-dependent antibody formation and protection against atherosclerosis.* Arterioscler Thromb Vasc Biol, 2001. **21**(1): p. 108-14.
232. Fredrikson, G.N., et al., *Inhibition of atherosclerosis in apoE-null mice by immunization with apoB-100 peptide sequences.* Arterioscler Thromb Vasc Biol, 2003. **23**(5): p. 879-84.
233. Hochleitner, B.W., et al., *Fluid shear stress induces heat shock protein 60 expression in endothelial cells in vitro and in vivo.* Arterioscler Thromb Vasc Biol, 2000. **20**(3): p. 617-23.
234. Frostegard, J., et al., *Induction of heat shock protein in monocytic cells by oxidized low density lipoprotein.* Atherosclerosis, 1996. **121**(1): p. 93-103.
235. Oehler, R., et al., *Endothelial cells downregulate expression of the 70 kDa heat shock protein during hypoxia.* Biochem Biophys Res Commun, 2000. **274**(2): p. 542-7.
236. Afek, A., et al., *Immunization of low-density lipoprotein receptor deficient (LDL-RD) mice with heat shock protein 65 (HSP-65) promotes early atherosclerosis.* J Autoimmun, 2000. **14**(2): p. 115-21.
237. Maron, R., et al., *Mucosal administration of heat shock protein-65 decreases atherosclerosis and inflammation in aortic arch of low-density lipoprotein receptor-deficient mice.* Circulation, 2002. **106**(13): p. 1708-15.
238. van Puijvelde, G.H., et al., *Induction of oral tolerance to HSP60 or an HSP60-peptide activates T cell regulation and reduces atherosclerosis.* Arterioscler Thromb Vasc Biol, 2007. **27**(12): p. 2677-83.
239. van Es, T., et al., *IL-15 aggravates atherosclerotic lesion development in LDL receptor deficient mice.* Vaccine. **29**(5): p. 976-83.
240. Petrovan, R.J., et al., *DNA vaccination against VEGF receptor 2 reduces atherosclerosis in LDL receptor-deficient mice.* Arterioscler Thromb Vasc Biol, 2007. **27**(5): p. 1095-100.
241. Jonasson, L., et al., *Expression of class II transplantation antigen on vascular smooth muscle cells in human atherosclerosis.* J Clin Invest, 1985. **76**(1): p. 125-31.
242. Stemme, S., J. Holm, and G.K. Hansson, *T lymphocytes in human atherosclerotic plaques are memory cells expressing CD45RO and the integrin VLA-1.* Arterioscler Thromb, 1992. **12**(2): p. 206-11.

243. Hansson, G.K., J. Holm, and L. Jonasson, *Detection of activated T lymphocytes in the human atherosclerotic plaque.* Am J Pathol, 1989. **135**(1): p. 169-75.
244. Hosono, M., et al., *Increased expression of T cell activation markers (CD25, CD26, CD40L and CD69) in atherectomy specimens of patients with unstable angina and acute myocardial infarction.* Atherosclerosis, 2003. **168**(1): p. 73-80.
245. Frostegard, J., et al., *Cytokine expression in advanced human atherosclerotic plaques: dominance of pro-inflammatory (Th1) and macrophage-stimulating cytokines.* Atherosclerosis, 1999. **145**(1): p. 33-43.
246. Kleindienst, R., et al., *Immunology of atherosclerosis. Demonstration of heat shock protein 60 expression and T lymphocytes bearing alpha/beta or gamma/delta receptor in human atherosclerotic lesions.* Am J Pathol, 1993. **142**(6): p. 1927-37.
247. Epstein, S.E., Y.F. Zhou, and J. Zhu, *Infection and atherosclerosis: emerging mechanistic paradigms.* Circulation, 1999. **100**(4): p. e20-8.
248. Mayr, M., et al., *Infections, immunity, and atherosclerosis: associations of antibodies to Chlamydia pneumoniae, Helicobacter pylori, and cytomegalovirus with immune reactions to heat-shock protein 60 and carotid or femoral atherosclerosis.* Circulation, 2000. **102**(8): p. 833-9.
249. George, J., et al., *Enhanced fatty streak formation in C57BL/6J mice by immunization with heat shock protein-65.* Arterioscler Thromb Vasc Biol, 1999. **19**(3): p. 505-10.
250. Xu, Q., et al., *Association of serum antibodies to heat-shock protein 65 with carotid atherosclerosis.* Lancet, 1993. **341**(8840): p. 255-9.
251. Xu, Q., et al., *Association of serum antibodies to heat-shock protein 65 with carotid atherosclerosis : clinical significance determined in a follow-up study.* Circulation, 1999. **100**(11): p. 1169-74.
252. Palinski, W. and J.L. Witztum, *Immune responses to oxidative neoepitopes on LDL and phospholipids modulate the development of atherosclerosis.* J Intern Med, 2000. **247**(3): p. 371-80.
253. Palinski, W., et al., *Increased autoantibody titers against epitopes of oxidized LDL in LDL receptor-deficient mice with increased atherosclerosis.* Arterioscler Thromb Vasc Biol, 1995. **15**(10): p. 1569-76.
254. Salonen, J.T., et al., *Autoantibody against oxidised LDL and progression of carotid atherosclerosis.* Lancet, 1992. **339**(8798): p. 883-7.
255. George, J., et al., *Immunolocalization of beta2-glycoprotein I (apolipoprotein H) to human atherosclerotic plaques: potential implications for lesion progression.* Circulation, 1999. **99**(17): p. 2227-30.
256. Wu, R., et al., *Antibodies against cardiolipin and oxidatively modified LDL in 50-year-old men predict myocardial infarction.* Arterioscler Thromb Vasc Biol, 1997. **17**(11): p. 3159-63.

257. Hasunuma, Y., et al., *Involvement of beta 2-glycoprotein I and anticardiolipin antibodies in oxidatively modified low-density lipoprotein uptake by macrophages.* Clin Exp Immunol, 1997. **107**(3): p. 569-73.
258. Zhou, X., et al., *Adoptive transfer of CD4+ T cells reactive to modified low-density lipoprotein aggravates atherosclerosis.* Arterioscler Thromb Vasc Biol, 2006. **26**(4): p. 864-70.
259. George, J., et al., *Adoptive transfer of beta(2)-glycoprotein I-reactive lymphocytes enhances early atherosclerosis in LDL receptor-deficient mice.* Circulation, 2000. **102**(15): p. 1822-7.
260. George, J., et al., *Cellular and humoral immune responses to heat shock protein 65 are both involved in promoting fatty-streak formation in LDL-receptor deficient mice.* J Am Coll Cardiol, 2001. **38**(3): p. 900-5.
261. Tedgui, A. and Z. Mallat, *Cytokines in atherosclerosis: pathogenic and regulatory pathways.* Physiol Rev, 2006. **86**(2): p. 515-81.
262. Leon, M.L. and S.H. Zuckerman, *Gamma interferon: a central mediator in atherosclerosis.* Inflamm Res, 2005. **54**(10): p. 395-411.
263. Harvey, E.J. and D.P. Ramji, *Interferon-gamma and atherosclerosis: pro- or anti-atherogenic?* Cardiovasc Res, 2005. **67**(1): p. 11-20.
264. Huber, S.A., et al., *T helper-cell phenotype regulates atherosclerosis in mice under conditions of mild hypercholesterolemia.* Circulation, 2001. **103**(21): p. 2610-6.
265. King, V.L., S.J. Szilvassy, and A. Daugherty, *Interleukin-4 deficiency decreases atherosclerotic lesion formation in a site-specific manner in female LDL receptor$^{-/-}$ mice.* Arterioscler Thromb Vasc Biol, 2002. **22**(3): p. 456-61.
266. Saederup, N., et al., *Fractalkine deficiency markedly reduces macrophage accumulation and atherosclerotic lesion formation in CCR2$^{-/-}$ mice: evidence for independent chemokine functions in atherogenesis.* Circulation, 2008. **117**(13): p. 1642-8.
267. Sakaguchi, S., *Naturally arising CD4+ regulatory t cells for immunologic self-tolerance and negative control of immune responses.* Annu Rev Immunol, 2004. **22**: p. 531-62.
268. Heller, E.A., et al., *Chemokine CXCL10 promotes atherogenesis by modulating the local balance of effector and regulatory T cells.* Circulation, 2006. **113**(19): p. 2301-12.
269. de Boer, O.J., et al., *Low numbers of FOXP3 positive regulatory T cells are present in all developmental stages of human atherosclerotic lesions.* PLoS One, 2007. **2**(8): p. e779.
270. Ait-Oufella, H., et al., *Natural regulatory T cells control the development of atherosclerosis in mice.* Nat Med, 2006. **12**(2): p. 178-80.
271. Robertson, E.J., et al., *Control of early anterior-posterior patterning in the mouse embryo by TGF-beta signalling.* Philos Trans R Soc Lond B Biol Sci, 2003. **358**(1436): p. 1351-7; discussion 1357.

272. Mor, A., et al., *Role of naturally occurring CD4+ CD25+ regulatory T cells in experimental atherosclerosis.* Arterioscler Thromb Vasc Biol, 2007. **27**(4): p. 893-900.
273. Yang, K., et al., *Generation of HSP60-specific regulatory T cell and effect on atherosclerosis.* Cell Immunol, 2006. **243**(2): p. 90-5.
274. Park, H., et al., *A distinct lineage of CD4 T cells regulates tissue inflammation by producing interleukin 17.* Nat Immunol, 2005. **6**(11): p. 1133-41.
275. Kolls, J.K. and A. Linden, *Interleukin-17 family members and inflammation.* Immunity, 2004. **21**(4): p. 467-76.
276. Gao, Q., et al., *A critical function of Th17 proinflammatory cells in the development of atherosclerotic plaque in mice.* J Immunol. **185**(10): p. 5820-7.
277. Fyfe, A.I., J.H. Qiao, and A.J. Lusis, *Immune-deficient mice develop typical atherosclerotic fatty streaks when fed an atherogenic diet.* J Clin Invest, 1994. **94**(6): p. 2516-20.
278. Kolbus, D., et al., *CD8+ T cell activation predominate early immune responses to hypercholesterolemia in Apoe(-)(/)(-) mice.* BMC Immunol. **11**: p. 58.
279. Wick, G., et al., *Atherosclerosis, autoimmunity, and vascular-associated lymphoid tissue.* FASEB J, 1997. **11**(13): p. 1199-207.
280. Schroder, A.E., et al., *Differentiation of B cells in the nonlymphoid tissue of the synovial membrane of patients with rheumatoid arthritis.* Proc Natl Acad Sci U S A, 1996. **93**(1): p. 221-5.
281. Pablos, J.L., et al., *A HEV-restricted sulfotransferase is expressed in rheumatoid arthritis synovium and is induced by lymphotoxin-alpha/beta and TNF-alpha in cultured endothelial cells.* BMC Immunol, 2005. **6**: p. 6.
282. Prineas, J.W., *Multiple sclerosis: presence of lymphatic capillaries and lymphoid tissue in the brain and spinal cord.* Science, 1979. **203**(4385): p. 1123-5.
283. Mazzucchelli, L., et al., *BCA-1 is highly expressed in Helicobacter pylori-induced mucosa-associated lymphoid tissue and gastric lymphoma.* J Clin Invest, 1999. **104**(10): p. R49-54.
284. Ghosh, S., et al., *In situ diversification of the antibody repertoire in chronic Lyme arthritis synovium.* J Immunol, 2005. **174**(5): p. 2860-9.
285. Kerjaschki, D., et al., *Lymphatic neoangiogenesis in human kidney transplants is associated with immunologically active lymphocytic infiltrates.* J Am Soc Nephrol, 2004. **15**(3): p. 603-12.
286. Thaunat, O., et al., *Lymphoid neogenesis in chronic rejection: evidence for a local humoral alloimmune response.* Proc Natl Acad Sci U S A, 2005. **102**(41): p. 14723-8.
287. Mebius, R.E., *Organogenesis of lymphoid tissues.* Nat Rev Immunol, 2003. **3**(4): p. 292-303.
288. Gommerman, J.L. and J.L. Browning, *Lymphotoxin/light, lymphoid microenvironments and autoimmune disease.* Nat Rev Immunol, 2003. **3**(8): p. 642-55.

289. Cupedo, T. and R.E. Mebius, *Role of chemokines in the development of secondary and tertiary lymphoid tissues.* Semin Immunol, 2003. **15**(5): p. 243-8.
290. Nishikawa, S., et al., *Organogenesis of peripheral lymphoid organs.* Immunol Rev, 2003. **195**: p. 72-80.
291. Moos, M.P., et al., *The lamina adventitia is the major site of immune cell accumulation in standard chow-fed apolipoprotein E-deficient mice.* Arterioscler Thromb Vasc Biol, 2005. **25**(11): p. 2386-91.
292. Dal Canto, A.J., et al., *IFN-gamma action in the media of the great elastic arteries, a novel immunoprivileged site.* J Clin Invest, 2001. **107**(2): p. R15-22.
293. Ashbourne Excoffon, K.J., T. Moninger, and J. Zabner, *The coxsackie B virus and adenovirus receptor resides in a distinct membrane microdomain.* J Virol, 2003. **77**(4): p. 2559-67.
294. Greig, J.A., et al., *Influence of coagulation factor x on in vitro and in vivo gene delivery by adenovirus (Ad) 5, Ad35, and chimeric Ad5/Ad35 vectors.* Mol Ther, 2009. **17**(10): p. 1683-91.
295. Yang, Y., et al., *Cellular and humoral immune responses to viral antigens create barriers to lung-directed gene therapy with recombinant adenoviruses.* J Virol, 1995. **69**(4): p. 2004-15.
296. Hurez, V., et al., *Efficient adenovirus-mediated gene transfer into primary T cells and thymocytes in a new coxsackie/adenovirus receptor transgenic model.* BMC Immunol, 2002. **3**: p. 4.
297. Pluta, K. and M.M. Kacprzak, *Use of HIV as a gene transfer vector.* Acta Biochim Pol, 2009. **56**(4): p. 531-95.
298. Clapham, P.R. and A. McKnight, *Cell surface receptors, virus entry and tropism of primate lentiviruses.* J Gen Virol, 2002. **83**(Pt 8): p. 1809-29.
299. Gale, M., Jr. and M.G. Katze, *What happens inside lentivirus or influenza virus infected cells: insights into regulation of cellular and viral protein synthesis.* Methods, 1997. **11**(4): p. 383-401.
300. Bokhoven, M., et al., *Insertional gene activation by lentiviral and gammaretroviral vectors.* J Virol, 2009. **83**(1): p. 283-94.
301. Matlin, K.S., et al., *Pathway of vesicular stomatitis virus entry leading to infection.* J Mol Biol, 1982. **156**(3): p. 609-31.
302. Swainson, L., et al., *Lentiviral transduction of immune cells.* Methods Mol Biol, 2008. **415**: p. 301-20.
303. Verhoeyen, E., et al., *IL-7 surface-engineered lentiviral vectors promote survival and efficient gene transfer in resting primary T lymphocytes.* Blood, 2003. **101**(6): p. 2167-74.
304. Richter, M., et al., *Adeno-associated virus vector transduction of vascular smooth muscle cells in vivo.* Physiol Genomics, 2000. **2**(3): p. 117-27.
305. Maeda, Y., et al., *Gene transfer into vascular cells using adeno-associated virus (AAV) vectors.* Cardiovasc Res, 1997. **35**(3): p. 514-21.

306. Maeda, Y., et al., *Efficient gene transfer into cardiac myocytes using adeno-associated virus (AAV) vectors.* J Mol Cell Cardiol, 1998. **30**(7): p. 1341-8.
307. Maeda, Y., et al., *Adeno-associated virus-mediated vascular endothelial growth factor gene transfer into cardiac myocytes.* J Cardiovasc Pharmacol, 2000. **36**(4): p. 438-43.
308. Vassalli, G., et al., *Adeno-associated virus (AAV) vectors achieve prolonged transgene expression in mouse myocardium and arteries in vivo: a comparative study with adenovirus vectors.* Int J Cardiol, 2003. **90**(2-3): p. 229-38.
309. Zincarelli, C., et al., *Comparative cardiac gene delivery of adeno-associated virus serotypes 1-9 reveals that AAV6 mediates the most efficient transduction in mouse heart.* Clin Transl Sci. **3**(3): p. 81-9.
310. Dishart, K.L., et al., *Third-generation lentivirus vectors efficiently transduce and phenotypically modify vascular cells: implications for gene therapy.* J Mol Cell Cardiol, 2003. **35**(7): p. 739-48.
311. White, S.J., et al., *Targeted gene delivery to vascular tissue in vivo by tropism-modified adeno-associated virus vectors.* Circulation, 2004. **109**(4): p. 513-9.
312. Parkes, R., et al., *High efficiency transfection of porcine vascular cells in vitro with a synthetic vector system.* J Gene Med, 2002. **4**(3): p. 292-9.
313. Morishita, R., et al., *In vivo transfection of cis element "decoy" against nuclear factor-kappaB binding site prevents myocardial infarction.* Nat Med, 1997. **3**(8): p. 894-9.
314. Zhao, Y., et al., *High-efficiency transfection of primary human and mouse T lymphocytes using RNA electroporation.* Mol Ther, 2006. **13**(1): p. 151-9.
315. Zhao, X., et al., *High transfection efficiency of porcine peripheral blood T cells via nucleofection.* Vet Immunol Immunopathol. **144**(3-4): p. 179-86.
316. Fiorentino, D.F., M.W. Bond, and T.R. Mosmann, *Two types of mouse T helper cell. IV. Th2 clones secrete a factor that inhibits cytokine production by Th1 clones.* J Exp Med, 1989. **170**(6): p. 2081-95.
317. Fiorentino, D.F., et al., *IL-10 inhibits cytokine production by activated macrophages.* J Immunol, 1991. **147**(11): p. 3815-22.
318. de Waal Malefyt, R., et al., *Effects of IL-13 on phenotype, cytokine production, and cytotoxic function of human monocytes. Comparison with IL-4 and modulation by IFN-gamma or IL-10.* J Immunol, 1993. **151**(11): p. 6370-81.
319. D'Andrea, A., et al., *Interleukin 10 (IL-10) inhibits human lymphocyte interferon gamma-production by suppressing natural killer cell stimulatory factor/IL-12 synthesis in accessory cells.* J Exp Med, 1993. **178**(3): p. 1041-8.
320. Gruber, M.F., C.C. Williams, and T.L. Gerrard, *Macrophage-colony-stimulating factor expression by anti-CD45 stimulated human monocytes is transcriptionally up-regulated by IL-1 beta and inhibited by IL-4 and IL-10.* J Immunol, 1994. **152**(3): p. 1354-61.

321. de Waal Malefyt, R., et al., *Interleukin 10 (IL-10) and viral IL-10 strongly reduce antigen-specific human T cell proliferation by diminishing the antigen-presenting capacity of monocytes via downregulation of class II major histocompatibility complex expression.* J Exp Med, 1991. **174**(4): p. 915-24.
322. Ding, L., et al., *IL-10 inhibits macrophage costimulatory activity by selectively inhibiting the up-regulation of B7 expression.* J Immunol, 1993. **151**(3): p. 1224-34.
323. Kubin, M., M. Kamoun, and G. Trinchieri, *Interleukin 12 synergizes with B7/CD28 interaction in inducing efficient proliferation and cytokine production of human T cells.* J Exp Med, 1994. **180**(1): p. 211-22.
324. Willems, F., et al., *Interleukin-10 inhibits B7 and intercellular adhesion molecule-1 expression on human monocytes.* Eur J Immunol, 1994. **24**(4): p. 1007-9.
325. Taga, K., H. Mostowski, and G. Tosato, *Human interleukin-10 can directly inhibit T-cell growth.* Blood, 1993. **81**(11): p. 2964-71.
326. Schandene, L., et al., *B7/CD28-dependent IL-5 production by human resting T cells is inhibited by IL-10.* J Immunol, 1994. **152**(9): p. 4368-74.
327. de Waal Malefyt, R., H. Yssel, and J.E. de Vries, *Direct effects of IL-10 on subsets of human CD4+ T cell clones and resting T cells. Specific inhibition of IL-2 production and proliferation.* J Immunol, 1993. **150**(11): p. 4754-65.
328. Jinquan, T., et al., *CXC chemokine receptor 4 expression and stromal cell-derived factor-1alpha-induced chemotaxis in CD4+ T lymphocytes are regulated by interleukin-4 and interleukin-10.* Immunology, 2000. **99**(3): p. 402-10.
329. Groux, H., et al., *Interleukin-10 induces a long-term antigen-specific anergic state in human CD4+ T cells.* J Exp Med, 1996. **184**(1): p. 19-29.
330. Buer, J., et al., *Interleukin 10 secretion and impaired effector function of major histocompatibility complex class II-restricted T cells anergized in vivo.* J Exp Med, 1998. **187**(2): p. 177-83.
331. Akdis, C.A., et al., *Role of interleukin 10 in specific immunotherapy.* J Clin Invest, 1998. **102**(1): p. 98-106.
332. Groux, H., et al., *A CD4+ T-cell subset inhibits antigen-specific T-cell responses and prevents colitis.* Nature, 1997. **389**(6652): p. 737-42.
333. Asseman, C., et al., *An essential role for interleukin 10 in the function of regulatory T cells that inhibit intestinal inflammation.* J Exp Med, 1999. **190**(7): p. 995-1004.
334. Cassatella, M.A., et al., *Interleukin 10 (IL-10) inhibits the release of proinflammatory cytokines from human polymorphonuclear leukocytes. Evidence for an autocrine role of tumor necrosis factor and IL-1 beta in mediating the production of IL-8 triggered by lipopolysaccharide.* J Exp Med, 1993. **178**(6): p. 2207-11.

335. Groux, H., et al., *A transgenic model to analyze the immunoregulatory role of IL-10 secreted by antigen-presenting cells.* J Immunol, 1999. **162**(3): p. 1723-9.
336. Potteaux, S., et al., *Leukocyte-derived interleukin 10 is required for protection against atherosclerosis in low-density lipoprotein receptor knockout mice.* Arterioscler Thromb Vasc Biol, 2004. **24**(8): p. 1474-8.
337. Han, X., et al., *Interleukin-10 overexpression in macrophages suppresses atherosclerosis in hyperlipidemic mice.* FASEB J. **24**(8): p. 2869-80.
338. Graham, F.L., et al., *Characteristics of a human cell line transformed by DNA from human adenovirus type 5.* J Gen Virol, 1977. **36**(1): p. 59-74.
339. Scherer, W.F., J.T. Syverton, and G.O. Gey, *Studies on the propagation in vitro of poliomyelitis viruses. IV. Viral multiplication in a stable strain of human malignant epithelial cells (strain HeLa) derived from an epidermoid carcinoma of the cervix.* J Exp Med, 1953. **97**(5): p. 695-710.
340. Millington, O.R., et al., *Imaging interactions between the immune and cardiovascular systems in vivo by multiphoton microscopy.* Methods Mol Biol. **616**: p. 193-206.
341. Zinselmeyer, B.H., et al., *In situ characterization of CD4+ T cell behavior in mucosal and systemic lymphoid tissues during the induction of oral priming and tolerance.* J Exp Med, 2005. **201**(11): p. 1815-23.
342. Millington, O.R., et al., *Lymphocyte tracking and interactions in secondary lymphoid organs.* Inflamm Res, 2007. **56**(10): p. 391-401.
343. Schneider, H., et al., *Reversal of the TCR stop signal by CTLA-4.* Science, 2006. **313**(5795): p. 1972-5.
344. Beltman, J.B., A.F. Maree, and R.J. de Boer, *Analysing immune cell migration.* Nat Rev Immunol, 2009. **9**(11): p. 789-98.
345. Herbst, M.M., et al., *Sequence and expression analysis of deer mouse interferon-gamma, interleukin-10, tumor necrosis factor, and lymphotoxin-alpha.* Cytokine, 2002. **17**(4): p. 203-13.
346. Jacobsen, L.B., et al., *FuGENE 6 Transfection Reagent: the gentle power.* Methods, 2004. **33**(2): p. 104-12.
347. Baker, A.H., *Vascular Disease: Molecular Biology and Gene Transfer Protocols.* Vol. 30. 1999, Totowa: Humuna Press. 442.
348. Maffia, P., et al., *Inducing experimental arthritis and breaking self-tolerance to joint-specific antigens with trackable, ovalbumin-specific T cells.* J Immunol, 2004. **173**(1): p. 151-6.
349. Hsieh, C.S., et al., *Development of TH1 CD4+ T cells through IL-12 produced by Listeria-induced macrophages.* Science, 1993. **260**(5107): p. 547-9.
350. Macatonia, S.E., et al., *Dendritic cells produce IL-12 and direct the development of Th1 cells from naive CD4+ T cells.* J Immunol, 1995. **154**(10): p. 5071-9.

351. Gilham, D.E., et al., *Cytokine stimulation and the choice of promoter are critical factors for the efficient transduction of mouse T cells with HIV-1 vectors.* J Gene Med. **12**(2): p. 129-36.
352. Lutz, M.B., et al., *An advanced culture method for generating large quantities of highly pure dendritic cells from mouse bone marrow.* J Immunol Methods, 1999. **223**(1): p. 77-92.
353. Tournier, J.N., et al., *Fever-like thermal conditions regulate the activation of maturing dendritic cells.* J Leukoc Biol, 2003. **73**(4): p. 493-501.
354. Miller, M.J., et al., *Two-photon imaging of lymphocyte motility and antigen response in intact lymph node.* Science, 2002. **296**(5574): p. 1869-73.
355. Okada, T., et al., *Antigen-engaged B cells undergo chemotaxis toward the T zone and form motile conjugates with helper T cells.* PLoS Biol, 2005. **3**(6): p. e150.
356. Mempel, T.R., S.E. Henrickson, and U.H. Von Andrian, *T-cell priming by dendritic cells in lymph nodes occurs in three distinct phases.* Nature, 2004. **427**(6970): p. 154-9.
357. Amino, R., et al., *Imaging malaria sporozoites in the dermis of the mammalian host.* Nat Protoc, 2007. **2**(7): p. 1705-12.
358. Parasassi, T., et al., *Two-photon microscopy of aorta fibers shows proteolysis induced by LDL hydroperoxides.* Free Radic Biol Med, 2000. **28**(11): p. 1589-97.
359. Biswas, K.S., et al., *Multi-photon microscopy in the evaluation of human saphenous vein.* J Surg Res, 2001. **95**(1): p. 37-43.
360. Zoumi, A., et al., *Imaging coronary artery microstructure using second-harmonic and two-photon fluorescence microscopy.* Biophys J, 2004. **87**(4): p. 2778-86.
361. Lilledahl, M.B., et al., *Characterization of vulnerable plaques by multiphoton microscopy.* J Biomed Opt, 2007. **12**(4): p. 044005.
362. Le, T.T., et al., *Label-free molecular imaging of atherosclerotic lesions using multimodal nonlinear optical microscopy.* J Biomed Opt, 2007. **12**(5): p. 054007.
363. Ohata, H., et al., *Optical bioimaging: from living tissue to a single molecule: calcium imaging in blood vessel in situ employing two-photon excitation fluorescence microscopy.* J Pharmacol Sci, 2003. **93**(3): p. 242-7.
364. Megens, R.T., et al., *Two-photon microscopy of vital murine elastic and muscular arteries. Combined structural and functional imaging with subcellular resolution.* J Vasc Res, 2007. **44**(2): p. 87-98.
365. Megens, R.T., et al., *Intravital imaging of phagocyte recruitment.* Thromb Haemost. **105**(5): p. 802-10.
366. Drechsler, M., et al., *Hyperlipidemia-triggered neutrophilia promotes early atherosclerosis.* Circulation. **122**(18): p. 1837-45.
367. Garside, P. and J.M. Brewer, *Real-time imaging of the cellular interactions underlying tolerance, priming, and responses to infection.* Immunol Rev, 2008. **221**: p. 130-46.

368. Koltsova, E.K., et al., *Dynamic T cell-APC interactions sustain chronic inflammation in atherosclerosis.* J Clin Invest. **122**(9): p. 3114-26.
369. Thaunat, O., et al., *Immune responses elicited in tertiary lymphoid tissues display distinctive features.* PLoS One. **5**(6): p. e11398.
370. Penaranda, C., et al., *Prevention of diabetes by FTY720-mediated stabilization of peri-islet tertiary lymphoid organs.* Diabetes. **59**(6): p. 1461-8.
371. Brown, K., S.H. Sacks, and W. Wong, *Tertiary lymphoid organs in renal allografts can be associated with donor-specific tolerance rather than rejection.* Eur J Immunol. **41**(1): p. 89-96.
372. Sura, R., J.F. Colombel, and H.J. Van Kruiningen, *Lymphatics, tertiary lymphoid organs and the granulomas of Crohn's disease: an immunohistochemical study.* Aliment Pharmacol Ther. **33**(8): p. 930-9.
373. Bowen, G.P., et al., *Adenovirus vector-induced inflammation: capsid-dependent induction of the C-C chemokine RANTES requires NF-kappa B.* Hum Gene Ther, 2002. **13**(3): p. 367-79.
374. Hsu, C.P., et al., *Overexpression of human intestinal oligopeptide transporter in mammalian cells via adenoviral transduction.* Pharm Res, 1998. **15**(9): p. 1376-81.
375. Deriy, L., et al., *Expression of alpha-gal epitopes on HeLa cells transduced with adenovirus containing alpha1,3galactosyltransferase cDNA.* Glycobiology, 2002. **12**(2): p. 135-44.
376. Lee, N., et al., *Hypercytokinemia and hyperactivation of phospho-p38 mitogen-activated protein kinase in severe human influenza A virus infection.* Clin Infect Dis, 2007. **45**(6): p. 723-31.
377. Hunig, T., *The storm has cleared: lessons from the CD28 superagonist TGN1412 trial.* Nat Rev Immunol. **12**(5): p. 317-8.
378. Kohno, T., et al., *Interleukin-10-mediated inhibition of angiogenesis and tumor growth in mice bearing VEGF-producing ovarian cancer.* Cancer Res, 2003. **63**(16): p. 5091-4.
379. Shen, C.F. and A. Kamen, *Hyperosmotic pressure on HEK 293 cells during the growth phase, but not the production phase, improves adenovirus production.* J Biotechnol. **157**(1): p. 228-36.
380. Cai, G., et al., *A new inducible adenoviral expression system that responds to inflammatory stimuli in vivo.* J Gene Med, 2006. **8**(12): p. 1369-78.
381. Ji, H.B., et al., *T cell-specific expression of the murine CD3delta promoter.* J Biol Chem, 2002. **277**(49): p. 47898-906.
382. Nakajima, A., et al., *Antigen-specific T cell-mediated gene therapy in collagen-induced arthritis.* J Clin Invest, 2001. **107**(10): p. 1293-301.
383. Shaw, M.K., et al., *Local delivery of interleukin 4 by retrovirus-transduced T lymphocytes ameliorates experimental autoimmune encephalomyelitis.* J Exp Med, 1997. **185**(9): p. 1711-4.

384. Al-Khami, A.A., S. Mehrotra, and M.I. Nishimura, *Adoptive immunotherapy of cancer: Gene transfer of T cell specificity*. Self Nonself. **2**(2): p. 80-84.
385. Bogdan, C., Y. Vodovotz, and C. Nathan, *Macrophage deactivation by interleukin 10.* J Exp Med, 1991. **174**(6): p. 1549-55.
386. Alonso Arias, R., A. Lopez-Vazquez, and C. Lopez-Larrea, *Imunology and the challenge of transplantation.* Adv Exp Med Biol. **741**: p. 27-43.
387. Tervo, H.M., I. Allespach, and O.T. Keppler, *High-level transfection of primary rabbit T lymphocytes.* J Immunol Methods, 2008. **336**(1): p. 85-9.
388. Goffinet, C. and O.T. Keppler, *Efficient nonviral gene delivery into primary lymphocytes from rats and mice.* FASEB J, 2006. **20**(3): p. 500-2.
389. Lai, W., C.H. Chang, and D.L. Farber, *Gene transfection and expression in resting and activated murine CD4 T cell subsets.* J Immunol Methods, 2003. **282**(1-2): p. 93-102.
390. Carneiro, F.A., et al., *Membrane recognition by vesicular stomatitis virus involves enthalpy-driven protein-lipid interactions.* J Virol, 2002. **76**(8): p. 3756-64.
391. Miller, D.G., M.A. Adam, and A.D. Miller, *Gene transfer by retrovirus vectors occurs only in cells that are actively replicating at the time of infection.* Mol Cell Biol, 1990. **10**(8): p. 4239-42.
392. Qasim, W., et al., *T cell transduction and suicide with an enhanced mutant thymidine kinase.* Gene Ther, 2002. **9**(12): p. 824-7.
393. Symes, J.C., et al., *Retrovirally transduced murine T lymphocytes expressing FasL mediate effective killing of prostate cancer cells.* Cancer Gene Ther, 2009. **16**(5): p. 439-52.
394. Cavalieri, S., et al., *Human T lymphocytes transduced by lentiviral vectors in the absence of TCR activation maintain an intact immune competence.* Blood, 2003. **102**(2): p. 497-505.
395. Alba, R., et al., *Biodistribution and retargeting of FX-binding ablated adenovirus serotype 5 vectors.* Blood. **116**(15): p. 2656-64.
396. Alba, R., et al., *Identification of coagulation factor (F)X binding sites on the adenovirus serotype 5 hexon: effect of mutagenesis on FX interactions and gene transfer.* Blood, 2009. **114**(5): p. 965-71.
397. Poiesi, C., et al., *HIV-1 p17 binds heparan sulfate proteoglycans to activated CD4(+) T cells.* Virus Res, 2008. **132**(1-2): p. 25-32.
398. Kaur, S., et al., *Heparan sulfate modification of the transmembrane receptor CD47 is necessary for inhibition of T cell receptor signaling by thrombospondin-1.* J Biol Chem. **286**(17): p. 14991-5002.
399. Jones, K.S., et al., *Heparan sulfate proteoglycans mediate attachment and entry of human T-cell leukemia virus type 1 virions into CD4+ T cells.* J Virol, 2005. **79**(20): p. 12692-702.
400. Muzio, M., et al., *Differential expression and regulation of toll-like receptors (TLR) in human leukocytes: selective expression of TLR3 in dendritic cells.* J Immunol, 2000. **164**(11): p. 5998-6004.

401. Morel, A.S., G. Coulton, and M. Londei, *Regulation of major histocompatibility complex class II synthesis by interleukin-10.* Immunology, 2002. **106**(2): p. 229-36.
402. Chen, J. and X.S. Liu, *Development and function of IL-10 IFN-gamma-secreting CD4(+) T cells.* J Leukoc Biol, 2009. **86**(6): p. 1305-10.
403. Wei, K., F. Kuhnert, and C.J. Kuo, *Recombinant adenovirus as a methodology for exploration of physiologic functions of growth factor pathways.* J Mol Med (Berl), 2008. **86**(2): p. 161-9.
404. Laugwitz, K.L., et al., *Adenoviral gene transfer of the human V2 vasopressin receptor improves contractile force of rat cardiomyocytes.* Circulation, 1999. **99**(7): p. 925-33.
405. Schmidt, M.R., et al., *Expression of a human coxsackie/adenovirus receptor transgene permits adenovirus infection of primary lymphocytes.* J Immunol, 2000. **165**(7): p. 4112-9.
406. Huang, S., R.I. Endo, and G.R. Nemerow, *Upregulation of integrins alpha v beta 3 and alpha v beta 5 on human monocytes and T lymphocytes facilitates adenovirus-mediated gene delivery.* J Virol, 1995. **69**(4): p. 2257-63.
407. Kitamura, N., et al., *Correlation between mRNA expression of Th1/Th2 cytokines and their specific transcription factors in human helper T-cell clones.* Immunol Cell Biol, 2005. **83**(5): p. 536-41.
408. Whitmire, J.K., B. Eam, and J.L. Whitton, *Tentative T cells: memory cells are quick to respond, but slow to divide.* PLoS Pathog, 2008. **4**(4): p. e1000041.
409. Lai, W., et al., *Transcriptional control of rapid recall by memory CD4 T cells.* J Immunol. **187**(1): p. 133-40.
410. Pahl, H.L., *Activators and target genes of Rel/NF-kappaB transcription factors.* Oncogene, 1999. **18**(49): p. 6853-66.
411. Bernfield, M., et al., *Functions of cell surface heparan sulfate proteoglycans.* Annu Rev Biochem, 1999. **68**: p. 729-77.
412. Kim, C.W., et al., *Members of the syndecan family of heparan sulfate proteoglycans are expressed in distinct cell-, tissue-, and development-specific patterns.* Mol Biol Cell, 1994. **5**(7): p. 797-805.
413. Bradshaw, A.C., et al., *Requirements for receptor engagement during infection by adenovirus complexed with blood coagulation factor X.* PLoS Pathog. **6**(10): p. e1001142.
414. Leopold, P.L., et al., *Dynein- and microtubule-mediated translocation of adenovirus serotype 5 occurs after endosomal lysis.* Hum Gene Ther, 2000. **11**(1): p. 151-65.
415. Suomalainen, M., et al., *Microtubule-dependent plus- and minus end-directed motilities are competing processes for nuclear targeting of adenovirus.* J Cell Biol, 1999. **144**(4): p. 657-72.
416. Bremner, K.H., et al., *Adenovirus transport via direct interaction of cytoplasmic dynein with the viral capsid hexon subunit.* Cell Host Microbe, 2009. **6**(6): p. 523-35.

417. Huthoff, H. and G.J. Towers, *Restriction of retroviral replication by APOBEC3G/F and TRIM5alpha.* Trends Microbiol, 2008. **16**(12): p. 612-9.
418. Bieniasz, P.D., *Restriction factors: a defense against retroviral infection.* Trends Microbiol, 2003. **11**(6): p. 286-91.
419. Baumann, J.G., et al., *Murine T cells potently restrict human immunodeficiency virus infection.* J Virol, 2004. **78**(22): p. 12537-47.
420. Clarke, S.R., et al., *Characterization of the ovalbumin-specific TCR transgenic line OT-I: MHC elements for positive and negative selection.* Immunol Cell Biol, 2000. **78**(2): p. 110-7.
421. von Andrian, U.H. and C.R. Mackay, *T-cell function and migration. Two sides of the same coin.* N Engl J Med, 2000. **343**(14): p. 1020-34.
422. Shiow, L.R., et al., *CD69 acts downstream of interferon-alpha/beta to inhibit S1P1 and lymphocyte egress from lymphoid organs.* Nature, 2006. **440**(7083): p. 540-4.
423. Jenkins, M.K., et al., *In vivo activation of antigen-specific CD4 T cells.* Annu Rev Immunol, 2001. **19**: p. 23-45.
424. Croft, M., *Co-stimulatory members of the TNFR family: keys to effective T-cell immunity?* Nat Rev Immunol, 2003. **3**(8): p. 609-20.
425. Seder, R.A. and R. Ahmed, *Similarities and differences in CD4+ and CD8+ effector and memory T cell generation.* Nat Immunol, 2003. **4**(9): p. 835-42.
426. Homann, D., L. Teyton, and M.B. Oldstone, *Differential regulation of antiviral T-cell immunity results in stable CD8+ but declining CD4+ T-cell memory.* Nat Med, 2001. **7**(8): p. 913-9.
427. Mora, J.R. and U.H. von Andrian, *T-cell homing specificity and plasticity: new concepts and future challenges.* Trends Immunol, 2006. **27**(5): p. 235-43.
428. Chong, B.F., et al., *E-selectin, thymus- and activation-regulated chemokine/CCL17, and intercellular adhesion molecule-1 are constitutively coexpressed in dermal microvessels: a foundation for a cutaneous immunosurveillance system.* J Immunol, 2004. **172**(3): p. 1575-81.
429. Reinhardt, R.L., et al., *Visualizing the generation of memory CD4 T cells in the whole body.* Nature, 2001. **410**(6824): p. 101-5.
430. Ouyang, Y.L., et al., *Vomitoxin-mediated IL-2, IL-4, and IL-5 superinduction in murine CD4+ T cells stimulated with phorbol ester calcium ionophore: relation to kinetics of proliferation.* Toxicol Appl Pharmacol, 1996. **138**(2): p. 324-34.
431. Curran, K.J., H.J. Pegram, and R.J. Brentjens, *Chimeric antigen receptors for T cell immunotherapy: current understanding and future direction.* J Gene Med.
432. Fujio, K., et al., *Gene therapy of arthritis with TCR isolated from the inflamed paw.* J Immunol, 2006. **177**(11): p. 8140-7.

433. Urbanska, K., et al., *A universal strategy for adoptive immunotherapy of cancer through use of a novel T cell antigen receptor.* Cancer Res.
434. Yee, C., et al., *Adoptive T cell therapy using antigen-specific CD8+ T cell clones for the treatment of patients with metastatic melanoma: in vivo persistence, migration, and antitumor effect of transferred T cells.* Proc Natl Acad Sci U S A, 2002. **99**(25): p. 16168-73.
435. Mathisen, P.M., et al., *Treatment of experimental autoimmune encephalomyelitis with genetically modified memory T cells.* J Exp Med, 1997. **186**(1): p. 159-64.
436. Rosenberg, S.A., et al., *Adoptive cell transfer: a clinical path to effective cancer immunotherapy.* Nat Rev Cancer, 2008. **8**(4): p. 299-308.
437. Almasbak, H., et al., *Transiently redirected T cells for adoptive transfer.* Cytotherapy. **13**(5): p. 629-40.
438. Walter, E.A., et al., *Reconstitution of cellular immunity against cytomegalovirus in recipients of allogeneic bone marrow by transfer of T-cell clones from the donor.* N Engl J Med, 1995. **333**(16): p. 1038-44.
439. Rooney, C.M., et al., *Infusion of cytotoxic T cells for the prevention and treatment of Epstein-Barr virus-induced lymphoma in allogeneic transplant recipients.* Blood, 1998. **92**(5): p. 1549-55.
440. Dudley, M.E., et al., *Cancer regression and autoimmunity in patients after clonal repopulation with antitumor lymphocytes.* Science, 2002. **298**(5594): p. 850-4.
441. Marijt, W.A., et al., *Hematopoiesis-restricted minor histocompatibility antigens HA-1- or HA-2-specific T cells can induce complete remissions of relapsed leukemia.* Proc Natl Acad Sci U S A, 2003. **100**(5): p. 2742-7.
442. Bonini, C., et al., *HSV-TK gene transfer into donor lymphocytes for control of allogeneic graft-versus-leukemia.* Science, 1997. **276**(5319): p. 1719-24.
443. Tiberghien, P., et al., *Administration of herpes simplex-thymidine kinase-expressing donor T cells with a T-cell-depleted allogeneic marrow graft.* Blood, 2001. **97**(1): p. 63-72.
444. Freytag, S.O., et al., *Phase I study of replication-competent adenovirus-mediated double suicide gene therapy for the treatment of locally recurrent prostate cancer.* Cancer Res, 2002. **62**(17): p. 4968-76.
445. Introna, M., et al., *Genetic modification of human T cells with CD20: a strategy to purify and lyse transduced cells with anti-CD20 antibodies.* Hum Gene Ther, 2000. **11**(4): p. 611-20.
446. Straathof, K.C., et al., *An inducible caspase 9 safety switch for T-cell therapy.* Blood, 2005. **105**(11): p. 4247-54.
447. Philip, B., *A highly compact epitope-based marker suicide gene for more convenient and safer T cell adoptive immunotherapy*, in *Blood*. 2010, American Society of Hematology. p. 2.